

TABLE OF CONTENTS

DECLARATION	i
ACKNOWLEDGEMENTS	iv
SUMMARY	vi
LIST OF FIGURES	xiii
LIST OF TABLES	xxi
LIST OF ABBREVIATIONS	xxii
CHAPTER ONE: LITERATURE REVIEW	1
1.1 INTRODUCTION	1
1.2 FOOT-AND-MOUTH DISEASE VIRUS	1
1.3 EPIDEMIOLOGY OF FMDV	2
1.3.1 DISTRIBUTION	2
1.3.2 EPIDEMIOLOGICAL PATTERNS FOR FMDV IN AFRICA	3
1.3.3 THE ROLE OF CARRIERS IN THE EPIDEMIOLOGY OF FMDV	7
1.3.4 TRANSMISSION OF FMD	8
1.4 CONTROL AND ERADICATION OF FMDV	9
1.5 PATHOGENESIS OF THE DISEASE	11
1.6 THE VIRION	12
1.7 FMD VIRAL STRUCTURAL PROTEINS	13
1.8 FMDV GENOME	15
1.9 VIRUS REPLICATION AND TRANSLATION	16
1.10 THE CELLULAR RECEPTORS OF FMDV	20
1.10.1 INTEGRIN-MEDIATED FMDV INFECTION	20
1.10.1.1 INTEGRIN ACTIVATION	21
1.10.1.2 FMDV INTEGRIN BINDING	22
1.10.1.3 INTEGRINS IDENTIFIED FOR FMDV ATTACHMENT	24
	viii

	(i)	$\alpha_v\beta_3$	24
	(ii)	$\alpha_v\beta_6$	24
	(iii)	$\alpha_v\beta_1$	25
	(iv)	$\alpha_v\beta_8$	25
	(v)	$\alpha_5\beta_1$	25
1.10.1.4		SUMMARY OF FMDV INTEGRIN RECEPTORS	26
1.10.2		HEPARAN SULPHATE (HS)	26
1.10.3		THIRD GROUP OF “UNKNOWN” FMDV RECEPTORS	28
1.11		DESIGN OF IMPROVED INACTIVATED VACCINES	31
1.12		FMDV DIAGNOSTIC ASSAYS	33
1.13		THE IMMUNE RESPONSE TO FMDV	36
	1.13.1	THE INNATE IMMUNE SYSTEM	36
	1.13.2	THE ADAPTIVE IMMUNE SYSTEM	38
		1.13.2.1 HUMORAL IMMUNE RESPONSES	38
		1.13.2.2 CELLULAR IMMUNE RESPONSES	39
1.14		ANTIBODIES	40
	1.14.1	ANTIBODY STRUCTURE AND DIVERSITY	40
1.15		ANTIBODY PHAGE DISPLAY TECHNOLOGY	42
1.16		AIMS OF THE STUDY	47

CHAPTER TWO: SYMMETRICAL ARRANGEMENT OF POSITIVELY CHARGED RESIDUES AROUND THE FIVE-FOLD PORE OF FOOT-AND-MOUTH DISEASE SAT TYPE VIRUS CAPSIDS RESULTS IN THE ENHANCED AFFINITY TO HEPARAN SULPHATE **50**

2.1	INTRODUCTION	50
2.2	MATERIALS AND METHODS	52
2.2.1	CELLS, VIRUSES AND PLASMIDS	52
2.2.2	PLAQUE TITRATION	54
2.2.3	RNA EXTRACTION, CDNA SYNTHESIS, PCR AMPLIFICATION AND NUCLEOTIDE SEQUENCING	54
2.2.4	SITE-DIRECTED MUTAGENESIS AND SUB-CLONING	54
2.2.5	<i>IN VITRO</i> RNA SYNTHESIS, TRANSFECTION AND VIRUS RECOVERY	56
2.2.6	HEPARIN PLAQUE REDUCTION ASSAY	56
2.2.7	HEPARINASE ASSAY	57
2.2.8	STRUCTURAL MODELLING AND LIGAND DOCKING	57
2.3	RESULTS	57
2.3.1	MULTIPLE SERIAL PASSAGES OF SAT VIRUSES IN CULTURED CELLS SELECT FOR VARIANTS WITH INCREASED VIRULENCE IN BHK-21 CELLS	57
2.3.2	GAIN OF NET POSITIVE CHARGE IN THE VP1 AND VP3 PROTEINS DURING GROWTH IN BHK-21 CELLS	60
2.3.3	GENERATION OF RECOMBINANT FMDV WITH ALTERED SURFACE CHARGES	61
2.3.4	EFFECT OF THE MUTATIONS ON THE INFECTIVITY AND CELL ENTRY OF CULTURED BHK-21 AND CHO CELLS	64
2.4	DISCUSSION	68

CHAPTER THREE: DEVELOPMENT AND VALIDATION OF A FOOT-AND-MOUTH DISEASE VIRUS SAT SEROTYPE-SPECIFIC 3ABC ASSAY TO DIFFERENTIATE INFECTED FROM VACCINATED ANIMALS	73
3.1 INTRODUCTION	73
3.2 MATERIALS AND METHODS	75
3.2.1 CLONING AND EXPRESSION OF SAT2/ZIM/7/83 TRUNCATED 3ABC POLYPEPTIDE	75
3.2.2 SDS-POLYACRYLAMIDE GEL ELECTROPHORESIS AND IMMUNOBLOTTING	76
3.2.3 NSP ELISAs	76
3.2.4 SERUM PANEL	77
3.2.5 COMPARISON OF THE SAT-NSP ELISA AND STATISTICAL ANALYSIS	78
3.3 RESULTS	80
3.3.1 EXPRESSION OF THE SAT-TR3ABC PROTEIN AND OPTIMIZATION OF THE SAT-NSP ELISA	80
3.3.2 COMPARISON OF THE SAT-NSP, IZSLER-NSP AND PRIOCHECK®-NSP KIT	81
3.4 DISCUSSION	88
CHAPTER FOUR: NOVEL SINGLE-CHAIN ANTIBODY FRAGMENTS AGAINST FOOT-AND-MOUTH DISEASE SEROTYPE A, SAT1 AND SAT3 VIRUSES USING A NKUKU® PHAGE DISPLAY LIBRARY	91
4.1 INTRODUCTION	91
4.2 MATERIALS AND METHODS	93
4.2.1 CELL CULTURES, VIRUS PROPAGATION AND PURIFICATION	93
4.2.2 SELECTION OF SCFVS AGAINST SAT1/KNP/196/91, SAT3/KNP/10/90 AND A22	95
4.2.3 POLYCLONAL PHAGE ELISA	95
4.2.4 MONOCLONAL PHAGE SCFV ELISA	96

4.2.5 MONOCLONAL SOLUBLE SCFV ELISA	96
4.2.6 DNA SEQUENCING AND SEQUENCE ANALYSIS OF PHAGE-DISPLAYED SCFVS	96
4.2.7 LARGE SCALE EXPRESSION AND PURIFICATION OF SOLUBLE SCFVS	97
4.2.8 BINDING SPECIFICITY OF SOLUBLE SCFVS	98
4.2.9 NEUTRALIZATION ASSAYS AND GENERATION OF VIRUS ESCAPE MUTANTS	98
4.2.9.1 CHARACTERIZATION OF VIRUS ESCAPE MUTANTS	99
4.2.10 INVESTIGATION OF THE SAT1 AND SAT3 SOLUBLE SCFVS AS CAPTURING ANTIBODIES IN AN INDIRECT ELISA	100
4.2.11 INVESTIGATION OF THE SAT1 AND SAT3 SCFVS AS DETECTING ANTIBODIES IN AN INDIRECT ELISA	101
4.2.12 ANALYSIS OF SAT1 AND SAT3 VIRUS SEQUENCES	102
4.3 RESULTS	102
4.3.1 BIOPANNING AGAINST FMDV SAT1/KNP/196/91; SAT3/KNP/10/90 AND A22	102
4.3.2 BINDING SPECIFICITY OF SOLUBLE SCFVS TO FMDV	106
4.3.3 NEUTRALIZATION AND ESCAPE MUTANT INVESTIGATIONS OF THE IDENTIFIED SCFVS	109
4.3.4 SAT VIRUS-SPECIFIC SCFVS AS A FMDV CAPTURING ANTIBODY IN A SANDWICH ELISA	111
4.3.5 SAT VIRUS-SPECIFIC SCFVS AS A FMDV DETECTING ANTIBODY IN AN ELISA	113
4.3.6 PREDICTION OF ELISA VARIABILITY FROM SEQUENCE DATA ANALYSIS	115
4.4 DISCUSSION	128
CHAPTER FIVE: CONCLUDING REMARKS	135
REFERENCES	140
APPENDICES	176
PUBLICATIONS AND CONGRESS CONTRIBUTIONS	183

LIST OF FIGURES

- Figure 1.1:** Geographical distribution of seven pools of Foot-and-mouth disease viruses. Taken from Jamal and Belsham (2013). 3
- Figure 1.2:** Schematic representation of the surface structure of FMDV capsid proteins, the subunits and the virus capsid. (A) Schematic, tertiary structure of VP1 (1D), VP2 (1B) and VP3 (1C). The eight β -strands are shown *i.e.* B, I, D, G, C, H, E and F. (B) Arrangement of VP1 – 3, the external capsid proteins, in a biological protomer. (C) The arrangement of five protomers making up a pentamer (a protomer is outlined). (D) Structure of the capsid, outlining the pentamer (in green) and the protomer (in black). The two-fold, three-fold and five-fold axes are indicated. Adapted from Sobrino *et al.*, 2001 and Jamal and Belsham, 2013. 14
- Figure 1.3:** Map of the FMDV genome showing the functional elements of the genome as well as the protein cleavage products. Taken from (Gao *et al.*, 2016). 16
- Figure 1.4:** Diagram depicting FMDV replication and translation. Following entry of FMDV RNA into the cytoplasm of the cell, the RNA has to be translated to generate viral proteins required for viral RNA replication. HS is Heparan sulphate. NSPs is non-structural proteins. Green line is viral positive strand (+) RNA. Orange line is viral negative strand (-) RNA. Taken from (Gao *et al.*, 2016). 18
- Figure 1.5:** FMDV receptor endocytosis pathways. (A) The pathogen (virus) bind to glycosaminoglycans (GAGs) to increase their concentration on the cell surface and facilitate virus internalization. (B) FMDV can either enter cells via a caveola-mediated or clathrin-mediated endocytic pathway. Taken from (Yamaguchi *et al.*, 2010). 20
- Figure 1.6:** Diagram depicting the integrin α and β subunits. The putative locations of the cysteine-rich repeats of the β subunit as well as the extracellular, transmembrane and the intracellular domains are indicated. Taken from <https://rituparnas.wordpress.com/2016/03/14/cell-junctions-and-cell-adhesion/> 22
- Figure 1.7:** A schematic diagram representing currently postulated integrin-mediated ‘inside-out’ signaling. The activities of both protein (serine/threonine) kinases and phosphatases are involved in the signaling regulation. Phosphorylation/dephosphorylation of integrin cytoplasmic domains (no

evidence yet) or of associated regulatory molecules (? in diagram), may allow for the interaction of other proteins (e.g. endonexin) with the integrin cytoplasmic domains. Calreticulin (CRT) associates only with the 'active' integrin form of α subunits, which are involved in the regulation of integrin-affinity states. Integrin-linked kinase (ILK) associates with the β integrin subunits and may play a role in regulating integrin-affinity states. The GTPases, R-ras and Rho A may be implicated in the regulation of integrin-affinity states [taken from (Dedhar and Hannigan, 1996)].

23

Figure 1.8: Heparan sulphate proteoglycan cell signalling features. Cellular responses are triggered by HSPG through signal transduction pathways where HSPG is a receptor or co-receptor in a cytoskeleton independent (A) or dependant (B) manner. Taken from (Dreyfuss *et al.*, 2009).

27

Figure 1.9: Model of the FMDV macropinocytic internalization pathway. Binding of FMDV to receptor tyrosine kinases (RTKs) may activate cellular actin modulators (Rac1, Pak1, and PKC) and other factors, such as NHEs (sodium-hydrogen exchanger) and dynamin. This starts actin rearrangement and plasma membrane ruffling. Internalisation of the virions occur into macropinosomes and the membrane fission events that separate the macropinosomes from the extracellular space occur in a myosin II-dependent manner. After closure, the early macropinosomes containing FMDV acquire Rab5 (Ras-related protein, a regulatory guanosine triphosphatase) and EEA1 (early endosomal autoantigen 1), which facilitate intracellular trafficking. The acidic pH of macropinosomes may trigger viral uncoating. As an alternative entry route of FMDV, virion binding to integrin receptors induces viral internalization via CME. The internalized vesicle is then delivered to early endosomes, and the endosomal acidic pH triggers viral uncoating. Taken from (Han *et al.*, 2016).

30

Figure 1.10: Representation of an antibody. There are two heavy polypeptide chains and two light polypeptide chains joined together by disulphide bonds. Each heavy chain is composed of one variable region (V_H) (blue block) and three constant regions (C_{H1} , C_{H2} , C_{H3}) (blue blocks) whilst each light chain is composed of one variable region (V_L , pink block) and one constant region (C_L , pink block). The antigen binding site is indicated, which is composed of one light and one heavy chain. The Fab and Fc regions are indicated. Figure adapted from <https://global.britannica.com/science/disulfide>

41

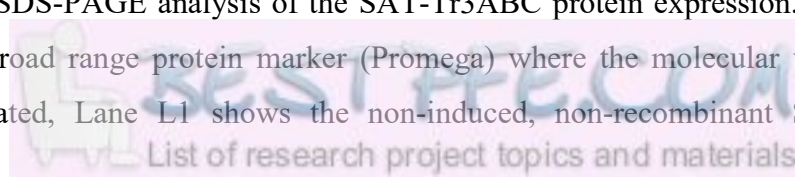
- Figure 1.11:** A schematic diagram of an antibody structure and derivative fragments. (A) IgG, 160kD; (B) Fab fragment, 50kD; (C) Fv fragment, 30kD, containing only the variable fragments of one heavy and one light chain; (D) scFv with linker, 30kDa, which is a randomly combined variable fragment of a heavy and light chain. Taken from Carmen and Jermutus (2002). 43
- Figure 1.12:** The basic principal of phage display. A bacteriophage has a genome that comprises of an origin of replication (Or) and genes g1 and g2 that encode two types of coat protein *i.e.* p1 and p2 respectively. A foreign protein, px (or random peptide, protein domains and antibody fragments), that is encoded by gene gx is displayed at the phage surface by the fusion of gx to p1 or p2. The number of copies of px displayed is dependent on which phage coat protein fusion occurred. Taken from Carmen and Jermutus (2002). 44
- Figure 1.13:** Representation of the structure of the M13 filamentous bacteriophage. Taken from Fukunaga and Taki, 2012. 45
- Figure 1.14:** Schematic representation showing the screening of an antibody phage display library to isolate target specific antibody fragments. (1) DNA encoding a vast amount of variant antibody fragments is cloned into the genome of a filamentous phage fused to one of the coat protein genes. (2) A separate phage particle contains each of the variant DNA and the antibody fragment is displayed on the phage coat protein. (3) Phage that is expressing the antibody fragment that is able to bind to the target analyte are selected using biopanning cycles of (a) binding, (b) washing and (c) elution. (4) The phages obtained after elution are used to reinfect *E.coli* cells and amplified by repeating the biopanning process. (5) After 3-4 rounds of selection, clones are then characterized. Taken from (Yun *et al.*, 2009). 46
- Figure 2.1:** Charge distribution and clustering of mutations on the capsid surface. (A) Electrostatic potential of wild-type SAT1 capsid showing uniform charge distribution on the particle surface. (B) Electrostatic potential of the mutant SAT1 capsid showing clustering of positive charge at 5-fold axis. The electrostatic potential was calculated using APBS plugin embedded within Pymol. The colouring represents positive charge (blue), negative charge (red) and neutral (white). (C) The projection of the capsid on a 5-fold axis shows the clustering of the positively charge mutations from the top view. (D) The

projection showing the size view and the surface exposure of the mutant side chains. 63

Figure 2.2: Infection of CHO-K1 cells by the recombinant mutants vSAU^{1158K}SAT2, vSAU^{1083K}SAT2 and vSAU^{3158R}SAT2 is inhibited by heparin. (A) There was a linear decrease in titres for vSAU^{VP1Δ83K,85R}SAT2 and vSAU^{VP1Δ110KRR}SAT2 infection of CHO-K1 cells with increasing concentration of heparin. Infection was completely abolished in the presence of 5 mg/ml heparin for vSAU^{VP1Δ83K,85R}SAT2, whilst vSAU^{VP1Δ110KRR}SAT2 was still able to infect CHO-K1 cells in the presence of 10 mg/ml heparin. Viruses having titres ranging from 5×10^7 to 7×10^7 PFU/ml were mock-treated or treated with 0.625, 1.25, 2.5, 5 or 10 mg/ml soluble heparin before infecting monolayers of CHO-K1 cells. Virus that had not been internalized was removed by washing with MES buffer (pH 5.5). The number of plaques formed on CHO-K1 cells was counted and expressed as the percentage of infectivity in relation to the non-heparin treated chimeric viruses. The standard deviations of the titres determined from duplicate wells are indicated. (B) The infection of vSAU^{VP1Δ2}SAT2 and vSAU¹¹¹⁰⁻¹¹¹²SAT2 on BHK-21 heparinase I and III treated cells were determined. The chimera, vSAU^{VP1Δ2}SAT2, was not able to infect heparinase I or III treated BHK-21 cells. However, vSAU¹¹¹⁰⁻¹¹¹²SAT2 virus titres reduced to 78% in heparinase I treated BHK-21 cells and to 82% for heparinase III treated BHK-21 cells. Monolayers of BHK-21 cells prepared in 24-well cell culture plates were treated with heparinase I and III enzymes (prepared in PBS) for 30 min at 37°C. After a wash step, virus was allowed to infect cell monolayers for 1 h at 37°C. This was followed by a final wash step, addition of GMEM and incubation of plates at 37°C. Virus infectivity titres were determined by plaque on BHK-21 cells at 24 h post-infection. 67

Figure 3.1: Map showing the provinces of South Africa (inset), highlighting the Mpumalanga (top) and Northern Cape regions (below) in detail. The vaccinated group of bovine sera originated from the FMD control zone region of Mpumalanga whilst the naïve bovine sera originated from the Northern Cape region. 79

Figure 3.2: (A): SDS-PAGE analysis of the SAT-Tr3ABC protein expression. Lane M is the broad range protein marker (Promega) where the molecular weights are indicated, Lane L1 shows the non-induced, non-recombinant SAT-3ABC



protein, L2 is the induced non-recombinant SAT-3ABC protein, L3 is the non-induced recombinant SAT-Tr3ABC protein whilst lanes L4 and L5 indicates successful expression of the recombinant SAT-Tr3ABC protein at *ca.* 37kDa (indicated by an arrow), by two clones. (B) Lanes L1 and L2 shows the western blot analysis of two clones of the expressed SAT-Tr3ABC protein. The position of the protein marker relative to the western blot is indicated. 80

Figure 3.3: Summary of the distribution of results for the (A) IZSLER-NSP, (B) SAT-NSP and (C) PrioCheck®-NSP tests from 617 cattle sampled within the FMD free zone (FMD naive), 1145 vaccinated cattle sampled during a SAT 1 outbreak of which 592 were test negative on a SAT1 liquid-phase blocking ELISA (VLN) and 553 were test positive on a SAT1 liquid-phase blocking ELISA (VLP), and 215 samples collected from FMDV experimentally challenged cattle (Experimental). The positive threshold for the IZSLER-NSP and SAT-NSP tests is 0.1 proportion positive and the PrioCheck®-NSP is considered positive at or above 0.5 proportion inhibition. The thresholds position is indicated by a red line in each graph. Outliers are plotted as individual points *. 82

Figure 4.1: Enrichment of phage-displayed scFvs for (A) SAT1/KNP/196/91, (B) SAT3/KNP/10/90 and (C) A22 using a polyclonal ELISA. Phage displayed scFvs that bound to SAT1/KNP/196/91, SAT3/KNP/10/90 and A22 were eluted and enrichment of virus specific phage displayed scFvs (black bars) was determined by a polyclonal phage ELISA of the outputs for three consecutive biopannings. The unpanned aliquot of the Nkuku® phage display library was a non-enriched control (selection round 0). The negative control used was 2% milk powder (labelled 2% MP, grey bars). The data are averages \pm SD of three repeats. 104

Figure 4.2: Indirect ELISA showing the specificity of scFvs *i.e.* (A) SAT1scFv1, (B) SAT3scFv1, (C) SAT3scFv2, (D) A22scFv5 and (E) A22scFv6. The remainder of the A22 scFv phage and soluble binders only reacted to A22 with no significant reaction to any of the other viruses or reagents (data not shown). Absorbance was measured at A_{450nm} . FMDV A22, A24, SAT1/KNP/196/91, SAT2/ZIM/7/83, SAT3/KNP/10/90 SDG purified viruses as well as BHK-21 cell extract, 2% sucrose (suc) and 2% milk powder (MP) was tested. The black bars indicate the phage-displayed scFvs whilst the grey bars indicate the soluble scFv tested. An ELISA signal two-fold that of the 2% MP soluble scFv




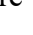
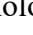
absorbance was considered a positive result and the cut-off is indicated by a red line. The data are means \pm SD of three repeats. 108

Figure 4.3: (A) The A22 virus escape mutant substitutions are indicated in an aa alignment of the VP1 GH-loop of A22. The aa alignment indicates the proline to serine (Pro149→Ser) substitution at position 149 of VP1 for SRV1 and a leucine to a phenylalanine (Leu150→Phe) substitution at position 150 of VP1 for SRV3 (bold and underlined). The RGD motif is blocked. (B) The substitutions are shown on the model of FMDV capsid proteins forming a crystallographic protomer. The aa substitutions are indicated in the salmon colour whilst VP1 is dark blue, VP2 is green, VP3 is magenta and the RGD sequence is shown in red. 110


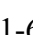

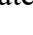
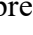
Figure 4.4: A sandwich ELISA with soluble scFvs as capturing antibodies. The SAT1scFv1 was tested with PEG concentrated SAT1 viruses (A) and SAT3scFv1 and SAT3scFv2 was tested with the SAT3 viruses (B). For the negative control (neg), 2% milk powder was included in the assays replacing the soluble scFvs coating the plate. The data are means \pm SD of two independent experiments. An ELISA signal more than two-fold that of the negative control A_{450nm} was considered a positive result and the cut-off is indicated by a red line. 112

Figure 4.5: Sandwich ELISA using soluble scFvs SAT1scFv1, SAT3scFv1 and SAT3scFv2 as detecting reagents. The standard diagnostic sandwich ELISA used for FMD antigen detection (OIE manual, 2017) (used as a positive control) was adapted, where the detection antibody was replaced with a soluble SAT scFv. The ELISA was executed to determine the detecting potential of soluble SAT1scFv1 to PEG concentrated SAT1 (A) and for SAT3scFv1 and SAT3scFv2 to PEG concentrated SAT3 (B) serotype viruses. For the negative control (neg), 2% milk powder was included in the assays replacing the virus component. The negative control ELISA background signal was deducted when plotting the ELISA A_{450nm} result. The data are means \pm SD of two independent experiments. 114

Figure 4.6: Neighbor-Joining tree (Saitou and Nei, 1987) of SAT1 viruses used in this study based on the aa sequences of the VP1, VP2, VP3 and VP4 region. The evolutionary distances were computed using the Poisson correction method and a bootstrap analysis of 1000 replication was applied. Evolutionary analyses were conducted in MEGA7 (Kumar *et al.*, 2016). The coloured squares indicate the

ELISA reactivity from Table 4.6 of SAT1scFv1 with the SAT1 viruses *i.e.* 0-20% , 21-40% , 41-60% , 61-80% , and 81-100% . The roman numerals in brackets indicate the order of antigenic relationship calculated as per r1 values where (i) represents the most closely related virus antigenically to the homologous virus (SAT1/KNP/196/91). The square brackets [] refer to the bootstrap value from the minimum evolution phylogeny computation. The topotype groupings (Bastos *et al.*, 2001, Maree *et al.*, 2011) are indicated in bold roman numerals.

119

Figure 4.7: Neighbor-Joining tree (Saitou and Nei, 1987) of SAT3 viruses used in this study based on the aa sequences of the P1 region. The evolutionary distances were computed using the Poisson correction method and a bootstrap analysis of 1000 replication was applied. Evolutionary analyses were conducted in MEGA7 (Kumar *et al.*, 2016). The coloured squares indicate the ELISA reactivity from Table 4.6 of SAT3scFv1 and SAT3scFv2 with the SAT3 viruses *i.e.* 0-20% , 21-40% , 41-60% , 61-80% , and 81-100% . The roman numerals in brackets indicate the order of antigenic relationship calculated as per r1 values where (i) represents the most closely related virus antigenically to the homologous virus (SAT3/KNP/10/90). The square brackets [] refer to the bootstrap value from the minimum evolution phylogeny computation. The topotype groupings (Bastos *et al.*, 2003a) are indicated in bold roman numerals.

120

Figure 4.8: Plots representing the aa variation for VP3 (A), VP2 (B), and VP1 (C) for the aligned SAT1 viruses. The pink bars represent the beta strands of the FMDV structure, whilst the green represent the alpha helices. The SAT1 viruses were aligned to the SAT1/KNP/196/91 virus, which was used for panning. Regions of aa variation are shown by the red vertical bars and the clear areas represent conserved regions. Regions of chaotropy or high entropy were identified as having an entropy >1 and hypervariable regions were defined as five or more variable aa positions in a window of 10 aa in the alignment. The blue horizontal line indicates an entropy of 1. Previously identified antigenic sites and hypervariable regions are indicated by the blue bar/blocks based on Grazioli *et al.*, 2006 and Maree *et al.*, 2011 and these regions corresponded to or were located in close proximity to regions of chaotropy observed for the SAT1 viruses from this study.

122

Figure 4.9: Plots representing the aa variation for VP3 (A), VP2 (B), and VP1 (C) for the aligned SAT3 viruses. The pink bars represent the beta strands of the FMDV structure, whilst the green represent the alpha helices. The SAT3 viruses were aligned to the SAT3/KNP/10/90 virus, which was used for panning. Regions of aa variation are shown by the red vertical bars and the clear areas represent conserved regions. Regions of chaotropism were identified as having an entropy >1 and were defined as sites on the capsid protein that had five or more variable aa residues within a window of 10 residues. The blue line indicates an entropy of 1. 123

Figure 4.10: The aa variation (entropy >1) occurring during sequence alignments was plotted on a ribbon protein diagram of a crystallographic pentamer of SAT1 (protein data bank ID: 2wzr, r2wrsf; Reeve *et al.*, 2010) (A) and a modelled pentamer for SAT3 viruses (B). The protein subunits and structural features are colour coded for VP1 (red), VP2 (light blue), VP3 (yellow) and VP4 (green). The pore, located at the 5-fold axis of the capsid (black circle), is shown in the middle of the structure. The 3-fold axis is depicted by the black triangles. The spheres indicate the aa variation (entropy >1) in VP1 (blue), VP2 (pink) and VP3 (purple). 126

LIST OF TABLES

Table 2.1:	Summary of the SAT1 and SAT2 viruses resulting from cytolitic passages in BHK-21 cells, the plaque morphologies and their titres in PFU/ml on BHK-21, CHO-K1, CHO-677, CHO-745 and CHO-Lec2 cells.	59
Table 2.2:	Summary of the amino acid substitutions to a positively charged residue in the outer capsid proteins of serially passaged SAT1 and SAT2 viruses.	60
Table 2.3:	Titres (PFU/ml) of inter-serotype or intra-serotype FMDV chimera viruses with positive charged residue substitutions in the VP1 or VP3 capsid proteins. Plaque morphology on BHK-21 cells are indicated.	66
Table 3.1:	Correlation and agreement among three FMD non-structural protein ELISA evaluated in cattle from South Africa.	84
Table 3.2:	Cross-classified test results for 1020 FMD vaccinated cattle sampled during a SAT1 outbreak and evaluated using three non-structural protein (NSP) ELISA and a SAT1 liquid-phase blocking ELISA (LPBE) in South Africa.	85
Table 3.3:	FMD prevalence and diagnostic accuracy estimates for 823 animals tested with three non-structural protein ELISAs in experimentally infected FMDV cattle and naïve animals.	86
Table 3.4:	Comparison of NSP ELISA assay detection of 3ABC positive samples from the experimentally infected cattle sera.	87
Table 4.1:	Detailed list of FMDV SAT1, SAT2, SAT3, and A viruses used in this study.	94
Table 4.2:	Oligonucleotides used for sequencing the escape mutant viruses.	100
Table 4.3:	Amino acid sequence alignment of the complementary determining regions (CDR) of the heavy and light chains of the SAT1/KNP/196/91, SAT3/KNP/10/90 and A22-specific soluble scFvs panned from the Nkuku® library.	105
Table 4.4:	Concentration of post-dialysed scFv's for SAT1/KNP/196/91, SAT3/KNP/10/90 and A22 binders.	106
Table 4.5:	The 50% tissue culture infectious dose (TCID ₅₀) of A22 when neutralized by the A22 scFvs.	109
Table 4.6:	Virus titre, r ₁ values and percentage (%) ELISA reactivity observed for the SAT1 and SAT3 viruses tested when SAT1scFv1, SAT3scFv1 and SAT3scFv2 were used as detecting antibodies in a sandwich ELISA.	116
Table 4.7:	Collation of regions of entropy >1 for the SAT1 and SAT3 FMDV alignments for the outer capsid proteins.	127

LIST OF ABBREVIATIONS

α	alpha
A	absorbance
Å	angstrom
aa	amino acid
Ala or A	alanine
ARC	Agricultural Research Council
Arg or R	arginine
Asn or N	asparagine
Asp or D	aspartic acid
β	beta
B	bovine
BHK	baby hamster kidney
BME	Eagle's basal medium
bp	base pair
BSL3	biosecurity level 3
BTY	bovine thyroid
°C	degrees Celsius
<i>ca.</i>	<i>circa</i> (approximately)
CAV-9	coxsackievirus A9
cDNA	complementary deoxyribonucleic acid
CDR	complementary determining region
CHO	chinese hamster ovary
C _H	C-terminal constant heavy domain
CI	confidence interval
cm	centimetre
C _L	C-terminal constant light domain
CO ₂	carbon dioxide
CP	cattle passage
CPE	cytopathic effect
<i>cre</i>	<i>cis</i> -acting replication element
CRT	Calreticulin
CS	chondroitin sulphate
Cys or C	Cysteine
δ	delta
D	diversity
DC	dendritic cells
DIVA	differentiate between naturally infected and vaccinated animals
DS	dermatan sulphate
DNA	deoxyribonucleic acid
dNTP	deoxynucleoside-5'-triphosphate
DPI	days post infection
dsn	diagnostic sensitivity
dsp	diagnostic specificity
DRC	Democratic Republic of Congo
EA	East Africa
e.g.	exempli gratia (for example)
eIF	eukaryotic initiation factor
EDTA	ethylenediaminetetra-acetic acid
ELISA	enzyme-linked immunosorbent assay
ER	endoplasmic reticulum
EscM	escape mutant
<i>et al.</i>	<i>et alia</i> (and others)
EtBr	ethidium bromide

etc	et cetera
Fab	antigen binding fragment
FAO	Food and Agriculture Organization of the United Nations
Fc	Fragment crystallizable
FcR	Fc receptor
FBS	foetal bovine serum
Ff	filamentous phage
FMD	foot-and-mouth disease
FMDV	foot-and-mouth disease virus
Fv	fragment variable region
γ	gamma
<i>g</i>	gravitational force
GAG	glycosaminoglycan
GlcA	glucuronic acid
Gln or Q	Glutamine
Glu or E	Glutamic acid
Gly or G	Glycine
GMEM	Glasgow minimum essential medium
H	heavy
h	hour
HCl	hydrochloric acid
HEPES	4-(2-hydroxyethyl)-1-piperazineethanesulfonic acid
His or H	Histidine
HIV	human immunodeficiency virus
H ₂ O ₂	hydrogen peroxide
HRP	horseradish peroxidase
HS	heparan sulphate
H ₂ SO ₄	hydrogen peroxide
HSPG	heparan sulphate proteoglycan
HSV	herpes simplex virus
<i>i.e.</i>	<i>id est</i> (that is)
IdoA	iduronic acid
IB-RS-2 or RS	Instituto Biologico-Renal Suino-2
IFN	interferon
Ig	immunoglobulin
IGAD	Intergovernmental Authority on Development
IL	interleukin
Ile or I	isoleucine
ILK	Integrin-linked kinase
IPTG	isopropyl β -D-1-thiogalactopyranoside
IRES	internal ribosome entry site
J	joining
JMJD6	Jumonji C-domain containing protein 6
kb	kilobase pair
kcal	kilo calorie
kDA	kilodalton
κ	kappa
KGE	Lys-Gly-Glu
KNP	Kruger National Park
KS	keratin sulphate
λ	lambda
L	litre
LB	luria broth
LPBE	liquid-phase blocking enzyme-linked immunosorbent assay
L ^{pro}	leader proteinase

LAMP	loop-mediated isothermal amplification
LAK	lymphokine-activated killer
Leu or L	Leucine
LFD	lateral flow device
Lys or K	Lysine
M	Molar
mA	milliamperes
MAb	monoclonal antibody
MEMAlpha	Alpha minimum essential medium
ME-SA	Middle East-South Asia
MHC	major histocompatibility complex
µg	microgram
M	molar
mg	milligram
MgCl ₂	magnesium chloride
min	minutes
ml	millilitre
mm	millimetre
mM	millimolar
mRNA	messenger ribonucleic acid
N/A	not available or not applicable
ND	not done
NaCl	sodium chloride
NaN ₃	sodium azide
NCR	non-coding region
NHE	Na ⁺ /H ⁺ exchangers
NK	natural killer
nm	nanometre
nt	nucleotides
NSP	non-structural protein
OD	optical density
OIE	Office International des Epizooties
OP	oesophageal-pharyngeal
Or	origin of replication
ORF	open reading frame
OVR	Onderstepoort Veterinary Research
3D ^{pol}	3D polymerase (RNA-dependant RNA polymerase)
3C ^{pro}	3C proteinase
PAGE	polyacrylamide gel electrophoresis
PBMC	peripheral blood mononuclear cell
PBS	phosphate-buffered saline
PBS/T	1 × PBS containing 0.1% (v/v) Tween-20
PBS-0.05%T	1 × PBS containing 0.05% (v/v) Tween-20
PCP	progressive control pathway
PCR	polymerase chain reaction
PEG	polyethylene glycol
PG	proteoglycan
pH	potential of hydrogen
PFU	plaque forming units
Phe or F	Phenylalanine
PI	percentage inhibition
PK	pig kidney
Pro or P	Proline
PTBP	polypyrimidine tract-binding protein
RGD	Arg-Gly-Asp

RNA	ribonucleic acid
rpm	revolutions per minute
RPMI	Roswell Park Memorial Institute-1640 medium
RTK	receptor tyrosine kinases
RT-PCR	reverse transcriptase-polymerase chain reaction
s	seconds
SADC	Southern African Development Community
SAT	Southern African Territories
sc	single chain
SA	sialic acid
scFv	single chain variable fragment
SD	standard deviation
SDG	sucrose density gradient
SDS	sodium dodecyl sulphate
Ser or S	Serine
SPCE	Solid phase competition ELISA
TADP	Transboundary Animal Diseases Programme
TAE	Tris-acetate-EDTA
TCID ₅₀	50% tissue culture infective dose
TE	Tris-EDTA
TEMED	tetramethylethylenediamine
TFCAs	transfrontier conservation areas
Thr or T	Threonine
TNF	Tumor necrosis factor
TNE	Tris-NaCl-EDTA
TPB	tryptose phosphate broth
Tris	Tris-hydroxymethyl-aminomethane
TY	tryptone-yeast extract-NaCl
TYE	tryptone-yeast extract-NaCl-agar
Tyr or Y	Tyrosine
U	units
µg	microgram
µl	microlitre
µm	micrometre
UK	United Kingdom
USA	United States of America
UTR	untranslated region
V	variable
VDD	Vaccines and diagnostic development programme
v/v	volume per volume
Val or V	Valine
via	by way of
viz	videlicet “namely”
VGM	virus growth medium
V _H	N-terminal variable heavy domain
V _L	N-terminal variable light domain
VLN	FMDV vaccinated and LPBE negative
VLP	FMDV vaccinated and LPBE positive
VN	virus neutralization
VNT	virus neutralization test
VP	viral protein
VP _g	viral genome-linked protein
vRNA	viral RNA
w/v	weight per volume

CHAPTER 1

LITERATURE REVIEW

1.1 INTRODUCTION

Foot-and-mouth disease (FMD) is a highly infectious disease of livestock. All domestic and wild cloven-hoofed species such as the bovidae (cattle, zebu, domestic buffaloes, yaks), sheep, goats, swine and all wild ruminants are susceptible to FMD whereas camelidae (camels, dromedaries, llamas, vicunas) have low susceptibility to the disease (Thomson and Bastos 2004). The damaging effects of FMD on livestock production make FMD an economically important, debilitating disease. Despite all the information accumulated over the years on the disease and vaccine development, FMD still occurs extensively around the world and is one of the most transmissible animal diseases (Kitching 1998). Typically, when an animal becomes infected, most members of the herd or flock will also become infected. Outbreaks of the disease can result in high mortality of young animals due to myocarditis, as well as decreased production of milk and meat. The costs of eradication and control are enormous and trade restrictions could severely affect economies that are reliant on agricultural produce. These facts have led the World Organisation for Animal Health (OIE) to include FMD on its list of highly infectious diseases. Areas that are 'free' of FMD have been able to achieve freedom due to the maintenance of quarantine measures, vaccination and/or geographical isolation (Knowles and Samuel 2003).

1.2 FOOT-AND-MOUTH DISEASE VIRUS

The virus that causes FMD is the foot-and-mouth disease virus (FMDV). Loeffler and Frosch in 1897 demonstrated that a filterable infectious agent smaller than bacteria caused the disease and this was the first description of a virus producing an animal disease. FMDV belongs to the family *Picornaviridae* and is one of two members of the *Aphthovirus* genus. Equine rhinitis A virus is the only non-foot-and-mouth disease virus member of this genus (Pringle 1999). Replication of FMDV is prone to error such that viral populations consist of mutant spectra

(quasispecies) rather than a defined genomic sequence (Domingo *et al.*, 1985, 2002). Most variation occurs within the capsid-coding region of the FMD genome resulting in antigenic variation [reviewed in (Grubman and Baxt 2004)]. FMDV has a high potential for genetic and antigenic variation; this has led to the virus classification of seven immunologically distinct serotypes *i.e.* A, O, C, Asia1, the Southern African territories types: SAT1, SAT2 and SAT3. Serotypes O and A were identified by Vallee and Carre in 1922, whilst type C was identified by Waldmann and Trautwein in 1926 (Brooksby 1967). The other serotypes *i.e.* SAT1, SAT2, SAT3 and type Asia 1 was first described in Galloway *et al.*, 1948 and Brooksby 1967.

FMDV has a narrow pH stability range with the optimal pH between 7.2 and 7.6. At pH levels above 9 and below 6, the FMD virus capsid becomes unstable and the ribonucleoprotein is dissociated when FMDV is inactivated by acidification (Van Vlijmen *et al.*, 1998). The acid-lability of FMDV is vital for efficient viral uncoating and endocytic entry into the host cell. The virus can survive in lymph nodes and bone marrow at neutral pH, but it is destroyed in muscle when the pH is <6.0 *i.e.* after *rigor mortis*. FMDV survives best in aerosols and microdroplets, where relative humidity exceeds 60% (Alexandersen *et al.*, 2002).

1.3 EPIDEMIOLOGY OF FMDV

1.3.1 DISTRIBUTION

To date, the FMDV is still very active, however, the serotypes are not distributed uniformly around the world and areas that are FMD-free are investing enormous resources to maintain their status by implementing strict control measures especially regarding imports and exports of animals and animal products to prevent the occurrence of FMDV. Seven geographical FMDV pools have been described for endemic areas (Figure 1.1) (Rweyemamu *et al.*, 2008a; Paton *et al.*, 2009).

Pool 1 incorporates East Asia and South East Asia with serotypes O, A and Asia 1 being prevalent. Pool 2 involves the Indian subcontinent, which are the Southern Asian countries *i.e.* India, Nepal, Bhutan, Bangladesh and Sri Lanka where most of the outbreaks are a result of serotype O followed by serotype A and Asia 1 respectively (Sanyal *et al.*, 2010; Subramaniam *et al.*, 2013). The Middle East and Eurasia make up pool 3 and comprise outbreaks of serotypes A, O, Asia 1 and more recently the incursion of SAT2 (Jamal *et al.*, 2011).

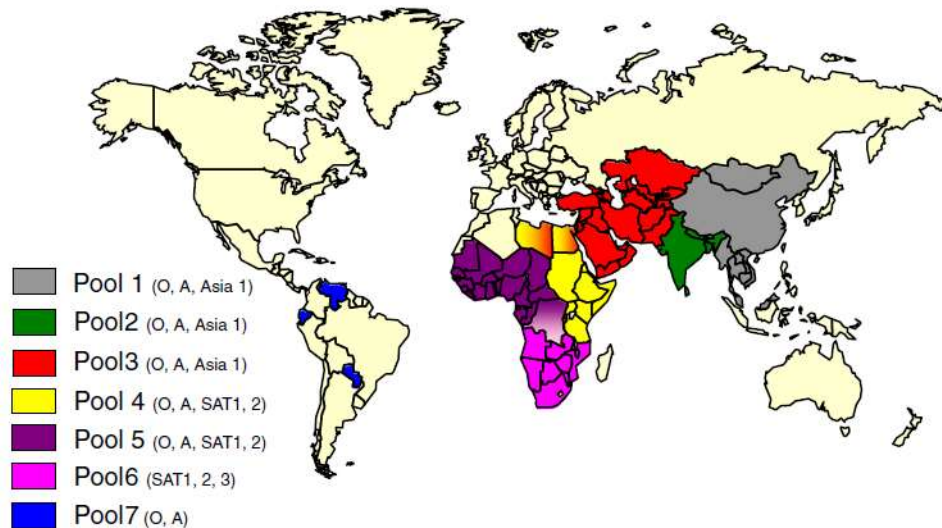


Figure 1.1: Geographical distribution of seven pools of Foot-and-mouth disease viruses. Taken from Jamal and Belsham (2013).

Pools 4, 5 and 6 include the endemic pools of Africa where pool 4 involves eastern and northern Africa (A, O, SAT1 and SAT2), pool 5 includes West and central Africa (A, O, SAT1 and SAT2) and pool 6 is southern Africa (SAT1, SAT2 and SAT3). Studies have shown that the SAT2 serotype is the most widely distributed SAT-serotype and is the cause of most of the outbreaks in wildlife and livestock whilst SAT1 is the second most distributed followed by SAT3 (Dyason 2010; Hall *et al.*, 2013). In South America, pool 7, small areas of the continent may still be considered as endemic but clinical cases are rare, in fact, FMD outbreaks that occurred in Venezuela in 2013 now represent the most recent confirmed FMD cases in South America. Serotype A and O, both belonging to toptotype Euro-SA make up pool 7. It is important to note that FMDV serotype C was last recorded in Kenya in 2004 (Sangula *et al.*, 2011).

1.3.2 EPIDEMIOLOGICAL PATTERNS FOR FMDV IN AFRICA

** Excerpts taken from co-authored article: Maree FF, Kasanga CJ, Scott KA, Opperman PA, **Chitray M**, Sangula AK, Sallu R, Sinkala Y, Wambura PN, King DP, Paton DJ, Rweyemamu MM. (2014). Review: Challenges and prospects for the control of foot-and-mouth disease: an African perspective. DovePress Journal: Veterinary Medicine: Research and Reports (5) 119–138.

Molecular epidemiology of FMDV has become fundamental in FMD research. Determining the nucleotide sequence of the viral ribonucleic acid (RNA) has enabled the characterization

of genetic relationships between strains and provides accurate evidence for epidemiological studies (Beck and Strohmaier, 1987; Samuel *et al.*, 1988). Epidemiological studies based on nucleotide sequence comparisons of FMDV show that if the number of differences in the sequences compared are large, then the virus strains are distantly related. The construction of phylogenetic trees results in visualising virus relationships. Using sequence data of the VP1 region, P1 region as well as the complete FMDV genome has become common to determine virus relationships. Molecular epidemiology based on nucleotide sequence determination has also been useful to successfully trace the origin of FMD outbreaks, inter-species transmissions as well as trans-continental introductions (Zadoks and Schukken, 2006) and overall aid in the control of FMD.

To understand the complexity of FMD epidemiology in Africa and to assist decision making and improve the continental control of FMD, it is important to further divide the virus pools into epidemiological clusters (Rweyemamu *et al.*, 2008a). Rweyemamu *et al.* (2008a) proposed eight epidemiological clusters for Africa based on the distribution of serotypes and topotypes in different regions in Africa, animal movement patterns, impact of wildlife and farming systems. The epidemiological clusters for Africa have the following characteristics:

Indian Ocean Island Countries (Madagascar, Mauritius, and Seychelles) are free of FMD, with a recognized status of FMD freedom without vaccination. The South Southern African Development Community (SADC) cluster includes Swaziland, Lesotho, South Africa, Botswana, and Namibia, the southern and western part of Zimbabwe, and the southern part of Mozambique. The commercial livestock sectors of South SADC countries, with the exception of Zimbabwe and Mozambique, are free from FMD and meet the conditions of the OIE for zonal or country freedom from FMD without vaccination. Over the last 5 years, the region has suffered from an increasing number of outbreaks in cattle, most of which has been caused by SAT2 viruses. Cross-border epidemiological events have occurred on a number of occasions in South SADC, and in some cases, outbreaks were caused by viruses from different topotypes. The epidemiology of FMD in this region is characterized by virus circulation between the wildlife host, the African buffalo, and domestic animals, as well as spread among domestic animals, without the involvement of wildlife (Thomson and Vosloo, 2004). In some of these countries, there are segregated wildlife areas that harbor African buffalo known to be infected, asymptotically, with FMDV serotypes SAT1, SAT2, and SAT3. These wildlife parks are segregated from livestock through a system of game-proof fencing and vigorous surveillance. In these countries, game ranching or other wildlife conservation activities with FMD-infected

African buffalo are not allowed within FMD-free zones. However, for this epidemiological cluster, the primary source of FMD seems to be the risk posed by the wild buffalo herds, (Sutmoller *et al.*, 2000; Hargreaves *et al.*, 2004) as evidenced by many outbreaks in or near transfrontier conservation areas (TFCAs), such as the Kavango-Zambezi TFCA (*Special FMD Bulletin: FMD Occurrence in Southern Africa Shows a Worrying Upward Trend with Unusual Patterns of Transboundary Spread*, 2011).

The North SADC cluster comprises the northern part of Zimbabwe, Zambia, northern Mozambique, Malawi, and southern Tanzania. The North SADC cluster countries have to deal with at least four serotypes of the virus (A, O, SAT1, and SAT2), and maybe even five (SAT3), each with multiple subtypes in the region. This may require the incorporation of more than one strain of a given serotype into a single vaccine to allow effective control in this region. Viral diversity and thus antigenic diversity is a complicating factor in effective vaccination against FMD in this cluster. Cross-border spread of the disease is common, and SAT1 and/or SAT2 outbreaks in Mozambique, Malawi, and Zambia between 2002 and 2013 were either because of outbreaks spreading from neighbouring countries or to internal buffalo–cattle contact. Northern Malawi and Northern Zambia are under constant threat of FMD spread from southern Tanzania (Rweyemamu *et al.*, 2008a; Kasanga *et al.*, 2012, 2015; Sinkala *et al.*, 2012).

The Angola cluster may also include the western Democratic Republic of Congo (DRC). Very little is known about the true incidence of FMD within this cluster, and no official information is available on the isolation of FMDV from Angola since 1974. However, an FMD outbreak has been recorded in Angola in 2009, although no virus could be isolated. The southern part of Angola forms part of the Kavango-Zambezi TFCA and it may be appropriate to include it within the South SADC cluster.

The East African Community cluster is comprised of Tanzania, Uganda, Kenya, Rwanda, and Burundi, plus the eastern part of the DRC. In addition to large livestock populations, this cluster has the highest concentration of wildlife in the world. The transmission and maintenance of FMD in this region is complex, as farming practices, trade, and wildlife contribute to the maintenance and spread of the virus. Farming is dominated by agro-pastoral and pastoral communities and is characterized by communal grazing and migrations. Eastern DRC is heavily dependent on trade in livestock from Uganda, Tanzania, Rwanda, and Burundi. The cluster probably contains several FMD primary endemic foci and cross-border epidemiological

events suggest that animal movement plays an important role in virus dissemination (Kasanga *et al.*, 2015). At least four serotypes (A, O, SAT1, and SAT2) are endemic in this cluster (Balinda *et al.*, 2010a; b; Kasanga *et al.*, 2012, 2015; Sangula *et al.*, 2010a; b) with serological evidence for a fifth serotype (C) (Sangula *et al.*, 2011). A sixth serotype (SAT3) was isolated in wildlife (African buffalo) in Uganda in 1970 (Hedger, 1972), although it has never been isolated from livestock in this cluster. SAT3 was also reported in Uganda in 1997 (Bastos *et al.*, 2003a; b) and in the DRC in 2005, but was not genotyped (Sumption *et al.*, 2008). Isolates of serotypes A, O, SAT1, and SAT2 from Tanzania and Kenya (2004–2009) were genetically related (Kasanga *et al.*, 2012, 2015). Similarly, viruses from Uganda and Kenya (1998–2008) were related (Balinda *et al.*, 2010b). FMDV isolates belonging to serotypes SAT1 (topotype IV) and SAT2 (topotype X) have been isolated from African buffalo (Ayebazibwe *et al.*, 2010a). As discussed above, there are also wide genetic and antigenic variations in the virus strains in this epidemiological cluster. The role of the African buffalo in the maintenance and transmission of FMD serotypes (e.g., A and O) (Ayebazibwe *et al.*, 2010b) that occur in this cluster has not been systematically studied.

The Intergovernmental Authority on Development (IGAD) cluster comprises Sudan, South Sudan, Eritrea, Ethiopia, Djibouti, Somalia, Northern Kenya, and Northern Uganda. Similar to the East African Community cluster, this cluster probably harbors major FMD primary endemic foci. Ethiopia and Sudan have the highest cattle populations in Africa (Rweyemamu *et al.*, 2008a). Historically, isolates of serotypes A, O, SAT1, and SAT2 from Sudan and Ethiopia were genetically related to isolates from Uganda, Kenya, and Tanzania, most likely as a result of cross-border movement, a situation that has not changed.

The Soudan/Sahel cluster comprises Western Sudan, Niger, Chad, Burkina Faso, Mali, Northern Nigeria, Senegal, and Mauritania. The farming system in this ecosystem is predominantly pastoral, characterized by long-distance movement of livestock due to either transhumance or trade. This cluster probably also contains important FMD primary endemic areas and at least four serotypes (A, O, SAT1, and SAT2) of the virus have been found. Furthermore, it may be an important disease-corridor cluster, linking the IGAD cluster with West Africa and probably West Africa with North Africa. The 1999 FMD strain in Algeria was found to be related to the West African type O topotype (Rweyemamu *et al.*, 2008a). Similarly, isolates of serotype O from Niger (2007) and Nigeria (2007 and 2009) were genetically related to viruses found in Eritrea (2004 and 2011), Ethiopia (2005, 2006, 2008, and 2010–2012), and

Sudan (2005, 2008–2011) (World Reference Lab reports 2005-2011). Viruses belonging to serotype A were isolated from cattle samples from Togo (2005), Nigeria (2009) in West Africa, and Cameroon (2005) in Central Africa, which had close genetic relationships with viruses from Eritrea (1998) and Sudan (2006 and 2011) in East Africa (World Reference Lab reports 2005-2011; Bronsvoort *et al.*, 2004a).

Although the epidemiology of FMD in the coastal belt countries of West and Central Africa has not been deeply studied, it seems that this cluster probably becomes infected from the Soudan/Sahel cluster. It could therefore be described as secondarily endemic. North Africa/Maghreb cluster countries Morocco, Algeria, and Tunisia have not reported FMD since 1999, most likely because of routine preventive vaccination and other measures. Libya and Egypt have sporadic FMD and take routine preventive vaccination. Libya reported a SAT2 outbreak in 2003 (topotype VII), probably as a result of live animal introductions from neighboring countries to the south, breaching the Sahara barrier. The virus was genetically related to outbreaks in cattle in Saudi Arabia in 2000 and Eritrea in 1998 (Valarcher *et al.*, 2004). In 2012, Libya experienced another SAT2 outbreak (topotype VII), this time genetically related to isolates from Sudan (2007) and Nigeria (2008). Egypt also reported a SAT2 outbreak in 2012, the first occurrence of this serotype since 1950, and at least three sub-lineages (one Libyan and two Egyptian) (Ahmed *et al.*, 2012) were identified. Egypt also reported African type A viruses in 2006, 2007, 2009, and 2012, as well as ME-SA (Middle East–South Asia) types O and A. Yemen reported EA (East Africa)-3 type O in 2007 and 2009. Thus, North African countries will remain at risk from the south and east, but across the majority of their territories and at-risk populations should effectively maintain FMD freedom.

1.3.3 THE ROLE OF CARRIERS IN THE EPIDEMIOLOGY OF FMDV

The epidemiology of FMD in Africa is influenced by two different patterns *i.e.* a cycle involving wildlife and a cycle that is independent of wildlife but maintained within domestic animals (Bengis *et al.*, 1986; Thomson *et al.*, 1992; Vosloo *et al.*, 2005; Michel and Bengis, 2012). The control of FMDV can be problematic especially with the existence of FMDV ‘carriers’. Carriers can be described as animals in which the virus persists in the pharyngeal region for more than four weeks after FMDV infection but do not show any clinical signs or symptoms of FMDV (persistently infected animals) (Salt 1993). Additionally, unvaccinated infected animals can become carriers and also, the carrier state is not caused by vaccination but

a vaccinated animal must be exposed to FMDV in order to become a carrier (Sutmoller *et al.*, 2003). More than 50% of ruminants can become carriers, whether they have been vaccinated or not (Alexandersen *et al.*, 2003). To date, the mechanism by which the carrier state is established and maintained is still unknown. Cattle, sheep and goats have been shown to be carriers for differing periods of time (Panina *et al.*, 1989). Pigs were shown to be non-carriers until a study by Carrillo *et al.* (2007) who showed that after 26 days of contact with FMDV infected animals; two pigs had become infected with FMDV but did not show any clinical symptoms indicating that the virus had persisted for four weeks, resembling the FMDV carrier state.

Africa is the only region where FMDV is maintained in wildlife *i.e.* the African buffaloes (*Syncerus caffer*), which can carry the virus for up to 5 years, act as maintenance hosts for all three of the FMDV SAT types (Condy *et al.*, 1985). This makes the eradication of FMDV in sub-Saharan Africa unattainable as these buffaloes have the ability to transmit the virus to other susceptible wild (e.g. impala) and domestic species that they may come into contact with in and around the Kruger National Park and other game reserves. In addition, the three FMDV SAT types normally infect buffalo calves when maternal immunity wanes, usually by the age of 6 to 12 months and during the acute infection stage, virus is excreted from the calves in almost equal quantities as cattle (Condy and Hedger, 1974; Thomson *et al.*, 1992; 2003). The FMDV carrier state provides a way for the virus to be maintained in nature, which may contribute to the emergence of new antigenically variant viruses due to the quasispecies dynamics of FMDV (Donaldson and Kitching, 1989; Domingo *et al.*, 2003).

1.3.4 TRANSMISSION OF FMD

The transmission of FMDV usually occurs by direct contact between susceptible animals and animals excreting virus during transport, markets, shows, etc. Indirect transmission occurs via contact with contaminated objects or materials or animal products. Farmers, veterinarians, vehicles etc. can also be a source of indirect contact. Airborne transmission is favoured by humid and cold weather, where virus aerosols can be carried by the wind (Donaldson, 1972). Three factors determine FMD transmission *i.e.* the quantity, duration and means by which the virus is released into the environment, the virus's ability to survive outside the host and the amount of virus required to initiate infection at the primary infection sites of animals that are exposed. A factor that plays a role in FMDV transmission is the stability of the virus under

suitable conditions e.g. cool temperatures, neutral or alkaline conditions or organic material protecting it from the environment (Sellers *et al.*, 1971). FMDV can survive outside the body of infected animals and can be preserved by refrigeration and freezing but at temperatures above 50°C it becomes inactivated. Charleston *et al.* (2011) investigated direct FMDV transmission and proposed that conditions conducive for transmission occurs for only a brief period. It was shown that infectiousness is complex and linked to virus dynamics as well as host responses and clinical signs (Charleston *et al.*, 2011; Chase-Topping *et al.*, 2013). Interestingly, detectable levels of virus in the air was associated to transmission although it was stated that this does not necessarily mean that air-borne spread is itself a major route of transmission (Chase-Topping *et al.*, 2013).

1.4 CONTROL AND ERADICATION OF FMDV

Due to the economic importance of FMD, control and ultimate eradication of FMD is the aim of various regions of the world. Some areas have managed to eradicate the disease but in large areas of Asia and Africa, FMD persists. Countries that are free of FMD are under threat of disease due to the often illegal international movement of animals and animal products. In endemically infected areas animals are usually vaccinated regularly with an inactivated vaccine to prevent outbreaks (Brown, 1999). FMDV that is incorporated into the vaccine is treated with an inactivant, which destroys viral infectivity but retains viral antigenicity (Brown, 1999). A vaccine can contain one or more strains of any of the FMD types depending on the area where it is used. Vaccines that are inactivated and purified cause the production of antibodies only against the viral structural proteins exposed on the virion surface *i.e.* VP1 – 3. Vaccinated animals do not produce antibodies against the FMDV non-structural proteins whereas vaccinated/non-vaccinated, infected animals do. Thus, this serves as a way to differentiate between a vaccinated and infected animal, which is useful to detect an outbreak or to declare a country free from FMD infection (Sobrino *et al.*, 2001; Barteling, 2002).

In countries usually free of FMD, the steps taken to maintain this status is through stringent zoo-sanitary measures. These include import controls on animals and animal products from FMD affected regions; rapid detection and culling of cases; locating the source of infection and potential spread as well as movement control of animals and contaminated materials and surveillance until freedom is re-gained. Endemic regions follow a similar process except policies involving vaccination and quarantine rather than slaughter of affected animals have

been adopted. In a country with a completely susceptible livestock population and as an alternative to mass culling, ring vaccination may be carried out. This involves the vaccination of all susceptible animals in a prescribed area around an outbreak. Success with ring vaccinations is dependant on how rapid FMDV is diagnosed and typed so that vaccination can be performed. Vaccines used in the control of FMD in endemic regions are mostly used for mass prophylactic application. Such vaccines are multivalent to provide protection against multiple serotypes, and should have a potency of at least 3 PD50 per dose (Rweyemamu *et al.*, 2006; 2008b). Inactivated vaccines induce short-lived immunity, and it is recommended that naïve animals receive two initial vaccinations (a primary and secondary dose) 3–4 weeks apart, followed by re-vaccination every 4–6 months (Cloete *et al.*, 2008; Hunter, 1998) to prevent spread of disease within populations. However, in the African environment, this may differ for different manufacturers, depending on the potency of the vaccine, and some manufacturers recommend five vaccinations per annum. There is a definite need to assess whether different adjuvants may enhance the duration of immunity against SAT antigens. For these reasons vaccination campaigns should be performed regularly, based on 1) the epidemiological circumstances and risk of disease spread, 2) the value and life expectancy of species, and 3) the economic status of the country. The interval between vaccinations is critical to prevent a “window of susceptibility” and where the continuous or sporadic presence of virus in carrier animals is present.

The control of FMDV in sub-Saharan Africa is difficult due to the occurrence of five of the seven FMDV serotypes, each with multiple antigenic sub-types where animals recovered from infection with one FMDV serotype or sub-type are susceptible to re-infection with any of the other five serotypes or sub-types within a serotype (Thomson, 1994). In addition to the vaccine-matching constraints, some viruses adapt with difficulty to cell culture, slowing the introduction of new vaccine strains, reducing vaccine yield and potentiating the selection of undesirable antigenic changes through prolonged passage (Sa-Carvalho *et al.*, 1997; Zhao *et al.*, 2003). Vaccination does not induce sterile immunity, and animals may still be able to infect non-vaccinated animals and may also become persistently infected (Sutmoller and Gaggero, 1965; Sutmoller *et al.*, 1967; Salt, 1993; Mackay *et al.*, 1998). In addition, the presence of the FMDV wildlife maintenance host, the African buffalo and the lack of controlled borders and animal movement in Africa contribute to the difficulty in achieving FMDV control in Africa. The creation and expansion of transfrontier conservation areas (TFCA) in southern and eastern Africa to enhance biodiversity conservation and improve economic benefits of nature-based

tourism and other related activities among rural communities living at the interface, presents a particular challenge to managing transboundary animal diseases (Brito *et al.*, 2016). The interaction between buffalo and livestock from surrounding communities has been described for some of the countries encompassed in these TFCA such as South Africa (Jori *et al.*, 2009; Abu Samra *et al.*, 2013), Zimbabwe (Caron *et al.*, 2013; Miguel *et al.*, 2013; Jori *et al.*, 2016), Botswana (Eyelaar *et al.*, 2015; Jori *et al.*, 2015), and Zambia (Sinkala *et al.*, 2014). Common areas for pasture and water are shared between rural communities living on the outskirts of TFCAs and with other livestock owners and wild animals. The boundaries of protected areas can be delimited by a physical barriers such as a veterinary cordon fence or a river, allowing occasional contacts between cattle and buffalo (Jori *et al.*, 2011). The veterinary cordon fence is to control the transmission of pathogens from wildlife to livestock and to mitigate human/wildlife conflict in wildlife areas (Jori *et al.*, 2011). However, the fence is not a steadfast barrier and although it has undergone several changes to improve its efficiency, the fence is exposed to various environmental and human pressures, including flooding, breaks due to wildlife movement, and damage due to component theft (Jori *et al.*, 2009). A joint Food and Agriculture Organization of the United Nations/ Office International des Epizooties (FAO/OIE) tool *i.e.* the progressive control pathway for foot-and-mouth disease (PCP-FMD) has been developed by the FAO to support and facilitate countries endemic for FMD to progressively reduce the impact of FMD and the load of FMD virus. This program was introduced in 2009 and endemic countries are showing improved development on their FMD PCP stages.

1.5 PATHOGENESIS OF THE DISEASE

Infection with FMDV can occur in a number of ways e.g. via inhalation, ingestion, iatrogenic or via damaged epithelia and contact with contaminated persons or objects (Sobrino *et al.*, 2001). All secretions and excretions of the infected animal contain high levels of virus but decline 4 – 5 days after infection due to the presence of FMD-specific antibodies (Bartley *et al.*, 2002). The primary route of infection by FMDV is via the upper respiratory tract where the virus shows a strong tropism for epithelial cells and the epithelial cells of the oropharynx and associated lymphoid tissues are the initial viral replication sites (Jackson *et al.*, 2000a; 2003, Arzt *et al.*, 2011; 2017). As the FMDV infection progresses in an animal, it disseminates throughout the body with secondary sites of replication in other epithelial tissues. Infection of an animal with FMDV results in a humoral response and the virus specific antibodies protect

an animal against re-infection or infection of the same or related virus (Grubman and Baxt, 2004).

FMD is characterized by high fever, salivation as well as lameness due to vesicular lesions and erosions on the feet. Vesicular lesions also occur on the snout and teats. The severity of the disease can vary depending on the infectious dose, the virus strain, the level of immunity and the species. FMDV infects various cloven-hoofed animals with a different degree of severity that can also vary between animals within the same species. The deterioration of the animal's body condition can lower animal productivity by 25%. The incubation period of the disease is *ca.* 3 – 14 days and virus excretion from infected animals begins before the development of clinical signs (Thomson, 1994). In cattle between 2 – 3 days post infection, it is observed that FMDV causes pyrexia, anorexia, shivering and a reduction in milk. Thereafter, due to the vesicles (aphthae) on buccal and nasal mucous membranes, between the claws and coronary band, the following occurs: smacking of lips, grinding of teeth, drooling, lameness and stamping or kicking of the feet. After 24-48 hours (depending on the FMD serotype), the vesicles rupture which result in erosions (Alexandersen *et al.*, 2002). The lesions that occur in infected sheep and goats are not very pronounced. Lesions occur on the dental pad of the sheep, but foot lesions are more common. The initial pyrexia phase may not be noticeable (Sáiz *et al.*, 2002). Pigs tend to develop severe foot lesions especially if they are kept on hard floors. There is usually a high mortality rate in piglets. Pigs are less susceptible to aerosol infection but excrete more virus in aerosols than do cattle (Quan *et al.*, 2004).

1.6 THE VIRION

FMDV is a non-enveloped virus containing a single-stranded ribonucleic acid (RNA) genome of positive polarity. The viral RNA is infectious, thus the virus particle serves to protect the genome while it is outside of cells and to aid the delivery of the RNA to the cytoplasm of the cell where infection can initiate. The surface of the virus particle is relatively smooth when compared to the other picornaviruses since it lacks peaks and depressions. The virus has a roughly spherical capsid, which results in icosahedral symmetry (Figure 1.2). The diameter of the virus is 23 ± 2 nm in diameter and the virion consists of *ca.* 70% protein, 30% RNA and a small amount of lipid (Bachrach *et al.*, 1964; Grubman *et al.*, 1979; Jamal and Belsham, 2013). The total weight of an infectious virion is *ca.* 8.5×10^6 Da. The viral protein coat consists of 60 copies of each of the four viral capsid proteins *i.e.* VP1, VP2, VP3 and VP4 (Parry *et al.*, 1989). VP1 to VP3 have molecular weights of *ca.* 30kDa, which form the external surface of the

icosahedral shell and constitute the bulk of the viral capsid (Vasquez *et al.*, 1979; Fry *et al.*, 1999). The small VP4, in conjunction with the amino termini of VP1 and VP2 form an interface between the capsid and the internal RNA genome. After cleavage of the structural precursor, P1, three polypeptides *i.e.* VP0 (precursor of VP4 and VP2 present in immature virions), VP1 and VP3 assemble into asymmetric units or protomers. VP0 is cleaved into VP4 and VP2 in the final stages of viral assembly (Pallansch *et al.*, 1984; Grubman and Baxt, 2004). This cleavage is considered autocatalytic and is observed during the encapsidation of RNA (Curry *et al.*, 1996). Five copies of VP1 are clustered around the 5-fold symmetry whilst VP2 and VP3 are positioned at the two- and three-fold axes of symmetry (Acharya *et al.*, 1990). Five protomers associate to form a pentamer and twelve pentamers enclose a newly synthesised RNA molecule to form a virus particle.

1.7 FMD VIRAL STRUCTURAL PROTEINS

VP1 - 3 have similar structural patterns, which consist of an eight-stranded β -barrel composed of two four stranded β -sheets (Figure 1.2). The loops that join these strands together with the C-termini of VP1 - 3 are exposed on the surface of the capsid. However, the N-termini are located facing its interior. The antigenicity of the viral particles is dependent on the amino acid residues that are exposed on the surface of the capsid (Mateu *et al.*, 1995; Usherwood and Nash 1995).

VP1 is comprised of *ca.* 213 residues in FMDV serotype O (Ferrer-Orta and Fita 2004). A disordered protrusion is present on the particle surface, which is situated between the β G and β H-strands of the capsid protein VP1, also known as the β G- β H loop (at residues *ca.* 141-161 in serotype O), which is a prominent feature of the virion. Two VP1 protein regions show the highest antigenicity *i.e.* the β G- β H loop (the virus major antigenic site) and residues 200-213 of the C-terminal end (a minor viral antigenic site). Within the β G- β H loop there is a conserved amino acid sequence *i.e.* Arg-Gly-Asp (RGD) at residues *ca.* 145 to 147. The RGD sequence has a dual function as it can recognize integrins that serve as cellular receptors for FMDV and in binding antibody (Mason *et al.*, 1994; Domingo *et al.*, 2002).

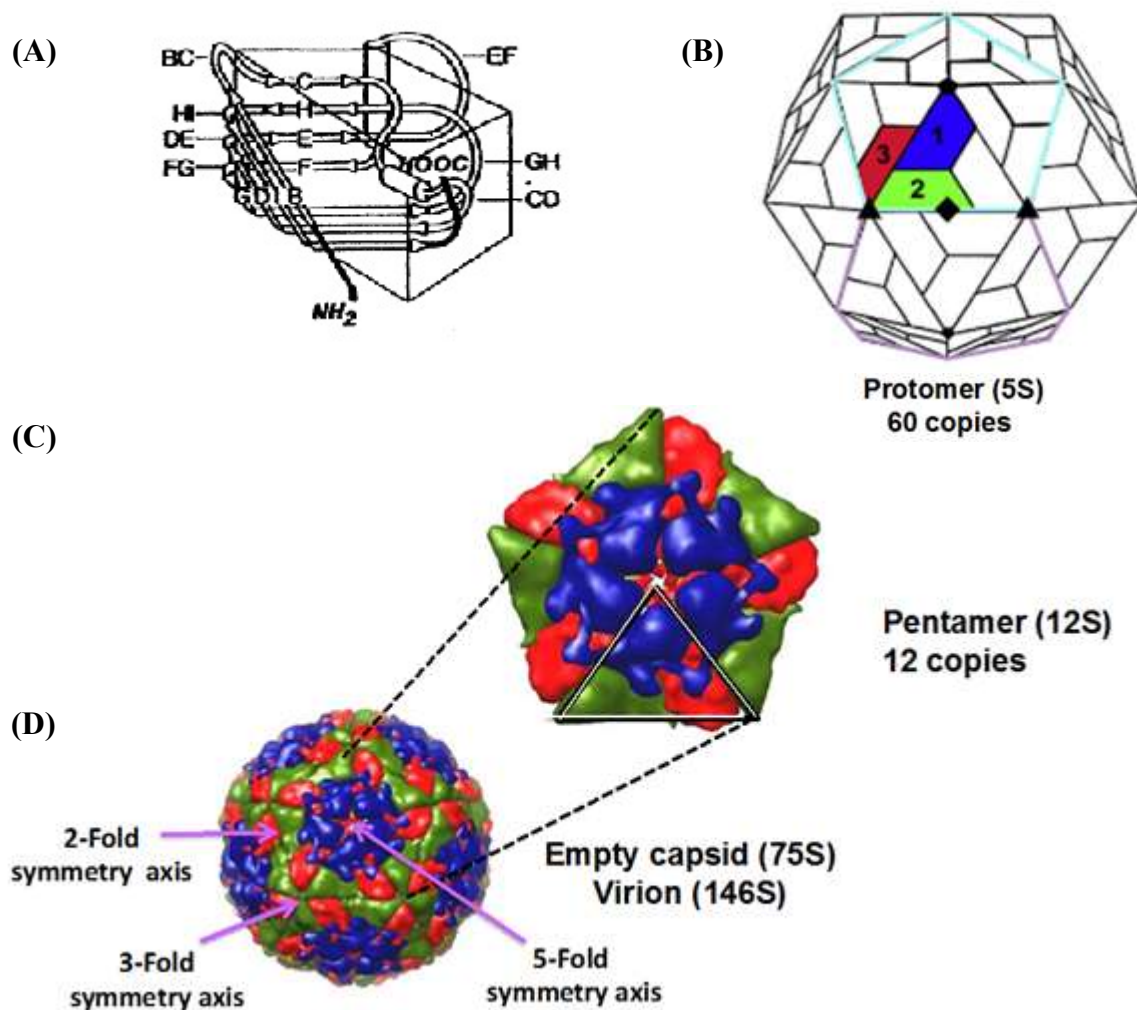


Figure 1.2: Schematic representation of the surface structure of FMDV capsid proteins, the subunits and the virus capsid. (A) Schematic, tertiary structure of VP1 (1D), VP2 (1B) and VP3 (1C). The eight β -strands are shown *i.e.* B, I, D, G, C, H, E and F. (B) Arrangement of VP1 – 3, the external capsid proteins, in a biological protomer. (C) The arrangement of five protomers making up a pentamer (a protomer is outlined). (D) Structure of the capsid, outlining the pentamer (in green). The two-fold, three-fold and five-fold axes are indicated. Adapted from Sobrino *et al.*, 2001 and Jamal and Belsham, 2013.

The flexibility of the loop and its loose connection to the capsid is due to the residues that lack secondary structure, which are found flanking the loop. A long ‘arm’ is formed with the 17 C-terminal residues of VP1, which is quite unique and is on the surface of the capsid and extends at a constant radius to the 5-fold axis from the VP1 of one sub-unit over VP3 (Acharya *et al.*, 1989).

In FMDV serotype O the VP2 protein is comprised of *ca.* 218 residues, whilst the VP3 protein is comprised of *ca.* 220 residues, the latter being the most conserved among the structural proteins of picornaviruses (Ferrer-Orta and Fita 2004). The association of the N-termini VP3

molecules form a five-stranded β -barrel at the 5-fold axis, which 'knits' the protomers into pentamers (Jackson *et al.*, 2003; Ferrer-Orta and Fita 2004). The VP4 protein varies considerably in length when compared to the other capsid proteins and is comprised of approximately 85 residues in serotype O (Ferrer-Orta and Fita 2004).

1.8 FMDV GENOME

The FMDV genome is a positive sense, single-stranded infectious RNA, where a single copy is contained within each virus particle (Belsham and Bostock 1988). FMDV viral RNA is approximately 8,500 nucleotides (nt) in length. A small virus-encoded peptide, VPg, is covalently attached to the 5' terminus and there is a genetically encoded polyriboadenylic acid or poly (A) tail at the 3' end. At the 5' end an untranslated region (UTR) of *ca.* 1,300nt is found followed by a large open reading frame (ORF) that is *ca.* 6,996 nt and a short 3' UTR of *ca.* 90nt (Figure 1.3).

The large ORF within the RNA encodes a single polypeptide, which is co- and post-translationally cleaved by viral proteases to give rise to the structural and non-structural proteins (Belsham 1993). There are four distinct regions in the FMDV polyprotein *i.e.* the Leader (L), P1 – 2A, P2 and P3. The polyprotein is processed in a series of proteolytic cleavage steps to give rise to the virion capsid proteins as well as other non-capsid viral proteins. There are two different sites on the RNA at which the initiation of protein synthesis occurs, which are responsible for generating two forms of L^{pro} (see section 1.5).

The P1 region is the viral capsid precursor and consists of the proteins 1A (VP4), 1B (VP2), 1C (VP3), 1D (VP1) and 2A (short oligopeptide). The L, P2 and P3 are precursors for the non-structural proteins. The non-structural proteins play a role in protein processing and RNA replication (Mason *et al.*, 2003). An S fragment is present within the 5' UTR (*ca.* 400nt long). The S-fragment is the name given to the smaller of the two RNA fragments, which are generated when viral RNA is treated with oligo(dG) and RNaseH (Rowlands *et al.*, 1978).

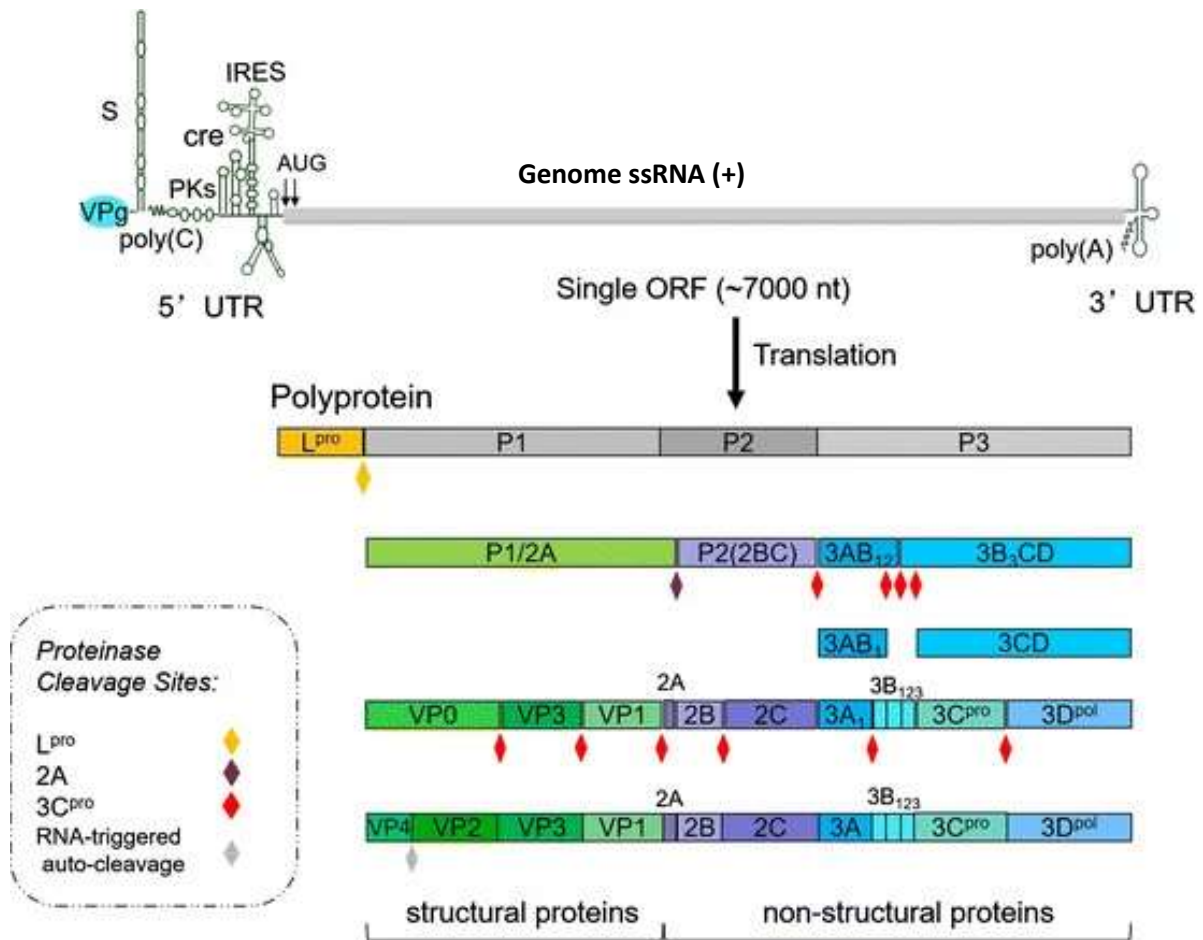


Figure 1.3: Map of the FMDV genome showing the functional elements of the genome as well as the protein cleavage products. Taken from (Gao *et al.*, 2016).

On the 3' end of the S-fragment there is a region containing cytidyl (C) residues (*ca.* 50 – 250nt), which is referred to as the polyribocytidylic or poly C tract (Mason *et al.*, 2003). Downstream of the poly C tract, a region of *ca.* 720nt, consisting of inverted repeats and predicted to form pseudoknots, occurs. The internal ribosomal entry site (IRES) of *ca.* 435nt long is highly structured and located several hundred nucleotides away from the 5' end of the genome (Clarke *et al.*, 1985; Domingo *et al.*, 2002).

1.9 VIRUS REPLICATION AND TRANSLATION

FMDV RNA has all the information required for the virus to take control of the host cell machinery. Entry of FMDV into host cells occurs by the virus attaching to viral receptors present on the host cell (Figure 1.4). The virus is then internalised by endocytosis to form an endosome (Madhus *et al.*, 1984a; 1984b). Once the virus is inside an endosome, the low pH environment triggers uncoating of the virus and the viral RNA is translocated across the

endosomal membrane into the cytosol (Jackson *et al.*, 1997; Fry *et al.*, 1999). The virus undergoes eclipse (initial part of infection, no complete virus particles present) and uncoating in a single step where the 146S virion degrades into 12S protein subunits and RNA (Baxt and Morgan 1985). The viral replication cycle occurs in the cytoplasm and polypeptide processing is via protease activity (Figure 1.4). However, before any viral processes can occur, the virus must inhibit certain host processes and redirect them into viral multiplication. Inhibition of host cell translation occurs by cleavage of p220 [220 000 dalton polypeptide component of the cap-binding protein complex (Etchison *et al.*, 1982)], which is induced by the L protein (Belsham, 1993).

Since the FMD RNA is a single-stranded plus sense RNA, it acts as a messenger RNA for the host cell translation machinery and as a template for RNA replication (Figure 1.4) via the viral RNA polymerase so that both viral RNA and virus proteins are produced (Belsham, 1993). These viral proteins are necessary for the formation of the RNA replication complex as well as to produce the capsid proteins that are required to form new virus particles. The synthesis of viral RNA occurs by the virus encoded RNA-dependant RNA polymerase (3D^{pol}). This process requires other viral proteins such as VPg (3B), which acts as the primer for RNA synthesis (Belsham and Martínez-Salas 2004). The IRES forms a secondary structure, which is able to bind ribosomes and deliver them directly to the polyprotein initiation codon in a cap-independent manner. Translation initiation factors involved in cap-dependent mRNA translation, such as the eukaryotic translation initiation factor, eIF-4B, and the cellular polypyrimidine tract-binding protein (PTBP), have been reported to play a role in stimulation of the internal translation initiation at the picornaviral IRES (Meyer *et al.*, 1995). Translation results in a single large polyprotein, which is cleaved into the FMDV structural and non-structural proteins.

Co-translational cleavage of the L/P1 junction (by L proteinase) occurs. The leader protein is a papain-like cysteine proteinase (L^{pro}), which cleaves between its C terminus and the N terminus of VP4. There are two forms of the L proteinase *i.e.* Lb and the less abundant Lab, where Lb is the truncated version, which arises after the initiation of translation at the second AUG start codon (Belsham, 1993). Lab and Lb can cleave the L/P1 junction and ensure the proteolytic degradation of the cellular cap-binding protein complex (eIF-4G), which results in the shutoff of host translation (Devaney *et al.*, 1988).

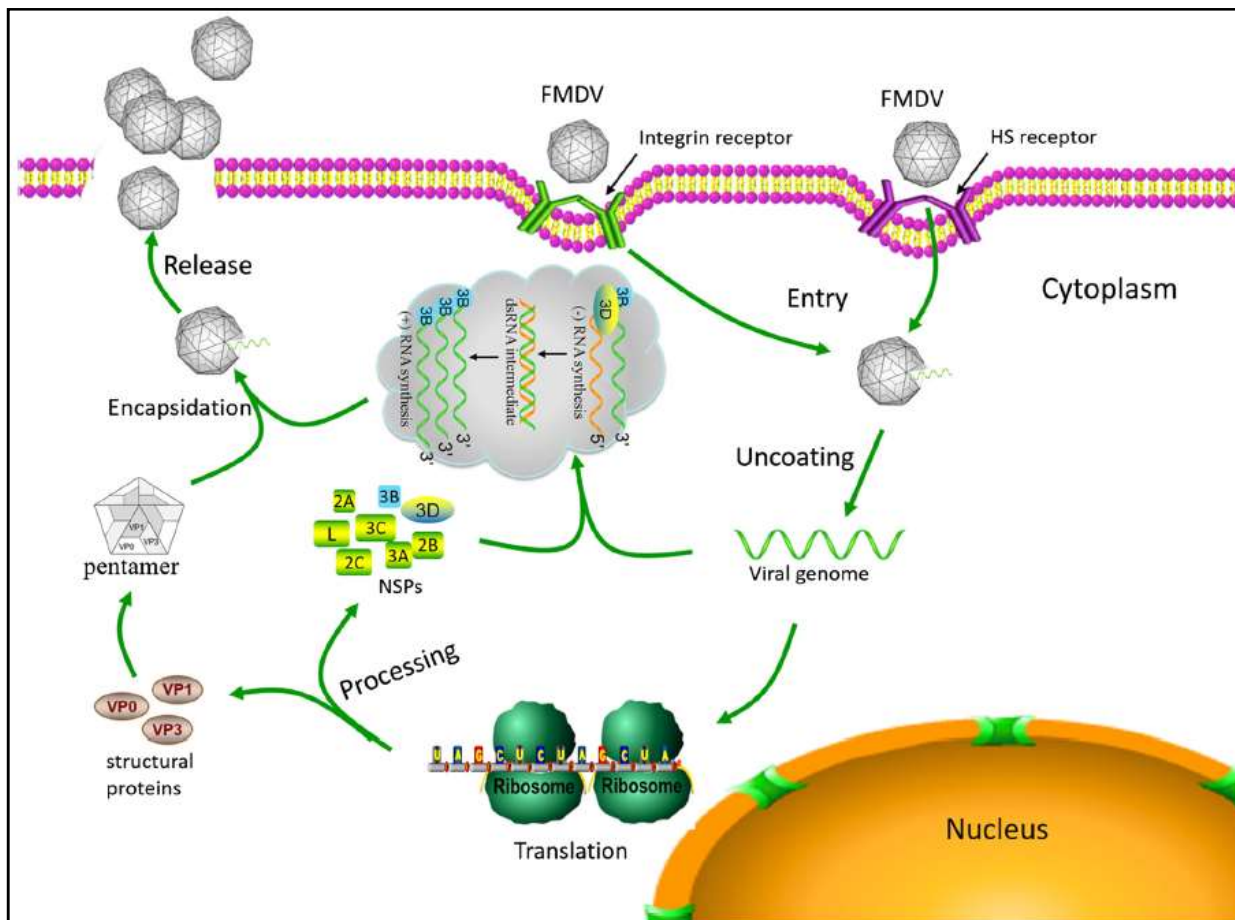


Figure 1.4: Diagram depicting FMDV replication and translation. Following entry of FMDV RNA into the cytoplasm of the cell, the RNA has to be translated to generate viral proteins required for viral RNA replication. HS is Heparan sulphate. NSPs is non-structural proteins. Green line is viral positive strand (+) RNA. Orange line is viral negative strand (-) RNA. Taken from (Gao *et al.*, 2016).

Thereafter, co-translational cleavage of the 2A/2B junction (by 2A) produces a P1-2A product. Post-translational cleavage of P1 via the 3C^{pro} viral protease produces VP0 (1AB), VP3 (1C) and VP1 (1D). The assembly of the virus involves the formation of capsid protomers where 5 protomers assemble into pentamers followed by packaging of the VPg-RNA to form provirions (Belsham, 1993). The final proteolytic cleavage, which is the final step in virion maturation, occurs at VP0 but only upon encapsidation of the RNA and produces VP2 and VP4 (Harber *et al.*, 1991). This is necessary to form infectious virus particles. The virions are then released from the host cell by lysis. Due to the absence of proofreading by the viral replicase, there are high levels of variation of FMDV types that arise from viral RNA replication, which is error prone (Domingo *et al.*, 2002).

The 2BC precursor of the P2 region is processed to 2B and 2C by the 3C^{pro} (Vakharia *et al.*, 1987). The functions of the 2B and 2C proteins are not well understood (Sobrino *et al.*, 2001), but they have a strong hydrophobic nature (Carrillo *et al.*, 2005) and are involved in many membrane bound activities at sites of FMDV replication in vesicles in the host cytoplasm (Grubman and Baxt, 2004). The 2C has been confirmed to have ATPase activity (Sweeney *et al.*, 2010). The 2B can be located in the endoplasmic reticulum (ER), the site of genome replication. The 2C can also be found to a lesser extent in the ER, however it is mostly located within the Golgi apparatus, in the membrane-associated virus replicating complexes. The 2BC complex blocks the mammalian protein secretory pathway by inhibiting host protein traffic between the ER and the Golgi apparatus (Moffat *et al.*, 2005; 2007). This interference in the secretory pathway could result in a decrease in the expression of the major histocompatibility complex (MHC) class I molecules on the surface of the infected cells thus hampering the host's cell mediated immune response (Grubman *et al.*, 2008). The 2BC complex in other picornaviruses increases membrane permeability (both the ER and cell membranes) eventually facilitating release of the virus progeny (Aldabe *et al.*, 1997; Van Kuppeveld *et al.*, 1997), while the 2C is implicated in virus encapsidation (Vance *et al.*, 1997).

The P3 region is separated from the P2 and processed by 3C^{pro} (Vakharia *et al.*, 1987) to yield the 3A peptide, three distinct copies of the 3B peptide (VPg), 3C^{pro} and 3D^{pol}, the RNA-dependent RNA polymerase. The 3C^{pro} is the major virus protease processing up to ten of the thirteen cleavage sites in the FMDV polyprotein (Bablanian and Grubman, 1993; Belsham, 2005). The 3C^{pro} also induces proteolytic processing of histone H3, which may inhibit the mammalian transcription process (Falk *et al.*, 1990). The 3C^{pro} initiates the cleavage of translation initiation factors eIF-4A (part of the cap-binding complex) and eIF-4G, making conditions unfavourable for normal mammalian translation (Belsham, 2005). The 3D^{pol} enzyme is necessary in replication (Newman *et al.*, 1979) and requires the uridylylated form of the 3B/VPg peptide to act as a primer (Nayak *et al.*, 2005; 2006). The function of the 3A protein is unclear in FMDV (Sobrino *et al.*, 2001; Domingo *et al.*, 2002) and heterogeneity of this protein has previously been associated to differences in pathogenesis and virulence among other genome factors (Girauda *et al.*, 1990; Knowles *et al.*, 2001; Nunez *et al.*, 2001; Maroudam *et al.*, 2010; Pacheco *et al.*, 2013). The 3A peptide is also hydrophobic in nature (Forss *et al.*, 1984; Carrillo *et al.*, 2005) and is found in association with the 3ABC complex in the perinuclear area of the cells enabling 3C cleavage of histones (Capozzo *et al.*, 2002). In

other picornaviruses, the 3AB complex delivers or anchors the 3B/VPg protein to the replication complex (Lama *et al.*, 1994; Towner *et al.*, 1996).

1.10 THE CELLULAR RECEPTORS OF FMDV

The FMDV life cycle pertaining to the virus-host interactions is researched extensively, however, although a lot of evidence has been gathered over the years, a vast amount of unknowns exists. Similar to other non-enveloped viruses, for FMDV to initiate infection, it needs to undergo host cell adsorption by attaching to the host cell surface and undergoing receptor-mediated endocytosis (Neff *et al.*, 1998). For FMDV, two families of cellular receptors have been identified *i.e.* integrins and heparan sulphate proteoglycans (HSPG) (Jackson *et al.*, 1996; 2003) to initiate infection by distinct endocytic pathways within the host cells. The use of integrin receptors for FMDV infection involves clathrin-mediated endocytosis (Neff *et al.*, 1998; Jackson *et al.*, 2002; 2004), whilst the virus can undertake another route *i.e.* caveola-mediated endocytosis for heparan sulphate receptor binding (O’ Donnell *et al.*, 2008; Ruiz-Sáenz *et al.*, 2009) (Figure 1.5). More recently, research has shown that FMDV can utilize a third group of “unknown” receptors for cell entry (refer to section 1.10.3).

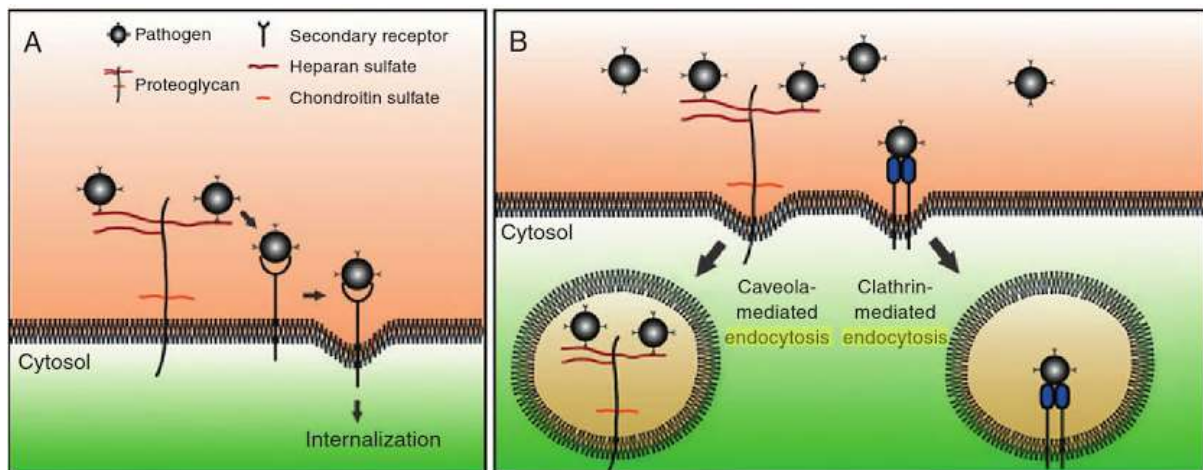


Figure 1.5: FMDV receptor endocytosis pathways. (A) The pathogen (virus) bind to glycosaminoglycans (GAGs) to increase their concentration on the cell surface and facilitate virus internalization. (B) FMDV can either enter cells via a caveola-mediated or clathrin-mediated endocytic pathway. Taken from (Yamaguchi *et al.*, 2010)

1.10.1 INTEGRIN-MEDIATED FMDV INFECTION

Integrins can be described as cell surface adhesion receptors and are type I membrane proteins (Hynes, 1992). These cellular receptors contribute to a number of important processes in

development and in adult organisms (Hynes, 1992). The integrins consist of α - β heterodimeric glycoproteins (Figure 1.6) and there are at least 18 α and 8 β subunits, which associate to form over 20 different combinations of α - β (Jackson *et al.*, 2000a). Each α subunit is noncovalently associated with a β subunit. A wide variety of cells express integrins and most cells express several integrins. Also, individual integrins can bind to more than one ligand and similarly, individual ligands are recognized by more than one integrin (Hynes, 1992). The first binding site to be defined as an integrin recognition site was the RGD sequence, which is present in fibronectin, vitronectin and other adhesive proteins (Hynes, 1992). The RGD sequence in the VP1 β G- β H loop is highly conserved in all FMDV serotypes and is involved in integrin binding (Fox *et al.*, 1989; Baxt and Becker, 1990; Knowles and Samuel, 2003). To date, only eight integrins have been found to bind to their ligands by recognizing the RGD motif viz $\alpha_V\beta_1$, $\alpha_V\beta_3$, $\alpha_V\beta_5$, $\alpha_V\beta_6$, $\alpha_V\beta_8$, $\alpha_5\beta_1$, $\alpha_8\beta_1$ and $\alpha_{IIb}\beta_3$ (Jackson *et al.*, 2000b). The specificity of the ligand binding of integrins is determined by the $\alpha\beta$ combination while the sequences flanking the RGD motif and its hypervariable characteristics are involved in determining both the binding specificity and affinity of integrins for their ligands (Pfaff *et al.*, 1994; Kunicki *et al.*, 1997). The amino acid changes immediately flanking the VP1 β G- β H loop RGD of FMDV have been shown to influence the ability of several FMDV serotypes to bind and infect cells in culture (Mason *et al.*, 1994; Mateu *et al.*, 1996; Leippert *et al.*, 1997). Both integrin subunits are transmembrane glycoproteins, each with a single hydrophobic transmembrane segment. Each subunit is composed of a large N-terminal extracellular domain, a smaller transmembrane region and in most cases a short cytoplasmic tail (50 amino acids or less) (Jackson *et al.*, 2004). All β subunits have a four-fold repeat of a cysteine-rich segment (Figure 1.6) (Calvete *et al.*, 1991).

1.10.1.1 INTEGRIN ACTIVATION

Integrins exist in at least two conformations *i.e.* active, where it is able to bind the ligand and inactive, where it is unable to bind the ligand. Changing from the inactive to active state occurs via ‘inside-out’ signalling or integrin activation, which involves two different mechanisms (Figure 1.7). The first mechanism is avidity modulation mediated by the clustering of heterodimers at the cell surface whilst the second mechanism is affinity modulation mediated via conformational changes in the integrin ectodomain (Jackson *et al.*, 2002).

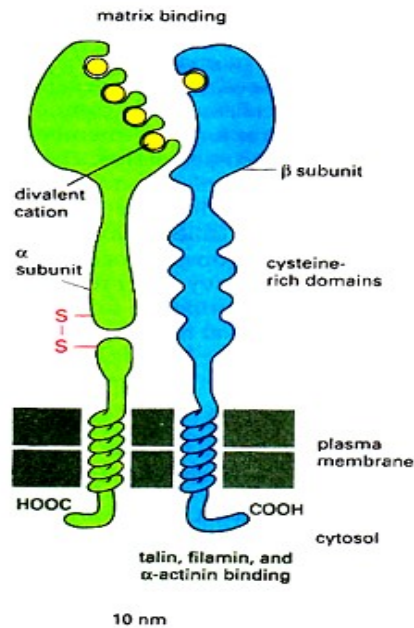


Figure 1.6: Diagram depicting the integrin α and β subunits. The putative locations of the cysteine-rich repeats of the β subunit as well as the extracellular, transmembrane and the intracellular domains are indicated. Taken from <https://rituparnas.wordpress.com/2016/03/14/cell-junctions-and-cell-adhesion/>

Integrin activation is energy dependant and cell type specific, which requires both α and β subunit cytoplasmic domains (O'Toole *et al.*, 1994). Both activation and inactivation of various integrins can be mediated from within cells. Although the exact mechanisms are not fully elucidated, presumptive evidence indicates that both of the integrin activation processes involve the cytoplasmic domains of the integrins, as well as cellular proteins (Hynes, 1992; O'Toole *et al.*, 1994).

1.10.1.2 FMDV INTEGRIN BINDING

Baxt *et al.* (1984) were able to deduce that the VP1 protein of FMDV acts as a carrier of major antigenic determinants and as the viral attachment protein, which reacts with the cellular receptor. Compared to the four viral proteins, VP1 is the outermost. Treatment of FMDV with trypsin results in the loss of FMD infectivity due to the Arg144 of VP1 cleavage, which results in non-infectious virus particles that are not able to bind to the cellular receptors (Fox *et al.*, 1989). This led to the suggestion that Arg144 of the VP1 β G- β H loop (serotype O) must play a role in virus attachment to the cellular receptor. Arg144 of VP1 for serotype A, O and C was demonstrated to be the attachment site of the virus to the host cell receptor (Baxt and Becker 1990). As described in section 1.10.1, it is not just the Arg144 position that is required for

integrin binding but the highly conserved Arg-Gly-Asp (RGD) motif. Due to virus evolution in cell culture, FMD viruses propagated in cell culture can utilize alternative pathways, independent of integrin-binding, to recognize and enter cells.

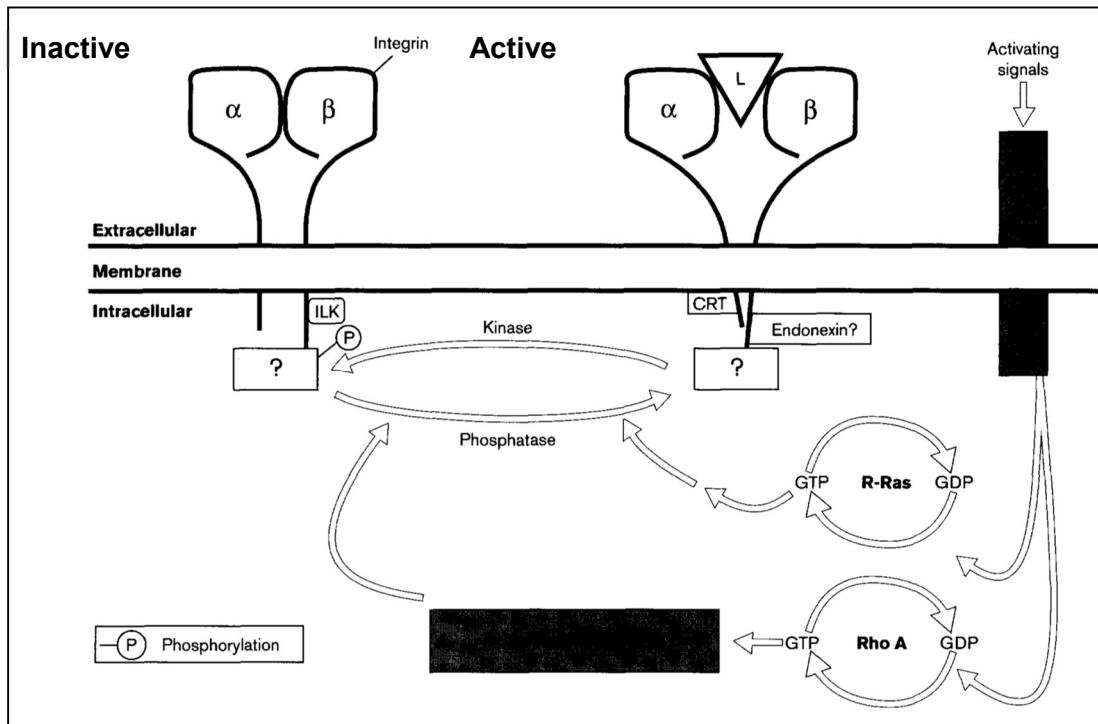


Figure 1.7: A schematic diagram representing currently postulated integrin-mediated ‘inside-out’ signaling. The activities of both protein (serine/threonine) kinases and phosphatases are involved in the signaling regulation. Phosphorylation/dephosphorylation of integrin cytoplasmic domains (no evidence yet) or of associated regulatory molecules (? in diagram), may allow for the interaction of other proteins (e.g. endonexin) with the integrin cytoplasmic domains. Calreticulin (CRT) associates only with the ‘active’ integrin form of α subunits, which are involved in the regulation of integrin-affinity states. Integrin-linked kinase (ILK) associates with the β integrin subunits and may play a role in regulating integrin-affinity states. The GTPases, R-ras and Rho A may be implicated in the regulation of integrin-affinity states [taken from (Dedhar and Hannigan, 1996)].

The RGD sequence in the VP1 β G- β H loop is highly conserved but the sequences flanking the RGD are hypervariable, which does not affect receptor binding (Stanway 1990). This introduces two important points:

- (i) The changes in the flanking RGD sequences result in mutations producing antigenic diversity without altering receptor binding.
- (ii) The specificity of binding to different integrins may be affected due to the changes in the flanking RGD sequences.

1.10.1.3 INTEGRINS IDENTIFIED FOR FMDV ATTACHMENT

(i) $\alpha_v\beta_3$

The first to be identified as the primary receptor for FMDV was the integrin $\alpha_v\beta_3$, also referred to as the vitronectin receptor (Berinstein *et al.*, 1995). Competition binding studies of coxsackievirus A9 (CAV-9) and FMDV in monkey kidney cells and baby hamster kidney cells (BHK-21) (Chang *et al.*, 1989; Roivainen *et al.*, 1994) as well as antibodies blocking the $\alpha_v\beta_3$ integrin (Berinstein *et al.*, 1995) suggested that FMDV could use $\alpha_v\beta_3$ as a receptor for entry in certain cells. In addition, studies by Neff *et al.* (1998), concluded that FMDV type A12 replication was dependent on expression of the integrin $\alpha_v\beta_3$. However, in cattle and pigs the expression of $\alpha_v\beta_3$ is in the epithelium of many organs such as the small intestine, kidney, endometrium, etc. Considering that the initial infection sites of FMDV are the lung and pharyngeal areas, it was thought that other integrins must be receptors for FMDV.

(ii) $\alpha_v\beta_6$

The expression of $\alpha_v\beta_6$ has been observed in many sites such as epithelia of the uterus, bladder, respiratory tract and salivary gland (Breuss *et al.*, 1995). This led Jackson and co-workers (2000a) to investigate if $\alpha_v\beta_6$ could act as a receptor for FMDV by transfecting the human colon carcinoma cell line to express $\alpha_v\beta_6$ at the cell surface and they found that these cells became susceptible to FMDV infection as a result of transfection with the β_6 subunit. In addition, it was shown that virus binding to $\alpha_v\beta_6$ and infection of the β_6 -transfected cells is RGD-dependent and this established $\alpha_v\beta_6$ as a cellular receptor for FMDV.

Miller *et al.*, 2001 demonstrated that the β_6 cytoplasmic domain is not required for virus binding; however, this domain is essential for infection, indicating a critical role in post-attachment events. Furthermore, it was shown that $\alpha_v\beta_6$ -mediated infection is dependent on active endosomal acidification, which implies that infection, mediated by $\alpha_v\beta_6$ most likely proceeds through endosomes (Miller *et al.*, 2001). Using immunofluorescence confocal microscopy and real-time RT-PCR, Monaghan *et al.* (2005), proved that integrin $\alpha_v\beta_6$ and not $\alpha_v\beta_3$ serves as a major receptor for cell entry, *in vivo*, and determines the tropism of FMDV for the epithelia normally targeted by this virus where $\alpha_v\beta_6$ is expressed constitutively at levels sufficient to allow initiation of infection.

(iii) $\alpha_V\beta_1$

Jackson and co-workers (2002) investigated whether $\alpha_V\beta_1$ could serve as a receptor for FMDV by transfecting Chinese hamster ovary cells (CHO-B2) cells (which are integrin deficient) to express two integrins *i.e.* $\alpha_V\beta_1$ and $\alpha_5\beta_1$. Since $\alpha_5\beta_1$ and $\alpha_V\beta_3$ was previously shown to not mediate infection by FMDV (Neff *et al.*, 1998; Jackson *et al.*, 2000b), the results proved that FMDV infection occurred with the CHO-B2 cells utilizing the $\alpha_V\beta_1$ receptor. It was also shown that $\alpha_V\beta_1$ serves as a major receptor for FMDV serotype O attachment on CHO-B2 cells, since virus binding was inhibited >98% by a function-blocking monoclonal antibody (MAb). Furthermore, RGD-containing peptides were shown to specifically inhibit virus attachment and infection mediated by $\alpha_V\beta_1$ (Jackson *et al.*, 2002).

(iv) $\alpha_V\beta_8$

SW480 cells stably transfected with integrin β_8 complementary DNA (cDNA) resulted in the expression of $\alpha_V\beta_8$ at the cell surface and competition experiments demonstrated that virus binding and infection are inhibited by function-blocking MAbs specific for the $\alpha_V\beta_8$ heterodimer or the α_V chain confirming that the $\alpha_V\beta_8$ receptor was also used by FMD virus for infection (Jackson *et al.*, 2004).

(v) $\alpha_5\beta_1$

Another integrin known to bind to the ligands through the RGD motif and are expressed on epithelial and lymphoid cells is the $\alpha_5\beta_1$ (Ruoslahti, 1996). However, not all the FMD viruses having the RGD motif is able to bind all the integrins to initiate infection and the $\alpha_5\beta_1$ has repeatedly been negative for FMDV in this regard (Baranowski *et al.*, 2000; Jackson *et al.*, 2000a; Duque and Baxt, 2003). Jackson and co-workers (2000a) used a solid-phase receptor-binding assay where the binding of FMDV to purified samples of the human integrin $\alpha_5\beta_1$ was investigated when the heparan sulphate and other RGD-binding integrins were absent. It was found that the binding of FMDV resembled authentic ligand binding to $\alpha_5\beta_1$ based on its dependence on divalent cations and specific inhibition by RGD peptides (Jackson *et al.*, 2000a). This binding was dependant on the conformation of the integrin, which occurred after induction of the high-affinity ligand-binding state. In addition, the ability of FMDV serotype O to bind integrins $\alpha_5\beta_1$ and $\alpha_V\beta_3$ has been shown to be influenced by the amino acid residues immediately following the β_G - β_H loop RGD motif (Jackson *et al.*, 2000a). FMD viruses that have a leucine residue following the RGD motif can serve as ligands for both $\alpha_5\beta_1$ and $\alpha_V\beta_3$,

whereas those that have an arginine residue at this position serve as better ligands for $\alpha v\beta 3$ but become poor ligands for $\alpha 5\beta 1$ (Jackson *et al.*, 2000a).

1.10.1.4 SUMMARY OF FMDV INTEGRIN RECEPTORS

The efficiency with which a receptor is used is dependent upon the FMD viral serotype and structural difference on the viral surface (Duque *et al.*, 2004). Duque and Baxt (2003) showed that FMDV type O viruses used $\alpha v\beta 6$ with the highest efficiency, following in descending order by $\alpha v\beta 1$, $\alpha v\beta 3$ and $\alpha v\beta 5$. In addition, type A viruses used $\alpha v\beta 3$ with a high efficiency and $\alpha v\beta 6$ with either an equal or lesser efficiency. The FMDV type A₂₄ Cruzeiro used $\alpha v\beta 1$ with a low efficiency. Overall, it was concluded that all FMDV type A and O viruses used $\alpha v\beta 5$ with low efficiency and that FMDV type O1 uses $\alpha v\beta 6$ and $\alpha v\beta 1$ as receptors *in vitro* (Duque and Baxt, 2003). Maree and co-workers (2013) showed that FMDV SAT2 was able to infect and replicate in COS cells expressing the $\alpha v\beta 6$ integrins but displayed poor infectivity of cells expressing $\alpha v\beta 3$, which is in agreement with the low affinity of type O1 viruses for $\alpha v\beta 3$ (Neff *et al.*, 2000; Jackson *et al.*, 2002; Burman *et al.*, 2006).

1.10.2 HEPARAN SULPHATE (HS):

Proteoglycans (PGs) are sulphated macromolecules composed of glycosaminoglycan (GAG) chains covalently bound to a protein core (Figure 1.8). PGs are widely distributed in animal tissues and appear to be synthesized by almost all cell types. The GAG components consist of hexosamine [D-glucosamine (GlcN) or D-galactosamine] and either hexuronic acid [D-glucuronic acid (GlcA)] or L-iduronic acid (IdoA), which carry random patterns of sulphation and are negatively charged (Jackson *et al.*, 2003). The common GAGs include the galactosaminoglycans *i.e.* chondroitin sulphate (CS) and dermatan sulphate (DS), and the glucosaminoglycans *i.e.* heparan sulphate (HS) and keratan sulphate (KS). Another receptor implicated in FMDV cell adhesion is HS. HSPG has a complex heterogeneous structure and the biological activities modulated by the interaction of proteins to HS include cell recognition, cell proliferation, cell differentiation, cell migration, cell survival, defense mechanism, endocytosis etc. (Fry *et al.*, 1999; Dreyfuss *et al.*, 2009).

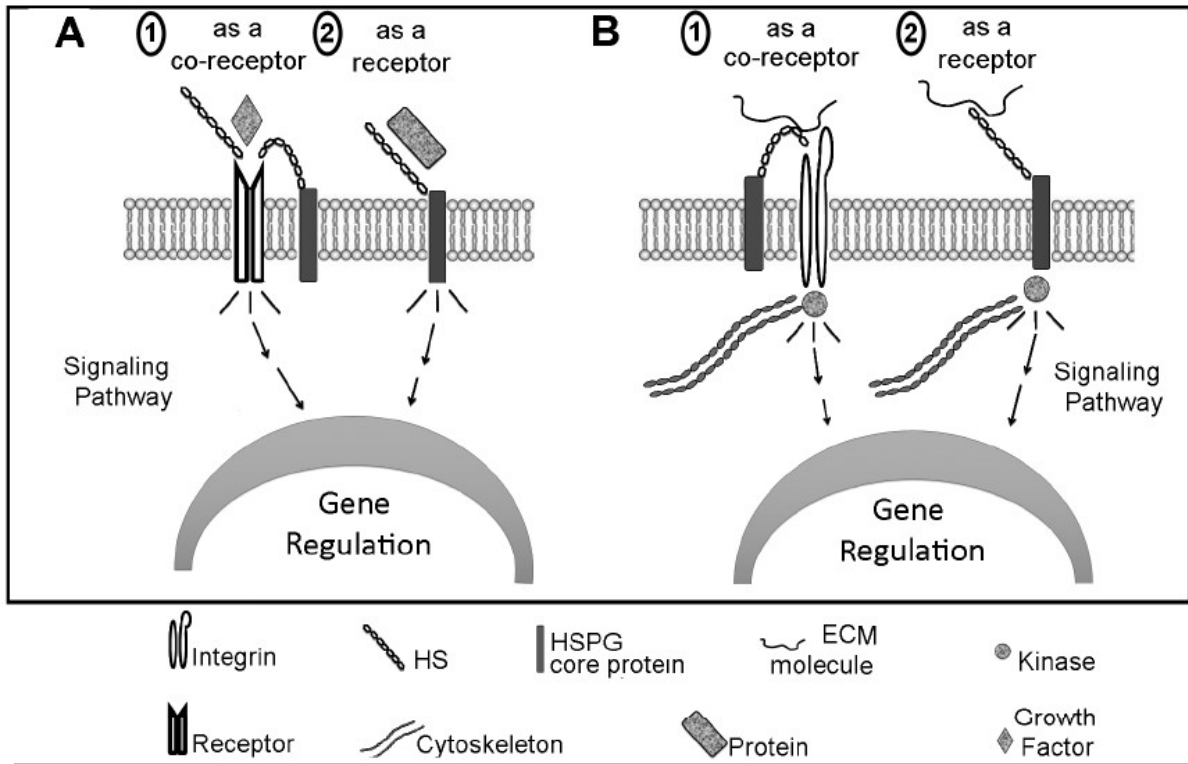


Figure 1.8: Heparan sulphate proteoglycan cell signalling features. Cellular responses are triggered by HSPG through signal transduction pathways where HSPG is a receptor or co-receptor in a cytoskeleton independent (A) or dependant (B) manner. Taken from (Dreyfuss *et al.*, 2009).

HSPG was originally thought to be a co-receptor for the O-type viruses during cell entry (Jackson *et al.*, 1996). Subsequently, FMDV serotypes O, A, C, Asia1 and SAT1 have been shown to bind HSPGs (Baranowski *et al.*, 1998; 2000; Jackson *et al.*, 1996; Maree *et al.*, 2011). The FMDV type O virus O₁BFS was the first FMD virus identified as being able to use HSPG as cellular receptors (Jackson *et al.*, 1996) while certain strains of FMDV O1 use HSPG as the predominant receptor. Adaptation of FMDV to cell culture can result in the selection of virus variants that have a high affinity for HS and a single amino acid change can alter receptor usage (Jackson *et al.*, 1996; Sa-Carvalho *et al.*, 1997). This is true for FMDV type O viruses, which bind to HSPG in cell culture due to the substitution of an histidine for an arginine at position 56 of VP3 (Sa-Carvalho *et al.*, 1997; Fry *et al.*, 1999). The additional positive charge on the surface of the virion could mediate electrostatic binding to HS, which is negatively charged (Sa-Carvalho *et al.*, 1997). Sulphated heparan is thought to bind to a shallow depression of the FMDV subtype O1 protomer, making contact with all three major capsid proteins (Fry *et al.*, 1999). The integrin recognition site is unaffected by heparan binding and the two receptor binding sites appear to be independent of each other (Baranowski *et al.*, 2000). However,

(Jackson *et al.*, 1996), suggested that HSPG was the first step to virus-cell interaction followed by virus-integrin interaction. Studies have shown the HS receptor mediated FMDV infection by utilizing the caveola-dependant endocytosis pathway (Ruiz-Sáenz *et al.*, 2009; O' Donnell *et al.*, 2008). The functional relation between HSPG and integrin receptors remains lacking as different FMDV strains can use different receptors. Studies have led to the belief that HSPG might be a replacement receptor for FMDV or an alternative pathway for entry into cells after virus infection (Baranowski *et al.*, 1998).

1.10.3 THIRD GROUP OF “UNKNOWN” FMDV RECEPTORS

FMDV investigations have led to the belief that there are a third group of cellular receptors for FMDV cell entry. Besides binding directly to cellular receptors, some viruses are able to infect cells through the an antibody receptor involved in antigen recognition, which is located at the membrane of certain immune cells *i.e.* the Fc receptor (FcR), in the presence of virus-specific antibodies (FcR-mediated adsorption) (Peiris *et al.*, 1981; Schlesinger and Brandriss, 1981; Takeda *et al.*, 1988). Mason *et al.* (1994) first reported that genetically engineered FMD viruses, lacking the RGD binding site, can infect CHO cells expressing the immunoglobulin Fc receptor, which was later confirmed by Baxt and Mason (1995), where FMDV was able to infect macrophages via FcR-mediated adsorption. These studies suggests that the natural receptor for FMDV may only serve in docking the virus to cells and that actual uptake by susceptible cells can be dissociated from binding (Rieder *et al.*, 1996). Based on this theory, Rieder *et al.* (1996) proposed that the functional FMDV receptor could be obtained by joining the antigen binding domain of an FMDV-specific antibody molecule to a cell-surface molecule. Thus, the first study to demonstrate a synthetic virus cell-surface receptor was by Rieder *et al.* (1996) where it was shown that a new receptor was generated by fusing a virus-binding, single chain antibody to intracellular adhesion molecule 1. Interestingly, cells that were not normally susceptible to FMDV infection became infected once treated with DNA encoding the single chain antibody/intracellular adhesion molecule 1 protein and RGD-deleted virions that were non-infectious in animals and other cell types grew to high titres and formed plaques on these cells (Rieder *et al.*, 1996).

Baranowski *et al.* (2000) showed that recombinant FMDVs that had a change at the integrin recognition RGD motif and did not require binding to HSPG was viable and able to replicate in human K-562 cells. Thus, the use of integrin $\alpha v \beta_3$ and the alternate HSPG receptor was

absent but through an unknown alternative, replication was possible. Another study showed that a mutant FMDV virus was able to replicate in cultured cells, even after the RGD sequence was artificially mutated to a Lys-Gly-Glu (KGE) and HSPG as well as integrin utilization was ruled out suggesting multiple receptors and viral components being involved for mediating FMDV infection (Zhao *et al.*, 2003). A variant of the A/IRN/2/87 (called A/IRN/87/A-) was shown to retain its infectivity in cattle even though it had a major VP1 β G- β H loop deletion that resulted in the loss of integrin binding (Fowler *et al.*, 2010; 2014). Additionally, this variant virus was shown to infect CHO-K1 cells (lacks the FMDV integrin but has HSPG) as well as the HSPG-deficient cell line, CHO-677, indicating unknown receptor use (Chamberlain *et al.*, 2015). Berryman *et al.* (2013) confirmed the presence of a non-integrin non-HSPG receptor being utilized by FMDV on CHO cells in addition to discovering a novel non-RGD-dependant use of α v β ₆.

In another study, a soluble integrin-resistant FMDV that acquired capsid mutations was able to adapt to HSPG deficient cell line CHO-677 and upon investigation, it was found that this virus had increased affinity to membrane-bound Jumonji C-domain containing protein 6 (JMJD6) (Lawrence *et al.*, 2016a). When cells were pre-treated with N- and C- terminal JMJD6 antibodies or by concurrent incubation of mutant virus and JMJD6, impaired virus infectivity was observed in cultured cells although this was not the case when treated with HS or α v β ₆ (Lawrence *et al.*, 2016a). The results indicate that JMJD6 contributes to FMDV infectivity and may be a previously unidentified receptor when certain VP1 mutations are present (Lawrence *et al.*, 2016a). In a follow-up study, chemical uptake inhibitors showed that *in vitro*, the JMJD6-FMDV complexes entered cells via clathrin-mediated endocytosis whilst *in vivo* the JMJD6-FMDV exhibited a preference for JMJD6⁺ cells (Lawrence *et al.*, 2016b). Thus, the availability of this alternate receptor may likely be dependent on the route of inoculation (Lawrence *et al.*, 2016b).

In addition to FMDV being shown to utilize the clathrin and/or caveola-mediated endocytosis pathways, a recent study shows evidence for the use of the macropinocytosis pathway by FMDV to invade cells (Han *et al.*, 2016). In this study, FMDV was observed to enter host cells by macropinocytosis and the clathrin-mediated pathway. Macropinocytosis varies from other pinocytotic pathways in that after the virus binds to the cell membrane, activating receptor tyrosine kinases (RTK) or other signalling molecules, which further activate the intracellular multi-branched signalling cascades (Han *et al.*, 2016). The proposed macropinocytotic pathway

(Figure 1.9) involves the binding of FMDV to the cell membrane, activating RTKs, which may result in the activation of cellular actin modulators *i.e.* Rac1, Pak1, PKC and other factors such as NHEs and dynamin which in turn triggers actin rearrangement and plasma membrane ruffling (Han *et al.*, 2016). The virions internalise into macropinosomes and intracellular trafficking occurs, the details thereafter are indicated in Figure 1.9.

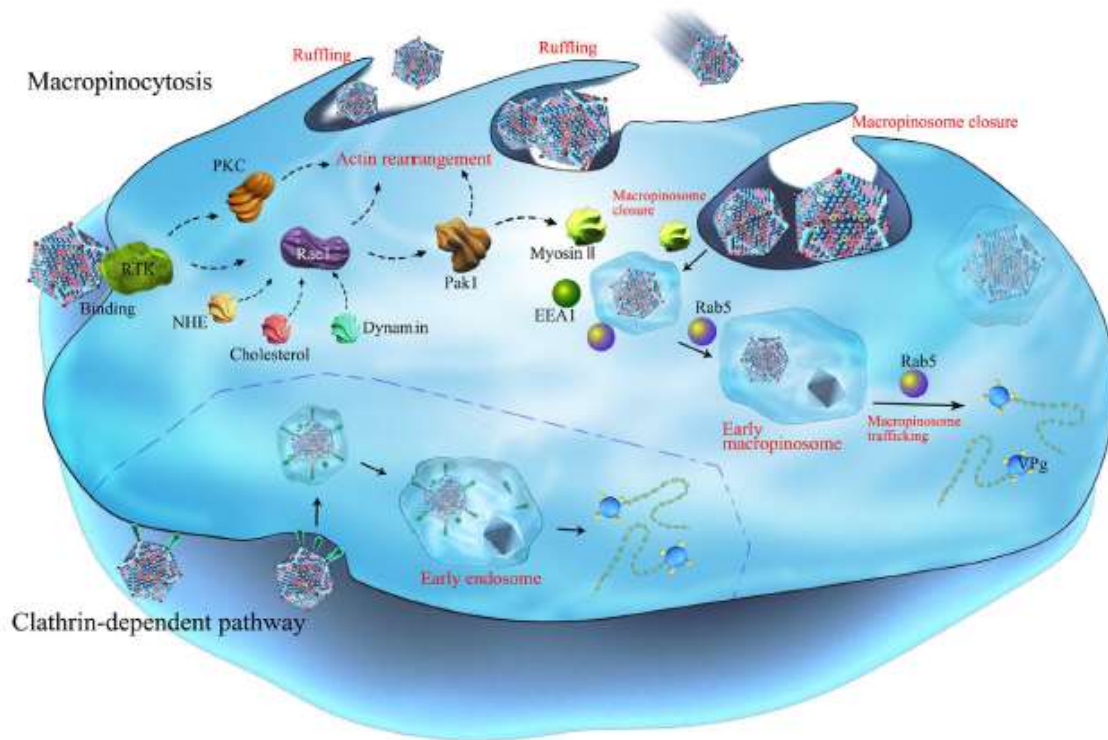


Figure 1.9: Model of the FMDV macropinocytic internalization pathway. Binding of FMDV to receptor tyrosine kinases (RTKs) may activate cellular actin modulators (Rac1, Pak1, and PKC) and other factors, such as NHEs (sodium-hydrogen exchanger) and dynamin. This starts actin rearrangement and plasma membrane ruffling. Internalisation of the virions occur into macropinosomes and the membrane fission events that separate the macropinosomes from the extracellular space occur in a myosin II-dependent manner. After closure, the early macropinosomes containing FMDV acquire Rab5 (Ras-related protein, a regulatory guanosine triphosphatase) and EEA1 (early endosomal autoantigen 1), which facilitate intracellular trafficking. The acidic pH of macropinosomes may trigger viral uncoating. As an alternative entry route of FMDV, virion binding to integrin receptors induces viral internalization via CME. The internalized vesicle is then delivered to early endosomes, and the endosomal acidic pH triggers viral uncoating. Taken from (Han *et al.*, 2016).

1.11 DESIGN OF IMPROVED INACTIVATED VACCINES

** Taken from co-authored article: Maree FF, Kasanga CJ, Scott KA, Opperman PA, **Chitray M**, Sangula AK, Sallu R, Sinkala Y, Wambura PN, King DP, Paton DJ, Rweyemamu MM. (2014). Review: Challenges and prospects for the control of foot-and-mouth disease: an African perspective. *DovePress Journal: Veterinary Medicine: Research and Reports* (5) 119–138.

The development of reverse genetic approaches provide promising advances for FMDV vaccines. Additionally, new alternative vaccines that do not require infectious virus as well as efforts to understand the role of innate immunity and cytokines to induce protection and boost the immune response offer tremendous potential for the control of FMD in endemic regions. Genome-length viral RNA (vRNA) derived from cDNA clones of FMDV is infectious when transfected into suitable mammalian cells (Zibert *et al.*, 1990; Rieder *et al.*, 1994; Almeida *et al.*, 1998; Van Rensburg *et al.*, 2004). These cDNA clones are readily amenable to genetic engineering to introduce changes to the virus genome that allows for the replacement of the external capsid-coding region or structural, surface-exposed antigenic loops with the corresponding regions of an emerging virus. The outcome of such a chimeric virus is the transfer of the spectrum of neutralizing epitopes from the etiological agent to the recombinant virus (Zibert *et al.*, 1990; Rieder *et al.*, 1994; Almeida *et al.*, 1998; Van Rensburg *et al.*, 2002; 2004) and the ability to antigenically simulate the outbreak virus and induce protective immunity in host animals (Rieder *et al.*, 1994; Maree *et al.*, 2010; Blignaut *et al.*, 2011). Furthermore, it has been shown that inter-serotype chimeric vaccines with the capsid proteins of SAT1 within a SAT2 background (Blignaut *et al.*, 2011) and O serotype within an A serotype background (Rieder *et al.*, 1994; Fowler *et al.*, 2008) confer protective immunity. However, capsid swapping may transfer other undesirable traits such as capsid instability and poor cell culture adaptation, which are limitations that can be overcome by site-directed mutagenesis of the amino acid(s) associated with improved performance for FMDV vaccine candidate strains (Maree *et al.*, 2010).

The development of new FMDV vaccine strains relies strongly on virus growth and high antigen yields of the new strain in the production cell line (Pay and Rweyemamu, 1978; Preston, *et al.*, 1982; Doel, 2003). We have demonstrated that SAT-type viruses, previously impossible to adapt to cell culture, can be structurally modified by introducing an adaptation

phenotype which is able to interact with sulphated glycosaminoglycans, enabling improved vaccine production (Maree *et al.*, 2010). Several glycosaminoglycan-binding sites have been identified for the various serotypes that can be used for this purpose (Rieder *et al.*, 1994; Jackson *et al.*, 1996; Sa-Carvalho *et al.*, 1997; Baranowski *et al.*, 1998; 2000; Fry *et al.*, 1999; 2005; Maree *et al.*, 2010). Furthermore, alternative cell entry pathways exist and can be applied in future to improve cell adaptation (Baranowski *et al.*, 1998; 2000; Berryman *et al.*, 2013; Lawrence *et al.*, 2016a).

The stability of vaccines is of crucial importance in Africa, where the logistical process to get the vaccine from the manufacturer to the animal may take months and in many remote regions is in the absence of a cold-chain. Vaccines with improved stability and less reliant on a cold-chain are needed and could improve the longevity of immune responses elicited in animals (Doel and Baccarini, 1981). FMD is known to be unstable, especially for O and SAT2 serotypes (Doel and Baccarini, 1981), in mildly acidic pH conditions or at elevated temperatures, leading to dissociation of the capsid (146S particle) and loss of immunogenicity. The residues at the capsid inter-pentamer interfaces, and their interactions, are important for the infectivity and stability of the virion (Mateo *et al.*, 2003; 2008), and mutations adjacent to these interfaces have an effect on the conformational stability of FMDV (Filman *et al.*, 1989; Twomey *et al.*, 1995; Airaksinen *et al.*, 2001; Mateo *et al.*, 2007). However, experimental studies on the relative importance of residues and molecular interactions in viral capsid assembly, disassembly, and/or stability are still very limited. Recent research has compared more thermostable serotype A viruses with unstable O and SAT2 viruses, together with crystallography structures, sequence data, and *in silico* calculations of stability, to predict residue substitutions that could increase stability at inter-pentameric interfaces. With reverse genetic approaches, stabilizing mutations have been introduced into infectious copy clones. SAT2 and O viruses with improved stability have been developed and their antigens were tested in animal models and show promise for use as vaccines (Kotecha *et al.*, 2015).

Future research should also attempt to utilize directed evolution or rational engineering of antigenic sites through mutation of a few of the antigenically relevant positions to broaden and improve the antigenic spectrum of FMDV vaccine strains within a serotype. Ultimately, this approach in combination with cell culture adaptation and capsid stabilization can be utilized in

the development of custom-engineered vaccines for Africa that will provide high, stable antigen yield with broad antigenic coverage across serotypes.

1.12 FMDV DIAGNOSTIC ASSAYS

** Excerpts taken from co-authored article: Maree FF, Kasanga CJ, Scott KA, Opperman PA, **Chitray M**, Sangula AK, Sallu R, Sinkala Y, Wambura PN, King DP, Paton DJ, Rweyemamu MM. (2014). Review: Challenges and prospects for the control of foot-and-mouth disease: an African perspective. *DovePress Journal: Veterinary Medicine: Research and Reports* (5) 119–138.

The accurate diagnosis of FMDV infection is of utmost importance for the control and eradication of the disease especially in endemic regions. The initial diagnosis of FMD is normally based on clinical signs, but this can easily be confused with other vesicular diseases (Rémond *et al.*, 2002). Hence, it is vital that the recognition of signs of the disease by the farmer is promptly conveyed to the relevant veterinary authorities to verify clinical symptoms, and suspect samples should then be sent to the reference laboratory for confirmation. Rapid and precise data generated by laboratories provides vital support to FMD control and vaccination programs. To prove clinical diagnosis of FMD, laboratory confirmation testing (Kitching and Hughes, 2002) includes either the detection of active virus, virus antigen or viral genome, or serological indication of virus occurrence (Kitching *et al.*, 2005). However, in many African countries, samples received by the laboratory can be of poor quality due to an ineffective cold-chain and long transport periods. These factors make laboratory diagnosis challenging, and it is evident that endemic regions, like sub-Saharan Africa, requires diagnostic tools that are fit for purpose in these settings to allow for rapid diagnosis and the appropriate measures taken for control.

Existing diagnostic techniques for the detection of FMD are mainly based on the following principles:

- The identification of the infectious agent by virus isolation involving propagation on susceptible cell cultures (Jamal and Belsham, 2013). The ideal sample to diagnose FMD is epithelium from unruptured or fresh vesicles (OIE manual, 2017). However, in advanced disease or convalescent and carrier animals, oesophageal-pharyngeal (OP) fluid obtained by probang cup, are considered options to recover FMDV.

- The detection of viral antigen by enzyme-linked immunosorbent assay (ELISA) systems using FMDV-specific antibody or capturing reagents
- Molecular detection of viral nucleic acid by reverse-transcription polymerase chain reaction (RT-PCR) and the genetic analysis of the nucleotide sequence, mostly of the VP1-coding region (Di Nardo *et al.*, 2011).
- Detection of FMDV-specific antibody in animals previously exposed to the virus. The VNT is usually used as a confirmatory test for sera found positive by ELISA (Paton *et al.*, 2005).

These techniques are primarily suited for well-equipped laboratories which are usually either national or regional reference laboratories (Rweyemamu and Garland, 2006). The virus cell culture system, for example, requires careful handling of specimens to prevent environmental and cross-contamination, trained personnel, and a BSL3 (biosecurity level 3) laboratory. The success of virus isolation is dependent on the sample quality and requires special transport conditions from the sampling point to the laboratory (Jamal and Belsham, 2013). ELISA has been used for the detection of viral antigen and serotyping (OIE, 2017). Both the solid-phase competition ELISA and the liquid-phase blocking ELISA for serological detection of FMDV-specific antibodies against structural proteins are relatively simple procedures and easily implementable in diagnostic laboratories in endemic regions (Mackay *et al.*, 2001; Paiba *et al.*, 2004; King *et al.*, 2012). The VNT on the other hand, requires technical skill to be performed accurately and is dependent on cell culture facilities (Mackay *et al.*, 1998; Donaldson and Kitching, 2000) which may not be conducive for laboratories in endemic regions. Molecular techniques, like RT-PCR and real-time RT-PCR have the advantage that a wide range of samples (e.g. esophageal/pharyngeal scrapings, tissue and serum) can be tested rapidly (Amaral-Doel *et al.*, 1993; Marquardt *et al.*, 1995) and are now widely considered to be front-line diagnostic tests for the detection of FMD (Reid *et al.*, 2009). Furthermore, RT-PCR is the first step to determine the nucleotide sequences and contributes to molecular epidemiology studies and provides a tool to support regional and country-wide FMD control programs in an outbreak situation. To various degrees, these technologies are being implemented and applied in many diagnostic laboratories across the African continent, although these approaches are sometimes still too expensive to be implemented as routine across the whole of the African environment.

There is a possibility that some animals will not have shown any FMD clinical signs but would have had replication of FMDV. Such animals are a threat to other susceptible animals and may

carry the virus for many years. As stated in section 1.4, vaccinated animals do not produce antibodies against the FMDV NSPs whereas infected animals whether vaccinated or not, do produce antibodies against the FMDV NSPs. Thus, a single test that can identify infection would be of great benefit, especially in endemic regions. The development of the FMDV NSP ELISA assay has proven beneficial, sensitive and reproducible for this purpose and there are a wide variety of commercially available kits and in-house laboratory assays developed (Bergmann *et al.*, 1993; Mackay *et al.*, 1998; Sørensen *et al.*, 1998; Bronsvort *et al.*, 2004b). Presently, such tests are imperative for confirming whether a country is free from FMD virus (replication) even where there is no observed clinical disease. This is vital to trade issues in live animals and animal products. A variety of ELISA kits, containing expressed 3ABC or 3AB polyproteins in either *Escherichia coli* or baculovirus, or peptides of the polyprotein are available and have been validated mostly outside Africa (De Diego *et al.*, 1997; Sørensen *et al.*, 1998). However, the expressed 3ABC polyprotein or peptides are derived from the classical “European” types (A, O and C). In unpublished data by Dr Francois Maree, nucleotide and deduced amino acid sequences were determined for the 3C-coding region of 42 SAT isolates distributed across Africa and revealed 32% of variable amino acid residues in a complete alignment. In a neighbour joining phylogenetic tree based on the 3C-coding region the African SAT isolates clustered in four distinct phylogenetic units. Firstly, the southern African SAT1, 2 and 3 viruses grouped together, secondly, East and West African SAT isolates grouped with Euro-Asian types A, O and C, thirdly, Ugandan SAT1, 2 and 3 isolates and fourthly, West African SAT2 isolates. The amino acid variation within the 3C protein was not random but resided in hypervariable regions that could be mapped to the surface of the crystallographic structure of 3C. These overlapped with MAb binding sites identified for serotypes A and O. Similarly, 46.5% and 50% variable amino acid positions were observed for the 3A and 3B proteins respectively, many of which overlapped with MAb binding sites. Conceivably the variation within NSPs may consequently affect the antigenicity of these proteins which may impinge on the performance of the current 3ABC ELISA tests. This hypothesis was investigated by experimental infection of cattle with SAT1, 2 and 3 viruses and measuring the antibody levels against the 3ABC. Indeed, significant variation and poor correlation in NSPs within and between SAT viruses were observed. Due to the genetic heterogeneity of the FMDV 3C, 3B and 3A proteins of the SAT types viruses, it is speculated that the current tests may not be sensitive in the southern African subregion and further investigations are crucial.

Additional novel diagnostic assays such as immune-chromatographic lateral flow devices (LFDs) (Reid *et al.*, 2001; Jae *et al.*, 2009; Yang *et al.*, 2013), portable real-time PCR platforms (King *et al.*, 2008; Sammin *et al.*, 2010; Shirley *et al.*, 2010), loop-mediated isothermal amplification (LAMP) assay (Dukes *et al.*, 2006; James *et al.*, 2010), biosensors (Sánchez-Aparicio *et al.*, 2009), microarrays (Baxi *et al.*, 2006), gold nanoparticle improved immuno-PCR (Ding *et al.*, 2011) and nucleic acid sequence-based amplification (Collins *et al.*, 2002; Lau *et al.*, 2008) have been shown to enable rapid and reliable diagnosis, surveillance screening, and strain typing for FMDV. Although these assays have promising capabilities for sub-Saharan Africa and can improve many of the current problems faced, many limiting factors prevent the routine use of certain assays. For example, many of the novel assays are yet to be optimized for the FMDV SAT serotypes (where a high degree of sequence variability exists); the costs involved per test will determine how widely these assays will be used; the field-based novel assays will require training of personnel and some laboratory-based tests require specialized equipment, which is not readily available and personnel capable of correctly interpreting and analyzing the datasets produced. Thus, open communication between national and international reference labs becomes important as a support system to endemic regions. In addition, the possibility of diagnostic banks where diagnostic kits become readily available in outbreak situations can alleviate many of the problems faced by endemic regions.

1.13 THE IMMUNE RESPONSE TO FMDV

The immune system can be divided into the innate and adaptive immune systems. The innate immune system involves non-specific defence mechanisms which include barriers and chemical defences such as skin, and stomach acid, which is activated once a foreign particle enters the host. An antigen specific immune response defines the more complex adaptive immunity where the antigen must be processed and recognized before this immune system creates numerous immune cells specifically designed to attack an antigen. Adaptive immunity creates a “memory” for future responses of a specific antigen (Palm and Medzhitov, 2009). Both these immune systems are required for an effective immune response to a pathogen such as FMDV.

1.13.1 THE INNATE IMMUNE SYSTEM

The complement system links the innate and adaptive immune responses through a range of mechanisms including enhancing humoral immunity, regulating antibody effector mechanisms

and modulating T cell function (Carroll, 2004). Macrophages and monocytes are cells of the innate immune system that can phagocytose and destroy viral pathogens, however macrophages have been shown to harbour virus infections (Rigden *et al.*, 2002). Macrophage activity has been shown to be vital for the immune defence against FMDV (McCullough *et al.*, 1986; 1988; 1992). The macrophage is able to rapidly phagocytose the antibody-opsonised FMDV complex via the Fc receptors (McCullough *et al.*, 1988) relating to efficient protection *in vivo* (McCullough *et al.*, 1986; 1988; 1992). Interestingly, FMDV non-structural proteins have been observed in porcine monocyte-macrophages although it is not well understood (Baxt and Mason, 1995).

Dendritic cells (DC) play a central role in inducing the innate and adaptive responses. These cells are antigen-presenting cells thus it processes the antigen material and presents on the cell surface to the T-cells of the immune system. The published literature of FMDV and DC is limited to porcine and murine DC. Gregg *et al.*, 1995 first reported on DC infection by FMDV where they reported on the cytopathic effects of the virus after infection of porcine skin DC, however, Bautista *et al.*, 2005 showed that such skin DC are obstinate to FMDV infection due to expression of IFN type I in response to the FMDV infection. Various subsets of porcine DC *i.e.* plasmacytoid DC, monocyte-derived DC and bone marrow-derived DC were found to be susceptible to FMDV infection (Guzylack-Piriou *et al.*, 2006; Harwood *et al.*, 2008). Interestingly, following FMDV infection of DCs, non-structural viral proteins and dsRNA were detected for up to 24 hours post-infection and small quantities released between 2-8 hours post infection (Summerfield *et al.*, 2009). As found with the macrophages, whether the progeny virus is released before the productive virus replication is aborted or exocytosed uptake of the virus, is unknown (Harwood *et al.*, 2008). Juleff *et al.* (2008) showed that by using monoclonal antibodies specific for conformational, non-neutralizing epitopes of the FMDV capsid, viral structural proteins were identified that were restricted to the light zone of a follicular dendritic cell network of germinal centres within mandibular lymph nodes, lateral retropharyngeal lymph nodes and palatine tonsils up to 38 days post contact infection.

Other cells that play an important role in the control of the early phase of FMDV infection is natural killer (NK) cells also known as lymphokine-activated killer (LAK) cells, which are able to target and kill infected or tumor cells without harming healthy cells (Lanier, 2005). These LAK cells were present in FMDV re-stimulated bovine PBMC (peripheral blood mononuclear cell) of vaccinated cattle, and shown to have cytotoxic activity against FMDV-infected target

cells (Amadori *et al.*, 1992). Sanz-Parra *et al.* (1998) showed a rapid loss of MHC class I on infected epithelial cells, which is postulated to be the trigger of NK cells or this effect of the virus may play a role in viral evasion from MHC class I restricted cytotoxic T-lymphocyte responses. Another immune cell *i.e.* the $\gamma\delta$ T-cell could proliferate and produce cytokines as a result of FMDV antigen presence (Takamatsu *et al.*, 2006). A mouse model showed innate-like CD9⁺ splenic B cells playing a role in FMDV-specific thymus-independent neutralizing IgM response, although it is not known if this occurs in the natural host (Ostrowski *et al.*, 2007). Although T- and B- lymphocytes play a major role in the adaptive immune response to FMDV, it is possible that T-lymphocytes and NK cells plays a role in the innate immune response as well through the release of IFN- γ , which acts together with type I IFNs (Zhang *et al.*, 2002; Moraes *et al.*, 2007). Non-immunological epithelial and endothelial cells induces the innate immune system via IFNs, chemokines and other cytokines. Ku *et al.*, 2005 demonstrated keratinocytes producing TNF- α when pigs were infected with FMDV. In addition, FMDV infection resulted in IL-1 α , TNF- α , and IFN- $\alpha/\beta/\gamma$ mRNA being observed in epithelial cells of the bovine tongue, coronary band and dorsal soft palate when laser microdissection and RT-PCR techniques were utilized (Zhang *et al.*, 2009). FMDV L^{pro} has been shown to shut-off the host cap-dependant mRNA translation by cleaving the host translation initiation factor eIF-4G (Devaney *et al.*, 1988). Additionally, L^{pro} can also inhibit nuclear factor kappa B (NFkB) signalling and suppress the levels of cytokine and chemokine mRNA in infected epithelial cells (de Los Santos *et al.*, 2007).

1.13.2 THE ADAPTIVE IMMUNE SYSTEM

1.13.2.1 HUMORAL IMMUNE RESPONSES

Humoral immunity is mediated by B cell (generated in the bone marrow) produced antibody and FMDV-mediated humoral responses have been well studied since the key to FMDV protection is the induction of high levels of neutralizing antibodies. Following FMDV immunisation or infection, an infected animal will produce high levels of neutralizing antibodies against the FMDV structural proteins (Pay and Hingley, 1987; Salt, 1993). B cell receptors recognize the antigen and there are various classes and subclasses of virus neutralizing antibodies studied for FMDV which are present in the serum and probang samples of FMDV infected animals.

One of the first neutralizing antibody responses elicited is IgM, which is detected in serum, 3 to 7 days after challenge, peaking between 5 and 14 days and a slow decline to an undetectable

level occurring at about 56 days post infection (Doel, 1996; Golde *et al.*, 2008; Juleff, 2009). Following rapid isotype switching, IgG1 and IgG2 antibodies is detected from 4 days post challenge and reach a peak at 14 to 20 days (Collen, 1994; Salt *et al.*, 1996; Doel, 2005; Juleff, 2009). Studies have shown that pigs and cattle that are protected against FMD following vaccination, produce higher levels of IgG1 than IgG2 (Barnett *et al.*, 2002; Juleff, 2009; Capozzo *et al.*, 2011). Peak IgA titres can be detected in FMDV serum samples at 7 to 14 days and 14 days in probang samples (Juleff, 2009). Interestingly, IgA titres can either decline to undetectable levels or persist in carrier animals thus providing a tool for identifying FMDV carrier animals (Salt *et al.*, 1996). *In vivo* antibody virus neutralization is complex and includes the interaction of antibody with cells and molecules of the innate immune system and under these conditions, non-neutralizing antibody can contribute to protection (Reading and Dimmock, 2007). The virus neutralization antibody test resulted in the information regarding *in vitro* FMDV neutralization being obtained, which includes cell attachment inhibition resulting in the loss of FMDV infectivity (McCullough *et al.*, 1987, 1992). The humoral response is rapid after FMDV infection or vaccination and can provide protection against re-infection with a homologous FMDV strain (Pay and Hingley, 1987; McCullough *et al.*, 1992; Salt, 1993), whilst following FMDV infection, the immune response can provide protection for several years and the levels of protection correlate well with serum neutralizing antibody titres (Brocchi *et al.*, 1998).

1.13.2.2 CELLULAR IMMUNE RESPONSES

Cell-mediated immunity in response to an antigen does not involve antibodies but relates to the activation of phagocytes, antigen-specific cytotoxic T-lymphocytes and the release of various cytokines where the T-helper lymphocytes (Th/CD4+) and T-cytotoxic lymphocytes (Tc/CD8+) are considered to be the most significant. The immune response involving T cells are pathogen-specific and are controlled by the MHC class I and II molecules (Germain, 1994). It is not fully understood how T cells protect against FMDV since varying T cell mediated antiviral responses (CD4+ and CD8+) have been observed both *in vitro* and *in vivo* (Glass *et al.*, 1991; Blanco *et al.*, 2001; Bautista *et al.*, 2003). Following FMDV infection or vaccination in cattle, MHC class I restricted CD8+ T cell responses were present in cattle and a CD8+ T cell epitope (present in VP1) induced virus-infected cell killing by $\alpha\beta$ CD8+ T cells, but not CD4+ T cells (Guzman *et al.*, 2008). Contrastingly, CD4+ T cell responses have also been shown to be important in protection against FMDV (Glass *et al.*, 1991; Li *et al.*, 2008; Gerner *et al.*, 2009; Golde *et al.*, 2011). Dendritic cells degrade FMDV antigens into peptides and the

peptides fuse with FMDV specific MHC class II molecules producing Th1 (IFN- γ) as well as Th2 (IL-4, IL-5 and IL-13) responses (Golde *et al.*, 2008). Specific Th-lymphocytes then recognize the processed antigen and B-lymphocyte proliferation is induced and differentiation into antibody-producing cells and memory cell development occurs (Tizard, 2000; McCullough, 2004).

1.14 ANTIBODIES

Also known as immunoglobulins (Ig), antibodies are globular glycoprotein molecules found in body fluids or on B cells where they act as antigen receptors to identify and neutralize immunogens such as bacteria and viruses (Litman *et al.*, 1993; Janeway *et al.*, 2001). Antibodies are either expressed on the surface of B cells or are secreted by terminally differentiated cells from this lineage (plasma cells) into the circulation or external secretions (Goldman and Prabhakar, 1996). Using the physiological properties of antibodies, researchers have been using antibodies as reagents in a vast array of assays and tests. Essentially, there are two primary types of antibody reagents *i.e.* monoclonal antibodies (MAb) and polyclonal antibodies. Polyclonal antibodies tend to exhibit variability between different batches produced in different animals at different times, there is a higher potential for cross reactivity as it recognizes multiple epitopes (Ritter, 2000). Contrastingly, large quantities of identical MAbs can be produced where there is homogeneity with each batch produced and MAbs have reduced cross reactivity (Ritter, 2000). MAbs are produced either using hybridoma technology or recombinant antibody technology. Hybridoma technology has its limitations as it is expensive, requires expertise and the use of laboratory animals (Köhler and Milstein, 1975; Willats, 2002; Pandey, 2010) and many molecules are not immunogenic or can be toxic and thus cannot be used (Dintzis *et al.*, 1976). However, the development of recombinant monoclonal antibody technology to select MAbs via antibody phage display using filamentous bacteriophages, has become advantageous in the fields of immunology, cell biology, research and diagnostics (Carmen and Jermutus, 2002). To understand phage display technology, antibodies and their diversity will be explained.

1.14.1 ANTIBODY STRUCTURE AND DIVERSITY

All antibodies have a basic structure (Figure 1.10) which comprises of two heavy (H) polypeptide chains (*ca.* 50kDa) and two light (L) polypeptide chains (*ca.* 25kDa) and are held together by disulphide bonds in a Y-shaped structure (Edelman *et al.*, 1969; Schroeder and Cavacini, 2010). The light chains of an antibody can be classified as either kappa (κ) or lambda

(λ) type based on small differences in polypeptide sequence and each L chain has two successive domains, *i.e.* a C-terminal constant domain (C_L) and an N-terminal variable domain (V_L) (Harlow and Lane, 1988; Roitt *et al.*, 1998; Rajan, 2001). The heavy chain also has one N-terminal V_H but may have either three or four C-terminal C_H domains (Williams and Barclay, 1988). There are five immunoglobulin classes *i.e.* IgG, IgM, IgA, IgD and IgE, each having different heavy chains. The antibody variable region consists of V_L and V_H and this region determines antigen binding specificity whilst the constant regions determine the antibody's ability to bind to complement and FcR (fragment crystallizable receptor) on phagocytic cells (Maverakis *et al.*, 2015). The amino acid sequence of V_L and V_H varies between different antibodies of the same class. The arms of the Y antibody contains one C and one V domain from each heavy and light chain of the antibody and this region is called the Fab (fragment, antigen-binding) region (Putnam *et al.*, 1979). Involved in modulating immune cell activity is the base of the Y and this region is called the Fc (fragment, crystallizable) region (Janeway *et al.*, 2001). The fragment variable region, Fv region, contains only the two variable domains (V_H and V_L) and are the smallest fragment made from the enzymatic cleavage of IgG and IgM class antibodies (Johnson, 2013) (Figure 1.10).

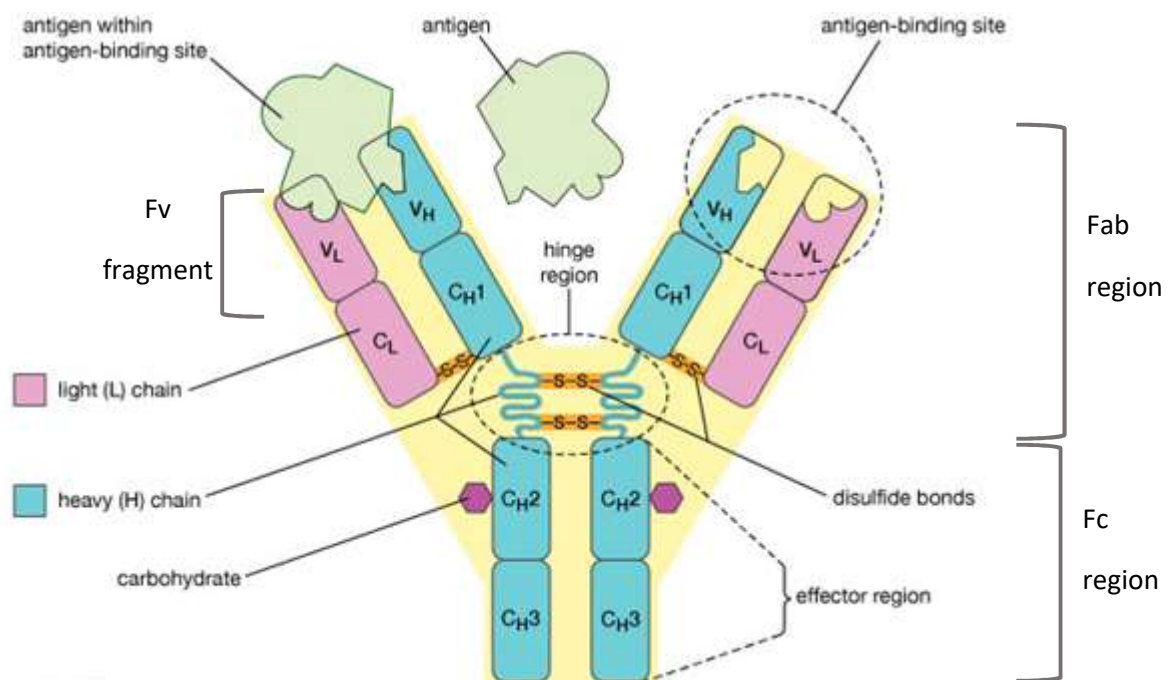


Figure 1.10: Representation of an antibody. There are two heavy polypeptide chains and two light polypeptide chains joined together by disulphide bonds. Each heavy chain is composed of one variable region (V_H) (blue block) and three constant regions (C_{H1} , C_{H2} , C_{H3}) (blue blocks) whilst each light chain is composed of one variable region (V_L , pink block) and one constant region (C_L , pink block). The antigen binding site is indicated, which is composed of

one light and one heavy chain. The Fab and Fc regions are indicated. Figure adapted from <https://global.britannica.com/science/disulfide>

Interactions of the Ig and antigen take place between the paratope *i.e.* the site of the Ig at which the antigen binds, and the epitope *i.e.* the site on the antigen that is bound (Schroeder and Cavacini, 2010). *In vivo*, immunoglobulins tend to be produced against intact antigens in soluble form, and thus preferentially identify surface epitopes that can represent conformational structures that are non-contiguous in the antigen's primary sequence. This ability to identify component parts of the antigen independently of the rest makes it possible for the B cell to discriminate between two closely related antigens, each of which can be viewed as a collection of epitopes. It also permits the same antibody to bind divergent antigens that share equivalent or similar epitopes, a phenomenon referred to as cross-reactivity. The amino acid differences of the V_H and V_L domains are located on three loops commonly known as complementarity determining regions (CDR1, CDR2 and CDR3) and within the CDRs are conserved framework regions. A large repertoire of antibodies with a vast degree of variability is generated when the heavy chain locus is combined with the range of genes for the other domains of the antibody, resulting in variable (V), diversity (D) and joining (J) recombination (Market and Papavasiliou, 2003). V, D and J are gene segments and due to there being multiple copies of each type of gene segment as well as different combinations to generate each immunoglobulin variable region, a huge number of antibodies with diverse paratopes and antigen specificities result (Market and Papavasiliou, 2003).

1.15 ANTIBODY PHAGE DISPLAY TECHNOLOGY

Molecular biology advances have resulted in the use of *Escherichia Coli* to produce recombinant antibodies via phage display technology. The reduction in the size of the antibody to either a Fab, a Fv or single chain Fv (scFv) with a linker (Figure 1.11), allows for these fragments to be expressed in bacterial cells and displayed by fusion to phage coat proteins (Griffiths and Duncan, 1998). A scFv is a fusion protein of the variable regions of V_H and V_L and can be connected with a short linker peptide of 10 to 25 amino acids (Huston *et al.*, 1988). The linker is usually rich in glycine (for flexibility) as well as serine or threonine (for solubility) and can either connect the N-terminus of the V_H with the C-terminus of the V_L , or *vice versa* (Schroeder and Cavacini, 2010).

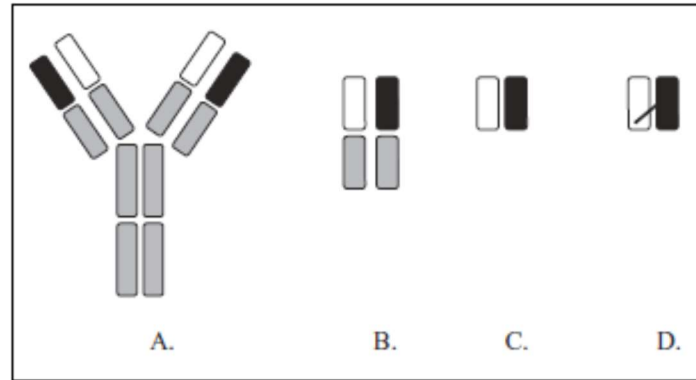


Figure 1.11: A schematic diagram of an antibody structure and derivative fragments. (A) IgG, 160kD; (B) Fab fragment, 50kD; (C) Fv fragment, 30kD, containing only the variable fragments of one heavy and one light chain; (D) scFv with linker, 30kDa, which is a randomly combined variable fragment of a heavy and light chain. Taken from Carmen and Jermutus (2002).

In addition to antibody fragments, phage display also allows for the expression of peptides or proteins on the surface of the phage particles (Smith, 1985; Winter *et al.*, 1994; Kay and Hoess, 1996). To accomplish this phage display, the nucleotide sequence encoding the protein to be displayed is incorporated into a phage or phagemid genome as a fusion to a gene encoding a phage coat protein. Thus, as the phage particles are assembled, the protein to be displayed is expressed at the surface of the mature phage and the sequence encoding the protein is confined within the same phage particle (Carmen and Jermutus, 2002) (Figure 1.12).

Bacteriophages such as the Ff filamentous phage, (M13 and its close relatives fd and fl), Lambda and T7 have been used successfully for phage display (Rodi and Makowski, 1999; Danner and Belasco, 2001). The size of the Ff phage family is not inhibited by the DNA contained within them, thus the insertion of foreign sequences within their genome is sustained by the assembly of longer phage particles (Willats, 2002). In phage display, the M13 is commonly used. It has a cylindrical shape, *ca.* 900nm long, 6-7nm in diameter and has a single-stranded DNA genome (6, 407bp) which encodes 11 genes (Webster, 1996; Makowski and Russel, 1997; Sambrook and Russell, 2001).

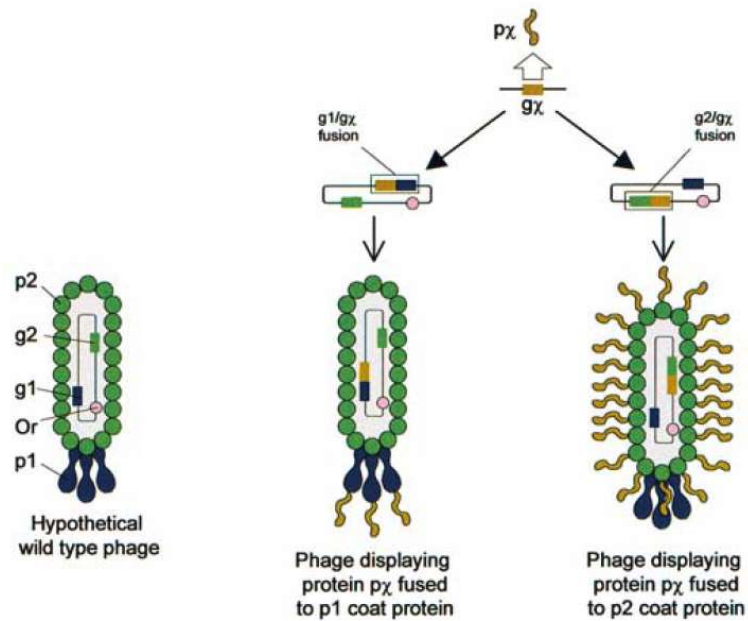


Figure 1.12: The basic principal of phage display. A bacteriophage has a genome that comprises of an origin of replication (Or) and genes g1 and g2 that encode two types of coat protein *i.e.* p1 and p2 respectively. A foreign protein, px (or random peptide, protein domains and antibody fragments), that is encoded by gene gx is displayed at the phage surface by the fusion of gx to p1 or p2. The number of copies of px displayed is dependent on which phage coat protein fusion occurred. Taken from Carmen and Jermutus (2002).

Five of the 11 genes are coat proteins with gene protein 8 (gp8) being present in *ca.* 2700 copies and responsible for encapsulating the phage DNA (Figure 1.13). The distal end comprises of 5 copies each of gp7 and gp9 whilst the proximal end has 4-5 copies each of gp6 and gp3 (Carmen and Jermutus, 2002). Only male bacteria (*E. coli* cells having the F-plasmid, which encodes the F-pilus) are infected by M13 and the association of gp3 and F-pilus facilitates infection. An advantageous characteristic of filamentous phages is that it does not lyse the infected host cell but is released from the cell membrane whilst the host cell continues to grow.

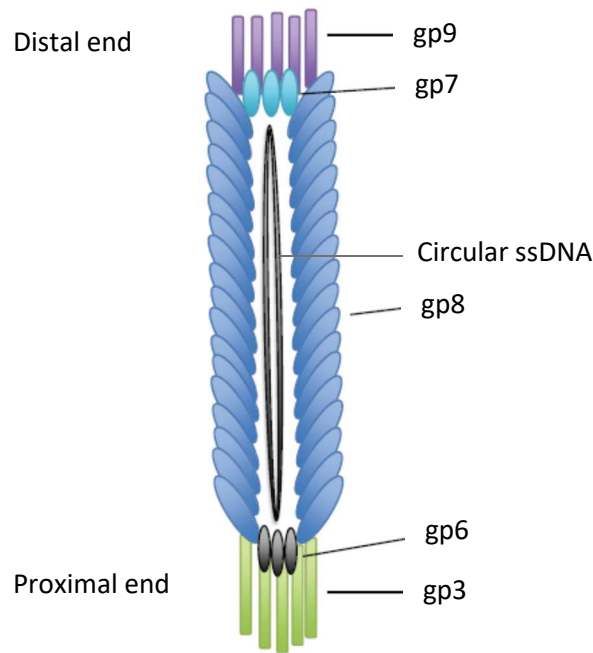


Figure 1.13: Representation of the structure of the M13 filamentous bacteriophage. Taken from Fukunaga and Taki, 2012.

A key advantage of phage display of antibody fragments versus hybridoma technology is that the generation of specific scFv/Fab to a particular antigen can be completed within a few weeks compared to hybridomas taking months. Additionally, the quantity of target antigen required for phage display (micrograms) is much less than what is needed for hybridoma antibody production (milligrams) (Carmen and Jermutus, 2002; Willats, 2002). The initial step for phage display is an antibody library, which can be either naïve or immune and comprises of an ideal population of $10^9 - 10^{11}$ clones (Sparks *et al.*, 1996; Hoogenboom, 1997; 1998). A naïve library consists of genomic information coding for antibody variable domains derived from B cells of non-immunised donors whereas for the immune library it is from immunised donors (Clackson *et al.*, 1991). Thus, the immune library will have an antibody range restricted to antibodies generated in response to a particular immunogen, although the naïve library can advantageously be used for an unlimited array of immunogens. To construct these libraries involves reverse transcription of the mRNA followed by polymerase chain reaction (PCR) to amplify the V_H and V_L gene segments from the cDNA template (Carmen and Jermutus, 2002; Willats, 2002). The rearranged antibody segments are then cloned into a phagemid display vector followed by the generation of the antibody repertoire *E. coli* cells (Carmen and Jermutus, 2002; Willats, 2002). Once the transformation step is optimised, a library size in the range of 10^8 - 10^{11} can be achieved only after numerous electroporation steps, however the size

of the library may be relative to the affinities of the isolated antibodies (Perelson and Oster, 1979).

Once the phage antibody library is obtained, it must be screened to isolate target specific antibody fragments (Figure 1.14). There are a few basic steps that make up the biopanning process (Figure 1.14): i) The library of phage particles are exposed to a target for which a binding protein is sort; ii) A washing step removes non-bound phages; iii) Phages that are bound to the target are eluted and amplified. Typically the bio-panning process is repeated at least 4 times where eluted phages are used to re-infect *E.coli* cells so that a population of best binders are enriched (Parmley and Smith, 1988).

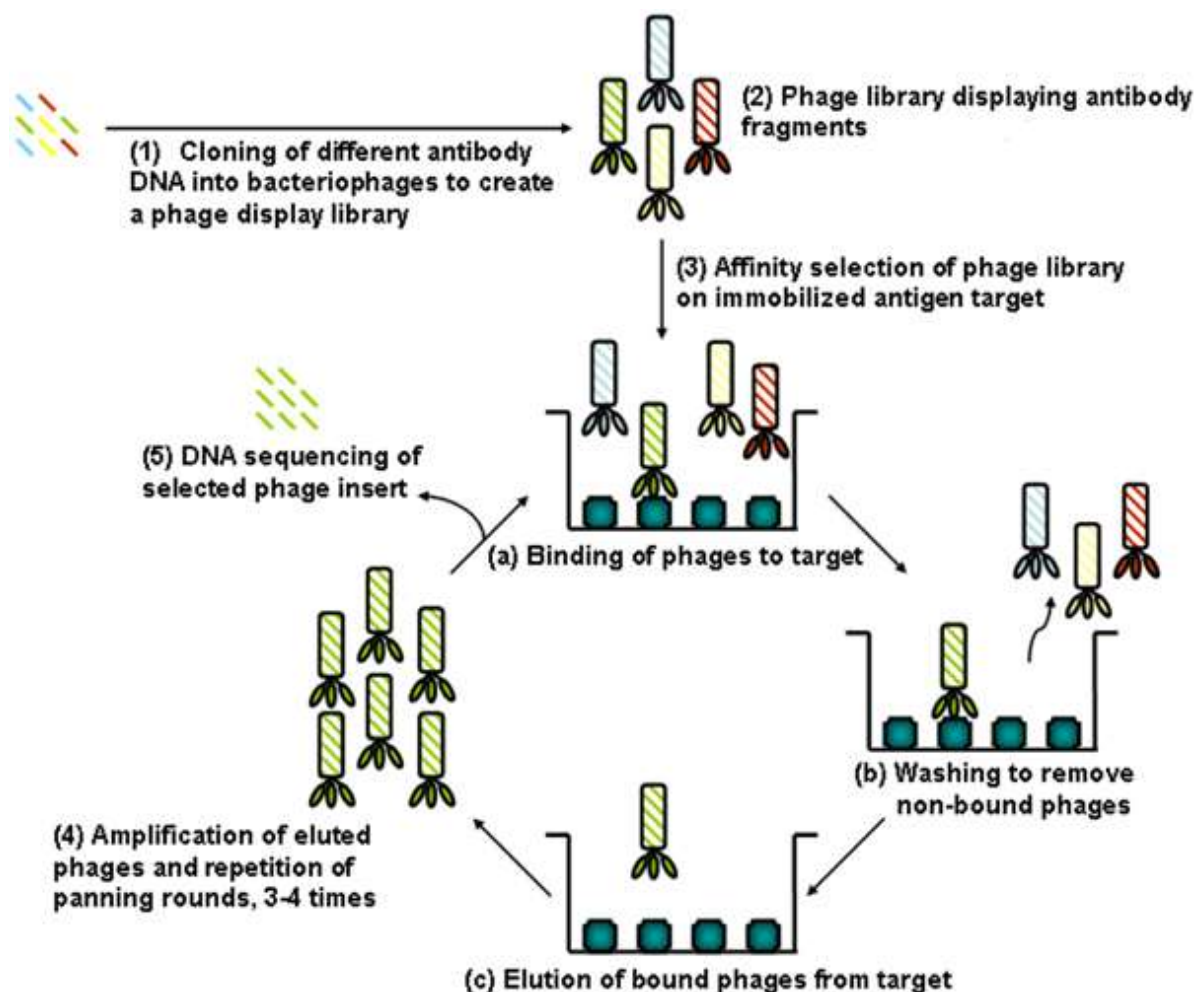


Figure 1.14: Schematic representation showing the screening of an antibody phage display library to isolate target specific antibody fragments. (1) DNA encoding a vast amount of variant antibody fragments is cloned into the genome of a filamentous phage fused to one of the coat protein genes. (2) A separate phage particle contains each of the variant DNA and the antibody fragment is displayed on the phage coat protein. (3) Phage that is expressing the antibody fragment that is able to bind to the target analyte are selected using biopanning cycles of (a) binding, (b) washing and (c) elution. (4) The phages obtained after elution are used to re-infect

E.coli cells and amplified by repeating the biopanning process. (5) After 3-4 rounds of selection, clones are then characterised. Taken from (Yun *et al.*, 2009).

1.16 AIMS OF THE STUDY

Although FMD is one of the oldest viral diseases known to man, it is still a major current threat for the world economies, which rely greatly on animal product imports and exports. Besides the effect on world economies, the local farmers and poor communities that rely on livestock for their livelihoods are severely affected by FMD outbreaks and the trade restrictions and injunctions that then arise. Regions that are endemic for FMD place a great deal of emphasis and resources into the control of the disease and countries that are FMD free conduct major research into better vaccines and diagnostic assays for FMDV, to be well-equipped and prepared should the threat of FMD occur. The Kruger National Park (KNP,) is the endemic region in South Africa due to the presence of the African buffalo (*Syncerus caffer*), the maintenance host of FMDV through persistent infections (Vosloo *et al.*, 2002; Thomson *et al.*, 2003). The communities, game farms and farmers adjacent to the KNP harbouring livestock are faced with unique challenges with the constant threat of FMD. Thus, control measures such as fences to separate livestock and wildlife and expensive vaccination programs are adopted in southern Africa in an attempt for control. Despite these efforts and the fact that vaccines are trivalent containing strains of all three FMDV serotypes that exist in South Africa (SAT1, SAT2 and SAT3), FMD outbreaks are continually occurring, in the control zone neighbouring the KNP.

Consequently, the need for improved vaccines is essential and vaccines should be produced based on currently circulating field strains. Vaccines are produced from chemical inactivation of virus grown in large-scale production cultures of BHK-21 cells. However, not all field virus strains can be adapted easily to suspension cell cultures. Thus, the production of custom-engineered FMD vaccines can be facilitated using infectious cDNA technology, which makes it possible to engineer chimeric viruses containing the antigenic region of a field strain and allows for the introduction of cell-culture receptor binding sites. This will facilitate fast and effective cell-culture adaptation of engineered viruses and allow for rapid amplification within a few passages in BHK-21 cells to create master virus seed stocks and circumvent the need to isolate on primary cell lines for further adaptation.

In addition to vaccination, the use of serological tests that can distinguish between naturally infected and vaccinated animals (DIVA) is of utmost importance to (i) quick and accurately diagnose exposure of livestock to FMDV and; (ii) gain FMD-free status following an outbreak. The use of serological tests that can distinguish between vaccinated and infected animals (DIVA) is of utmost importance to gain FMD-free status following an outbreak. The FMDV non-structural proteins (NSPs) are expressed only by replicating viruses. Inactivated vaccines are purified to remove cellular proteins and NSPs, and therefore only animals that have been infected with live virus should develop antibodies to these proteins. Because vaccination prevents clinical disease but does not necessarily prevent infection or persistence, it is useful to be able to identify animals, which are infected or have been exposed to live virus irrespective of their vaccination status. ELISAs based on the detection of antibodies to the 3ABC polyprotein have been shown to be sensitive and reproducible. A variety of kits containing expressed 3ABC or 3AB polyproteins in either *E.coli*, baculovirus or peptides of the polyprotein are available and have been validated outside Africa. However, the expressed 3ABC polyprotein/peptides are derived from the FMDV types A, O and C (Clavijo *et al.*, 2004; Sørensen *et al.*, 2005; Brocchi *et al.*, 2006). Due to the high genetic heterogeneity of the FMDV 3ABC polypeptide of the SAT serotype viruses (Van Rensburg *et al.*, 2002; Nsamba *et al.*, 2015), the current 3ABC ELISAs may not be sensitive in the southern African region. There is a need to design a 3ABC ELISA assay that are relevant for the southern African region.

Knowledge of the antigenic structure of FMD can greatly improve the understanding of the interaction between the virus and the immune system that results in neutralization of virus *in vivo*. Identification of those residues that comprise the antigenic determinants of the virus will allow the identification of those mutations in outbreak strains that potentially lessen the efficacy of a vaccine. Thus, if sufficient epitopes are identified, it may be possible to predict the protection afforded by a vaccine against a specific outbreak strain. Phage display libraries have been used with success to map epitopes for FMDV for serotype O viruses (Harmsen *et al.*, 2007; Yu *et al.*, 2011) and the SAT2 serotype (Opperman *et al.*, 2012; 2013). For the SAT2 serotype, the phage display library *i.e.* the Nkuku® library (Van Wyngaardt *et al.*, 2004) was successfully used to obtain three scFvs and to generate virus neutralization escape mutants. This study proves that the Nkuku® library could be further used to map epitopes for other FMDV serotypes. In addition, there are many studies that show the use of scFvs as potential diagnostic reagents (Mechaly *et al.*, 2008; Ribeiro *et al.*, 2013; Keller *et al.*, 2015).

Taking into account these predicaments faced with regards to FMDV, the following specific objectives for this study were:

1. Investigating the effect of symmetrically arranged, positively charged residues on the foot-and-mouth disease virus capsid in cell entry.
2. Development and validation of a foot-and-mouth disease virus SAT serotype-specific 3ABC assay to differentiate infected from vaccinated animals.
3. To isolate and characterize single-chain antibody fragments against foot-and-mouth disease serotype A, SAT1 and SAT3 viruses using a Nkuku® phage display library.

CHAPTER 2

SYMMETRICAL ARRANGEMENT OF POSITIVELY CHARGED RESIDUES AROUND THE FIVE-FOLD PORE OF FOOT-AND-MOUTH DISEASE SAT TYPE VIRUS CAPSIDS RESULTS IN THE ENHANCED AFFINITY TO HEPARAN SULPHATE

2.1 INTRODUCTION

Foot-and-mouth disease virus (FMDV) is a small, non-enveloped, icosahedral virus with a polyadenylated, single-stranded, positive-sense RNA genome belonging to the *Aphthovirus* genus in the *Picornaviridae* family (Knowles and Samuel, 2003). The virus capsid comprises 60 copies each of four virus-encoded structural proteins, VP1 to VP4. The outer shell of the capsid contains VP1, VP2 and VP3, whilst VP4 lines the interior surface (Acharya *et al.*, 1989). FMDV is an important pathogen that causes a highly contagious, vesicular disease affecting cloven-hoofed animals, including cattle, pigs, goats, sheep and buffalo, with severe economic consequences worldwide (Alexandersen and Mowat, 2005).

FMDV naturally infects epithelial cells and to date studies have shown FMDV can adhere to any of four members of the α_v subgroup of the integrin family of cellular receptors, *i.e.* $\alpha_v\beta_1$, $\alpha_v\beta_3$, $\alpha_v\beta_6$ and $\alpha_v\beta_8$ (Berinstein *et al.*, 1995; Jackson *et al.*, 1997, 2000a, 2002, 2004; Neff *et al.*, 1998; 2000; Duque and Baxt, 2003). Attachment to these receptors is mediated via a highly conserved Arg-Gly-Asp (RGD) motif (Fox *et al.*, 1989; Baxt and Becker, 1990; Mason *et al.*, 1994; Leippert *et al.*, 1997), located within the structurally disordered β_G - β_H loop of VP1 (Acharya *et al.*, 1989; Curry *et al.*, 1995; Lea *et al.*, 1995). Following FMDV-receptor interactions, the virus is internalized, and the viral genome released into the cytosol after acid-induced capsid dissociation (Cavanagh *et al.*, 1978; Grubman and Baxt, 2004).

Although FMDV infection is mediated by the RGD motif, RGD-independent infection can also occur (Baranowski *et al.*, 1998; Zhao *et al.*, 2003; Rieder *et al.*, 2005; Maree *et al.*, 2011; Chamberlain *et al.*, 2015; Lawrence *et al.*, 2016a). Molecules such as cell-surface glycosaminoglycans (GAGs) have been implicated in FMDV infections in cultured cells and may be involved in RGD-independent infection (Jackson *et al.*, 1996; Sa-Carvalho *et al.*, 1997; Zhao *et al.*, 2003). However, whilst the interactions between FMDV variants and heparin is known at atomic resolution for two strains of the virus, the molecular basis of this interaction and mechanism of cell entry by other strains are largely not well understood (Fry *et al.*, 1999; 2005). O'Donnell *et al.*, 2008 showed that heparan sulphate (HS) binding to FMDV enters via caveola-mediated endocytosis whilst recently, Lawrence *et al.* (2016a) demonstrated that FMDV can utilize the Jumonji C-domain containing protein (JMJD6) as part of an RGD-independent infection.

It has been documented that variants of FMDV, virulent to cultured cells, emerge following serial cytolitic infections (Charpentier *et al.*, 1996; Sevilla and Domingo, 1996; Martínez *et al.*, 1997). By comparison to parental field virus, these culture-adapted, virulent FMDV strains displayed a shorter replication cycle in BHK-21 cells and an enhanced ability to kill cells (Sevilla and Domingo, 1996). It is thought that FMDV adaptation to cell culture is made possible by the selective pressure of the viral quasi-species, exerted by cell surface molecules that may act as virus receptors (Baranowski *et al.*, 1998). However, it has been noted that field Southern African Territories (SAT) serotype viruses are difficult to adapt to BHK-21 cells, thus hampering large-scale propagation of vaccine antigen (Pay *et al.*, 1978; Preston *et al.*, 1982).

Adaptation of FMDV field isolates to enable efficient replication in cultured cells is accompanied by changes in viral properties, including the acquisition of the ability to bind to alternative cellular receptors such as cell-surface GAGs (Jackson *et al.*, 1996; Sa-Carvalho *et al.*, 1997; Zhao *et al.*, 2003; Maree *et al.*, 2011). The interactions of a diverse group of ligands, such as growth factors, chemokines, herpes simplex virus (HSV), human immunodeficiency virus (HIV), respiratory syncytial virus, alphaviruses, dengue virus, adeno-associated virus and FMDV, to highly sulphated GAGs are typically via a positively charged domain (Fromm *et al.*, 1995; Jackson *et al.*, 1996; Sa-Carvalho *et al.*, 1997; Chen *et al.*, 1997; Krusat and Streckert, 1997; Byrnes and Griffin, 1998; Klimstra *et al.*, 1998; Summerford and Samulski, 1998; Fry *et al.*, 1999; 2005; Zhao *et al.*, 2003). Zhao *et al.* (2003) reported that cell culture adaptation of FMDV serotype O selects for variant viruses with positively charged residues situated at

antigenically relevant positions in the VP1 capsid protein, showing that an increase in positively charged residues at the 5-fold axis plays a role during virus cell culture adaptation. Although the genetic alterations associated with increased virulence during cytolitic passages of the SAT serotype FMD viruses in BHK-21 cells are largely unknown, it has been noted that amino acid substitutions accumulate in their capsids during serial passaging (Maree *et al.*, 2010; Berryman *et al.*, 2013; Sarangi *et al.*, 2015). Surprisingly there is a common site of attachment between A10 and O1BFS (Fry *et al.*, 1999; 2005).

In a study by Nsamba 2015a, amino acid substitutions within the capsid proteins of SAT1 and SAT2 viruses that are consistent with a binding site, at a position close to the icosahedral five-fold axis, for a moiety of roughly the size and charge of a sulphated GAG was identified. Heparan sulphate proteoglycan (HSPG) is an example of such a GAG. We extended these investigations in this study and by utilizing infectious chimeric, genome-length clones, containing the outer capsid-coding sequence of either SAT2/SAU/6/00 or SAT1/NAM/307/98, we investigated some of these mutations in detail with respect to their effect on infectivity, cell binding and HS dependence in cultured cells. The results of this study combined with Nsamba, 2015a, proposes that these mutant viruses have a specific affinity for HS, thus implying that binding to cell surface HSPG is most likely required for entry into cultured cells.

2.2 MATERIALS AND METHODS

2.2.1 Cells, viruses and plasmids

Baby hamster kidney (BHK) cells, strain 21, clone 13 (ATCC CCL-10), used during virus passage and plaque assays, was maintained in Glasgow minimum essential medium (GMEM, Sigma), supplemented with 10% (v/v) foetal bovine serum (FBS, Hyclone), 1× antibiotic-antimycotic solution (Invitrogen), 1 mM L-glutamine (Invitrogen) and 10% (v/v) tryptose phosphate broth (TPB, Sigma-Aldrich). Wild-type Chinese hamster ovary (CHO) cells, strain K1 (ATCC CCL-61), were grown in Ham's F-12 nutrient medium (GIBCO™), supplemented with 10% (v/v) FBS and 1% (v/v) antibiotics. The same maintenance medium was used for the CHO-K1 derivative cell lines, CHO-677 (pgsD-677) (ATCC CRL-2244), which is HSPG deficient (HS⁻), and CHO-745 (pgsA-745) (ATCC CRL-2242), which is HS⁻ and chondroitin sulphate (CS⁻) deficient. The CHO-Lec2 (Pro-5WgaRII6A) (ATCC CRL-1736) cell line, which is sialic acid (SA⁻) deficient, was grown in Alpha minimum essential medium (MEMAlpha) (GIBCO) supplemented with 10% (v/v) FBS and 1% (v/v) antibiotics.

A part of this study is a continuation of the PhD work done by Nsamba, 2015a where 15 FMDV isolates, belonging to the SAT1 and SAT2, serotypes were isolated on either primary pig kidney or bovine thyroid cells, followed by amplification on Instituto Biologico Renal Suino-2 (IB-RS-2) cell monolayers. These viruses were either supplied by the World Reference Laboratory (WRL) for FMD at the Institute for Animal Health, Pirbright (United Kingdom), or are part of the virus bank at the Agricultural Research Council (ARC), Onderstepoort Veterinary Research (OVR) (South Africa) and were further analysed for the purposes of this study. The viruses were collected from either cattle or wildlife (Impala, *Aepyceros melampus* and African Buffalo, *Syncerus caffer*), and of the 15 virus isolates, 14 viruses were serially passaged eight times on BHK-21 cells and the SAT2/SAU/6/00 virus (from this study) was passaged 58 times on BHK-21 cells.

The nucleotide sequences generated for the fifteen cell culture-adapted FMDV isolates, were submitted to GenBank by Nsamba, 2015a. The respective accession numbers are as follows: GU194495 (SAT1/ KNP/148/91), GU194498 (SAT1/KNP/41/95), GU194497 (SAT1/ZIM/13/90), DQ009721 (SAT1/KEN/05/98), AF378302 (SAT1/TAN/1/99), AY442012 (SAT1/UGA/01/97), DQ009725 (SAT1/SUD/03/76), DQ009723 (SAT1/NIG/5/81), DQ009724 (SAT1/NIG/15/75), GU194502 (SAT1/NIG/06/76), GU194488 (SAT2/KNP/02/89), GU194489 (SAT2/KNP/51/93), AF367113 (SAT2/ZIM/10/91), DQ009731 (SAT2/UGA/02/02) and AY297948 (SAT2/SAU/6/00).

The construction of infectious genome-length plasmids for this study *i.e.* pSAT2, p^{NAM}SAT2 and p^{SAU}SAT2 (superscript indicates the donor capsid-coding sequence) has been described previously (Sa-Carvalho *et al.*, 1997; Van Rensburg *et al.*, 2004; Maree *et al.*, 2010; Berryman *et al.*, 2013). In order to construct the chimeric cDNA clones, the outer capsid-coding region of pSAT2 was replaced with the corresponding regions of SAT1/NAM/307/98 or SAT2/SAU/6/00 by making use of the flanking unique restriction enzyme sites, *SspI* and *XmaI*, in the VP2 and 2A-coding regions, respectively (Storey *et al.*, 2007; Maree *et al.*, 2010). The viruses recovered from pSAT2, pNAMSAT2 and pSAUSAT2 recombinant plasmid DNA were designated vSAT2, vNAMSAT2 (inter-serotype chimera) and vSAUSAT2 (intra-serotype chimera).

2.2.2 Plaque titration

Titration was performed by making use of a standard plaque assay method. Monolayers of BHK-21, CHO-K1, CHO-677, CHO-745 or CHO-Lec2 cells in 35-mm cell culture plates (Nunc) were infected with serially diluted viruses for 1 h, followed by the addition of a 2 ml tragacanth overlay (Grubman and Baxt 1979; Rieder *et al.*, 1993) and incubation for 48 h or 72 h at 37°C. The overlaid, infected monolayers were stained with 1% (w/v) methylene blue in 10% ethanol and 10% formaldehyde in phosphate buffered saline (PBS) (pH 7.4). Virus titres were calculated and expressed as plaque forming units per millilitre (PFU/ml).

2.2.3 RNA extraction, cDNA synthesis, PCR amplification and nucleotide sequencing

RNA was extracted from 200 µl infected cell lysates using a guanidium-based nucleic acid extraction method (Bastos, 1998) and utilized as templates for cDNA synthesis. Viral cDNA was synthesized with SuperScript III (Life Technologies) and oligonucleotide 2B208R (Reeve *et al.*, 2010). The *ca.* 3.0 kb leader and capsid-coding regions of the viral isolates were obtained by PCR amplification using Expand Long template *Taq* DNA polymerase (Roche) and SAT genome-specific oligonucleotides (Sa-Carvalho *et al.*, 1997). The consensus nucleotide sequences of the amplicons were determined using a primer-walking approach and the ABI PRISM BigDye Terminator Cycle Sequencing Ready Reaction Kit v3.0 (Perkin Elmer Applied Biosystems). The extension products were resolved on an ABI 3100 Genetic Analyzer (Applied Biosystems). Sequences were compiled and edited using Sequencher v5.4.6 (Gene Codes Corporation, Ann Arbor, MI, USA) sequence analysis software for Windows. The nucleotide and deduced amino acid sequences were aligned with ClustalX (Thompson *et al.*, 1997).

2.2.4 Site-directed mutagenesis and sub-cloning

The P1-2A region of SAT1/NAM/307/98 and SAT2/SAU/6/00 was cloned into pBlueScript (Stratagene) and the respective recombinant plasmids were designated pNAM-P1 and pSAU-P1. Mutagenesis primers, complementary to the P1-2A regions, were designed, containing the nucleotide substitutions (lower case, bold) to be introduced *i.e.*

NAMVP3-439 5'-GGCACAAACCCTCTCCCC**a**AAACACCGGAGATGGCATC-3';
NAMVP3-479 5'-CCTACACCTACGCTGAC**a**AGCCTGAACAGGCTTCAG-3';
SAUVP3-158 5'-GCCGCGCACTGCTATCACGCG**a**AATGGGACACTGGACTGAACTC-3';
SAUVP1-T158K GTACGCTGACAGCA**a**GCAC**a**CTTTGCCGTCAACCTTC;

SAUVP1-V50L/D55N AACATCCTTTcTTGTGGACCTCATG**a**ACACAAAGGAGAAG;
SAUVP1-83 5'-GTGGGC**aAa**CACCGGCGCGCCTTTTGGCAGCCTAAC-3';
SAUVP1-83/85
5'-CTTGAGATTGCATGTGTGGGC**aAa**CAC**ggcGc**GCCTTTTGGCAGCCTAAC-3';
SAUVP1-110-112
5'-GACAACCCCATGGTTTTCGCC**Aa**c**Gac**GTGTGACCCGCTTTGCCATCC-3'.

The QuikChange II XL Site-Directed Mutagenesis Kit (Stratagene) enabled the introduction of the desired mutations by an inverse PCR method, according to the manufacturer's instructions. The resulting plasmid DNA amplicons were transformed into XL10-Gold Ultra competent cells (Stratagene). The extracted plasmids were characterized by restriction enzyme digestion, followed by automated sequencing and selection of plasmid DNA containing the respective mutations.

The mutated P1-2A region of pNAM-P1 was cloned into the corresponding region of pSAT2 using the unique restriction sites, *SspI* and *XmaI*. Cloning and transformation procedures were performed as described previously (Sa-Carvalho *et al.*, 1997; Maree *et al.*, 2010). For the mutated P1-2A region of pSAU-P1, cloning into the corresponding region of pSAT2 was achieved with the In-Fusion HD Cloning Kit (Clontech). Briefly, pSAT2 was linearized by digestion with *SspI* and *XmaI*. A PCR primer set was designed for the mutated P1-2A region of pSAU-P1 with 15-bp extensions that are complementary to the ends of the linearized pSAT2 (F: 5'-GCTCGAGGACCGAATATTGACCACACGTCACGGAACCACGA-3' and R: 5'-AGAAGAAGGGCCCGGGTGGACTCAACGTCTCCTGCCT-3'). Following PCR amplification with the Advantage 2 PCR Kit (Clontech), the resulting amplicons were purified with the Zymoclean GEL DNA recovery Kit (Zymo Research) from an agarose gel. The In-Fusion cloning reaction, containing the purified amplicon and the linearized vector was transformed into Stellar competent cells (Clontech). Clones containing the desired mutations were selected and designated pNAM^{VP3Δ135K}SAT2, pNAM^{VP3Δ135K,175K}SAT2 (inter-serotype), pSAU^{VP3Δ158K}SAT2, pSAU^{VP1Δ50L,55N}SAT2, pSAU^{VP1Δ83K}SAT2, pSAU^{VP1Δ83K,85R}SAT2, pSAU^{VP1Δ110KRR}SAT2 and pSAU^{VP1Δ158K}SAT2 (intra-serotype).

2.2.5 *In vitro* RNA synthesis, transfection and virus recovery

The p^{NAM}SAT2, p^{NAM}^{VP3Δ135K}SAT2, p^{NAM}^{VP3Δ135K,175K}SAT2, p^{SAU}SAT2, p^{SAU}^{VP3Δ158K}SAT2, p^{SAU}^{VP1Δ50L,55N}SAT2, p^{SAU}^{VP1Δ83K}SAT2, p^{SAU}^{VP1Δ83K,85R}SAT2, p^{SAU}^{VP1Δ110KRR}SAT2 and p^{SAU}^{VP1Δ158K}SAT2 plasmids were linearized by digestion with *Swa*I and utilized as templates for *in vitro* RNA synthesis with the MEGAscript T7 Kit (Ambion). The RNA integrity was analyzed with agarose gel electrophoresis and quantified spectrophotometrically. *In vitro* synthesized RNA (ca. 3 μg) was mixed with Lipofectamine2000 (Invitrogen) and incubated for 20 min at room temperature, prior to being transfected into BHK-21 cell monolayers prepared in 35-mm cell culture plates. Incubation was continued in GMEM (GIBCO) containing 1% (v/v) FBS and 25mM HEPES for 48 h at 37°C with a 5% CO₂ influx.

Fresh BHK-21 monolayers in 35-mm cell culture wells were infected with 1/10th of freeze-thawed and clarified virus-containing supernatants and incubated for 48 h at 37°C. This cycle of passage continued until the cytopathic effect (CPE) observed was between 80 and 100%. Once viable viruses were recovered, automated sequencing was conducted to verify the presence of the engineered mutations.

2.2.6 Heparin plaque reduction assay

Viruses having titres ranging from 5×10^7 to 7×10^7 PFU/ml were prepared in 1 × PBS (pH 7.4) and added in a ratio of 1:1 to 1 × PBS containing heparin (Sigma-Aldrich). Viruses were incubated in the presence of heparin for 30 min at room temperature. Heparin concentrations of 0.625 mg/ml, 1.25 mg/ml, 2.5 mg/ml, 5 mg/ml and 10 mg/ml were used. Following incubation, 500 μl of the virus-heparin mixture was added to sub-confluent CHO-K1 cell monolayers and virus was allowed to attach to the cells for 15 min at room temperature. The cell monolayers were then washed with 1 × PBS (pH 7.4) and incubated at 37°C for a further 15 min in Ham's F-12 Nutrient medium containing 1% (v/v) FBS and 25 mM HEPES to enable virus internalization. Virus that had not been internalized was removed by washing with acidic MES (25 mM *N*-morpholino ethanesulfonic acid, pH 5.5, in 145 mM NaCl). Following a final wash step, 2 ml of tragacanth overlay was added and the monolayers were incubated at 37°C for 48 h. Subsequently, the cells were fixed with formaldehyde and stained with 1% methylene blue. Plaques were counted and virus titres (PFU/ml) were determined.

2.2.7 Heparinase assay

Monolayers of BHK-21 cells in 24-well tissue culture plates were washed three times with GMEM and treated with either heparinase I or heparinase III (Sigma) in $1 \times$ PBS for 30 min at 37°C. After enzyme treatment, the cells were washed three times with GMEM and vSAU^{VP1 Δ 83,85}SAT2 or vSAU^{VP1 Δ 10KRR}SAT2 viruses (100 PFU) were adsorbed onto the cells for 1 h at 37°C. Following a final wash, complete GMEM was added and the cells were incubated at 37°C for 24 h. Virus titres were determined by plaque assays on BHK-21 cells.

2.2.8 Structural modelling and ligand docking

The three-dimensional crystallographic protein structure of a FMDV SAT1 (2WZR) and a SAT2 capsid (5ACA) (Thompson *et al.*, 1997) was utilized as a template for the prediction of a protein homology model of the SAT2 virus. This was built manually using the crystallographic object-oriented toolkit (COOT) (Emsley and Cowtan, 2004) to avoid clashes between symmetry related protomers and was based on a sequence alignment generated using CLUSTALW (Thompson *et al.*, 1997). Only the local geometry was refined in COOT. Pentameric models were generated for each of the SAT1 and SAT2 structures using the non-crystallographic symmetry. In addition, the cell culture adapted mutations were modelled using COOT to make mutant virus structures for both SAT1 and SAT2. Structures were visualized with PyMol v0.98 (DeLano Scientific LLC) and the electrostatic surface potential was calculated using the APBS module of PyMol.

2.3 RESULTS

2.3.1 Multiple serial passages of SAT viruses in cultured cells select for variants with increased virulence in BHK-21 cells

SAT serotypes of FMDV exhibit altered viral properties after serial passaging in BHK-21 cells (Maree *et al.*, 2010). To further investigate this, Nsamba, 2015a, serially passaged fourteen SAT1 and SAT2 viruses eight times on BHK-21 cells (Table 2.1). The results were collated and summarised as indicated in Table 2.1. Complete CPE occurred within 24 h for the serially passaged viruses as opposed to 48 h for the parental viruses and the maximum titres observed were up to 10-fold higher than that of the parental viruses (Table 2.1). The viruses varied in their ability to adapt to BHK-21 cells. However, a feature consistent with adaptation was the appearance of small plaques on BHK-21 cells (results not shown). Here, we investigated whether the increased virulence in BHK-21 cells was associated with the ability to infect and replicate in CHO-K1 cells that lack the integrin receptors known to be utilized by FMDV for

cell entry, but has the alternative GAG receptors (Table 2.1). Investigations from this study also revealed that all of the BHK-21 adapted SAT1 and SAT2 viruses, except for SAT2/UGA/2/02 and SAT1/UGA/1/97, did not replicate in CHO-677 (HS⁻) or CHO-745 (HS⁻, CS⁻) cells (Table 2.1). Interestingly, titres of SAT2/UGA/2/02 and SAT1/UGA/1/97 on CHO-745 cells were in the order of 10³ PFU/ml and 10⁴ PFU/ml, respectively (Table 2.1). All viruses showed plaque formation on the CHO-Lec2 cells (SA⁻), demonstrating that cell entry of the SAT viruses are independent of sialic acid.

For reasons not well understood, many FMDV do not readily select small, clear-plaque variants upon passage in cultured BHK-21 cells. One SAT2 isolate, investigated in this study *i.e.* SAU/6/00, which had been responsible for a severe outbreak in dairy herds in Saudi Arabia in 2000, was passaged 58 times in BHK-21 suspension cells (SAU^{BHK58}) to determine the fate of the virus population. The plaque morphology of SAT2/SAU/6/00 on BHK-21 cells was medium-sized opaque plaques, whereas SAU^{BHK58} produced large, clear plaques and complete CPE at 24 hours post-infection (hpi) (Appendix A1). The opaque plaque virus in the SAU^{BHK58} population was undetectable. However, neither SAT2/SAU/6/00 nor SAU^{BHK58} were able to infect and replicate in CHO-K1 cells or its derivatives (Table 2.1, Appendix A1).

Using the data of Nsamba, 2015a, the percentage reduction in plaques in BHK-21 cells in the presence of 1mg/ml heparin was calculated and summarised in Table 2.1 were heparin reduced plaque formation by 69-98%. Interestingly, it was observed from investigations of this study that in CHO-K1 cells, the SAT1- and SAT2-adapted viruses were inhibited by 0.625 mg/ml heparin, with the exception of SAT2/UGA/2/02 and SAT1/UGA/1/97, which were able to produce plaques in the presence of 10 mg/ml heparin. The results confirm that SAT1 and SAT2 viruses with a broader cell tropism than field isolates can infect cells independently of the known integrin receptors for FMDV. For the majority of the viruses in this study, the results indicate that cell entry is most likely mediated by cell surface HSPG molecules.

Table 2.1: Summary of the SAT1 and SAT2 viruses resulting from cytolitic passages in BHK-21 cells, the plaque morphologies and their titres in PFU/ml on BHK-21, CHO-K1, CHO-677, CHO-745 and CHO-Lec2 cells.

Viruses	Cell lines and plaque morphology								
	Low passage isolate ¥	Plaque morphology $\#$	BHK-21* ¥	Plaque morphology*	+ Heparin (1 mg/ml) % reduction in number of plaques (BHK-21)	CHO-K1* ¥	CHO-677*	CHO-745*	CHO-Lec2*
KNP/148/91	4.5×10^4	L, opaque	1.2×10^8	M, S, clear	89	2.9×10^7	0	0	3.9×10^6
KNP/41/95	8.1×10^4	M, L, opaque	2.7×10^7	L, S, clear	80	4.5×10^6	0	0	1.4×10^6
ZIM/13/90	1.8×10^3	M, opaque	3.0×10^5	L, S, clear	91	1.5×10^5	0	0	6.5×10^4
KEN/5/98	5.4×10^3	M, L, opaque	9.4×10^5	L, S, clear	93	1.4×10^5	0	0	2.3×10^3
TAN/1/99	5.0×10^3	L, opaque	1.8×10^7	S, clear	95	7.6×10^5	0	0	2.9×10^4
UGA/1/97	4.5×10^2	M, opaque	1.0×10^7	M, S, clear	92	1.7×10^6	3.5×10^5	6.4×10^3	1.3×10^5
SUD/3/76	6.6×10^4	L, opaque	4.4×10^7	L, S, clear	97	3.4×10^6	0	0	8.0×10^6
NIG/5/81	4.0×10^3	M, opaque	7.2×10^6	L, S, clear	78	7.2×10^5	0	0	1.6×10^4
NIG/15/75	3.5×10^2	M, opaque	2.8×10^7	L, S, clear	82	1.8×10^6	0	0	3.5×10^5
NIG/6/76	1.6×10^2	M, opaque	6.8×10^6	L, S, clear	98	8.6×10^5		0	1.2×10^5
SAT2									
KNP/2/89	1.0×10^5	M, L, opaque	1.0×10^7	L,M,S, clear	96	1.4×10^6	0	0	1.7×10^4
KNP/51/93	2.9×10^3	L, opaque	8.6×10^5	L, S, clear	96	5.8×10^7	0	0	6.1×10^4
ZIM/10/91	3.8×10^2	L, opaque	2.0×10^7	L, S, clear	96	1.4×10^6	0	0	5.6×10^4
UGA/2/02	2.3×10^2	L, opaque	1.4×10^7	M, S, clear	69	2.1×10^6	1.6×10^5	1.0×10^4	6.6×10^5
SAU/6/00	1.0×10^5	M, opaque	1.6×10^5	L, clear	0	0	0	0	0

$\#$ The plaque morphologies prior to BHK-21 cytolitic passage are depicted as L for large plaques, M for medium plaques and S for small plaques. Prior to cytolitic passage. Large plaques were defined as those with a diameter of 6-8 mm; medium plaques were 3-5 mm in diameter. Plaque sizes are based on three repeats of titrations and average measure of 30 plaques.

* Subsequent to cytolitic passage. Small plaques had a diameter of 1-2 mm. ¥ Nsamba, 2015a study.

2.3.2 Gain of net positive charge in the VP1 and VP3 proteins during growth in BHK-21 cells

Analysis of the capsid proteins of the serially passaged SAT1 and SAT2 viruses revealed that the inner VP4 protein remained unchanged in all the viruses. In contrast, each virus had generally acquired three to five amino acid substitutions within VP1, VP2 and VP3 (Nsamba, 2015a). A total of 64 amino acid residue substitutions were, thus, observed amongst the fifteen serially passaged viruses of which 39% ($n = 21$) were to positively charged residues (Table 2.2). At least eight SAT1 viruses contained K or R residue substitutions at VP1 residue positions 111 and/or 112 (β F- β G loop), and five SAT1 and SAT2 viruses had similar substitutions at VP1 positions 83, 84 or 85 (Table 2.2).

Table 2.2: Summary of the amino acid substitutions to a positively charged residue in the outer capsid proteins of serially passaged SAT1 and SAT2 viruses.

<i>Viruses</i>	<i>Capsid Protein</i>	<i>Amino acid position and substitution</i>
SAT1		
KNP/148/91	VP2	Q74R
	VP1	G112R
KNP/41/95	VP1	E84K, N111K
ZIM/13/90	VP1	N111K, G112R
KEN/5/98	VP1	E84K, W87R
TAN/1/99	VP1	E112K, D181N
UGA/1/97	VP2	E133K
	VP1	E58K
SUD/3/76	VP1	C26R, N111K, G112R
NIG/5/81	VP1	N48K, N111K
NIG/15/75	VP1	N111K, D180N
NIG/6/76	VP1	N111K
NAM/307/98*	VP1	E135K, E175K
SAT2		
KNP/2/89	VP1	D83N Q85R
KNP/51/93	VP1	E83K, D110G
UGA/2/02	VP1	E83K
SAU/6/00#	VP1	V50L, D55N, T158K

*FMDV SAT1/NAM/307/98 amino acid substitutions were published previously in Maree *et al.* (2010).

Refer to Appendix A1 and A2.

SAU^{BHK58} did not replicate in CHO-K1 cells. Comparative amino acid sequence analysis of the outer capsid proteins of SAU^{BHK58} and SAT2/SAU/6/00 revealed five amino acid substitutions, including T99A, located in the β C- β D loop of VP2, D193N in VP3, and three substitutions in

VP1, *i.e.* V50L, D55N (β B- β C loop of VP1) and T158K (β G- β H loop of VP1). One substitution, residue 158 of VP1, was to a positively charged lysine (Table 2.2).

When plotted on the 3D structure of a SAT1 capsid (2WZR) and a SAT2 capsid (5ACA) using Pymol, most of the mutations were surface-exposed and located on protruding structural elements surrounding the five- and three-fold axes of the virion (Figure 2.1). The β F- β G loop substitutions, inducing a positive charge amino acid change at VP1 positions 111 and 112, were observed in eight of the 14 viruses and are highly surface-exposed, and adjacent to the five-fold pore of the capsid (Table 2.2; Figure 2.1). Another mutation that occurred more than once in SAT1 ($n = 2$) was a lysine residue at VP1 position 84 in the β D- β E loop (Table 2.2).

Five copies of positively charged residues at both positions (111-112 and 84) in the VP1 protein formed a tight cluster on the SAT1 capsid around the five-fold axis of symmetry (Figure 2.1). For the SAT2 serotype, lysine residues were observed in VP1 at position 83 in two viruses and an arginine substitution in VP1 at position 85 for SAT2/KNP/2/89. Although, residue 83 is not surface-exposed, amino acid 85 is exposed, forming a positively charged cluster around the five-fold axis (Figure 2.1). The positively charged cluster around the five-fold axis would likely permit binding to negatively charged sulphated proteoglycan molecules at the cell surface.

Additionally, it was shown using GRID that the most likely residue to interact with heparin as residue 112 of VP1, with a molecular interaction energy of -8.2 kcal/mol (analysis performed by Dr A Kotecha, University of Oxford). Collectively, the accumulated positively charged residues around the five-fold axis are especially interesting as those alone correlated with the observed phenotypes of viruses capable of binding CHO-K1 cells and were absent in viruses that lacked this ability.

2.3.3 Generation of recombinant FMDV with altered surface charges

To study the effect of individual mutations in a defined genetic background, we selected infectious, chimeric clones of FMDV, p^{SAU}SAT2 (intra-serotype) and p^{NAM}SAT2 (SAT1-SAT2 inter-serotype), to perform the mutational studies (Sa-Carvalho *et al.*, 1997; Maree *et al.*, 2010; Berryman *et al.*, 2013). Out of 25 different positively charged residue substitutions observed following the serial passage experiments (from Nsamba, 2015a study and this study), we selected eight patterns for the generation of recombinant viruses: (i) VP3 E135K; (ii) VP3

E135K, E175K; (iii) VP3 E158K; (iv) VP1 V50L, D55N; (v) VP1 T158K; (vi) VP1 E83K; (vii) VP1 E83K, T85R; and (viii) VP1 ¹¹⁰KGG¹¹² to ¹¹⁰KRR¹¹². The effect of these mutations on the surface charge distribution of VP1 and VP3 is detailed in Figure 2.1. All substitutions to positively charged residues occurred near already existing positively charged surface residues, resulting in the formation of an expanded, repeat cluster of positive charge on the virion surface, especially focused around the five-fold axis (Figure 2.1).

Production of progeny virus was determined upon transfection of BHK-21 cells with RNA transcripts derived from each cDNA clone. The corresponding recombinant viruses, designated vNAM^{VP3Δ135K}SAT2, vNAM^{VP3Δ135K,175K}SAT2 (inter-serotype), vSAU^{VP3Δ158K}SAT2, vSAU^{VP1Δ50L,55N}SAT2, vSAU^{VP1Δ83K}SAT2, vSAU^{VP1Δ83K,85R}SAT2, vSAU^{VP1Δ110KRR}SAT2 and vSAU^{VP1Δ158K}SAT2 (intra-serotype), were recovered and high-titre stocks were prepared in BHK-21 cells and used for subsequent biological analysis. All recombinant progeny maintained their chimeric integrity after seven passages in BHK-21 cells as evidenced by RT-PCR and nucleotide sequencing.

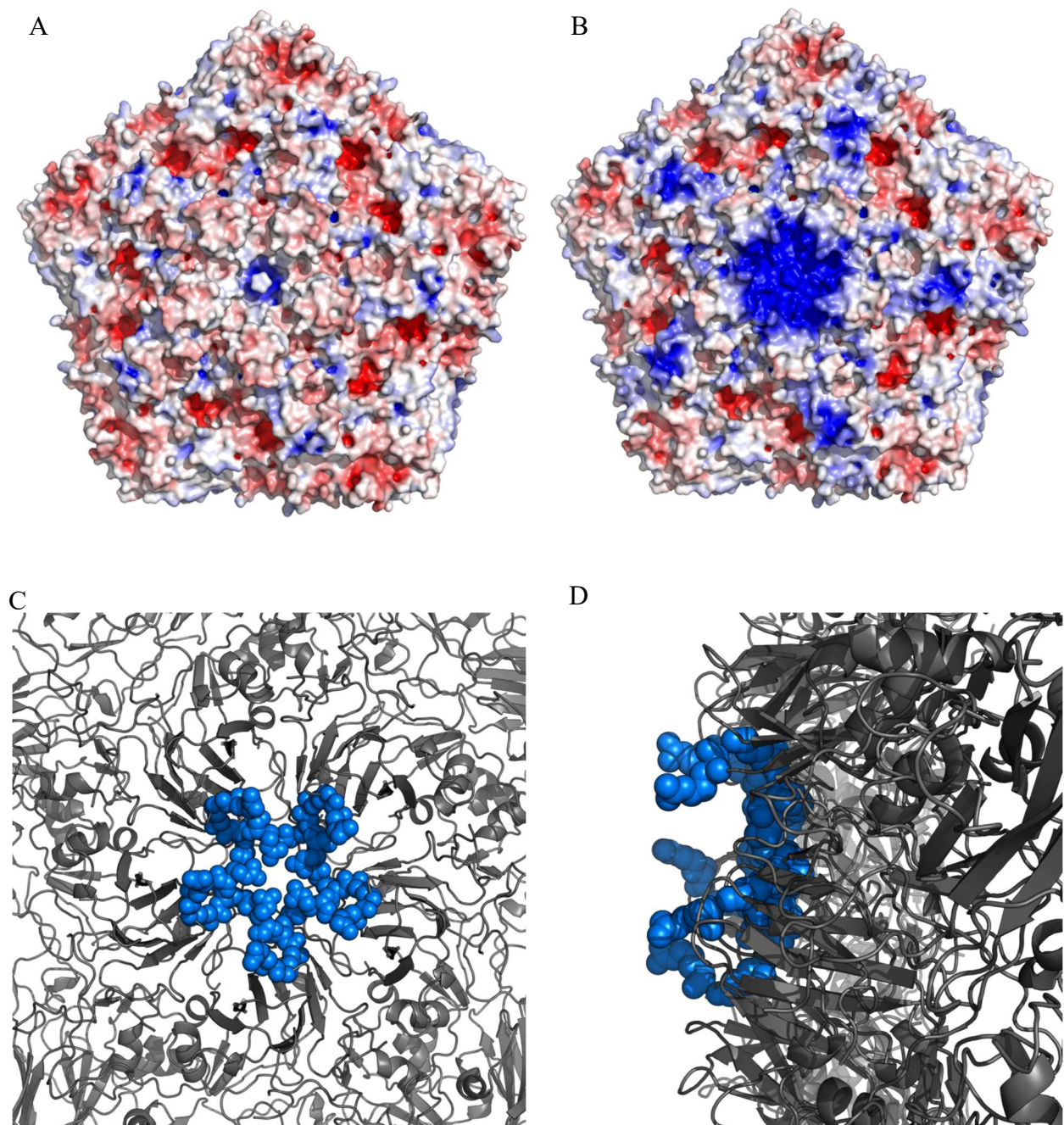


Figure 2.1: Charge distribution and clustering of mutations on the capsid surface. (A) Electrostatic potential of wild-type SAT1 capsid showing uniform charge distribution on the particle surface. (B) Electrostatic potential of the mutant SAT1 capsid showing clustering of positive charge at 5-fold axis. The electrostatic potential was calculated using APBS plugin embedded within Pymol. The colouring represents positive charge (blue), negative charge (red) and neutral (white). (C) The projection of the capsid on a 5-fold axis shows the clustering of the positively charge mutations from the top view. (D) The projection showing the side view and the surface exposure of the mutant side chains.

2.3.4 Effect of the mutations on the infectivity and cell entry of cultured BHK-21 and CHO cells

To confirm the significance of the introduced repeat clusters of positive charge on the virion, the relative infectivity of the mutant viruses was determined in cultured cells (Table 2.3). The introduction of positively charged residues at amino acid residue positions 135 and 175 of SAT1 VP3 in the inter-serotype chimera viruses, vNAM^{VP3Δ135K}SAT2 and vNAM^{VP3Δ135K,175K}SAT2, resulted in the same medium (3-5 mm) to large (6-8 mm) clear plaque morphologies on BHK-21 cells as the wild-type v^{NAM}SAT2 virus, but no growth on CHO-K1 or any of the other CHO cell lines (Table 2.3). Interestingly, the vNAM^{VP3Δ135K}SAT2 virus produced a 100-fold higher titre on BHK-21 cells, *i.e.* 2.51×10^8 PFU/ml at passage level 7 compared to the SAT1/NAM/307/98 wild-type virus, *i.e.* 1.26×10^6 PFU/ml at passage 8 on BHK-21 cells.

The ¹¹⁰KRR¹¹² of the vSAU^{VP1Δ110KRR}SAT2 mutant was the only mutation with an appreciable effect on the growth of the intra-serotype chimeric virus. The mutant resulted in large clear plaques and a titre of 100-fold higher (3.98×10^8 PFU/ml) than the wild-type virus in BHK-21 cells (Table 2.3). The intra-serotype chimera viruses with mutations in the VP1 N-terminus (vSAU^{VP1Δ50L,55N}SAT2) or the βG-βH loop (vSAU^{VP1Δ158K}SAT2) displayed medium (3-5 mm) to large (6-8 mm) opaque plaques on BHK-21 cells, and produced infectivity titres of 2.51×10^6 PFU/ml and 6.31×10^6 PFU/ml, respectively, which are similar to that of SAT2/SAU/6/00 (Table 2.3). However, small (1-2 mm) to medium clear plaques were observed on BHK-21 cells for the single mutants vSAU^{VP1Δ83K}SAT2 and vSAU^{VP3Δ158K}SAT2 with no significant effect on virus growth in BHK-21 cells (Table 2.3). Unexpectedly, the simultaneous replacement of E83 and T85 in the SAT2/SAU/6/00 VP1 protein with positive charged residues (mutant vSAU^{VP1Δ83K,85R}SAT2) significantly reduced the replication capacity of the mutant virus producing a titre of 7.94×10^4 PFU/ml (Table 2.3). Five mutant viruses, *i.e.* vSAU^{VP3Δ158K}SAT2, vSAU^{VP1Δ110KRR}SAT2, vSAU^{VP1Δ83K}SAT2, vSAU^{VP1Δ83K,85R}SAT2 and vSAU^{VP1Δ158K}SAT2, expanded its cell tropism and attained the ability to infect and replicate in CHO-K1 cells and the sialic acid-deficient (SA⁻) CHO-Lec2 cells. However, none of the mutant viruses were able to infect the HSPG-deficient (HS⁻) CHO-677 cells or the HS⁻ and chondroitin sulphate (CS⁻)-deficient CHO-745 cell line (Table 2.3).

To confirm the dependence of the mutant viruses on HSPG for cell entry, we used heparin as an inhibitor of virus growth. Mutant viruses were incubated with various concentrations of

heparin prior to performing plaque assays on CHO-K1 cells. Plaque formation was completely abolished for the vSAU^{VP3Δ158K}SAT2, vSAU^{VP1Δ83K}SAT2 and vSAU^{VP1Δ158R}SAT2 viruses at heparin concentrations of 0.625 mg/ml or higher (Figure 2.2A). Plaque formation of vSAU^{VP1Δ83K,85R}SAT2 and vSAU^{VP1Δ110KRR}SAT2 was linearly reduced with increasing concentrations of heparin until plaque formation was abolished for vSAU^{VP1Δ83K,85R}SAT2 at 5 mg/ml heparin and, at 10 mg/ml, vSAU^{VP1Δ110KRR}SAT2 had a titre of 0.7×10^2 PFU/ml (Figure 2.2A). This result suggest vSAU^{VP1Δ110KRR}SAT2 may enter and replicate in CHO-K1 cells in the presence of high concentration of heparin.

To confirm the involvement of HSPG in virus binding BHK-21 cells were treated with heparinase I or heparinase III prior to infection with intra-serotype chimeric viruses. Interestingly, vSAU^{VP1Δ83K,85R}SAT2 infection of BHK-21 cells was completely blocked by heparinase treatment of the cells, but with no effect on infectivity of v^{SAU}SAT2 (Figure 2.2B). However, the infectivity of vSAU^{VP1Δ110KRR}SAT2 was reduced by 78% following heparinase I treated BHK-21 cells and 82% with heparinase III treated BHK-21 cells when compared to the virus titres when no enzyme was present (Figure 2.2B).

Table 2.3: Titres (PFU/ml) of inter-serotype or intra-serotype FMDV chimera viruses with positive charged residue substitutions in the VP1 or VP3 capsid proteins. Plaque morphology on BHK-21 cells are indicated.

<i>Virus mutants*</i>	<i>Mutations in VP3</i>	<i>Mutations in VP1</i>	<i>Cell lines, plaque morphology and virus titres</i>					
			BHK-21	Plaque morphology	CHO-K1	CHO-677^a	CHO-745^b	CHO-Lec2^c
v ^{NAM} SAT2	None	None	1.26x10 ⁶	L, M, clear	N	N	N	N
vNAM ^{VP3Δ135K} SAT2	E135K	-	2.51x10 ⁸	L, M, clear	N	N	N	N
vNAM ^{VP3Δ135K,175K} SAT2	E135K, E175K	-	7.94x10 ⁶	L, M, clear	N	N	N	N
v ^{SAU} SAT2	None	None	1.6x10 ⁵	L, M, clear	N	N	N	N
vSAU ^{VP3Δ158K} SAT2	E158K	-	1.26x10 ⁵	M, S, clear	1.8x10 ³	N	N	1.4x10 ³
vSAU ^{VP1Δ50L,55N} SAT2	-	V50L-D55N	2.51x10 ⁶	L, M, clear	N	N	N	N
vSAU ^{VP1Δ158K} SAT2	-	T158K	6.31x10 ⁶	L, M, clear	2.9x10 ⁴	N	N	1.4x10 ⁴
vSAU ^{VP1Δ83K} SAT2	-	E83K	2.51x10 ⁶	M, S, clear	4.0x10 ⁶	N	N	1.6x10 ⁶
vSAU ^{VP1Δ83K,85R} SAT2	-	E83K; T85R	7.94x10 ⁴	M, S, clear	1.4x10 ⁴	N	N	1.2x10 ³
vSAU ^{VP1Δ110KRR} SAT2	-	KGG110-112KRR	3.98x10 ⁸	L, clear	4.7x10 ⁸	N	N	5.5x10 ⁵

^a CHO cell mutant, heparan sulphate deficient (HS⁻) cell line

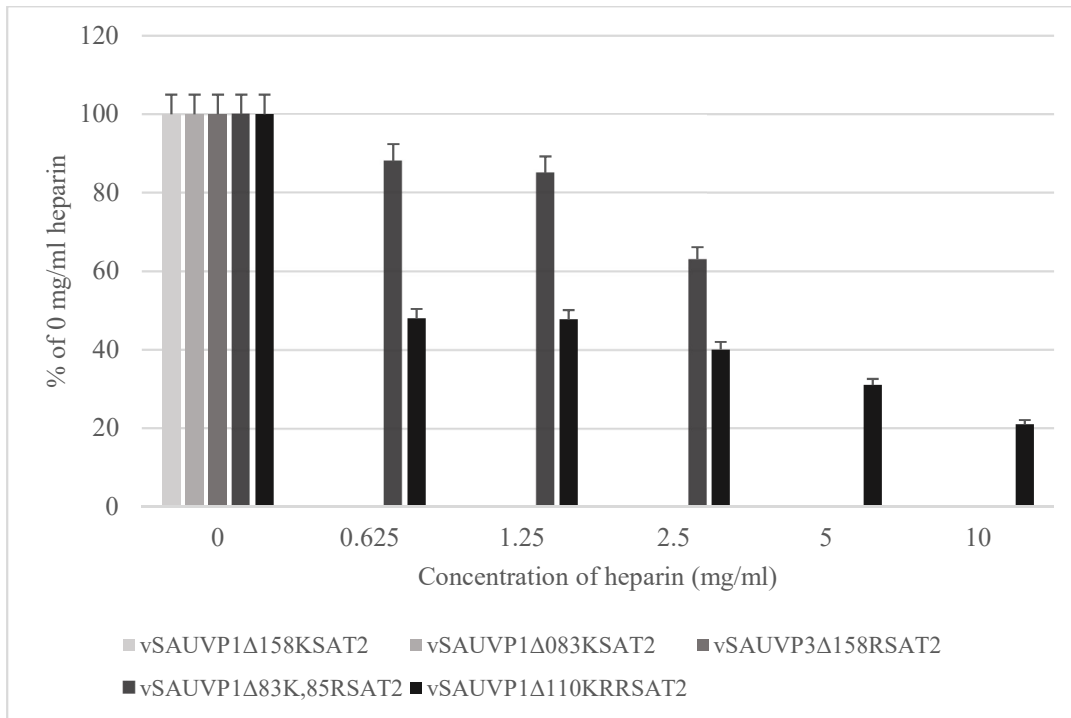
^b CHO cell mutant, heparan sulphate deficient (HS⁻) and chondroitin sulphate deficient (CS⁻) cell line

^c CHO cell mutant, sialic acid deficient (SA⁻) cell line

N indicates no growth.

L is for large plaques (6-8 mm in diameter), M for medium plaques (3-5 mm in diameter) and S for small plaques (1-2 mm in diameter).

A



B

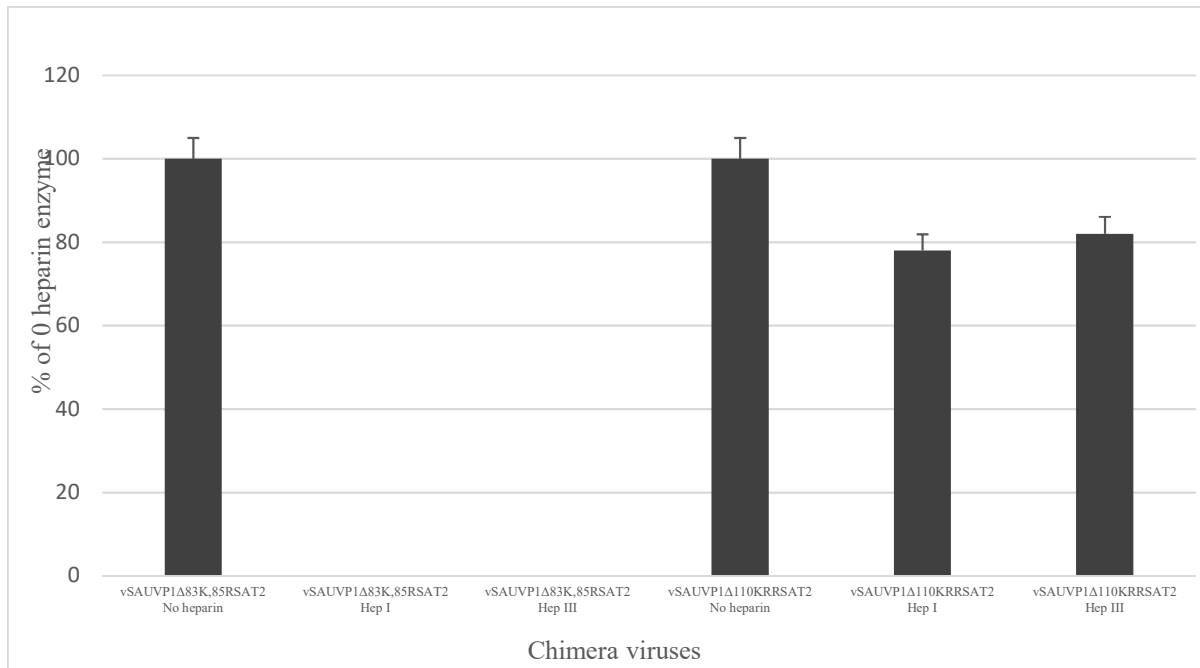


Figure 2.2: Infection of CHO-K1 cells by the recombinant mutants vSAU^{VP1Δ158K}SAT2, vSAU^{VP1Δ83K}SAT2 and vSAU^{VP3Δ158R}SAT2 is inhibited by heparin. (A) There was a linear decrease in titres for vSAU^{VP1Δ83K,85R}SAT2 and vSAU^{VP1Δ110KRR}SAT2 infection of CHO-K1 cells with increasing concentration of heparin. Infection was completely abolished in the presence of 5 mg/ml heparin for vSAU^{VP1Δ83K,85R}SAT2, whilst vSAU^{VP1Δ110KRR}SAT2 was still able to infect CHO-K1 cells in the presence of 10 mg/ml heparin. Viruses having titres ranging from 5×10^7 to 7×10^7 PFU/ml were mock-treated or treated with 0.625, 1.25, 2.5, 5 or 10 mg/ml soluble heparin before infecting monolayers of CHO-K1 cells. Virus that had not been

internalized was removed by washing with MES buffer (pH 5.5). The number of plaques formed on CHO-K1 cells was counted and expressed as the percentage of infectivity in relation to the non-heparin treated chimeric viruses. The standard deviations of the titres determined from duplicate wells are indicated. (B) The infection of vSAU^{VP1Δ83,85}SAT2 and vSAU¹¹¹⁰⁻¹¹¹²SAT2 on BHK-21 heparinase I and III treated cells were determined. The chimera, vSAU^{VP1Δ83,85}SAT2, was not able to infect heparinase I or III treated BHK-21 cells. However, vSAU¹¹¹⁰⁻¹¹¹²SAT2 virus titres reduced to 78% in heparinase I treated BHK-21 cells and to 82% for heparinase III treated BHK-21 cells. Monolayers of BHK-21 cells prepared in 24-well cell culture plates were treated with heparinase I and III enzymes (prepared in PBS) for 30 min at 37°C. After a wash step, virus was allowed to infect cell monolayers for 1 h at 37°C. This was followed by a final wash step, addition of GMEM and incubation of plates at 37°C. Virus infectivity titres were determined by plaque on BHK-21 cells at 24 h post-infection.

Collectively, our results indicate that positively charged residues on surface-exposed loops of VP1 and VP3 are involved in the expansion of cell tropism of SAT viruses. However, not all the mutations resulted in a growth advantage in BHK-21 cells. Only positively charged residues in VP1 at positions 110-112 caused a 10- to 100-fold higher titre in BHK-21 cells for SAT1 viruses (our previous work) and SAT2 viruses (Table 2.3).

2.4 DISCUSSION

Our findings suggest that binding to cell surface HSPG plays little or no role in the interaction between FMDV field isolates and host cells *in vivo*. Nonetheless, SAT viruses rapidly mutate to expand their cell tropism and utilize HSPG during cell culture adaptation. Although infection with low passage SAT1 and SAT2 viruses was predominantly HSPG-independent, several cell culture-adapted strains, each with increased clusters of positively charged residues at the five-fold axis, attached to cells through an HSPG-dependent mechanism. We identified critical amino acids at VP1 residues 111-112 and 84-85 involved in defining this phenotype. Interestingly, none of the SAT1 and SAT2 viruses acquired a positive charge residue at position 56 of the VP3 protein, reported previously for serotypes O and A during cell culture adaptation (Jackson *et al.*, 1996; Fry *et al.*, 2005). This is likely to be due to divergence of the SAT viruses having eliminated the cryptic GAG site in those viruses.

Cytolytic passages of FMDV in cell culture leads to rapid change in the preference of cell surface molecules for cell entry which is made possible by the selective pressure exerted by the cell surface molecules (Jackson *et al.*, 1996; Sa-Carvalho *et al.*, 1997; Baranowski *et al.*, 1998; Berryman *et al.*, 2013). To understand and exploit the dynamics involved in adaptation of SAT serotype viruses to cell culture, we showed that small, clear-plaque variants of SAT1 and SAT2 viruses are readily selected upon cytolytic passage in cell culture. HSPG usage was

demonstrated by the reduction in the number of plaques in the presence of heparin and the inability of the viruses to infect HSPG deficient cells. Remarkably most mutational patterns that arise during cytolitic passage of SAT viruses increase the net positive charge around the five-fold axis of the virion creating localized patches with the ability to bind a moiety of roughly the same size and charge of a sulphated glycan. Indeed, SAT viruses adopting such a mutation pattern were able to infect CHO-K1 cells, whilst plaque formation in BHK-21 cells was inhibited in the presence of soluble heparin as well as heparinase enzymes.

An increased number of surface positive charges after cytolitic passage in cell culture has been correlated with the ability to infect CHO-K1 cells and the use of HS receptors, and has been observed for a number of diverse virus families. Coxsackievirus A9 (McLeish *et al.*, 2012), Herpesviruses (WuDunn and Spear, 1989; Katsunori *et al.*, 1991), cytomegalovirus (Compton *et al.*, 1993), HIV (Roderiquez *et al.*, 1995; Moulard *et al.*, 2000), pseudorabies virus (Mettenleiter *et al.*, 1990), equine arteritis virus (Asagoe *et al.*, 1997), dengue virus (Chen *et al.*, 1997), porcine reproductive and respiratory syndrome virus (Jusa *et al.*, 1997), classical swine fever virus (Hulst *et al.*, 2000), respiratory syncytial virus (Krusat and Streckert, 1997), Sindbis virus (Klimstra *et al.*, 1998), tick-borne encephalitis (Mandl *et al.*, 2001), vaccinia virus (Chung *et al.*, 1998) and adeno-associated virus (Summerford and Samulski, 1998) have all been reported to select mutants with high affinity for binding to GAGs, especially HS, after repeated passage in cultured cells. For serotypes O and A residues from both VP1 and VP3 contribute to exposed positively charged clusters on the viral capsid (Fry *et al.*, 1999; 2005), and we find an analogous situation for SAT1 and SAT2 viruses with clusters of two to four basic amino acids (lysine or arginine).

The question arises as to whether the structural requirements for HS binding sites on complex protein structures, like FMDV, are created by chance as a result of random mutations or whether a structurally predisposed binding site exists on the capsid (Fry *et al.*, 1999). Analysis of the capsid region of non-HSPG binding strains revealed that a single basic residue, although rare, may occur in the VP1 β D- β E or β F- β G loops of SAT1 and SAT2 viruses; however, on its own it is insufficient to support HSPG interaction. A mutation of a spatially. closely positioned residue, that may be associated with optimization of cell entry will provide a selective advantage and will be strongly selected for (Baranowski *et al.*, 1998; 2000; O'Donnell *et al.*, 2005; Han *et al.*, 2016). VP1 residue positions 111-112 and 84-85 are both unique as they are arranged exposed on the surface close to the five-fold axes. Our data reveals that clustering of

positively charged residues at the 111-112 location enables interaction with HS. This infers that the virus particle has 12 HSPG binding patches, each located at a vertex of the icosahedron.

To confirm an HSPG-binding role for residues at position 111-112, we have recently reported on the construction of two infectious SAT1 genome-length clones, with substitutions of residues 111-112 to positively charged amino acids (Maree *et al.*, 2010; 2011). Both recombinant SAT1 viruses were capable of infecting CHO-K1 cells, suggesting infection via HSPG-binding. This is in agreement to the findings in a type A virus, where a single positively charged substitution at residue 110 of VP1 resulted in the ability to infect CHO-K1 cells (Berryman *et al.*, 2013).

Phenotypic characterization of the recombinant mutants revealed that the SAT2 variants with positively charged residues in VP1 or VP3 surface-exposed loops were able to infect CHO-K1 cells and plaque formation was inhibited by the presence of heparin. The growth of the engineered SAT2 single mutants 158K and 83K in VP1 and 158K in VP3 were completely inhibited by soluble heparin. However, none of these mutants showed any growth advantage on BHK-21 cells, compared to the wild-type chimeric v^{SAU}SAT2 virus. Our results suggest that KRR residues at positions 110-112 of VP1 are the most important residues for cell culture adaptation and expansion of cell tropism for SAT1 (Maree *et al.*, 2010) and SAT2 viruses (Table 2.3). These mutants had enhanced infectivity of BHK-21 cells. The combined K and R residues at positions 83 and 85 of VP1 also extended cell tropism of mutated FMDV and may even enhance infectivity of BHK-21 cells in certain circumstances, as observed for isolates that underwent repeated cytotytic passages on BHK-21 cells. Nevertheless, in mutational studies the v^{SAU}VP1 Δ 83K,85R SAT2 showed poor performance in BHK-21 cells despite the extended cell tropism. This highlights the unique position of residues 110-112 of VP1 as no other amino acid position in the P1 region can generate such a concentration of positively charged residues on the capsid. The interaction between HSPG, its cellular ligands and viruses is mostly electrostatic and the ability to infect CHO-K1 cells is tolerant to either R or K at VP1 position 110-112 (Fromm *et al.*, 1995; Maree *et al.*, 2010; McLeish *et al.*, 2012; Berryman *et al.*, 2013).

It remains possible that other residues contribute to HSPG binding in SAT1 and SAT2 viruses. Examples from our study include the VP1 W87R substitution of SAT1/KEN/5/98 that appeared simultaneously with the VP1 E84K mutation, and VP1 N48K together with the VP1 N111K substitution in SAT1/NIG/5/81. Both are spatially close to the VP1 β D- β E loop and contribute to the positively charged cluster around the five-fold axis. In several cases, the disappearance

of negatively charged amino acids or the appearance of residues with a partial positive charge has been observed in association with lysine or arginine residues. Although we found two examples of positively charged substitutions (VP2 Q74R and E133K) in the shallow depression at the junction of the three major capsid proteins, as described for type A and O viruses (Fry *et al.*, 1999; 2005), the role of these substitutions in the interaction of SAT1 capsids to HSPG is still unclear.

This study further strengthens the knowledge of the molecular mechanisms during expanded cell tropism of SAT viruses. FMDV has been shown to utilize other non-integrin and non-HS receptors (Baranowski *et al.*, 2000; Zhao *et al.*, 2003; Lawrence *et al.*, 2016a). Serotype O and C viruses that lack the RGD motif have been shown to infect HS-deficient cells (Baranowski *et al.*, 1998; Zhao *et al.*, 2003; Chamberlain *et al.*, 2015; Lawrence *et al.*, 2016a; Han *et al.*, 2016). Berryman *et al.* (2013) showed that a single amino acid substitution at VP1-110 (VP1 Q110K) allowed for HS-independent infection of CHO-677 cells. Additionally, Chamberlain *et al.* (Chamberlain *et al.*, 2015) provided evidence that residues in VP2 account for the cell culture adaptation and extended cell tropism of a variant of FMDV. Our results show that two SAT viruses (SAT1/UGA1/97 and SAT2/UGA/2/02) were able to infect CHO-677 (HS⁻) and CHO-745 (HS⁻, CS⁻) cells, indicating cell entry independent of sulphated proteoglycans or α v-integrin attachment. SAT1/UGA1/97 and SAT2/UGA/2/02 infectivity in CHO-K1 cells was also unaffected by the presence of heparin (Table 2.1). SAT1/UGA1/97 had VP2 E133K and VP1 E058K positively charged substitutions occurring together with two other significant surface-exposed changes (L115Q in VP2 and H046N in VP1), whilst SAT2/UGA/2/02 revealed seven amino acid changes with only one positively charged substitution, *i.e.* VP1 E083K (Nsamba, 2015a). Lawrence *et al.* (2016a) demonstrated that FMDV with a VP1 E95K/S96L and an RGD to a KGE substitution in the VP1 β G- β H loop are involved in the interaction with the cell membrane molecule, Jumonji C-domain containing protein 6 (JMJD6) during cell entry. In addition, FMDVs have been shown to utilize the macropinocytosis pathway to invade cells (Han *et al.*, 2016). The proposed macropinocytic pathway involves the binding of FMDV to receptor tyrosine kinases (RTK). In summary, as indicated many years ago by Mason *et al.* (1994), specific receptor mediated conformational changes are not required for FMDV to infect cells, it is sufficient to internalise the particle and provide a modest drop in pH to trigger uncoating.

Adaptation of FMDV to non-host cells, like cultured hamster cells, is a common step to expand the virus cell tropism during the vaccine production process, but is time-consuming and often unsuccessful (Roderiquez *et al.*, 1995; Moulard *et al.*, 2000). Knowledge of the HSPG-binding sites on FMDV and the role HSPG plays in assisting cell entry can be applied in the construction of chimeric viruses containing the symmetrical, positively charged clusters that enable interaction with HSPG. This might aid in avoiding the accumulation of random changes that lead to divergence of the vaccine strain from the virus populations circulating in nature. This study further emphasizes that there is much unknown knowledge regarding FMDV adaptation and cellular receptors for cell entry.

CHAPTER 3

DEVELOPMENT AND VALIDATION OF A FOOT-AND-MOUTH DISEASE VIRUS SAT SEROTYPE-SPECIFIC 3ABC ASSAY TO DIFFERENTIATE INFECTED FROM VACCINATED ANIMALS

****PUBLISHED ARTICLE (APPENDIX A5): Chitray M, Grazioli S, Willems T, Tshabalala T, De Vleeschauwerd A, Esterhuysen JJ, Brocchi E, De Clercq K and Maree FF. (2018). The development and evaluation of a SAT-specific 3ABC DIVA test for Foot-and-mouth disease virus in the Southern Africa context. *J. Virol Methods* **255**: 44-51.**

3.1 Introduction

Foot-and-mouth disease (FMD) is one of several contagious transboundary diseases that can spread rapidly within livestock populations with a devastating effect on the economy of a country or region. The causative agent, FMD virus (FMDV), an *Aphthovirus* in the family *Picornaviridae*, though clinically indistinguishable, exist as seven distinct serotypes (Knowles and Samuel, 2003). The epidemiology of FMD in Africa is unique in the sense that five of the seven serotypes of FMDV [Southern African Territories [(SAT) 1, 2, 3, A and O]], with the exception of types C and Asia-1, occur. Another unique feature is the two different epidemiological patterns in Africa *i.e.* a cycle involving wildlife, in particular the African buffalo (*Syncerus caffer*), and an independent cycle maintained within domestic animals (Vosloo *et al.*, 1996). The presence of large numbers of African buffalo provides a potential source of sporadic spill-over to domestic livestock (Hedger, 1972; Vosloo *et al.*, 1996). Although the precise mechanism of transmission of FMDV from buffalo to cattle is not well understood, it is facilitated by direct contact between these two species. Once cattle are infected they may maintain FMDV infections without the further involvement of buffalo (Dawe *et al.*, 1994). Outbreaks of the disease can cause high mortality of young animals due to myocarditis, as well as decreased production of milk and meat in older animals (Grubman and Baxt, 2004).

Considering the complex epidemiology of FMDV in Africa, in the Southern African Development Community (SADC) emphasis is placed on control rather than eradication of the disease. Countries implement control strategies to separate wildlife and livestock creating areas free of FMD, either through physical separation and movement restrictions or by creating an immunological ‘barrier’ via repeated vaccination of cattle herds potentially exposed to wildlife. The costs of control are substantial and trade restrictions severely affect economies that are reliant on agricultural production (reviewed in Maree *et al.*, 2014).

In southern Africa, where an increase in the incidence of outbreaks in livestock has been experienced over the last 10 years, a fast and reliable assay to distinguish between infected and vaccinated animals is essential in the decision making for the implementation of control measures. Direct detection methods of FMDV, including virus isolation, reverse-transcription polymerase chain reaction (RT-PCR), real-time RT-PCR and nucleotide sequencing are available (Reid *et al.*, 2003; Jamal *et al.*, 2013; Samuel and Knowles 2001, Knowles and Samuel 2003). Secondary detection methods include conventional FMDV enzyme-linked immunosorbent assay (ELISA) such as the liquid-phase blocking ELISA (LPBE), solid-phase competition ELISA (SPCE) and the virus neutralization test (VNT). These are useful for detecting antibodies to the FMDV structural proteins following infection or vaccination (The OIE Manual of Diagnostic Tests and Vaccines for Terrestrial Animals, 2017). In addition, previous studies have shown that serum antibodies specific for the non-structural protein (NSP), 3ABC, is a reliable marker of FMD virus replication in infected cattle (De Diego *et al.*, 1997; Mackay *et al.*, 1998; Sorensen *et al.*, 1998; Brocchi *et al.*, 2006). Thus, this serves as a way to differentiate between FMDV vaccinated and infected animals (DIVA).

A variety of 3ABC ELISA kits, containing expressed 3ABC or 3AB polyproteins in either *Escherichia coli* or *Spodoptera frugiperda* cells using baculovirus, or peptides of the polyprotein are available, which have been validated mostly outside Africa. Additionally, the expressed 3ABC polyprotein or peptides have been derived from the classical “European/South American” types (A, O and C) (Sorensen *et al.*, 1998; Clavijo *et al.*, 2004; Brocchi *et al.*, 2006) or Asia-1 serotype (Sharma *et al.*, 2014). However, the use, development and validation of DIVA tests in a region should take into account factors such as the viruses circulating in the region, in addition to vaccine quality, coverage and economy. The high genetic heterogeneity of the FMDV 3ABC polypeptide of the SAT serotype viruses (Van Rensburg *et al.*, 2002; Nsamba *et al.*, 2015b), prompted us to design a 3ABC ELISA using SAT-derived antigens. In

this study, we developed a SAT-specific NSP-ELISA and compared its performance with those of the commercially available PrioCheck®-NSP, Istituto Zooprofilattico Sperimentale della Lombardia e dell'Emilia Romagna (IZSLER)-NSP ELISA (De Diego *et al.*, 1997 and Brocchi *et al.*, 2006). The PrioCheck®-NSP and IZSLER-NSP are tests that have already been validated; however, in this study, useful information on the comparative performance of the tests as well as essential information on the validity of the two tests and a SAT-specific NSP ELISA in the SADC cattle population for FMDV is provided.

3.2 Materials and Methods

3.2.1 Cloning and expression of SAT2/ZIM/7/83 truncated 3ABC polypeptide

A soluble truncated version of the SAT2/ZIM/7/83 virus 3ABC polypeptide (SAT-Tr3ABC) was generated by removing the coding sequence of the C-terminal 52 amino acid residues of the 3C protease, including critical amino acids in the 3C active site. Sequence-specific primers with 5' and 3' introduced unique restriction enzyme sites (*Kpn*I and *Bam*H1) *i.e.* 5'-ggtaccatggctATTTCCATTCCTTCCCAAAGTCC and 5'-ccaaggatccAACCTTagcCCCAGCGCGGTACGC was utilized in an optimised PCR reaction containing dNTPs, buffer, MgCl₂ and Takara Ex TaqTM enzyme. The *ca.* 1,160 bp amplicon was agarose gel purified and digested with *Kpn*I and *Bam*H1 to allow cloning into the pET29a plasmid.

The SAT-Tr3ABC was cloned into the pET29a (Novagen) expression vector using standard procedures (Sambrook and Russell, 2001) and recombinant plasmids were used to transform competent BL21 *E. Coli* cells by heat shock (Sambrook and Russell, 2001). Expression of the SAT-Tr3ABC protein was induced by isopropyl-B-D-Thiogalactoside (IPTG) according to the pET System Manual (2003), 10th Ed., Novagen. Briefly, 1ml aliquots of Luria broth (LB) containing 100ug/ml of carbenicillin was inoculated with single colonies from the transformation. The inoculant was incubated overnight at 37°C, shaking at 220-250rpm. Thereafter, 500ul of the overnight cultures were inoculated into 10ml LB containing no selection antibiotics and incubated with shaking at 220-250rpm at 37°C until the optical density (OD) was OD₆₀₀~0.5-1.0 (approximately 2 hours). To induce the target protein, IPTG (Roche), was added to the cultures to obtain a final concentration of 1mM and incubated at 37°C shaking at 220-250rpm for 4 hours. To determine the protein expression, the samples were analysed via SDS-polyacrylamide gel electrophoresis (SDS-PAGE) gel. To obtain the soluble fraction of the

protein, the BugBuster™ Protein Extraction Reagent (Novagen) was utilized to lyse the cells. The crude lysate extract obtained was utilized as the SAT-Tr3ABC antigen for the SAT-specific NSP ELISA.

3.2.2 SDS-polyacrylamide gel electrophoresis and Immunoblotting

Crude bacterial lysates were prepared as described, mixed with an equal volume of Protein Solvent Buffer (PSB: 125 mM Tris-HCl [pH 6.8]; 4% [w/v] SDS; 20% [v/v] glycerol; 10% [v/v] 2-mercaptoethanol; 0.002% [w/v] bromophenol blue). Proteins were resolved by 10% (w/v) SDS-PAGE and transferred to Hybond-C nitrocellulose membrane (Amersham Pharmacia Biotech AB) with a semi-dry electro-blotter (SemiPhor, Hoefer Scientific Instruments) using standard protocols (Sambrook and Russell, 2001). The membrane was incubated with a 1:200 dilution of anti-SAT2/ZIM/7/83 infected bovine antisera. After washing, the membrane was incubated with horseradish peroxidase-conjugated mouse anti-bovine monoclonal antibody for detection. Bands corresponding to the *ca.* 37kDa protein were captured onto film and developed in a dark room.

3.2.3 NSP ELISAs

A SAT-specific 3ABC ELISA (SAT2/ZIM/7/83 truncated 3ABC) and two commercially available NSP ELISAs *i.e.* the PrioCheck®- NSP and the IZSLER-NSP 3ABC-monoclonal antibody (MAb) trapping ELISA were profiled against a bovine serum panel.

A detailed test protocol of the PrioCheck®-NSP blocking ELISA (Sørensen *et al.*, 1998) is available on the Thermofisher website. Briefly, the test plates of the kit contained FMDV NSP antigen captured by the coated MAb. The test is performed by dispensing the test samples to the wells of a test plate, after incubation the plate is washed, and the conjugate is added. The results for all samples were expressed as a percentage inhibition (PI) relative to the OD₄₅₀ max and samples showing $\geq 50\%$ inhibition are considered positive.

The IZSLER-NSP ELISA is described in detail in De Diego *et al.*, 1997, with the modification reported in Brocchi *et al.*, 2006. Briefly, this test uses an anti-3A specific MAb coated to the solid phase to trap the recombinant 3ABC polypeptide expressed in *E. coli*. After incubation of test sera the specific antibodies bound to the 3ABC are detected using a peroxidase-conjugated anti-species immunoglobulin. Results are interpreted as percent positivity in

relation to the OD generated by a positive control serum, with the threshold fixed at 10% (or OD serum/OD positive control = 0.1), as per the manufacturer's protocol.

The SAT-NSP ELISA uses the same capturing and detector anti-species immunoglobulin MAb as the IZSLER-NSP ELISA, however the O1 Kaufbeuren 3ABC antigen was replaced with the FMDV SAT2/ZIM/7/83 truncated 3ABC. The SAT-Tr3ABC antigen was used at the pre-determined optimal 1/50 dilution in dilution buffer (1 x PBS pH 7.4, containing 3% non-fat dried milk and 0.05% Tween 20). ELISA plates were washed with PBS containing 0.05% (vol/vol) Tween 20 and the ELISA plates were developed using substrate-chromogen solution, consisting of 4mM 3,3',5,5'-tetramethylbenzidine (Sigma-Aldrich) in substrate buffer (0.1M citric acid monohydrate, 0.1M, tripotassium citrate; pH 4.5) and 0.015% (vol/vol) H₂O₂. The OD was read at 450 nm using a Labsystems Multiskan Plus photometer. The test samples were done in duplicate and the OD value calculated as an average of the two values for each test sample. Thereafter the percentage positivity was calculated by dividing the average test sample value by the average of the strong positive control OD value. The percentage positivity result of 10-14 is considered as a weak positive result, whilst a value ≥ 15 is considered strong positive. Any value < 10 is considered negative.

3.2.4 Serum Panel

A panel of bovine serum samples (n= 1977), obtained from the Agricultural Research Council, Onderstepoort Veterinary Research, Transboundary Animal Diseases (ARC-OVR-TAD), was constituted for the study. The panel consisted of sera from FMD naïve bovines (n=617), bovines vaccinated with a trivalent vaccine containing SAT1, SAT2 and SAT3 antigen (n=1145) and experimentally FMDV infected cattle (samples collected from day 3 to 146 days post-infection from cattle intra-dermolingually challenged with either a SAT1/KNP/196/91, SAT1/NIG/5/81, SAT2/KNP/19/89, SAT2/UGA/2/02 or SAT3/KNP/10/90 virus) (n=215). The vaccinated sera were samples obtained during surveillance in the FMD control zone in the Mpumalanga region of South Africa (Figure 3.1) where the ARC-OVR-TAD confirmed a SAT1 outbreak occurring at that time. This group of sera consisted of 592 cattle that were negative on a SAT1, SAT2 and SAT3 liquid-phase blocking ELISA (LPBE) and therefore was classified into the group designated vaccinated and LPBE negative (VLN). Additionally, from the vaccinated group of sera, 553 were positive on the SAT1 LPBE, which were classified as vaccinated and LPBE positive (VLP). The naïve bovine sera originated from the FMD free Northern Cape region in South Africa (Figure 3.1). Each serum sample was aliquoted in triplicate for the three NSP

assays that were performed. The SAT-NSP was performed at the ARC-OVR-TAD institute in South Africa whilst the IZSLER-NSP was undertaken at the IZSLER institute in Brescia, Italy and the PrioCheck®-NSP kit was completed at the CODA-CERVA-VAR institute in Belgium for all samples.

3.2.5 Comparison of the SAT-NSP ELISA and statistical analysis

Diagnostic test results for the three NSP ELISAs were described using box and whisker plots for unvaccinated cattle sampled from the FMD free zone (naïve), vaccinated cattle sampled during a SAT1 outbreak that were VLN, cattle sampled during a SAT1 outbreak that were VLP, and cattle experimentally infected with one of the three SAT serotypes. Correlation between the diagnostic test results was described by calculating Spearman's rho. Test agreement was evaluated at the recommended positive thresholds by measuring absolute agreement and calculating the kappa statistic. Statistical evaluations were performed in commercially available software (MINITAB Statistical Software, Release 13.32, Minitab Inc, State College, PA, USA and IBM SPSS Statistics Version 23, International Business Machines Corp., Armonk, NY, USA) and results were interpreted at the 5% level of significance.

Sensitivity and specificity of the three NSP ELISAs were analysed using the LPBE results together with subsets of the experimentally infected animals as well as the naïve animal sera where the prevalence of NSP positives in this dataset was 28.9% (n=823). The sensitivity, specificity and accuracy of confidence limits rely on binomial distribution, Youden index confidence limits rely on normal approximation (Wald method for likelihoods) and the AUC (area under the ROC curve) is estimated by trapezoidal method (Simel *et al.*, 1991, Zhou *et al.*, 2002). Confidence intervals for the test sensitivity and specificity were calculated using the Exact method (Clopper and Pearson, 1934). Calculations were performed using the Epi library in the R program (<http://www.rproject.org>, The R Foundation for Statistical Computing, R Version 2.7.2, 2008-08-25).

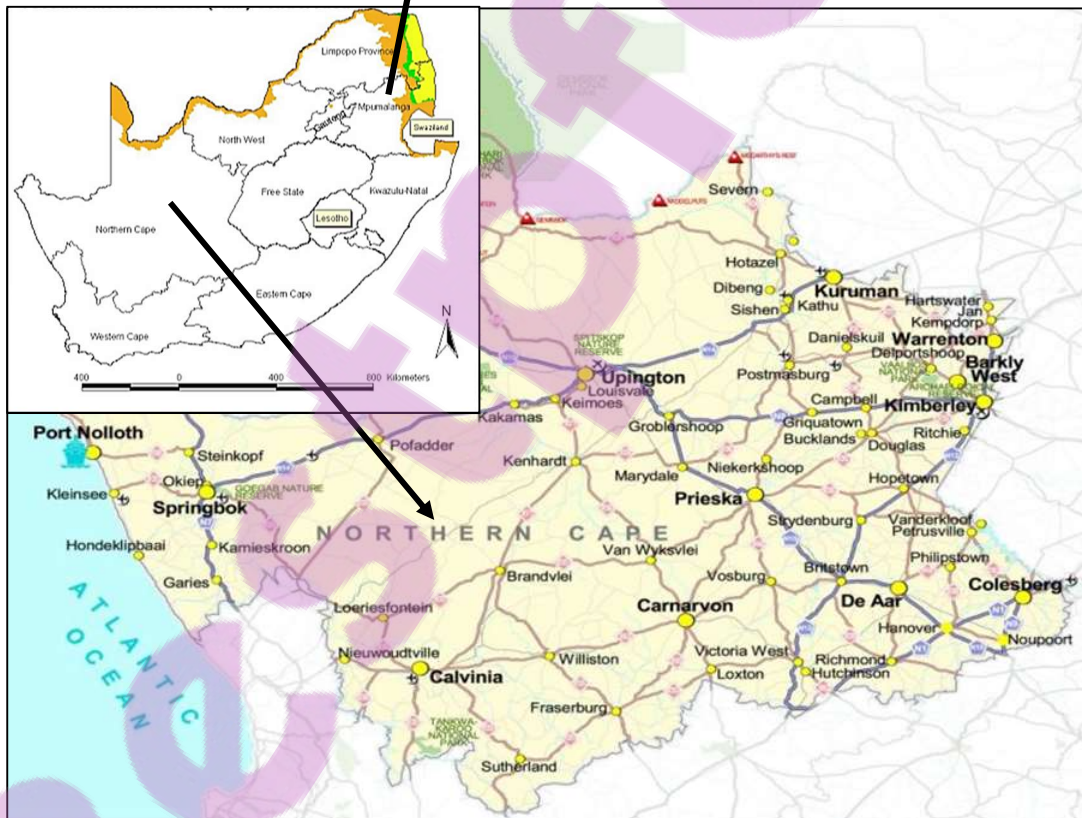
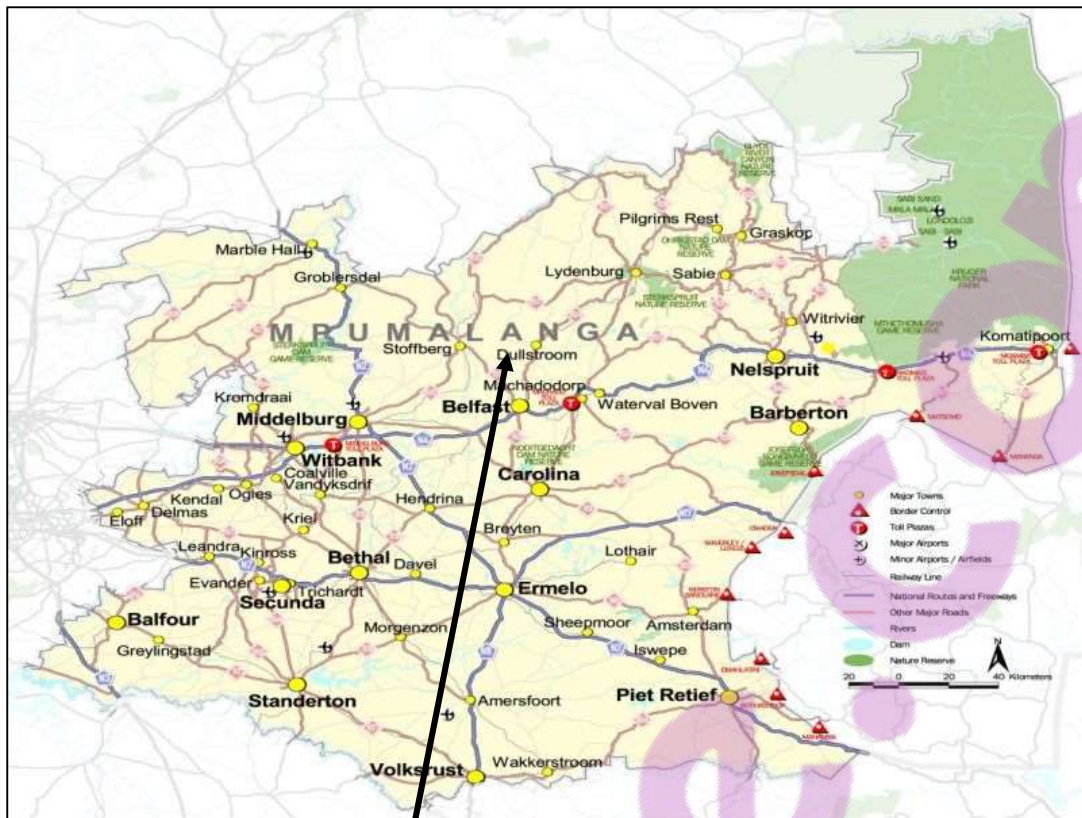


Figure 3.1: Map showing the provinces of South Africa (inset), highlighting the Mpumalanga (top) and Northern Cape regions (below) in detail. The vaccinated group of bovine sera originated from the FMD control zone region of Mpumalanga whilst the naïve bovine sera originated from the Northern Cape region.

3.3 Results

3.3.1 Expression of the SAT-Tr3ABC protein and optimization of the SAT-NSP ELISA

A truncated 3ABC coding sequence was recovered from SAT2/ZIM/7/83 viral RNA by reverse transcriptase PCR and directionally cloned into the pET29a bacterial expression vector. Expression was induced by IPTG and SDS-PAGE analysis (Figure 3.2A) showed an abundant protein of *ca.* 37kDa produced from induced *E.coli* cells. To confirm the integrity of the protein an immunoblot was performed, showing polyclonal sera from SAT2/ZIM/7/83 infected animals specifically react to the SAT-Tr3ABC protein (Figure 3.2B). This crude bacterial lysate was used as the antigen for the SAT-NSP ELISA at a 1:50 dilution.

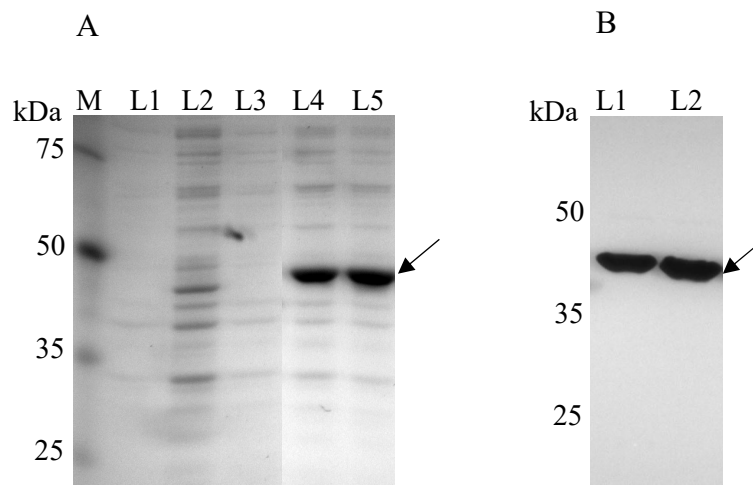


Figure 3.2: (A): SDS-PAGE analysis of the SAT-Tr3ABC protein expression. Lane M is the broad range protein marker (Promega) where the molecular weights are indicated, Lane L1 shows the non-induced, non-recombinant SAT-3ABC protein, L2 is the induced non-recombinant SAT-3ABC protein, L3 is the non-induced recombinant SAT-Tr3ABC protein whilst lanes L4 and L5 indicates successful expression of the recombinant SAT-Tr3ABC protein at *ca.* 37kDa (indicated by an arrow), by two clones. (B) Lanes L1 and L2 shows the western blot analysis of two clones of the expressed SAT-Tr3ABC protein. The position of the protein marker relative to the western blot is indicated.

Experimental samples positive on SAT2 LPBE were used for optimisation of the SAT-NSP ELISA. OD₄₅₀ readings were ~0.3 higher for the IZSLER-NSP ELISA than the SAT-NSP ELISA OD values (data not shown) and were therefore comparable. The OD value for cut off between positive and negative samples were found to be the same for the SAT-NSP and the IZSLER-NSP (De Diego *et al.*, 1997) ELISAs and were taken as an OD₄₅₀ reading of 0.2.

3.3.2 Comparison of the SAT-NSP, IZSLER-NSP and PrioCheck®-NSP kit

The performance of the three NSP ELISAs, presented in the boxplots in Figure 3.3, were compared using 617 naïve cattle sera, 592 VLN sera, 553 VLP sera and 215 sera from cattle experimentally infected with either a SAT1, SAT2 or SAT3 virus (see section 2.4) and LPBE positive. All three NSP ELISAs showed similar results for the naïve sera group, with a few false-positives showing borderline values. Results for the vaccinated groups, originated from an area where a SAT1 outbreak was confirmed, were more variable, although the three assays were in agreement that the majority of VLN and VLP sera was negative for NSP antibodies. For the VLN group, the SAT-NSP and IZSLER-NSP detected 1.6% of the samples NSP positive, comparable to the PrioCheck®-NSP with 0.7%. For the VLP group, the three assays performed similarly, and diagnosed 18.5%, 16.0% and 15.2% as positive for NSP for the SAT-NSP, IZSLER-NSP and the PrioCheck®-NSP, respectively (results not shown). In both VLN and VLP groups, the samples positive to NSP were outliers in each test, ranging up to values significantly higher than the false-positive observed in the naïve group and thus suggesting that these NSP positive samples are true-positive results from animals exposed to infection. The results for the samples of the experimentally challenged group are mostly positive with each NSP-test and distributed over a range of positive values (according to the tests principles and respective thresholds) that reflects variable antibody levels.

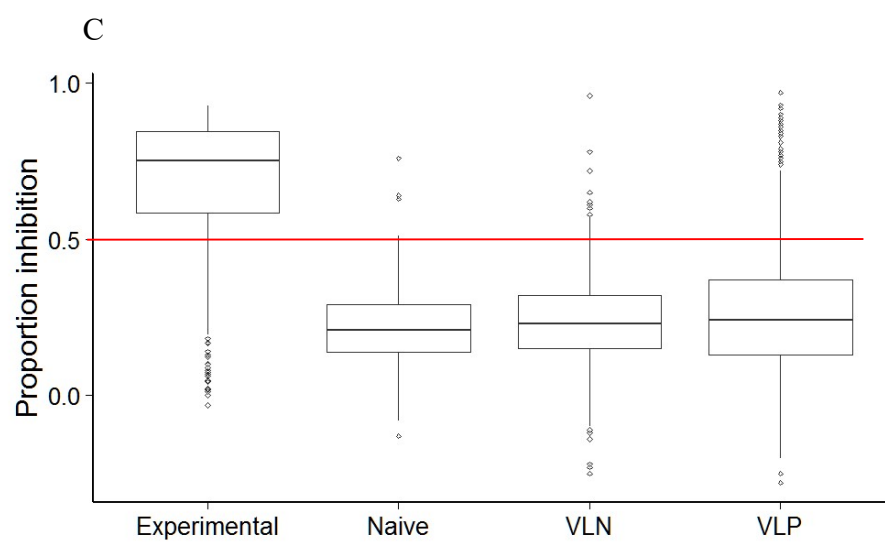
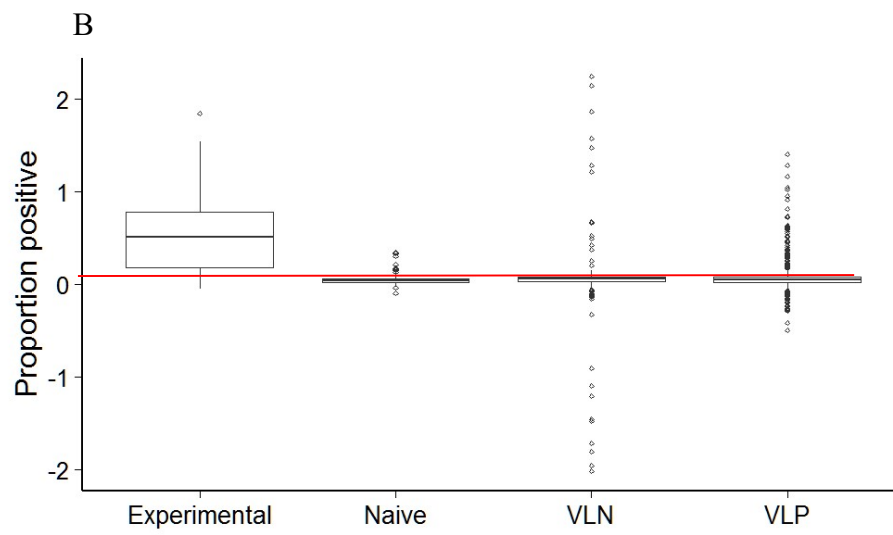
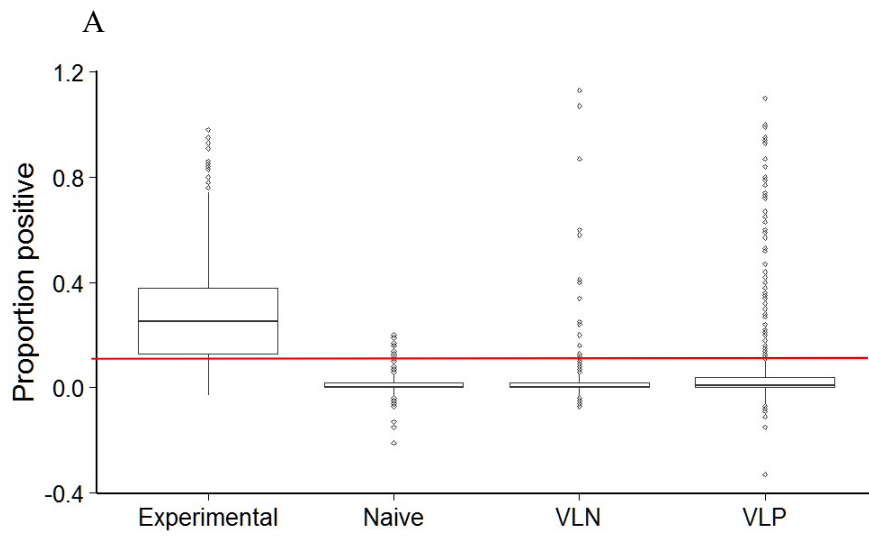


Figure 3.3: Summary of the distribution of results for the (A) IZSLER-NSP, (B) SAT-NSP and (C) PrioCheck®-NSP tests from 617 cattle sampled within the FMD free zone (FMD naïve), 1145 vaccinated cattle sampled during a SAT1 outbreak of which 592 were test negative on a SAT1 liquid-phase blocking ELISA (VLN) and 553 were test positive on a SAT1 liquid-phase blocking ELISA (VLP), and 215 samples collected from FMDV experimentally challenged cattle (Experimental). The positive threshold for the IZSLER-NSP and SAT-NSP tests is 0.1 proportion positive and the PrioCheck®-NSP is considered positive at or above 0.5 proportion inhibition. The thresholds position is indicated by a red line in each graph. Outliers are plotted as individual points *.

The agreement between the three NSP assays as well as the strength of correlation was determined based on the results obtained for the four sera groups/populations (Table 3.1). Results on the three NSP tests were not significantly correlated within the FMD naïve and VLN groups, but there was substantial absolute agreement (> 93%) for all the assays combinations. The correlation among assay results was substantially larger in the VLP group. Correlation among the three NSP assays was strongest in the group of cattle that were experimentally infected but agreement was descriptively similar to what was observed in the VLP group of cattle.

Out of 1145 FMD vaccinated cattle, 1020 had complete test results for the three NSP assays and the SAT1 LPBE. Detailed results on this set of samples are shown in Table 3.2. Forty-seven percent (484/1020) were positive on LPBE but only 11% (110/1020) of them were also positive on one or more of the NSP assays. Taking into consideration the epidemiological scenario in this population, the 374 samples LPBE SAT1 positive and NSP-negative most probably correspond to animals vaccinated but not exposed to infection. Sera with a single NSP test positive, irrespective of the output of the SAT1 LPBE (26 for PrioCheck, 22 for IZSLER-NSP and 27 SAT-NSP out of 1020 tested), can be interpreted as NSP-false positive and reflect the assays specificity performance, as described below. Finally, there are 79 sera with 2 or 3 NSP assays positive, that should be evidence of exposure to infection in these animals. Of them, 50 are concordant positive in the three tests; among the remaining 29 the highest concordance level is observed between IZSLER-NSP and SAT-NSP tests (21 concordant sera), that share the same principle and the same reagents with exception of the antigen derivation.

Table 3.1. Correlation and agreement among three FMD non-structural protein ELISA evaluated in cattle from South Africa.

Sub-population	Test 1	Test 2	rho	P value	Agreement (%)	Kappa	P value
FMD free and unvaccinated n. sera 617	SAT-NSP	PrioCheck [®]	-0.027	0.510	95.8	-0.012	1.0
	SAT-NSP	IZSLER	0.063	0.127	95.1	0.098	0.013
	PrioCheck [®]	IZSLER	0.010	0.804	97.6	0.116	0.001
Vaccinated, LPBE negative n. sera 592	SAT-NSP	PrioCheck [®]	0.129	0.002	95.2	0.317	<0.001
	SAT-NSP	IZSLER	0.020	0.654	96.1	0.441	<0.001
	PrioCheck [®]	IZSLER	0.098	0.023	93.7	0.117	0.033
Vaccinated, LPBE positive n. sera 553	SAT-NSP	PrioCheck [®]	0.218	<0.001	89.9	0.608	<0.001
	SAT-NSP	IZSLER	0.288	<0.001	92.6	0.723	<0.001
	PrioCheck [®]	IZSLER	0.360	<0.001	91.9	0.659	<0.001
Experimental infections* n. sera 215	SAT-NSP	PrioCheck [®]	0.613	<0.001	85.4	0.532	<0.001
	SAT-NSP	IZSLER	0.508	<0.001	85.5	0.574	<0.001
	PrioCheck [®]	IZSLER	0.638	<0.001	92.8	0.777	<0.001

LPBE = liquid-phase blocking ELISA for structural proteins

*Includes all virus serotypes (SAT1-3) and sampling periods

Table 3.2. Cross-classified test results for 1020 FMD vaccinated cattle sampled during a SAT1 outbreak and evaluated using three non-structural protein (NSP) ELISA and a SAT1 liquid-phase blocking ELISA (LPBE) in South Africa.

	NSP assay			LPBE	
	PrioCheck®-NSP	IZSLER-NSP	SAT-NSP	Negative	Positive
1	N	N	N	492	374
2	N	N	P	7	20
3	N	P	N	10	12
4	N	P	P	6	15
5	P	N	N	14	12
6	P	N	P	4	2
7	P	P	N	0	2
8	P	P	P	3	47

N = Negative test result. P = Positive test result.

The diagnostic sensitivity (dsn) (95% CI) and diagnostic specificity (dsp) (95% CI) of the SAT-NSP ELISA was estimated as 76% (70%, 81%) and 96% (95%, 98%), respectively (Table 3.3), which was similar to the IZSLER-NSP ELISA with 78% (72%, 83%) dsn and 98% (96%, 99%) dsp (Table 3.3). The PrioCheck®-NSP, however, exhibited a greater dsn of 82% (77%, 87%) and a greater dsp of 99% (98%, 99%). These results correlated with the AUC_{ROC} of 0.91, 0.88 and 0.86 for the PrioCheck®-NSP, IZSLER-NSP and SAT-NSP respectively (Table 3.3). The accuracies of the three tests were calculated as between 91% and 94% (Table 3.3).

Table 3.3. FMD prevalence and diagnostic accuracy estimates for 823 animals tested with three non-structural protein ELISAs in experimentally infected FMDV cattle and naïve animals.

Population or test	Measure	Median (95% CI)	AUC_{ROC}	Youden Index	Accuracy
PrioCheck [®] -NSP	Sensitivity	0.823 (0.770, 0.867)	0.91	0.82	0.94
	Specificity	0.993 (0.983, 0.997)			
IZSLER-NSP	Sensitivity	0.777 (0.720, 0.826)	0.88	0.76	0.92
	Specificity	0.979 (0.965, 0.988)			
SAT-NSP	Sensitivity	0.760 (0.702, 0.810)	0.86	0.72	0.91
	Specificity	0.964 (0.946, 0.976)			

CI = confidence interval.

The time to first detection of positive NSP antibody responses in animals experimentally infected with FMDV differed for each serotype, but all three ELISAs detected NSP in SAT2-infected cattle at 5 days post infection (DPI) (Table 3.4). Similarly, all three assays detected NSP antibodies at 5-7 DPI with SAT1 or SAT3 viruses with the exception of SAT1/NIG/5/81-infected animal, which was positive at 14 DPI.

Table 3.4. Comparison of NSP ELISA assay detection of 3ABC positive samples from the experimentally infected cattle sera

Serotype	ELISA*	Virus	Animal number	Days post infection							
				0	2	5	7	9	11	14	21
SAT1	PrioCheck®-NSP	SAT1/KNP/196/91	8011	0	ND	2	76	73	76	88	90
	IZSLER-NSP		8011	0	ND	2	21	28	86	84	98
	SAT-NSP		8011	0	ND	9	64	82	83	82	84
	PrioCheck®-NSP	SAT1/NIG/5/81	ZPO2 0805	0	ND	ND	13	0	28	72	74
	IZSLER-NSP		ZPO2 0805	0	ND	ND	0	1	2	23	48
	SAT-NSP		ZPO2 0805	0	ND	ND	5	6	5	51	40
SAT2	PrioCheck®-NSP	SAT2/KNP/19/89	1125	0	25	70	50	69	78	79	82
	IZSLER-NSP		1125	0	2	21	10	29	37	14	21
	SAT-NSP		1125	0	7	16	17	29	33	47	38
	PrioCheck®-NSP		1111	0	35	70	69	75	77	ND	ND
	IZSLER-NSP		1111	0	4	33	35	54	52	ND	ND
	SAT-NSP		1111	0	8	30	40	46	34	ND	ND
SAT3	PrioCheck®-NSP	SAT3/KNP/10/90	0102	0	25	73	84	81	75	81	78
	IZSLER-NSP		0102	0	7	36	54	85	85	74	50
	SAT-NSP		0102	0	4	21	28	67	42	31	28
	PrioCheck®-NSP		1124	0	17	10	59	67	69	68	61
	IZSLER-NSP		1124	0	8	3	33	91	91	95	74
	SAT-NSP		1124	0	7	8	55	72	61	55	51

* Priocheck ELISA results are indicated as % inhibition (>50% = positive), IZSLER-NSP and SAT-NSP results are indicated as % positivity (>10% = positive)

3.4 Discussion

It is essential for countries with FMD outbreaks to regain the advantageous FMD-free status as soon as possible. In order to achieve this, affected countries need to confirm absence of disease and infection in livestock by undergoing clinical and serological surveillance. This makes the use of NSP assays vital. For this study, three NSP assays: one commercially available, one IZSLER in-house assay as well as one in-house assay developed in a South African laboratory, were compared for their ability to detect a marker of FMDV replication. Moreover, this study is unique due to the high number of sera collected from the field, allowing for a more accurate representation of the NSP test performance for South Africa, where a population of both vaccinated and FMDV infected animals co-exist. Additionally, this validation study provides useful information on the comparative performance of three NSP assays and the validity of a particular test result in a given population.

From the investigations of correlation and agreement amongst the SAT-NSP, PrioCheck®-NSP and IZSLER-NSP performances for all cattle sera, the NSP assays performed similarly for the various population groups. However, to expect a flawless performance of the NSP assays is not a realistic assumption, therefore, a small number of false negative and false positive results are likely to occur depending on the FMDV immune status. All three NSP assays had similar high specificity values within the naïve population. The NSP positive results obtained for the vaccinated and LPBE negative group *i.e.* 1.6% for the SAT-NSP and IZSLER-NSP and 0.7% for the PrioCheck®-NSP, could be due to the fact that the NSP ELISA assay can also detect previous exposure to FMDV regardless of the serotype of virus involved (De Diego *et al.*, 1997). Additionally, the occurrence of false-positive results should not be excluded and NSP antibodies may decline in some animals later than the structural protein antibodies (personal communication, E. Brocchi). It is known that the 3ABC antibodies can be detected for up to 1 year after FMDV infection (De-Diego *et al.*, 1997, Kitching 2002, Sørensen *et al.*, 1998), which explains those samples that were found to be LPBE negative, but 3ABC positive. Furthermore, several studies have shown that multiple vaccinations or vaccinations and exposure of cattle to FMD in the control zones neighbouring National Wildlife Parks in southern Africa, revealed a variation in NSP serological incidence (Sammin *et al.*, 2007; Miguel *et al.*, 2013; Jori *et al.*, 2016). Cattle in the communal area neighbouring the Kruger National Park are vaccinated three times per year with a trivalent SAT1, SAT2 and SAT3 vaccine. Lee *et al.* (2006) showed that multiple vaccinations resulted in a significant increase in anti-3ABC antibodies in calves. Additionally, Elnekave *et al.*, 2015, showed that anti-NSP

antibodies persist in naturally infected and repeatedly vaccinated cattle for more than three years.

Several conditions need to be considered related to sensitivity such as the immunological and infectivity status for vaccinated or non-vaccinated animals after infection with FMDV (Brocchi *et al.*, 2006). A relative high estimate for sensitivity was achieved concerning diagnostic accuracy for the PrioCheck®-NSP (82%) whilst the SAT-NSP was 76% and IZSLER-NSP 78%, for the FMDV challenged group, showing that the PrioCheck®-NSP is more accurate for the detection of SAT-specific 3ABC antibodies. Furthermore, taking the kinetics of the immune response to 3ABC into account, the three assays showed the same sensitivity. Antibodies to NSP are found later in the infection cycle (6-8 days post infection) than antibodies to the structural proteins (De-Diego *et al.*, 1997, Bruderer *et al.*, 2004), therefore, sera samples from this study that were found to be FMDV positive on LPBE, may not necessarily be found 3ABC positive on the NSP assay, thus resulting in the higher number of 3ABC negative results found for the challenged group and also for the VLP classified group. Another possibility is that the VLP group of cattle had high antibody titres to FMDV due to immune response to repeated vaccinations, rather than infection, and therefore were found to be LPBE positive. Bruderer *et al.* (2004) describes the heterogeneity found in the 3ABC responses from various experiments in animals vaccinated and then challenged with FMDV, showing that in South African cattle, only 88.9% elicited anti-3ABC antibodies.

Approximately, 50% of vaccinated animals were found to be LPBE negative, most likely due to long inter-vaccination periods (ranging from 4-12 months). Chemically inactivated FMD vaccines induced short-lived antibody responses similar to other inactivated vaccines with antibody levels declining below the detection threshold two months post-vaccination (Hunter 1998; Cloete *et al.*, 2008; Maree *et al.*, 2015; Lazarus *et al.*, 2017). The lack of a sustained immune response beyond four months of vaccination of cattle populations in southern Africa is well documented (Massicame, 2012; Jori *et al.*, 2014).

Parida *et al.* (2005) showed that NSP seroconversion did not occur, despite a four-fold rise in virus neutralizing antibody levels for vaccinated cattle exposed to FMDV-infected, in contact cattle. Furthermore, Bergmann *et al.* (2005) stated that a negative result to 3ABC antibodies cannot be taken as conclusive evidence that a single animal has not been exposed to FMDV, since the animal could be in the seroconversion phase which can be delayed in vaccinated

animals exposed to infection. Thus, this could also explain the 3ABC negative results for the challenged and for the VLP groups in this study.

The ROC analysis was performed to determine the diagnostic accuracy of the three NSP assays in this study, where the accuracy is measured by the area under the curve. In summary, an area under the ROC curve of 1 represents a perfect test thus the closer a result is to 1, the more accurate a test is (Hanley and McNeil, 1982). Therefore, for the PrioCheck®-NSP, IZSLER-NSP and SAT NSP, the area under the ROC curve was 0.91, 0.88 and 0.86 correspondingly, indicating that all three assays were accurate for the detection of SAT 3ABC antibodies.

A limitation of this study included the sample collection and differentiation into the various groupings. It was challenging to collect good quality sera in large numbers and volumes and the VLP and VLN groups of sera were categorised based on the serology data from the ARC-OVR-TAD. Additionally, large numbers of FMDV infected only sera were difficult to source for the validation study and the sera collected *i.e.* the “experimental group” were samples that were collected from animal trials at the ARC-OVR-TAD.

Interestingly, although a high genetic variation has been shown for the FMDV SAT serotypes 3ABC polypeptide (Van Rensburg *et al.*, 2002; Nsamba *et al.*, 2015b); all three NSP kits tested in this study, irrespective of the origin of the 3ABC antigen, has proven to be reliable and accurate for the detection of FMDV SAT 3ABC antibodies. The sensitivity of the SAT-NSP assay was comparable to the other two assays in detecting NSP-specific antibodies from SAT-infected livestock. The commercially available and widely used PrioCheck®-NSP kit proved to be an excellent NSP kit to use for the detection of SAT NSP antibodies whilst the IZSLER-NSP and SAT-NSP performed similarly and has also proven to be an accurate assay for FMDV NSP detection. The SAT-NSP assay is based on a SAT-specific 3ABC polyprotein with a truncation at the C-terminus as the antigen, which is captured onto ELISA plates by the 3A-specific monoclonal antibody used in the IZSLER-NSP ELISA, giving the advantage of using the antigen as a crude extract, thus avoiding laborious purification procedures. The SAT-NSP can be used as an alternative NSP assay to that which is commercially available for routine detection of anti-3ABC antibodies in sub-Saharan Africa for the FMDV SAT serotypes.

CHAPTER 4

NOVEL SINGLE-CHAIN ANTIBODY FRAGMENTS AGAINST FOOT-AND-MOUTH DISEASE SEROTYPE A, SAT1 AND SAT3 VIRUSES USING A NKUKU® PHAGE DISPLAY LIBRARY

4.1 Introduction

Diseases caused by RNA viruses are often difficult to control because of the high mutation rate and the continual emergence of novel genetic and antigenic variants that allow escape from immunity. The degree to which immunity induced by one virus is effective against another is largely dependent on the antigenic differences between them. Foot-and-mouth disease (FMD) virus (FMDV) is an example of an antigenically variable pathogen with a capacity to evade the immune response (Mateu *et al.*, 1988; Martinez *et al.*, 1992; Domingo *et al.*, 1993). Of the seven clinically indistinguishable serotypes, the Southern African Territories (SAT) types FMD viruses display appreciably greater genomic and antigenic variation (Maree *et al.*, 2011).

The antigenic differences within serotypes are mostly contributed by the structural protrusions located in the three surface-exposed capsid proteins of the virus, *i.e.* VP1 to VP3, because the majority of FMDV-neutralizing antibodies are directed against these structural protrusions (Kitson *et al.*, 1990; Acharya *et al.*, 1989; Thomas *et al.*, 1988; Xie *et al.*, 1987). Neutralizing antigenic sites have been identified for serotype A (Thomas *et al.*, 1988; Baxt *et al.*, 1989; Bolwell *et al.*, 1989), O (Kitson *et al.*, 1990; Crowther *et al.*, 1993), C (Mateu *et al.*, 1990) and Asia-1 (Sanyal *et al.*, 1997). However, information regarding the antigenic determinants of SAT serotypes, which are confined geographically to Africa, is scarce (Maree *et al.*, 2014). Mapped SAT2 epitopes include: (i) β G- β H loop of VP1; (ii) residue 210 in the C-terminus of VP1; (iii) VP1 84-86, 109-111, VP2 71, 72, 133, 134 and (iv) VP1 159, VP2 71-72, 133-134, 148-150 (Crowther *et al.*, 1993; Davidson *et al.*, 1995; Grazioli *et al.*, 2006; Opperman *et al.*, 2012; 2014). Four independent antigenic determinants were identified for SAT1 viruses *i.e.* (i) two occurring in the β G- β H loop of VP1; (ii) two simultaneous residues one in VP3 (position

135 or 71 or 76) and one in VP1 (position 179 or 181); (iii) a conformation dependant site with VP1 position 181 and VP2 72 and (iv) VP1 position 111 (Grazioli *et al.*, 2006). To date, no neutralizing sites have been determined for viruses of the SAT3 serotype.

The development of large combinatorial antibody libraries based on antibody genes expressed and displayed on phages have revolutionized the selection and isolation of individual antibodies to an antigen (Smith and Petrenko, 1997). A key advantage of phage display of antibody fragments versus hybridoma technology is that the generation of specific single-chain variable fragment (scFv) or antigen binding fragment (Fab) to a particular antigen can be completed within a few weeks compared to hybridomas taking months. Additionally, the quantity of target antigen required for phage display (micrograms) is much less than what is needed for hybridoma antibody production (milligrams) (Carmen and Jermutus, 2002; Willats, 2002). Antibody libraries can be either immune (from immunised donors) or naïve (from non-immunised donors), where the immune library will have an antibody range restricted to antibodies generated in response to a particular immunogen, although the naïve library can advantageously be used for an unlimited array of immunogens (Van Wyngaardt *et al.*, 2004).

Phage display libraries have been used with success to map epitopes for FMDV for serotype O (Harmsen *et al.*, 2007; Yu *et al.*, 2011) and the SAT2 serotype (Opperman *et al.*, 2012). The Nkuku® phage-display library, which is a large semi-synthetic library of recombinant filamentous bacteriophages displaying single-chain antibody fragments derived from combinatorial pairings of chicken variable heavy and light chains, was used for this study (Van Wyngaardt *et al.*, 2004). This scFv phage display naïve library has been utilised to generate a variety of antibodies against antigens such as the bluetongue virus; African horse sickness virus; echovirus 1; coxsackievirus B3; FMDV of the SAT2 serotype as well as a mycobacterial 16 kDa antigen (Van Wyngaardt *et al.*, 2004; Fehrsen *et al.*, 2005; Rakabe, 2008; Sixholo *et al.*, 2011; Opperman *et al.*, 2012; Nukarinen, 2016). These studies prove that this library is sufficiently diverse for the recognition of a variety of different haptens, proteins and viruses.

FMDV diagnostics is continuously advancing to obtain the most rapid, accurate and reliable assays. Phage libraries have proven useful for the generation of diagnostic reagents detecting influenza virus (Rajput *et al.*, 2015), noroviruses (Hurwitz *et al.*, 2017), recombinant *Plasmodium falciparum* histidine rich protein 2 (Leow *et al.*, 2014), total proteins of *Strongyloides venezuelensis* (Levenhagen *et al.*, 2015) and human immunodeficiency virus

(Haard *et al.*, 2000). The scFvs for diagnostic purposes can bind a variety of antigens *i.e.* haptens, proteins as well as whole pathogens and have been shown to be successful in ELISAs (Luka *et al.*, 2011).

In this study, phage display technology was used to obtain specific scFvs from panning with a FMDV serotype A, SAT1 and SAT3 viruses. The scFvs resulting from the biopanning were investigated in virus neutralization assays and for their prospective use as FMDV diagnostic reagents in an ELISA. Additionally, ELISA data was used to determine r_1 values (relationship coefficient, the value that is used the most to express antigenic match) and antigenic relationships within serotypes. Variable regions on the capsid proteins of SAT1 and SAT3 isolates were combined with structural data to investigate varying ELISA profiles.

4.2. Materials and Methods

4.2.1 Cell cultures, virus propagation and purification

Baby hamster kidney (BHK) strain 21 clone 13 cells (ATCC CCL-10), used for virus propagation and SAT1 and SAT3 serotype neutralization assays, were maintained in Glasgow minimum essential medium (GMEM, Sigma), supplemented with 10% (v/v) foetal bovine serum (FBS, Hyclone), 1× antibiotic-antimycotic solution (Invitrogen), 1 mM L-glutamine (Invitrogen) and 10% (v/v) tryptose phosphate broth (TPB, Sigma-Aldrich). Instituto Biologico Renal Suino-2 (IBRS-2) cells used during virus neutralization tests were maintained in RPMI medium (Sigma-Aldrich) supplemented with 10% (v/v) foetal bovine serum (FBS, Hyclone) and 1 × antibiotics (Invitrogen). The Mycl-9E10 hybridoma (ECACC 85102202) was cultured in protein-free hybridoma medium (Invitrogen).

The SAT1/KNP/196/91 and SAT3/KNP/10/90 FMDV used for the biopanning, originated from buffalo in the Kruger National Park (KNP) in South Africa, isolated during 1991 and 1990 respectively (Table 4.1). Also used for biopanning was the A22 virus (Table 4.1), which was obtained from the Pirbright Institute, UK. The SAT1 and SAT3 viruses were propagated on BHK-21 cells whilst A22 was propagated on IB-RS-2 cells prior to sucrose density gradient (SDG) purification of 146S particles. Virus particles were concentrated with 8% (w/v) polyethylene glycol (PEG)-8000 (Sigma-Aldrich) and purified on 10% to 50% (w/v) sucrose density gradients, prepared in TNE buffer (50 mM Tris pH 7.4, 150 mM NaCl, 10 mM EDTA), as described by Knipe *et al.* (1997). Peak fractions corresponding to 146S virion particles (extinction coefficient $E_{259\text{nm}} [1\%] = 78.8$) were pooled and the amount of antigen (μg) was

calculated as described previously (Doel and Mowat, 1985). In a similar way, viruses utilized for the ELISA assays (Table 4.1) were PEG concentrated, where virus particles were concentrated with 8% (w/v) PEG-8000 (Sigma-Aldrich) and the resulting precipitated pellet was re-suspended in TNE buffer.

Table 4.1: Detailed list of FMDV SAT1, SAT2, SAT3, and A viruses used in this study

FMDV Serotype	Virus strain	Passage History*	Genbank accession number
SAT1	KNP/196/91	PK1RS5	DQ009716
SAT1	KNP/3/03	PK1RS1	KJ999914
SAT1	SAR/33/00	PK1RS2	KJ999908
SAT1	BOT/1/06	PK1RS1	KJ999919
SAT1	SAR/9/03	PK1RS1	KJ999911
SAT1	ZIM/14/98	BTY2RS2	KJ999925
SAT1	SAR/2/10	PK1RS2	KJ999913
SAT1	ZAM/2/93	PK1RS3	DQ009719
SAT1	KNP/10/03	PK1RS2	KJ999916
SAT1	SAR/9/81	B1BHK4B1RS2	DQ009715
SAT1	NAM/272/98	PK2RS1	KJ999921
SAT3	KNP/10/90	PK2RS2	KF647849
SAT3	KNP/14/96	PK1RS1	AY168813
SAT3	SAR/1/06	BHK5 BTY1	N/A
SAT3	KNP/8/02	PK2	N/A
SAT3	BOT/6/98	BTY1RS2	AY258050
SAT3	KNP/2/03	PK1RS1	N/A
SAT3	KNP/1/03	PK1RS1	N/A
SAT3	SAR/14/01	PK1RS2	N/A
SAT3	ZAM/5/93	PK1RS4BHK6	AY168800
SAT3	ZIM/5/91	BTY1RS4	AY168799
SAT3	KNP/6/08	PK1RS1	N/A
SAT3	ZIM/11/94	BTY2RS5	AY168808
SAT2	ZIM/7/83	B1BHK5B2RS2	DQ009726
A	A22/IRAQ	B2/TBTY2BHK2RS2	AY593764
A	A24/CRUZEIRO	B6BHK2RS3BHK3	AJ251476

*PK = Pig kidney cells, RS = Instituto Biologico Renal Suino-2 (IB-RS-2) cells, BTY = Bovine thyroid cells, B = Bovine, BHK = Baby hamster kidney cells, N/A = Not available.

4.2.2 Selection of scFvs against SAT1/KNP/196/91, SAT3/KNP/10/90 and A22

Selection of virus-specific scFvs from the Nkuku[®] phage display library [provided by Dr D.H. du Plessis, Agricultural Research Council (ARC), Onderstepoort Veterinary Research (OVR), Vaccines and Diagnostic Development programme (VDD)] was performed as described by Van Wyngaardt *et al.* (2004) and Opperman *et al.* (2012). Briefly, 2-ml immunotubes (Nunc Maxisorp), after being coated overnight with purified virus (30 µg/ml) was blocked with 2% milk powder (Elite) and incubated with library phage particles (10^{12} - 10^{13} transducing particles). Exponentially growing *Escherichia coli* TG1 cells (Stratagene, USA) were infected with eluted and neutralized phage-displayed scFvs that had bound to the specific viruses before plating on TYE plates supplemented with glucose and ampicillin. Subsequent to overnight incubation, the bacteria were collected and the phagemids rescued by the addition of M13KO7 helper phage. Infected bacterial cells were incubated overnight in $2 \times$ TY medium containing ampicillin and kanamycin. Phage-displayed scFvs were precipitated from the cell-free culture supernatant with one-fifth of the original culture volume of 20% (w/v) PEG-8000 in NaCl and were then suspended in $1 \times$ PBS for use in the next selection round. A total of three such selection rounds were performed. The input and output phages from each selection round was examined for enrichment by performing a titration and for the outputs of each consecutive selection round, a polyclonal ELISA was performed. The soluble monoclonal scFvs from the third selection round was tested for specific binding to SAT1/KNP/196/91, SAT3/KNP/10/90 or A22.

4.2.3 Polyclonal phage ELISA

Van Wyngaardt *et al.* (2004) and Opperman *et al.* (2012) described the polyclonal phage ELISA. In short, sucrose density purified virus (30 µg/ml) of either SAT1/KNP/196/91, SAT3/KNP/10/90 or A22 was used to coat 96-well Maxisorp immunoplates (Nunc) overnight at 4°C. To confirm the specificity of the phage-displayed scFvs to the respective viruses, 2% milk powder (Elite) was used as a blocking reagent and negative control. The PEG-precipitated phage-displayed scFvs, produced at each selection round, were detected with the MA b B62-FE2 (100 ng/ml, Progen Biotechnik) and horseradish peroxidase-conjugated polyclonal rabbit anti-mouse IgG (PO260, Dako). To develop the ELISA plates, substrate/chromogen solution consisting of 4 mM 3,3',5,5'-Tetramethylbenzidine (Sigma-Aldrich) in substrate buffer (0.1 M

citric acid monohydrate, 0.1 M tri-potassium citrate, pH 4.5) and 0.015% H₂O₂ was used. Following 10 min incubation at room temperature, the colour reaction was stopped with 1 M H₂SO₄ and the absorbance values were recorded at an absorbance of 450nm (A_{450nm}).

4.2.4 Monoclonal phage ELISA

Screening of individual phage-positive clones was performed following the third round of panning where individual clones were randomly picked from the titration plates of this selection round and inoculated into a 96-well cell-culture plate (Nunc) containing 2 x TY medium supplemented with 100 µg/ml ampicillin and 2% (w/v) glucose. The bacteria were grown overnight shaking at 30°C. Using a 96-well inoculation device (Sigma: Cat No R-2508), bacterial cells were transferred from the overnight plate to a second plate containing 150 µl of fresh medium per well followed by incubation for 2.5 h at 37°C. Subsequently, 50 µl of medium that contained 2×10^9 pfu/ml of the M13K07 helper phage was added to each well and the plate incubated for 30 min at 37°C without shaking. Thereafter, plates were centrifuged at $600 \times g$ for 10 min, the supernatants were removed and replaced with 150 µl of 2 x TY medium containing 100 µg/ml ampicillin and 25 µg/ml kanamycin prior to incubation overnight at 30°C with shaking. Following centrifugation at $600 \times g$ for 10 min to pellet bacterial cells, the supernatants, which contained the phage-displayed scFvs were removed and mixed 1:1 with 1 x PBS containing 4% (w/v) casein and 0.2% (v/v) Tween-20 prior to undergoing ELISA testing as described in section 4.2.3.

4.2.5 Monoclonal soluble scFv ELISA

The monoclonal soluble scFv ELISA has been described by Van Wyngaardt *et al.* (2004) and Opperman *et al.* (2012). The method is similar to the monoclonal phage ELISA described in section 4.2.4, except that soluble scFvs were induced by adding 2 x TY containing 100 µg/ml ampicillin and 3 mM IPTG instead of rescuing phages with M13. The anti-c-Myc MAb 9E10, expressed from the murine hybridoma Myc1-9E10 (CAMR, UK) and the polyclonal rabbit anti-mouse IgG conjugated to horseradish peroxidase (P0260; Dako) detected the secreted soluble scFvs. ELISA plates were developed as described in section 4.2.3.

4.2.6 DNA sequencing and sequence analysis of phage-displayed scFvs

Positive clones of phagemid DNA resulting from the monoclonal scFv ELISA from selection round three having high ELISA signals, were sequenced [ABI PRISM™ Big Dye™ Terminator

Cycling Ready Reaction Kit v.3.0 (Applied Biosystems)]. The clones were inoculated into 2 x TY medium containing 100 µg/ml ampicillin and 20% (w/v) glucose and phagemid DNA was isolated with a QIAprep® Spin Miniprep Kit (Qiagen) as per the manufacturer's instructions. The OP52 forward primer (5'-CCCTCATAGTTAGCGTAACG-3') and M13 reverse primer (5'-CAGGAAACAGCTATGAC-3'), as well as the ABI PRISM™ Big Dye™ Terminator Cycling Ready Reaction Kit v.3.0 (Applied Biosystems) was used to sequence the single clones (Van Wyngaardt *et al.*, 2004). An ABI 3100 automated sequencer resolved the extension products and all sequences were edited, assembled and translated using BioEdit v.7.0.9 (Hall, 1999) and Sequencher v5.4.6 (Gene Codes Corporation, Ann Arbor, MI, USA) software. Entropy plots for the SAT1 and SAT3 amino acid (aa) virus alignments were constructed using BioEdit v.7.0.9 (Hall, 1999). Hypervariable regions were defined as five or more variable aa positions in a window of 10 aa in the SAT1 and SAT3 virus capsid protein alignments.

4.2.7 Large scale expression and purification of soluble scFvs

Glycerol stocks (150 µl) of selected phage clones were inoculated in 90 ml of 2 x TY medium (16 g/L tryptone, 10 g/L yeast extract, 5 g/L NaCl) containing 100 µg/ml ampicillin and 20% (w/v) glucose and incubated overnight at 30°C with shaking. A 1:10 dilution of the overnight culture was prepared in 800 ml of fresh 2 x TY medium containing 100 µg/ml ampicillin and 20% (w/v) glucose and incubation, with shaking continued for a further 8 hrs after which the bacterial cells were pelleted at 4000 x g for 30 min. All traces of glucose-containing 2 x TY media was removed and the bacterial pellet resuspended in 1 L of 2 x TY media containing 100 mg/ml ampicillin and 1 M IPTG and incubated overnight at 30°C with shaking. The expressed soluble scFv was harvested by pelleting the bacterial cells at 4 000 x g for 30 min.

The bacterial pellets were resuspended in 50 ml of TSA buffer (0.05 M Tris, 0.1 M NaCl, 0.02% NaN₃, 0.02% sodium azide; pH 8.0) and treated with 0.01% (v/v) of 100 mg/ml lysozyme for 30 min at 30°C. Freshly prepared 200 mM phenylmethylsulfonyl fluoride [0.01% (v/v)] in isopropanol was added to the bacterial suspension and the suspension mixed by inverting. The bacterial suspension was sonicated for 3 min (30 sec pulses with 30 sec pauses), where after, the bacterial pellet was collected by centrifugation at 15 000 x g for 30 min and the clear lysate filtered through 0.8 µm and 0.45 µm filters respectively. The anti-*myc*-Sepharose column coupled with 143 mg of 9E10 Mab (prepared by Janine Frischmuth, the National Bioproducts Institute, Biotechnology division, Pinetown, South Africa) was washed

with TSA buffer before the clear lysate (containing soluble scFvs) was loaded through the column via a peristaltic pump. The column was washed with TSA buffer until the spectrophotometer reading at absorbance $A_{280\text{nm}}$ fell below 0.3. Soluble scFvs were eluted from the column with elution buffer (0.1 M glycine, 0.14 M NaCl, pH 2.2) and fractions collected. Peak fractions were pooled and the scFvs dialyzed, for 48 h at 4 °C, in 2 L PBS pH 7.4.

4.2.8 Binding specificity of soluble scFvs

The specificity of the soluble scFvs was tested with an ELISA essentially performed as described in section 4.2.5. ELISA plates were coated in duplicate with 30 µg/ml of purified SAT1/KNP/196/91, SAT2/ZIM/7/83, SAT3/KNP/10/90, A22 or A24 viruses (section 4.2.1) as well as with BHK-21 cell extract, 20% (w/v) sucrose and 2% (w/v) milk powder as negative controls.

4.2.9 Neutralization assays and generation of virus escape mutants

IB-RS-2 cells were used to determine the 50% tissue culture infective dose (TCID₅₀) of A22 (OIE Terrestrial Manual, 2017). Similarly, BHK-21 cells were used to determine the virus titres for SAT1/KNP196/91 and SAT3/KNP/10/90. The resulting virus titres was used to calculate the dilutions subsequently used in the virus neutralization test (VNT).

Virus dilutions containing approximately 500, 50 and 5 infectious particles for SAT1/KNP/196/91, SAT3/KNP/10/90 and A22 were prepared in the appropriate cell medium (RPMI for IB-RS-2 cells and GMEM for BHK-21 cells) and triplicate repeats were applied across a microtitre plate and diluted two-fold down the plate. Virus was incubated for 1 h at 37°C in an atmosphere of 5% CO₂ after undiluted scFvs were added to appropriate wells. A control plate without soluble scFvs was included. BHK-21 cells (for SAT1/KNP196/91 and SAT3/KNP/10/90) in Glasgow minimum essential medium (GMEM, Sigma) and IB-RS-2 cells (for A22) in RPMI medium supplemented with 1% (v/v) FCS and antibiotics (virus growth medium, VGM), with a cell count of 0.3×10^6 cells/ml for both cell lines, was subsequently added to the respective microtitre plates. Incubation of microtitre plates then occurred for 72 h at 37°C and fixation and staining with a methylene blue-formaldehyde stain to allow for inspection of the cytopathic effect, which was scored as a measure of neutralization.

To generate virus neutralization escape mutants, the viruses (SAT1/KNP/196/91, SAT3/KNP/10/90 and A22) were passaged under scFv pressure as described by Crowther *et al.* (1993) and Opperman *et al.* (2012). Equal volumes of *ca.* 25 infectious virus particles (SAT1/KNP/196/91, SAT3/KNP/10/90 and A22) were diluted two-fold in GMEM or RPMI medium on a microtitre plate before being mixed with an equal volume of the respective undiluted scFv, followed by 30 min incubation at 37°C. The virus-scFv complexes were added to either BHK-21 or IB-RS-2 monolayer cells and incubated for 1 h at 37°C. All scFvs were tested. Monolayers were washed twice with GMEM or RPMI (Sigma) medium before VGM containing a 1:50 dilution of scFv was added. Each virus was subjected to four consecutive passages under scFv pressure.

4.2.9.1 Characterization of virus escape mutants

Virus escape mutants were then characterized whereby RNA extraction was performed using the QIAmp viral RNA kit (Qiagen). cDNA was synthesized with SuperScript III first strand synthesis kit (Invitrogen), using the genome specific primer WDA 5'-GAAGGGCCCAGGGTTGGACTC-3'.

The Leader-P1-2A coding region of the escape viruses were amplified using the Expand Long Template PCR System (Roche) and forward primer NCR1 5'-TACCAAGCGACACTCGGGATCT-3' and reverse primer WDA 5'-GAAGGGCCCAGGGTTGGACTC-3'. Briefly, each 50 µl PCR reaction mixture consisted of 3 µl of the first strand cDNA reaction mixture, 0.3 µM of each oligonucleotide, 2.5 U of Expand Long Template DNA polymerase, 1 × Expand buffer, 0.75 mM MgCl₂ and 2 µM of each dNTP. A thermocycler (GeneAmp 9700, Applied Biosystems) was used to amplify and obtain the PCR product. After initial denaturation at 94°C of 2 min, the reactions were subjected to 35 cycles using the following temperature profile: denaturation at 94°C for 20 s, annealing at 55°C for 20 s and elongation at 68°C for 4 min with a final cycle of 68°C for 7 min to complete the synthesis of all strands. To visualize the PCR-amplified products, electrophoresis on a 1% (w/v) agarose (Roche) gel containing 0.5 µg/ml EtBr, using 1 x TAE (40 mM Tris-acetate, 2 mM EDTA; pH 8) electrophoresis buffer was performed. The λ-*Hind*III DNA molecular weight DNA marker (Promega) was used to estimate the size of the amplified DNA fragments. The desired sized amplicons were excised from the agarose gel and purified utilizing the QIAquick gel extraction kit (Qiagen) as per the manufacturer's instructions.

To determine the nucleotide sequence of the gel-purified amplicons, 0.16 μ M of the appropriate oligonucleotide (Table 4.2) and the ABI PRISM Big Dye Terminator Cycling Ready Reaction kit v3.0 (Applied Biosystems) was utilized. The extension products were resolved on an ABI PRISM™ 3100 automated sequencer (Applied Biosystems) and sequences analysed using the BioEdit v.7.0.9 (Hall, 1999) and Sequencher v5.4.6 (Gene Codes Corporation, Ann Arbor, MI, USA) software of the *ca.* 2.2-kb P1-coding region.

Table 4.2: Oligonucleotides used for sequencing the virus escape mutants

Oligonucleotide	*Sequence
L internal	5'GWTACGTCGATGARCC3'
NCR1	5'-TACCAAGCGACACTCGGGATCT-3'
WDA	5'-GAAGGGCCCAGGGTTGGACTC-3'
SEQ 16	5'-GTGGAACAAGCAGAGAGG T-3'
SEQ 18	5'-CAACTGCAACGTCCTTCTC-3'

*In selected oligonucleotides, the abbreviation represents ambiguities *i.e.* W=A or T, R=A or G

4.2.10 Investigation of the SAT1 and SAT3 soluble scFvs as capturing antibodies in an indirect ELISA

The SAT1 and SAT3 soluble scFvs were tested in an indirect ELISA to determine whether it can be used as capturing antibodies in routine testing of suspected FMDV cases. For this ELISA, the panel of viruses detailed in Table 4.1 were used. The PEG concentrated viruses were titrated in a liquid phase blocking ELISA (LPBE; OIE manual, 2017) to determine the optimal dilution where an absorbance value at 450nm (A_{450nm}) of *ca.* one was obtained. The virus dilution of 1:8 was chosen for the scFv ELISA as this was the highest dilution where an $A_{450nm} \sim 1$ (with standard deviation of 0.25) was still obtained for all the viruses tested. The undiluted scFvs (SAT1scFv1 0.03 mg/ml, SAT3scFv1 0.039 mg/ml and SAT3scFv2 0.09 mg/ml) were used to coat 96-well Maxisorp immunoplates (nunc) overnight at 4°C, following which, ELISA plates were washed with wash buffer *i.e.* PBS containing 0.05% (v/v) Tween 20. All ELISA wash steps included washing four times with wash buffer using an automated micro-titre plate washer. As a blocking reagent and negative control, 2% milk powder in 1 x PBS was used to confirm virus-specific scFvs by 1 h at 37°C incubation. Diluted PEG concentrated virus (1:8) was added to the scFv coated plates and incubated for 1 h at 37°C. Following incubation and washing, serotype specific guinea pig antiserum (typing/detecting

antibody, ARC-OVR-VDD) was added (working dilution for SAT1 and SAT2 was 1:100 and SAT3, A and O was 1:50) and plates were again incubated for 1 h at 37°C and then washed. The FMD specific conjugate (rabbit anti-guinea pig IgG conjugated to horseradish peroxidase, ARC-OVR-VDD) diluted at 1:80, was added to respective microtitre plate wells, followed by 1 h at 37°C incubation and washing. ELISA plates were developed using substrate-chromogen solution, consisting of 4mM 3,3',5,5'-Tetramethylbenzidine (Sigma-Aldrich) in substrate buffer (0.1M citric acid monohydrate, 0.1M, tripotassium citrate; pH 4.5) and after 10 min incubation at room temperature, the colorimetric reaction was stopped with 0.015% (v/v) H₂O₂. The A_{450nm} was determined using a Labsystems Multiskan Plus photometer (Thermo Fisher Scientific). The test samples were tested in duplicate and the absorbance calculated as an average of the two values for each test sample. A positive ELISA result was calculated as two-fold the A_{450nm} value of the average negative control.

4.2.11 Investigation of the SAT1 and SAT3 soluble scFvs as detecting antibodies in an indirect ELISA

The SAT1 and SAT3 soluble scFvs from this study were further investigated for their ability to act as a detecting antibody for the FMDV antigen in an ELISA format. Plates were coated with either SAT1, SAT2, SAT3, A or O specific rabbit antiserum. A 1:8 dilution of PEG concentrated virus (Table 4.1) was added to the coated 96-well Maxisorp immunoplates (nunc) and incubated for 1 h at 37°C. Following a wash step with wash buffer *i.e.* 1 × PBS containing 0.05% (v/v) Tween 20, undiluted scFvs (SAT1scFv1 0.03 mg/ml, SAT3scFv1 0.039 mg/ml and SAT3scFv2 0.09 mg/ml) were added and ELISA plates incubated for 1 h at 37°C. Microtitre plates were washed and the soluble scFvs that bound to the FMD antigen were detected with the B62-FE2 monoclonal antibody (100ng/ml; Progen Biotechnik) and horseradish peroxidase (HRP)-conjugated polyclonal rabbit anti-mouse IgG (PO260; Dako). The negative control contained 2% milk powder. The substrate/chromogen solution and A_{450nm} determination was performed as described in section 4.2.8 and a positive A_{450nm} value was considered \geq two-fold the average negative control value. The test samples were tested in duplicate and the absorbance calculated as an average of the two values for each test sample. The LPBE was adapted and essentially carried out in conjunction as a comparison of performance of the scFv detecting ELISA and was undertaken as described in the OIE manual (2017).



The detecting ELISA data was used to determine the scFv titre using the Spearman-Kärber method (Karber, 1931). The percentage positivity for each SAT scFv against the panel of SAT1 and SAT3 viruses was determined followed by the Log₁₀ titre *i.e.*

$$\text{Percentage positivity (PP)} = \frac{(\text{net OD of the two test serum wells})}{(\text{net OD of positive control})} \times 100$$

$$\text{Log}_{10} \text{ Titre} = \frac{\text{PP}}{100} - 0.5 + \log 8$$

Using the Log₁₀ titres, the antigenic relationship (*r*₁ values) between the SAT scFvs and the homologous virus *i.e.* viruses used in the biopanning was determined.

$$r_1 = \frac{\text{Titre of virus tested}}{\text{Titre of homologous virus}}$$

4.2.12 Analysis of SAT1 and SAT3 virus sequences

BioEdit 5.0.9 DNA sequence analysis software (Hall, 1999) was used to align the VP1, VP2, VP3 and VP4 nucleotide sequences of the SAT1 and SAT3 viruses (Table 4.1) where SAT1/KNP/196/91 and SAT3/KNP/10/90 nucleotide sequences respectively were used as the reference sequences. The sequences were translated and entropy plots were constructed using BioEdit 5.0.9 (Hall, 1999) to determine sites of variation within the protein alignments. Entropy values of >1 were taken as regions that are prone to variation as greater entropy corresponds to greater variability at the aa residue position (Caspersen *et al.*, 2002). These regions of chaotropism for the SAT1 and SAT3 virus sequence alignments were plotted onto a SAT1 pentamer (Reeve *et al.*, 2010; Protein Data Bank ID: 2wzr, r2wrsf) using the PyMOL Molecular Graphics System, Version 1.7.4.5 Schrödinger, LLC. Phylogenetic trees were constructed using amino acid sequence alignments using the neighbour-joining (NJ) and minimum evolution (ME) methods included in the MEGA 7.0 program (Kumar *et al.*, 2016). Node reliability was estimated by 1000 bootstrap replications for NJ. FMDV topotypes were categorized utilizing previously published SAT studies (Bastos *et al.*, 2001; 2003a; Vosloo *et al.*, 2005). Pairwise alignments and percentage amino acid conservation and variation was calculated from amino acid alignments in MEGA 7.0 (Kumar *et al.*, 2016).

4.3 Results

4.3.1 Biopanning against FMDV SAT1/KNP/196/91, SAT3/KNP/10/90 and A22

The large semi-synthetic Nkuku® phage display library based on chicken immunoglobulin genes, was panned by exposing the recombinant antibody repertoire to sucrose density gradient

(SDG) purified virions of the FMDV SAT1/KNP/196/91, SAT3/KNP/10/90 and A22. Phage displayed scFvs that bound to SAT1/KNP/196/91, SAT3/KNP/10/90 and A22 were eluted with trimethylamine and a polyclonal phage ELISA was used to evaluate enrichment (Figure 4.1) for each of the three biopannings. The phage outputs from the three consecutive selection rounds were tested and an aliquot of the library prior to panning was included as a non-enriched control (Figure 4.1). Output phages from selection round three resulted in A_{450nm} of 1.05, 1.35 and 2.48 for SAT1/KNP/196/91, SAT3/KNP/10/90 and A22, respectively (Figure 4.1 A, B, C). The Nkuku non-enriched control (selection round 0) produced A_{450nm} results of 0.13, 0.10 and 0.06 for SAT1/KNP/196/91, SAT3/KNP/10/90 and A22 respectively. Thus, the increased A_{450nm} from selection one to selection round three proves that enrichment did occur (Figure 4.1 A, B, C).

Specific phage binders to SAT1/KNP/196/91, SAT3/KNP/10/90 and A22 viruses were selected from single phage clones collected after selection round three and tested in a monoclonal scFv ELISA. Both the phage displayed and soluble scFv formats were tested. A total of 94 clones each for SAT1/KNP/196/91 and SAT3/KNP/10/90 and 188 clones for A22 from selection step three were screened. At least 20 clones expressed phage-displayed scFvs specific to SAT1/KNP/196/91 with ELISA signals more than two-fold greater than that of the negative milk powder control. Furthermore, of these, seven clones secreted soluble scFvs that bound to SAT1/KNP/196/91. Sequencing of the seven clones revealed one unique binder for SAT1/KNP/196/91, designated SAT1scFv1 (Table 4.3), which had seven identical clones ranging in ELISA signals from 1.3 to 1.7. Analysis of the 94 clones for SAT3/KNP/10/90 revealed three clones expressing phage-displayed scFvs specific to SAT3/KNP/10/90, all of which secreted soluble scFvs that bound to SAT3/KNP/10/90. Sequencing of these clones indicated two unique binders designated SAT3scFv1 (one clone, ELISA signal of 0.5) and SAT3scFv2 (two clones, ELISA signal 0.8) (Table 4.3). In addition, of the 188 clones for A22, 25 clones expressed phage-displayed scFvs specific to A22, whilst 9 clones secreted soluble scFvs that bound to A22 and sequencing revealed nine unique binders for A22 designated A22scFv1 to A22scFv9, ranging in ELISA signals from 1.5 to 2.7 (Table 4.3).

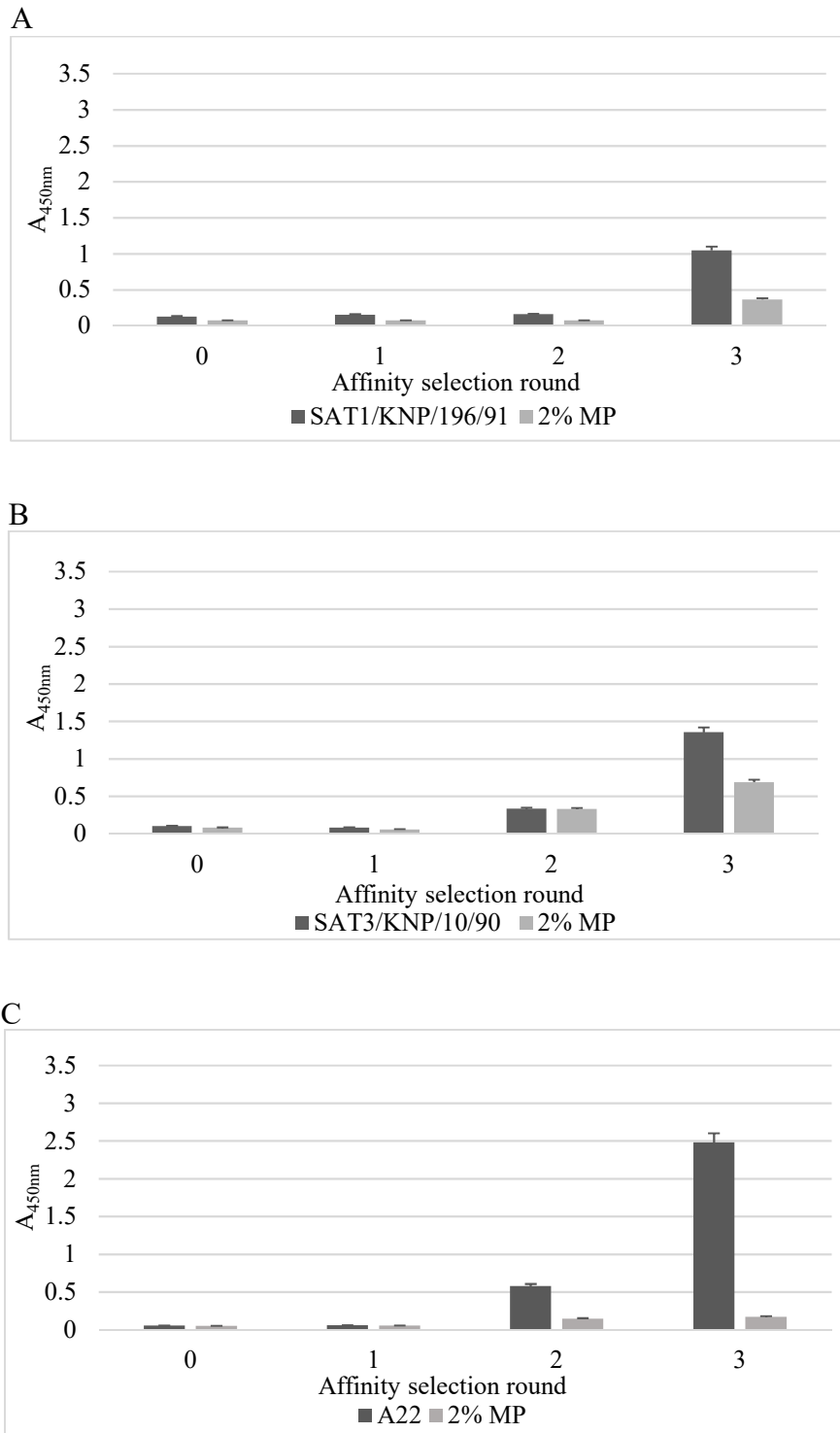


Figure 4.1: Enrichment of phage-displayed scFvs for (A) SAT1/KNP/196/91, (B) SAT3/KNP/10/90 and (C) A22 using a polyclonal ELISA. Phage displayed scFvs that bound to SAT1/KNP/196/91, SAT3/KNP/10/90 and A22 were eluted and enrichment of virus specific phage displayed scFvs (black bars) was determined by a polyclonal phage ELISA of the outputs for three consecutive biopannings. The unpanned aliquot of the Nkuku® phage display library was a non-enriched control (selection round 0). The negative control used was 2% milk powder (labelled 2% MP, grey bars). The data are averages \pm SD of three repeats.

Table 4.3: Amino acid sequence alignment of the complementary determining regions (CDR) of the heavy and light chains of the SAT1/KNP/196/91, SAT3/KNP/10/90 and A22-specific soluble scFvs panned from the Nkuku® library.

scFv	Heavy Chain			Light chain		
	Complementary Determining Region			Complementary Determining Region		
	CDR1	CDR2	CDR3	CDR1	CDR2	CDR3
SAT1scFv1	SSHGMF	EITN--TGSYAAYGAAV	CAKSSYEECTSSCWGNTGWID	SGDSSG----YGYG	YNNNKRPS	GTED-GITDAGI
SAT3scFv1	SSNGMA	AISSRD-GSGTGYGSAV	CAKPVKGM-----ID	SGGTYYA-----	YDNTNRPS	GAYDSS-TYAGI
SAT3scFv2	SSFNMG	AINND--GGGTAYGSAV	CAKSVDDSWNV-----DSID	SGGGSYAGS-YYYG	YDNTKRPS	GSYDSS---GGI
A22scFv1	SSYSMQ	GIGS--DGSdTAYGAAV	CTKCGYGGG-GYCWYAGDID	SGGGNE-----YG	YWNDRKPS	GSYDSSA---GI
A22scFv2	SSYEMQ	GIEN--DGSNPNYGAAV	CAKSAYGGSWGGYIPTDSID	SGG-SSS----YYG	YDNTNRPS	GSFDSSTTV-GI
A22scFv3	SDYAMG	GIGTSADGSSTAYGAAV	CTRIGAAE-----DID	SGG-SSS----YYG	YANTNRPS	GSSDSTY--VGI
A22scFv4	SSHGMG	SISR--DSSYTDYGPVAV	CTKSAGPYVNGDN-----ID	SGGGRYAGNYYYYG	YSNNQRPS	GSADSNSTDGVT
A22scFv5	SDYGMS	EITND--DSWTGYGAAV	CAKNDYYSLF-----ID	SG--DSN--YYGYS	YDNDRKPS	GSADSSA---VI
A22scFv6	SSFNMG	AINND--GGGTAYGSAV	CAKSVDDSWNV-----DSID	SGGGSYAGS-YYYG	YDNTKRPS	GSYDSS---GGI
A22scFv7	SSYGMG	GIEN--DGRYTGYGSAV	CAKDIYG-VGGGAFGADTID	SGG-SYS-----YG	YDNTNRPS	GSIDSSY-V-GI
A22scFv8	SSYSMQ	GIGS--DGSdTAYGAAV	CTKCGYGGG-GYCWYAGDID	SGGGG-----YYG	YSNNQRPS	GSYDNSA---GI
A22scFv9	SSYPMG	AISN--DGSYTGYGAAV	CAKDAYSYTTTGGWYVDEID	SGGGG-----YYG	YDNTNRPS	GGIDSTD---AA

Interestingly, sequencing revealed that SAT3scFv2 and A22scFv6 had an identical sequence in all three of the CDR's for the heavy and light chains and are essentially the same binder (Table 4.3). However, it must be noted that these biopannings were executed independently of each other and at different times and thus the possibility of cross-contamination is ruled out. The result inferred that the SAT3scFv2 and A22scFv6 binders recognize a conserved aa motif on both SAT3/KNP/10/90 and A22 viruses. The soluble scFvs were subsequently successfully purified by means of affinity chromatography (Table 4.4) and further characterized.

Table 4.4: Concentration of post-dialysed scFv's for SAT1/KNP/196/91, SAT3/KNP/10/90 and A22 binders.

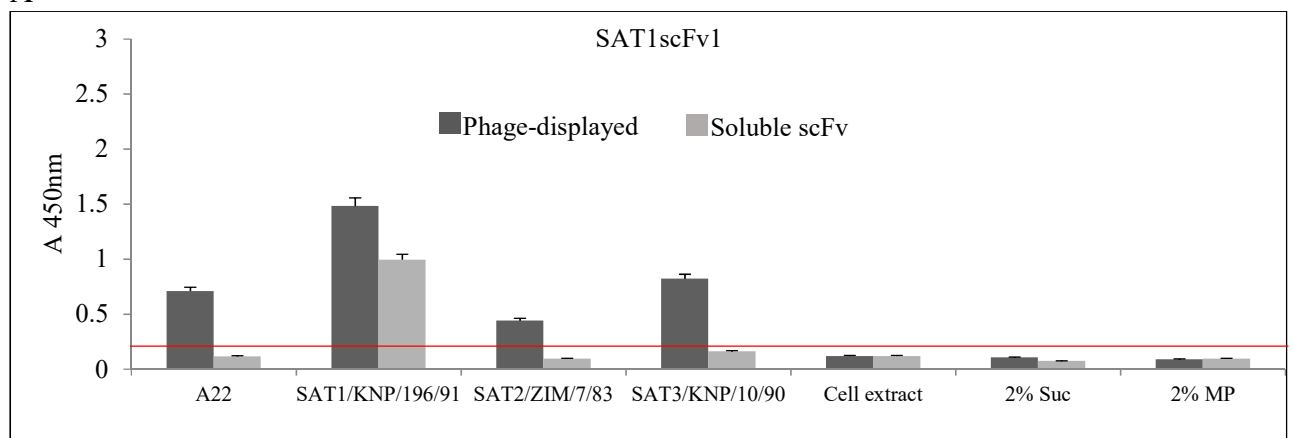
scFv	Purified concentration (mg/ml)
SAT1scFv1	0.03
SAT3scFv1	0.039
SAT3scFv2	0.09
A22scFv1	0.16
A22scFv2	0.23
A22scFv3	0.11
A22scFv4	0.08
A22scFv5	0.18
A22scFv6	0.04
A22scFv7	0.06
A22scFv8	0.18
A22scFv9	0.06

4.3.2 Binding specificity of soluble scFvs to FMDV

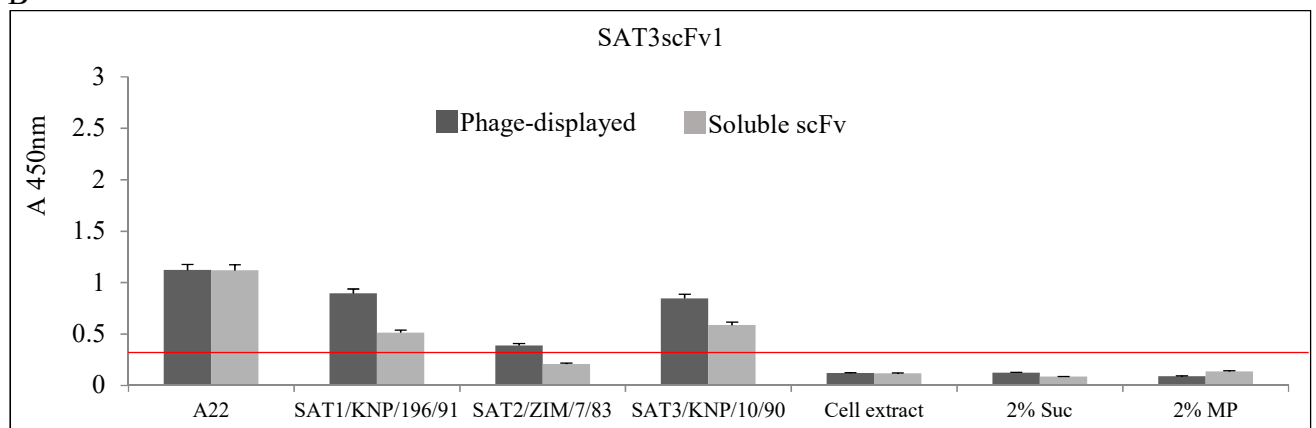
The specificity of the soluble scFvs (Table 4.3, 4.4) were determined by measuring their ability to bind to complete 146S virions of viruses from serotypes A, SAT1, SAT2 and SAT3. A specificity ELISA was performed using SDG purified A22, A24, SAT1/KNP/196/91, SAT2/ZIM/7/83 and SAT3/KNP/10/90 viruses. Also included in the specificity ELISA was BHK-21 cell extract as well as 2% sucrose and milk powder as negative controls to verify absence of non-specific reactions. Cross-reactivity was observed for the SAT1, SAT3 and two of the A22 binders from this study (Figure 4.2). SAT1scFv1 phage-displayed binder cross-reacted with A22, SAT2/ZIM/7/83 and SAT3/KNP/10/90, however, the soluble scFv did not exhibit cross-reactivity (Figure 4.2A). SAT3scFv1 phage-displayed and soluble scFv cross-reacted with A22 and SAT1/KNP/196/91 whilst there was borderline cross-reactivity with SAT2/ZIM/7/83 observed for the phage-displayed scFv (Figure 4.2B). The SAT3scFv2 and A22scFv6 have identical heavy and light chain complementary determining regions (CDRs)

aa sequences and the cross-reactivity between SAT3scFv2 and A22 as well as A22scFv6 and SAT3/KNP/10/90 was observed with both the phage-displayed and soluble scFv (Figure 4.2C, E). SAT3scFv2 phage-displayed scFv also cross-reacted with SAT1/KNP/196/91, whereas the soluble scFv did not cross-react (Figure 4.2C). A22scFv5 soluble scFv showed cross-reactivity to A24 virus and for the phage-displayed scFv, borderline cross-reactivity was observed (Figure 4.2D). There was no cross-reactivity observed with the A22scFv1, A22scFv2, A22scFv3, A22scFv4, A22scFv7, A22scFv8 and A22scFv9 binders with SAT1/KNP/196/91, SAT2/ZIM/7/83, SAT3/KNP/10/90 or A24 viruses. No cross-reactivity was observed with the reagents used for virus propagation and purification.

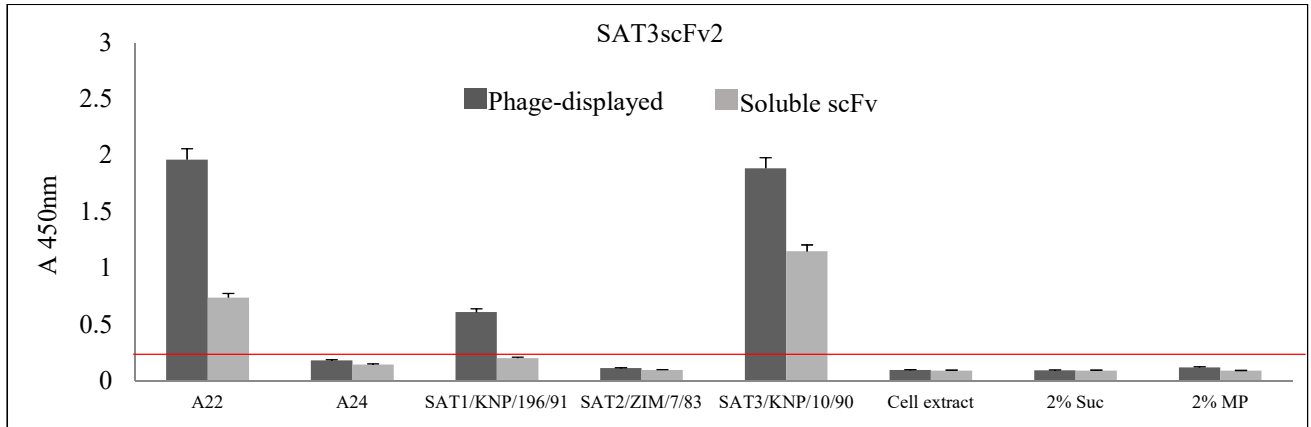
A



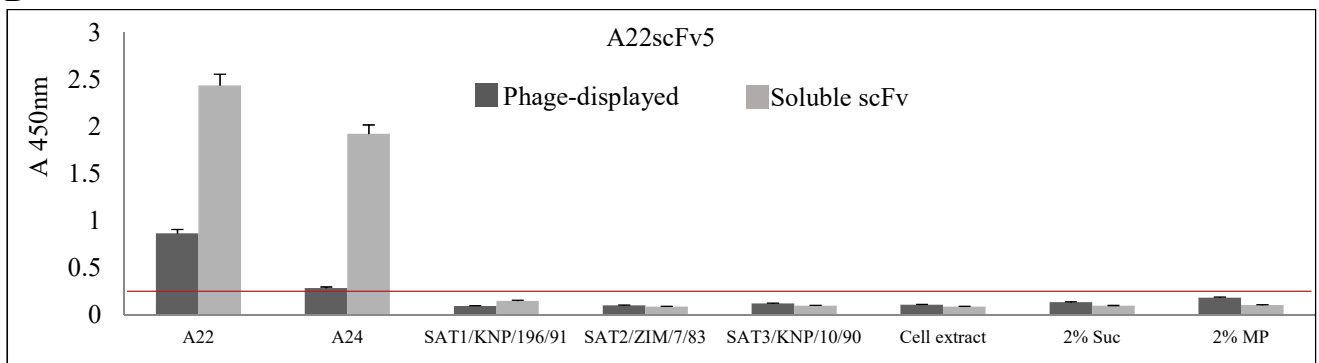
B



C



D



E

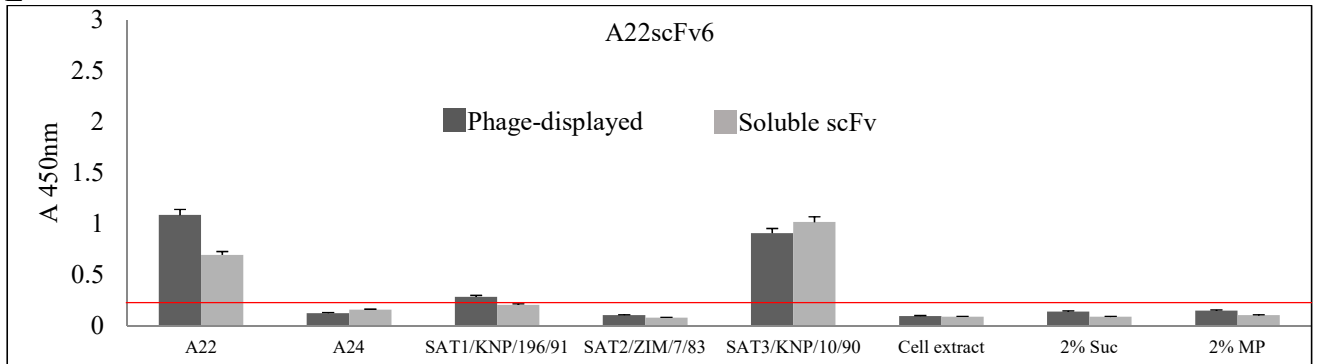


Figure 4.2: Indirect ELISA showing the specificity of scFvs *i.e.* (A) SAT1scFv1, (B) SAT3scFv1, (C) SAT3scFv2, (D) A22scFv5 and (E) A22scFv6. The remainder of the A22 scFv phage and soluble binders only reacted to A22 with no significant reaction to any of the other viruses or reagents (data not shown). Absorbance was measured at A_{450nm}. FMDV A22, A24, SAT1/KNP/196/91, SAT2/ZIM/7/83, SAT3/KNP/10/90 SDG purified viruses as well as BHK-21 cell extract, 2% sucrose (suc) and 2% milk powder (MP) was tested. The black bars indicate the phage-displayed scFvs whilst the grey bars indicate the soluble scFv tested. An ELISA signal two-fold that of the 2% MP soluble scFv absorbance was considered a positive result and the cut-off is indicated by a red line. The data are means \pm SD of three repeats.

The specificity investigations of the scFvs showed that the phage-displayed scFvs exhibited more prominent cross-reactivity when compared to the soluble scFvs. Due to this, further investigations for this study was continued with the soluble scFvs.

4.3.3 Neutralization and escape mutant investigations of the identified scFvs

The ability of the SAT1, SAT3 and A22 soluble scFv's to neutralize the SAT1/KNP/196/91, SAT3/KNP/10/90 or A22 viruses, respectively, *in vitro* was investigated. It was observed that SAT1scFv1 was unable to neutralize FMDV SAT1/KNP/196/91. Similarly, SAT3scFv1 and SAT3scFv2 soluble scFv binders were unable to neutralize the SAT3/KNP/10/90 virus. Additionally, A22scFv6, being essentially the same binder as SAT3scFv2, was unable to neutralize A22 virus *in vitro*. Nonetheless, three of the nine A22 soluble scFv binders, *i.e.* A22scFv1 (0.16 mg/ml), A22scFv2 (0.23 mg/ml) and A22scFv8 (0.18 mg/ml), were able to neutralize A22 *in vitro*. The neutralization titres (TCID₅₀) are indicated in Table 4.5.

Table 4.5: The 50% tissue culture infectious dose (TCID₅₀) of A22 when neutralized by the A22 scFvs

scFv*	Neutralization titre (TCID ₅₀ /50µl)
A22scFv1	0.5
A22scFv2	0.63
A22scFv8	0.63

* Titre of A22 (without scFvs) was TCID₅₀/50µl 1.25

FMDV A22 was serially passaged in the presence of soluble A22scFv1, A22scFv2 and A22scFv8 to select viruses from the A22 quasispecies population that escape neutralization by the soluble scFvs. Thus, the A22 viruses that escaped neutralization by soluble scFvs A22scFv1, A22scFv2 and A22scFv8 were designated scFv resistant virus (SRV) 1, 2 and 3 respectively. Following four consecutive passages under scFv pressure, the P1 nucleotide and aa sequences were determined for SRV1, SRV2 and SRV3. Comparative analysis of the aa sequences of the SRVs compared to the parental A22 sequence indicated that SRV1 exhibited one aa substitution *i.e.* a change from a non-polar proline (Pro) to a polar serine (Ser) change at VP1 aa position 149 *i.e.* RGD+3 (Pro149→Ser) (Figure 4.3). Interestingly SRV2 had no aa changes occurring in the P1 region, but SRV3 exhibited a single aa substitution of a leucine (Leu) to a phenylalanine (Phe) at position 150 of VP1 *i.e.* RGD+4 (Leu150→Phe) (Figure

4.3). The aa substitutions for SRV1 and SRV3 occurred in the surface exposed and structurally flexible VP1 β G- β H loop, downstream of the RGD sequence.

A

	135	140	150	160
A22	KYSAG	GTGR	<u>RGD</u>	LGP LAARVAAQLP ASFNFGAIQA
SRV1	KYSAG	GTGR	<u>RGD</u>	<u>LGS</u> LAARVAAQLP ASFNFGAIQA
SRV2	KYSAG	GTGR	<u>RGD</u>	LGP LAARVAAQLP ASFNFGAIQA
SRV3	KYSAG	GTGR	<u>RGD</u>	<u>FAARVAAQLP</u> ASFNFGAIQA

GH-loop

B

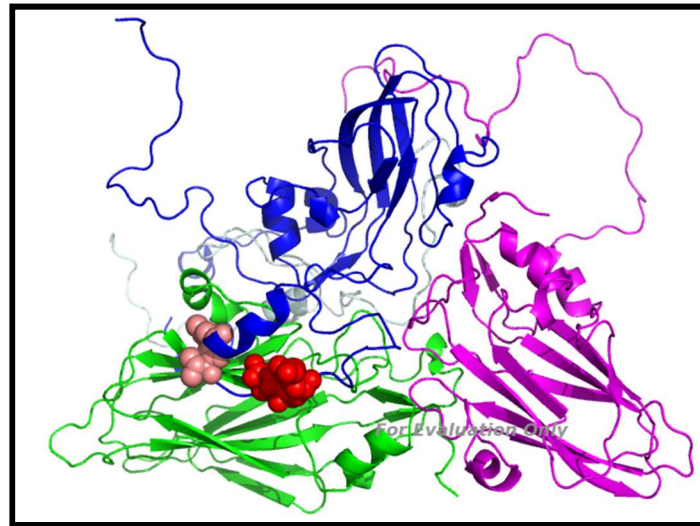


Figure 4.3: (A) The A22 virus escape mutant substitutions are indicated in an aa alignment of the VP1 GH-loop of A22. The aa alignment indicates the proline to serine (Pro149→Ser) substitution at position 149 of VP1 for SRV1 and a leucine to a phenylalanine (Leu150→Phe) substitution at position 150 of VP1 for SRV3 (bold and underlined). The RGD motif is blocked. (B) The substitutions are shown on the model of FMDV capsid proteins forming a crystallographic protomer. The aa substitutions are indicated in the salmon colour whilst VP1 is dark blue, VP2 is green, VP3 is magenta and the RGD sequence is shown in red.

The A22 virus was successfully neutralized by three soluble scFvs and SRVs for A22, showed a potential binding site for two of the scFvs in the GH-loop of the VP1 protein. However, SRV alone did not solve the binding footprint of the A22scFv1 and A22scFv8. It is reasonable to expect different binding footprints on the virion for the two scFvs even though they have a common binding site at VP1 aa position 149/150, since the three CDRs of the L-chain of A22scFv1 and A22scFv8 displayed different sequences (Table 4.3). The three CDRs of the H-chain of A22scFv1 and A22scFv8 are identical. Soluble scFvs for SAT1/KNP/196/91 and

SAT3/KNP/10/90 viruses did not neutralize the respective viruses. Thus, the SAT1 and SAT3 scFvs were investigated for its potential use as diagnostic reagents in an ELISA. Additionally, the reactivity profiles in the ELISA were used together with sequencing data to predict regions affecting scFv-virus binding.

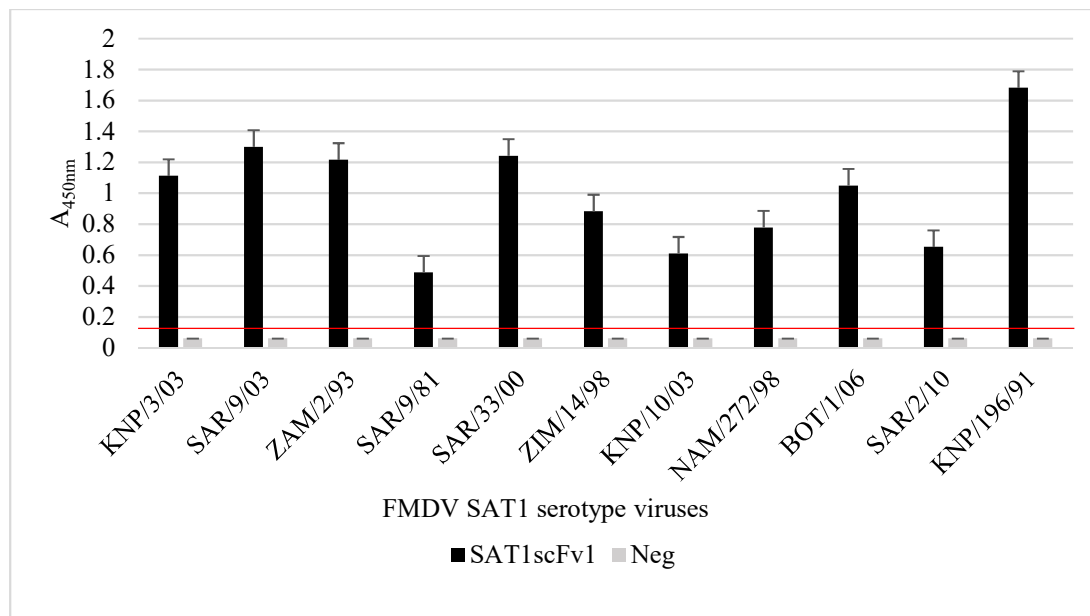
4.3.4 SAT virus-specific scFvs as a FMDV capturing antibody in a sandwich ELISA

To determine whether the SAT1 and SAT3 soluble scFv's retain the correct conformation to act as capturing reagents in a diagnostic sandwich ELISA, the soluble scFvs were coated directly onto maxisorp ELISA plates. The antigen-binding activity of the immobilized soluble SATscFv1 was tested against a panel of FMD SAT1 (n=11) viruses whilst soluble SAT3scFv1 and SAT3scFv2 was tested against a panel of SAT3 (n=12) viruses (Table 4.1). The panel of viruses were PEG concentrated and a 1:8 dilution of the viruses was used as the antigen in the sandwich ELISA where plates were coated with either undiluted SAT1scFv1 (0.03 mg/ml), SAT3scFv1 (0.039 mg/ml) or SAT3scFv2 (0.09 mg/ml).

The results revealed that soluble SAT1scFv1 successfully captured the panel of SAT1 viruses tested as ELISA signals of $A_{450\text{nm}} \geq 0.48$ and ≤ 1.68 were obtained (Figure 4.4A). Weak positive $A_{450\text{nm}}$ of >0.4 , <0.9 was observed when SAT1scFv1 captured SAT1/SAR/9/81, SAT1/ZIM/14/98, SAT1/KNP/10/03, SAT/NAM/272/98, and SAT1/SAR/2/10 (Figure 4.4A). Additionally, strong positive signals $A_{450\text{nm}} >1$, <1.7 for SAT1/KNP/3/03, SAT1/SAR/9/03, SAT1/ZAM/2/93, SAT1/SAR/33/00, SAT1/BOT/1/06 and SAT1/KNP/196/91 was observed when SAT1scFv1 was the capturing reagent (Figure 4.4A).

SAT3scFv1 and SAT3scFv2 soluble scFvs did not react as efficiently when utilized as a capturing reagent with the SAT3 viruses tested and displayed $A_{450\text{nm}}$ signals not significantly higher than the negative controls. Weak positive results were obtained for SAT3scFv1 with SAT3/KNP/6/08 ($A_{450\text{nm}}$ 0.6) (Figure 4.4B). SAT3scFv1 showed similar reactivity to SAT3/BOT/6/98 ($A_{450\text{nm}}$ 0.31), SAT3/KNP/1/03 ($A_{450\text{nm}}$ 0.31) and SAT3/ZIM/11/94 ($A_{450\text{nm}}$ 0.40) viruses indicating this scFv may recognize the same epitope on the virion for these viruses (Figure 4.4B). Additionally, absorbance values of both the SAT3 scFvs in the capturing ELISA against the virus used for the panning *i.e.* SAT3/KNP/10/90 was <0.2 .

A



B

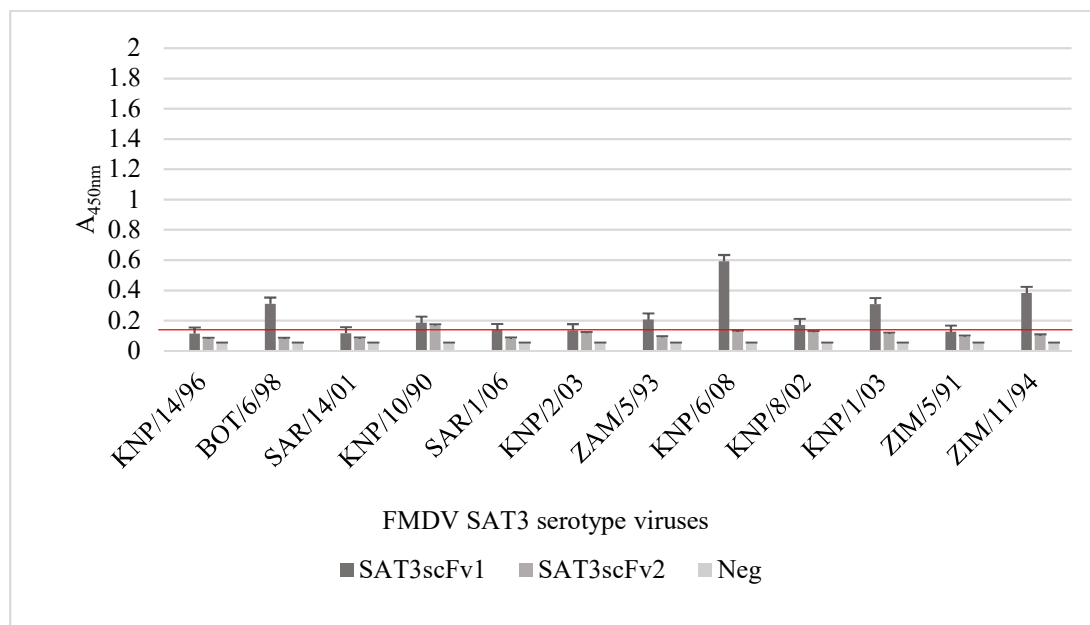


Figure 4.4: A sandwich ELISA with soluble scFvs as capturing antibodies. The SAT1scFv1 was tested with PEG concentrated SAT1 viruses (A) and SAT3scFv1 and SAT3scFv2 was tested with the SAT3 viruses (B). For the negative control (neg), 2% milk powder was included in the assays replacing the soluble scFvs coating the plate. The data are means \pm SD of two independent experiments. An ELISA signal more than two-fold that of the negative control A_{450nm} was considered a positive result and the cut-off is indicated by a red line.

Overall, the ELISA results using the scFvs as capturing reagents indicate that the soluble SAT1scFv1 was able to successfully bind to the polystyrene ELISA plate and react to viruses within the SAT1 serotype. The SAT3scFv1 and SAT3scFv2 exhibited no or borderline reactivity with the SAT3 viruses tested. The low signals may be attributed to the conformational changes of the scFvs when binding to the ELISA plate. Furthermore, differences in the viral proteins may result in the variable ELISA signals observed.

4.3.5 SAT virus-specific scFvs as a FMDV detecting antibody in an ELISA

The soluble scFvs, SAT1scFv1, SAT3scFv1 and SAT3scFv2, were investigated to be used as detecting antibodies in a sandwich ELISA. FMD virus was captured by polyclonal rabbit antiserum and the soluble scFvs was used to detect the 146S virus particles. SAT1scFv1 was tested against the SAT1 viruses whilst SAT3scFv1 and SAT3scFv2 were tested against SAT3 viruses indicated in Table 4.1. As indicated in section 4.3.4, a dilution of 1:8 of all the PEG concentrated SAT1 and SAT3 viruses were used in the ELISA whilst the scFvs were applied undiluted. The standard diagnostic sandwich ELISA used for antigen detection (OIE manual, 2017) was undertaken concurrently as a comparison of the scFv ELISA performance.

Results showed that the diagnostic antigen detection ELISA was able to detect all viruses tested and produced positive ELISA signals (Figure 4.5A, B). The ELISA assay using SAT1scFv1 as a detecting antibody revealed two characteristic reactivity profiles against the panel of SAT1 viruses, *i.e.* (i) $A_{450\text{nm}} > 1.4$ was observed for SAT1/SAR/9/03, SAT1/KNP/196/91 and SAT1/NAM/272/98 viruses and (ii) an $A_{450\text{nm}}$ absorbance value of ≥ 0.4 , ≤ 0.82 for the remaining eight SAT1 viruses in the panel (Figure 4.5 A).

The soluble SAT3scFv1 and SAT3scFv2 showed low absorbance signals for the SAT3 viruses tested (Figure 4.5B). Detectable absorbance signals ($A_{450\text{nm}}$) of 0.76 and 0.84 was observed for SAT3/KNP/10/90 and SAT3/KNP/6/08 respectively when SAT3scFv1 was the detecting antibody in the ELISA. All other $A_{450\text{nm}}$ values were below 0.26 for the SAT3 viruses tested with SAT3scFv1 and SAT3scFv2 (Figure 4.5B).

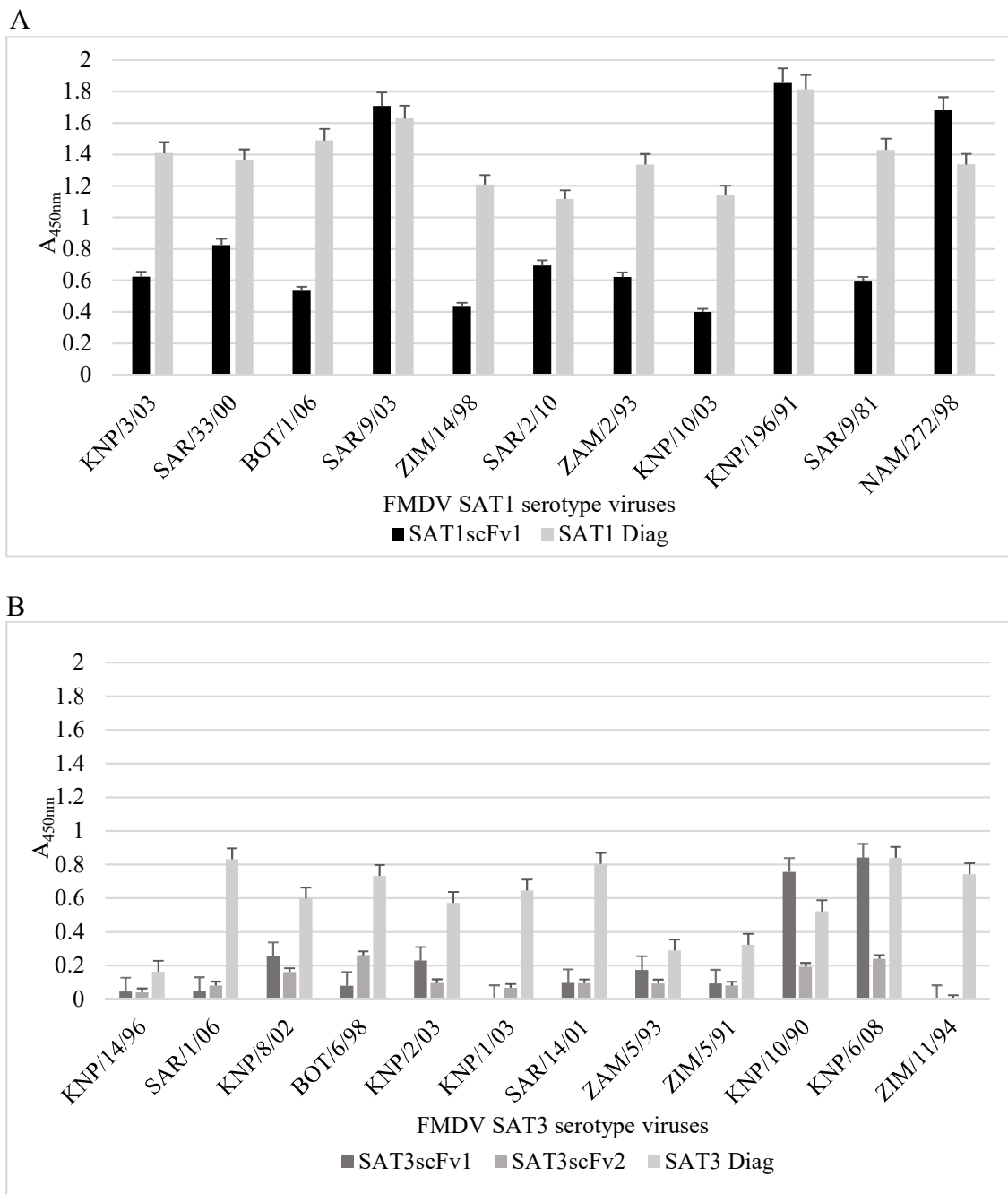


Figure 4.5: Sandwich ELISA using soluble scFvs SAT1scFv1, SAT3scFv1 and SAT3scFv2 as detecting reagents. The standard diagnostic sandwich ELISA used for FMD antigen detection (OIE manual, 2017) (used as a positive control) was adapted, where the detection antibody was replaced with a soluble SAT scFv. The ELISA was executed to determine the detecting potential of soluble SAT1scFv1 to PEG concentrated SAT1 (A) and for SAT3scFv1 and SAT3scFv2 to PEG concentrated SAT3 (B) serotype viruses. For the negative control (neg), 2% milk powder was included in the assays replacing the virus component. The negative control ELISA background signal was deducted when plotting the ELISA A_{450nm} result. The data are means \pm SD of two independent experiments.

4.3.6 Prediction of ELISA variability from sequence data analysis

The scFv capturing and detecting ELISA data show proof of concept as a diagnostic tool for FMDV SAT viruses. The outer capsid protein sequences of the SAT1 and SAT3 viruses were compared to determine whether virus sequence variation could explain the ELISA A_{450nm} profiles. Considering that the detecting scFv ELISA mimics the FMDV LPBE (OIE manual, 2017), but differs by replacing the detecting guinea pig antiserum with the soluble scFv's, this ELISA data was utilized to determine the scFv titre by means of the Spearman-Kärber method (Karber, 1931) (Table 4.6). The ELISA reactivity and antigenic relationship (r_1) between the viruses used for panning the Nkuku® library *i.e.* SAT1/KNP/196/91 and SAT3/KNP/10/90 (referred to as the homologous virus for SAT1 and SAT3 respectively) and the viruses tested in the panel was determined (Table 4.6).

At a concentration of 30 µg/ml, SAT1scFv1 reacted similarly to SAT1/KNP/196/91, SAT1/SAR/9/03 and SAT1/NAM/272/98 viruses, in the detecting ELISA (Figure 4.5), with r_1 values of 1, 0.95 and 0.93 respectively, indicating a close antigenic relationship. The reactivity of SAT1scFv1 to the remaining SAT1 viruses in the ELISA were reduced by more than 40% and resulted in r_1 -values of 0.45 to 0.61 (Table 4.6).

The SAT3scFv1 reacted similarly to SAT3/KNP/10/90 and SAT3/KNP/6/08 (Table 4.6), but reactivity was reduced more than 60% to SAT3/KNP/8/02 and SAT3/KNP/2/03 and more than 80% to the remaining SAT3 viruses (Table 4.6). SAT3scFv2 showed 81-100% reactivity to SAT3/KNP/10/90, SAT3/KNP/6/08, SAT3/KNP/8/02 and SAT3/BOT/6/98; 41-60% reactivity to SAT3/SAR/1/06, SAT3/KNP/2/03, SAT3/SAR/14/01, SAT3/ZAM/5/93 and SAT3/ZIM/5/91; whereas a 21-40% reactivity was observed for SAT3/KNP/14/96 and SAT3/KNP/1/03 (Table 4.6). Neither SAT3scFv1 or SAT3scFv2 could detect SAT3/ZIM/11/94 (Table 4.6).

Table 4.6: Virus titre, r_1 values and percentage (%) ELISA reactivity observed for the SAT1 and SAT3 viruses tested when SAT1scFv1, SAT3scFv1 and SAT3scFv2 were used as detecting antibodies in a sandwich ELISA

FMDV Serotype	Virus strain	SAT1scFv1		
		Titre (Log ₁₀)	r_1 value#%	% ELISA reactivity*
SAT1	KNP/196/91**	1.37	1 (i)	
SAT1	KNP/3/03	0.73	0.53 (ii)	
SAT1	SAR/33/00	0.83	0.61 (ii)	
SAT1	BOT/1/06	0.68	0.50 (ii)	
SAT1	SAR/9/03	1.3	0.95 (i)	
SAT1	ZIM/14/98	0.63	0.46 (ii)	
SAT1	SAR/2/10	0.77	0.56 (ii)	
SAT1	ZAM/2/93	0.73	0.53 (ii)	
SAT1	KNP/10/03	0.61	0.45 (ii)	
SAT1	SAR/9/81	0.71	0.52 (ii)	
SAT1	NAM/272/98	1.28	0.93 (i)	

FMDV serotype	Virus strain	SAT3scFv1			SAT3scFv2		
		Titre (Log ₁₀)	r ₁ value#¥	% ELISA reactivity*	Titre (Log ₁₀)	r ₁ value#¥	% ELISA reactivity*
SAT3	KNP/10/90**	1.29	1 (i)	■	0.97	1 (i)	■
SAT3	KNP/14/96	0.45	0.35 (iii)	□	0.52	0.54 (ii)	□
SAT3	SAR/1/06	0.45	0.35 (iii)	□	0.64	0.66 (ii)	□
SAT3	KNP/8/02	0.68	0.53 (ii)	□	0.87	0.90 (i)	■
SAT3	BOT/6/98	0.49	0.38 (iii)	□	1.2	1.24 (i)	■
SAT3	KNP/2/03	0.66	0.51 (ii)	□	0.68	0.70 (ii)	□
SAT3	KNP/1/03	0	0 (iii)	□	0.60	0.62 (ii)	□
SAT3	SAR/14/01	0.51	0.39 (iii)	□	0.68	0.70 (ii)	□
SAT3	ZAM/5/93	0.59	0.46 (iii)	□	0.67	0.69 (ii)	□
SAT3	ZIM/5/91	0.5	0.39 (iii)	□	0.64	0.66 (ii)	□
SAT3	KNP/6/08	1.33	1 (i)	■	1.1	1.1 (i)	■
SAT3	ZIM/11/94	0	0 (iii)	□	0	0 (iii)	□

** Homologous virus, used for the biopanning

* The A_{450nm} value for the panel of SAT1 and SAT3 viruses tested with each scFv was calculated as a percentage of the homologous virus (virus used for panning) A_{450nm} to obtain the percentage reactivity. The percentage reactivity were categorised as 0-20% □, 21-40% □, 41-60% □, 61-80% ■ and 81-100% ■.

r₁ values were determined using the ELISA data and the Spearman-Kärber method (Karber, 1931)

0.4 - 1 = Close relationship between virus tested and homologous virus (virus used for panning).

0.2 - 0.39 = The strains are antigenically related

<0.2 = Isolates are distantly related

¥ The roman numerals in brackets indicates the antigenic profiles observed of the virus tested to the homologous virus with (i) being most closely related. Two r₁ profiles were observed for SATscFv1 whilst three profiles were observed for SAT3scFv1 and SAT3scFv2.

To investigate the phylogenetic relationship of the viruses, neighbour-joining trees were constructed for SAT1 (Figure 4.6) and SAT3 (Figure 4.7) viruses respectively, using the FMDV capsid aa sequence alignment. Figures 4.6 and 4.7 show the different reactivity profiles in relation to the aa differences in the phylogenetic tree.

In a complete alignment of the capsid proteins of the 11 SAT1 viruses, 21% of the residue positions were variable. The neighbour-joining tree constructed for the SAT1 viruses show the phylogenetic groupings of the viruses into three distinct topotypes with 11.6% variable aa cut-off (Figure 4.6). Viruses grouping in topotype I included viruses originating in South Africa (1974-1991); topotype II included viruses from Botswana and Namibia; and topotype III viruses from Northwest Zimbabwe and Zambia. The three viruses in the SAT1scFv ELISA reactivity and r_1 profile (i) *i.e.* SAT1/KNP/196/91, SAT1/SAR/9/03 and SAT1/NAM/272/98 (Table 4.6), differ by 7.3%, 11.5% and 11.3% respectively, in pairwise aa alignments. The remaining SAT1 viruses differ by 4.2 – 11.3% of residue positions in any pairwise alignment.

The neighbour-joining and minimum evolution methods used to compute the phylogenetic inference of the capsid aa sequences of the SAT3 viruses from this study revealed three distinct groupings according to topotype (Figure 4.7). These groupings included topotype I (Southern Africa), topotype II (Northeast Zimbabwe) and topotype IV (Zambia, Botswana and Northwest Zimbabwe) (Figure 4.7). In a complete alignment of 12 SAT3 viruses, there was 19% of variable aa positions. There was a 4.2% aa difference between SAT3/KNP/10/90 and SAT3/KNP/6/08 representing r_1 profile (i) for SAT3scFv1 (Table 4.6). The r_1 profile (i) (Table 4.6) for SAT3scFv2 also included SAT3/KNP/6/08 as well as SAT3/KNP/8/02 and SAT3/BOT/6/98 where the aa differences in a pairwise alignment was 5.8% and 8.7% respectively with SAT3/KNP/10/90. All other SAT3 viruses had between 4.9% and 10.8% aa differences in any pairwise alignment to SAT3/KNP/10/90.

Amino acid variability was not random but were focussed in regions of hypervariability across the linear aa sequence of the outer capsid proteins. It is reasonable to assume that aa changes in residues that are surface-exposed may directly correlate with different reactivity profiles in the ELISA.

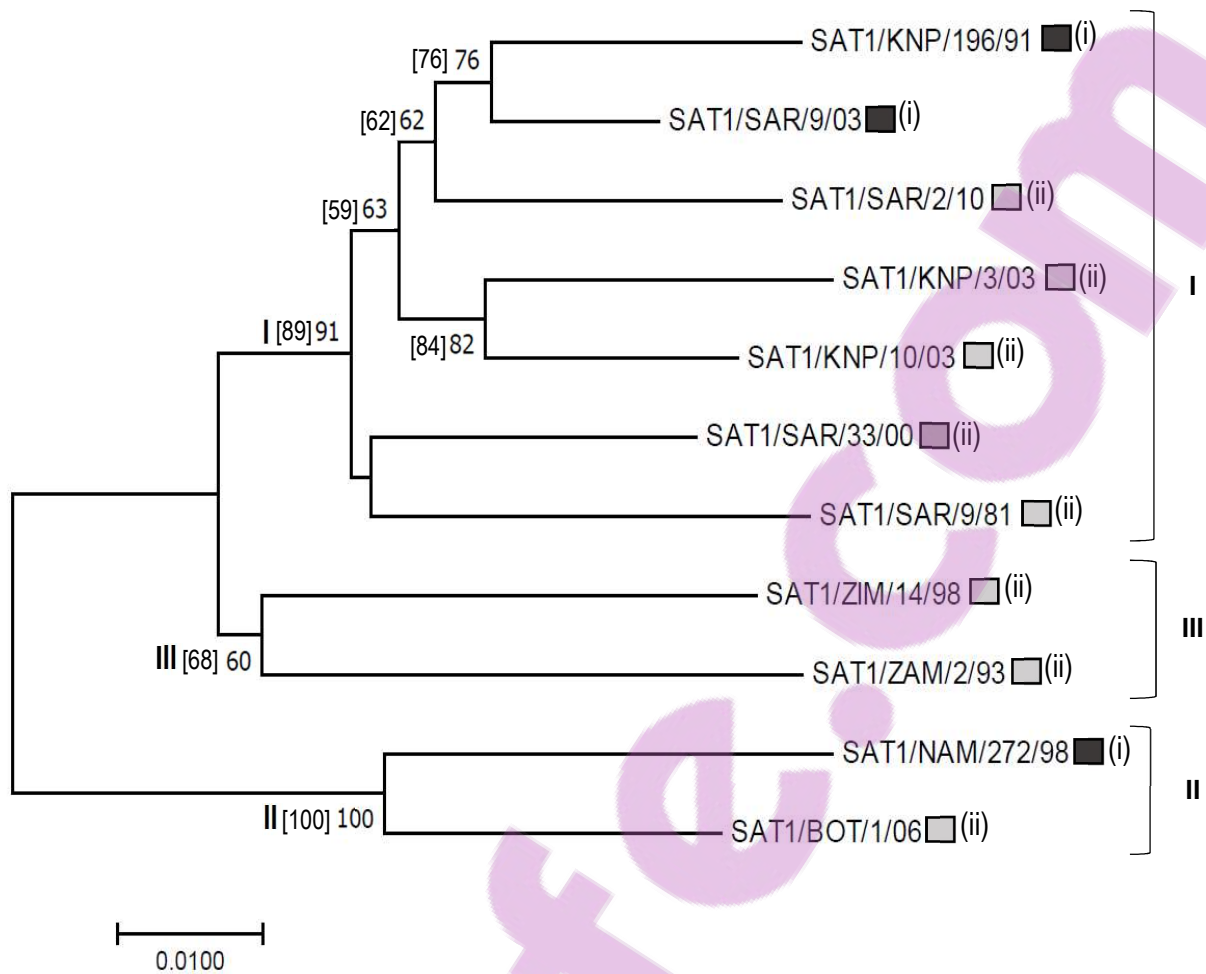


Figure 4.6: Neighbor-Joining tree (Saitou and Nei, 1987) of SAT1 viruses used in this study based on the aa sequences of the VP1, VP2, VP3 and VP4 region. The evolutionary distances were computed using the Poisson correction method and a bootstrap analysis of 1000 replication was applied. Evolutionary analyses were conducted in MEGA7 (Kumar *et al.*, 2016). The coloured squares indicate the ELISA reactivity from Table 4.6 of SAT1scFv1 with the SAT1 viruses *i.e.* 0-20%□, 21-40%□, 41-60%□, 61-80%■ and 81-100%■. The roman numerals in brackets indicate the order of antigenic relationship calculated as per r1 values where (i) represents the most closely related virus antigenically to the homologous virus (SAT1/KNP/196/91). The square brackets [] refer to the bootstrap value from the minimum evolution phylogeny computation. The topotype groupings (Bastos *et al.*, 2001, Maree *et al.*, 2011) are indicated in bold roman numerals.

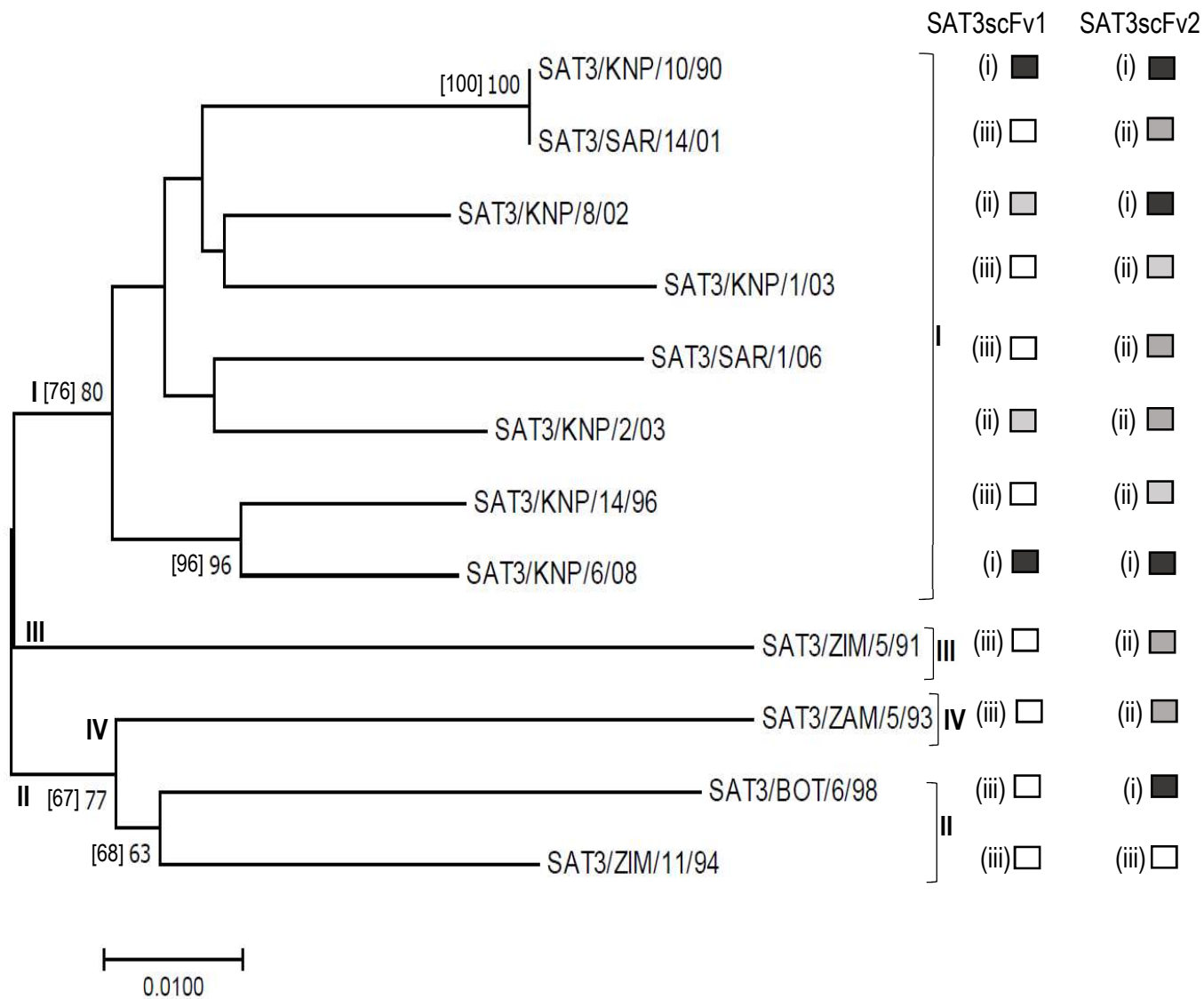
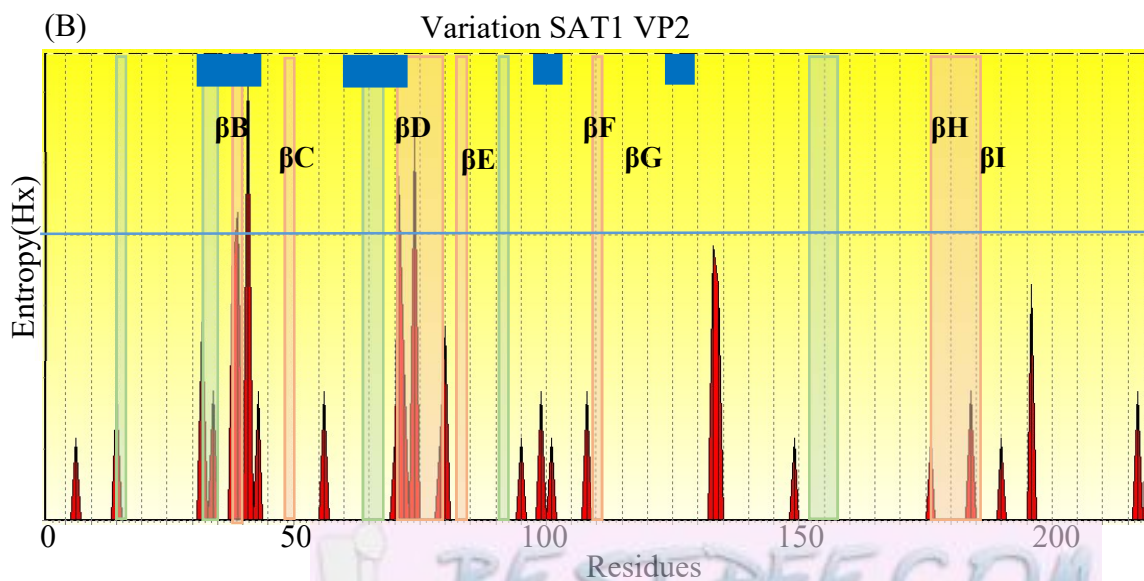
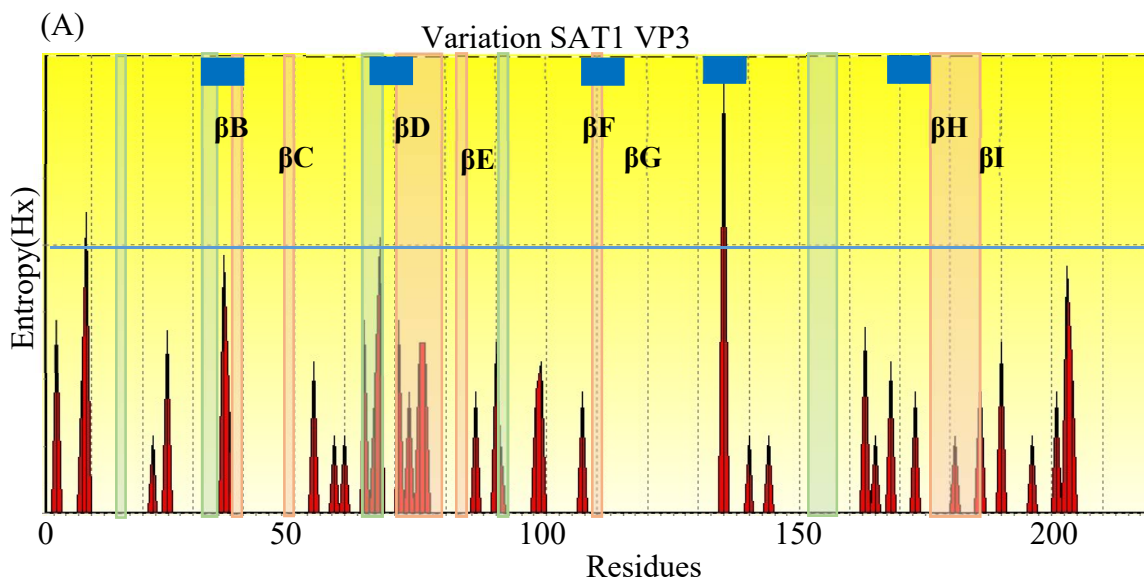


Figure 4.7: Neighbor-Joining tree (Saitou and Nei, 1987) of SAT3 viruses used in this study based on the aa sequences of the P1 region. The evolutionary distances were computed using the Poisson correction method and a bootstrap analysis of 1000 replication was applied. Evolutionary analyses were conducted in MEGA7 (Kumar *et al.*, 2016). The coloured squares indicate the ELISA reactivity from Table 4.6 of SAT3scFv1 and SAT3scFv2 with the SAT3 viruses *i.e.* 0-20% , 21-40% , 41-60% , 61-80% and 81-100% . The roman numerals in brackets indicate the order of antigenic relationship calculated as per r1 values where (i) represents the most closely related virus antigenically to the homologous virus (SAT3/KNP/10/90). The square brackets [] refer to the bootstrap value from the minimum evolution phylogeny computation. The topotype groupings (Bastos *et al.*, 2003a) are indicated in bold roman numerals.

The regions of aa residue variation within the capsid proteins of the SAT1 and SAT3 viruses were mapped using entropy plots constructed from the complete VP1, VP2 and VP3 aa alignments (Figure 4.8; 4.9). There were no intra-serotype aa changes occurring in VP4. The viruses that were used for the biopanning *i.e.* SAT1/KNP/196/91 and SAT3/KNP/10/90 were used as the reference sequence in the alignments of the SAT1 and SAT3 viruses respectively

(Figure 4.8; 4.9). Entropy values of >1 were taken as regions that are prone to variation as entropy is a measure of the lack of predictability for a residue position (Schneider and Stephens, 1990) (Figure 4.8; 4.9).

Hypervariable regions, in which 60% or more of the residue positions (varied using overlapping windows of 10 aa), were identified in the outer capsid proteins, *i.e.* VP1, VP2 and VP3. Within hypervariable regions, entropy was used to measure the uncertainty at each aa position within the SAT alignments (Schneider and Stephens, 1990). The variation (entropy >1) was 1% (3/221 amino acids) in VP3 (Figure 4.8A), VP2 was 2% (4/219 amino acids) (Figure 4.8B) whilst in the VP1 region, it was 6% (14/219 aa residues, Figure 4.8C) for the SAT1 viruses.



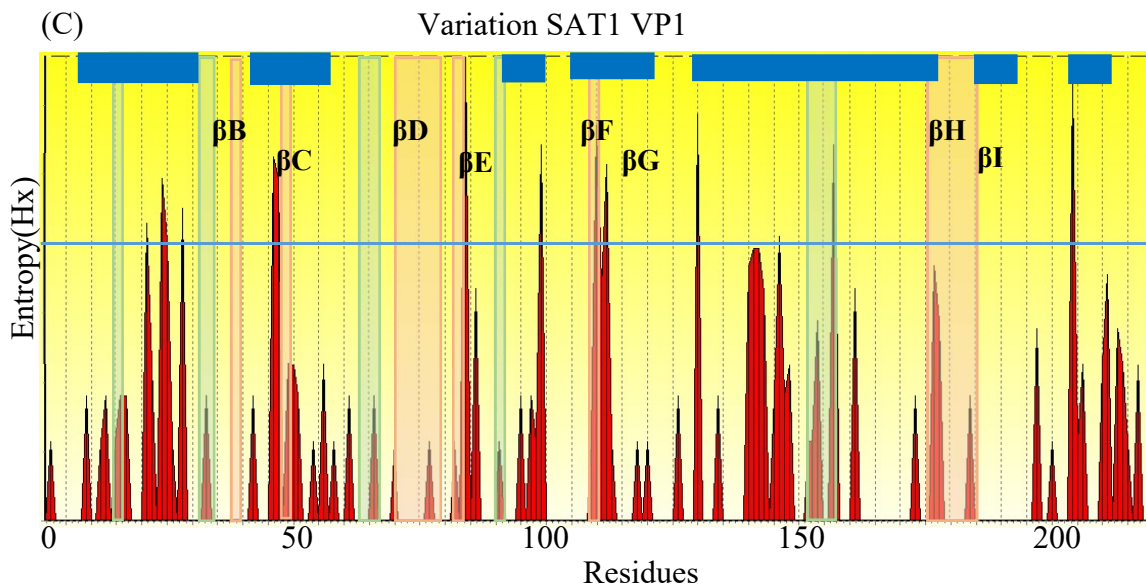


Figure 4.8: Plots representing the aa variation for VP3 (A), VP2 (B), and VP1 (C) for the aligned SAT1 viruses. The pink bars represent the beta strands of the FMDV structure, whilst the green represent the alpha helices. The SAT1 viruses were aligned to the SAT1/KNP/196/91 virus, which was used for biopanning. Regions of aa variation are shown by the red vertical bars and the clear areas represent conserved regions. Regions of chaotropy or high entropy were identified as having an entropy >1 and hypervariable regions were defined as five or more variable aa positions in a window of 10 aa in the alignment. The blue horizontal line indicates an entropy of 1. Previously identified antigenic sites and hypervariable regions are indicated by the blue bar/blocks based on Grazioli *et al.*, 2006 and Maree *et al.*, 2011 and these regions corresponded to or were located in close proximity to regions of chaotropy observed for the SAT1 viruses from this study.

No antigenic sites have been identified for FMDV SAT3 viruses to date. In this study, the aa variation observed from the alignment of the SAT3 viruses where the entropy was >1 was 1% (3/221 aa) for VP3 (Figure 4.9A) and VP2 (2/218aa) (Figure 4.9B) whilst the majority of variation occurring above an entropy of 1 was observed for VP1 (5%, 11/209 aa residues, Figure 4.9C).

Characteristics such as amino acid changes occurring from polar to non-polar, positive to negative, basic to acidic etc. is outlined in Appendix A3 and A4 and any of these differences may be playing a role with the differences observed for virus-scFv interactions in the ELISA assays.

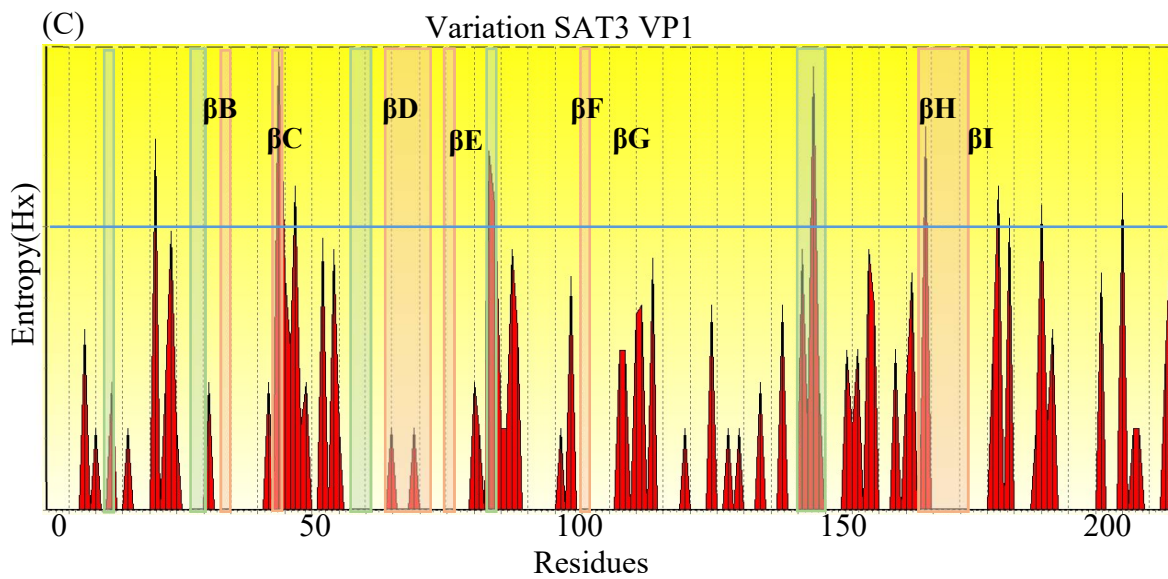
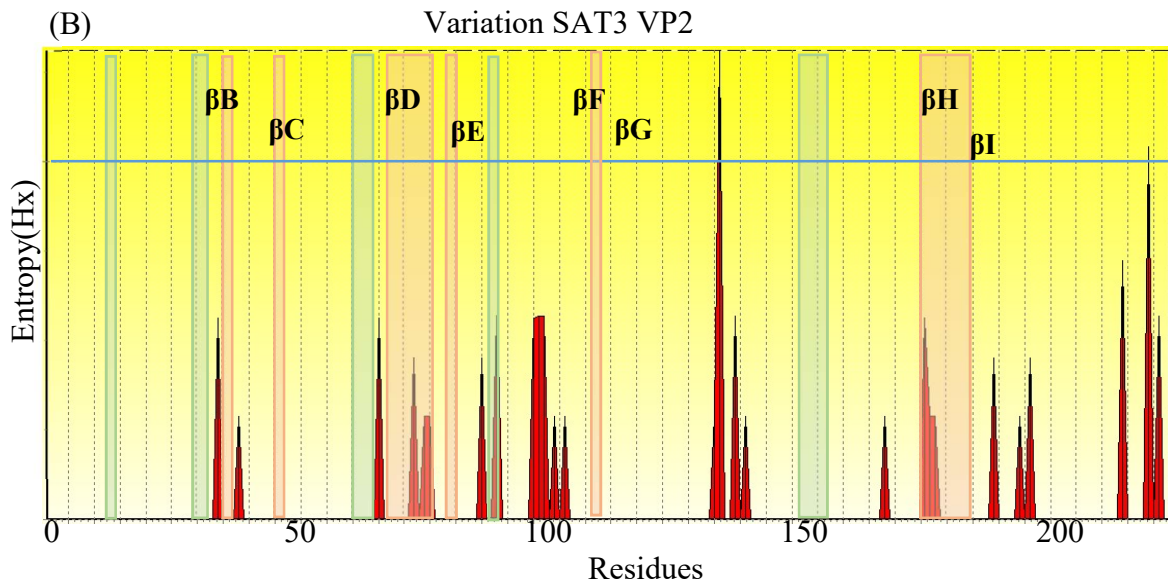
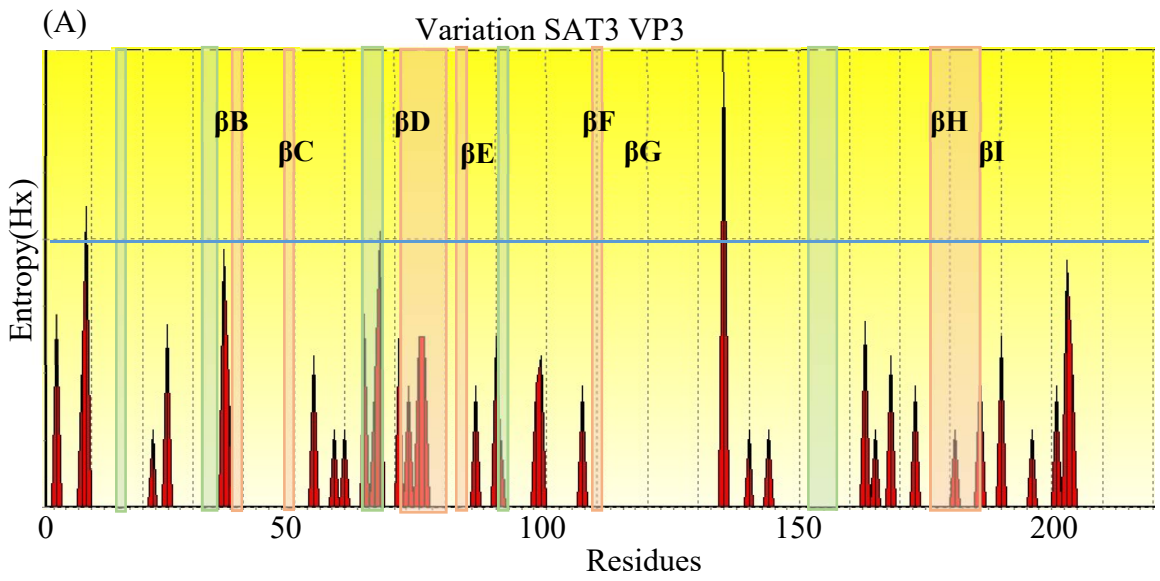


Figure 4.9: Plots representing the aa variation for VP3 (A), VP2 (B), and VP1 (C) for the aligned SAT3 viruses. The pink bars represent the beta strands of the FMDV structure, whilst the green represent the alpha helices. The SAT3 viruses were aligned to the SAT3/KNP/10/90 virus, which was used for panning. Regions of aa variation are shown by the red vertical bars and the clear areas represent conserved regions. Regions of chaotropy were identified as having an entropy >1 and were defined as sites on the capsid protein that had five or more variable aa residues within a window of 10 residues. The blue line indicates an entropy of 1.

Variable residue positions having an entropy >1, were plotted on the modelled pentamer structure of SAT1 (protein data bank ID: 2wzr, r2wrsf; Reeve *et al.*, 2010). This was performed to investigate the aa differences for the SAT1 and SAT3 viruses possibly interacting with the soluble scFvs from this study during the detecting scFv ELISA assay (Figure 4.10 A, B). Appendix A3 and A4 details the aa changes occurring from the SAT1 and SAT3 alignments.

Changes that were observed that may be significant in the scFv-FMDV interactions are: (i) a loss in a positively charged aa at VP1 position 110 (Appendix A3, Figure 4.8, Table 4.7) occurring for SAT1/SAR/9/81 (Lys-Asn), SAT1/KNP/10/03 (Lys-Ala) and SAT1/KNP/3/03 (Lys-Ala) viruses, all of which display 21-40% ELISA reactivity to the SAT1 scFv. (ii) SAT1/SAR/2/10 and SAT1/SAR/9/03, which were most closely related phylogenetically to SAT1/KNP/196/91, showed significant residue substitutions at VP2 position 196, VP3 positions 75-76 and VP1 25, 46-47, 54, 86, 99, 110-112 and residues in the GH-loop (Appendix A3) that may be responsible for the reduction in SAT1scFv1 reactivity in the ELISA. (iii) FMDV SAT1 VP2 aa positions 71, 74 and VP3 aa position 67 were found to have significant surface exposure (Table 4.7) and may play a role in virus-scFv binding.

For SAT3 viruses, regions with high entropy was observed, which overlapped with sites of hypervariability and antigenic regions from previous studies (Table 4.7). Specifically, antigenic sites identified from previous studies *i.e.* Site 1 for FMDV type A and O, FMDV type O site 2, and FMDV type A and O site 3 were found to be overlapping with regions of hypervariability for the FMDV SAT3 alignment from this study. SAT1 regions that were previously identified as having significant surface exposure and entropy also overlapped with SAT3 virus alignments from this study *viz* VP2 131, 214; VP3 131, 135, 139 and VP1 44, 47 (Table 4.7). Amino acid residues situated within regions of hypervariability and high entropy on surface exposed loops in the outer capsid proteins may be involved in the antigenicity of the

virion and may possibly affect the scFv binding to the FMD virus, resulting in varying ELISA profiles.

An interesting finding from this study was that SAT3scFv2 and A22scFv6 have identical sequences in all three of the CDR's for the heavy and light chains and are essentially the same binder. This leads to the postulation that these two binders recognize a conserved aa motif on both SAT3/KNP/10/90 and A22 viruses. Analysis of FMDV serotype A outer-capsid protein sequences with the serotype SAT3 viruses, revealed that VP1, VP2 and VP3 had 48% conserved aa residues. Thus, the conserved aa motif common between the A and SAT3 serotype viruses that is recognized by the SAT3scFv2 and A22scFv6 binders may be located within these conserved residues.

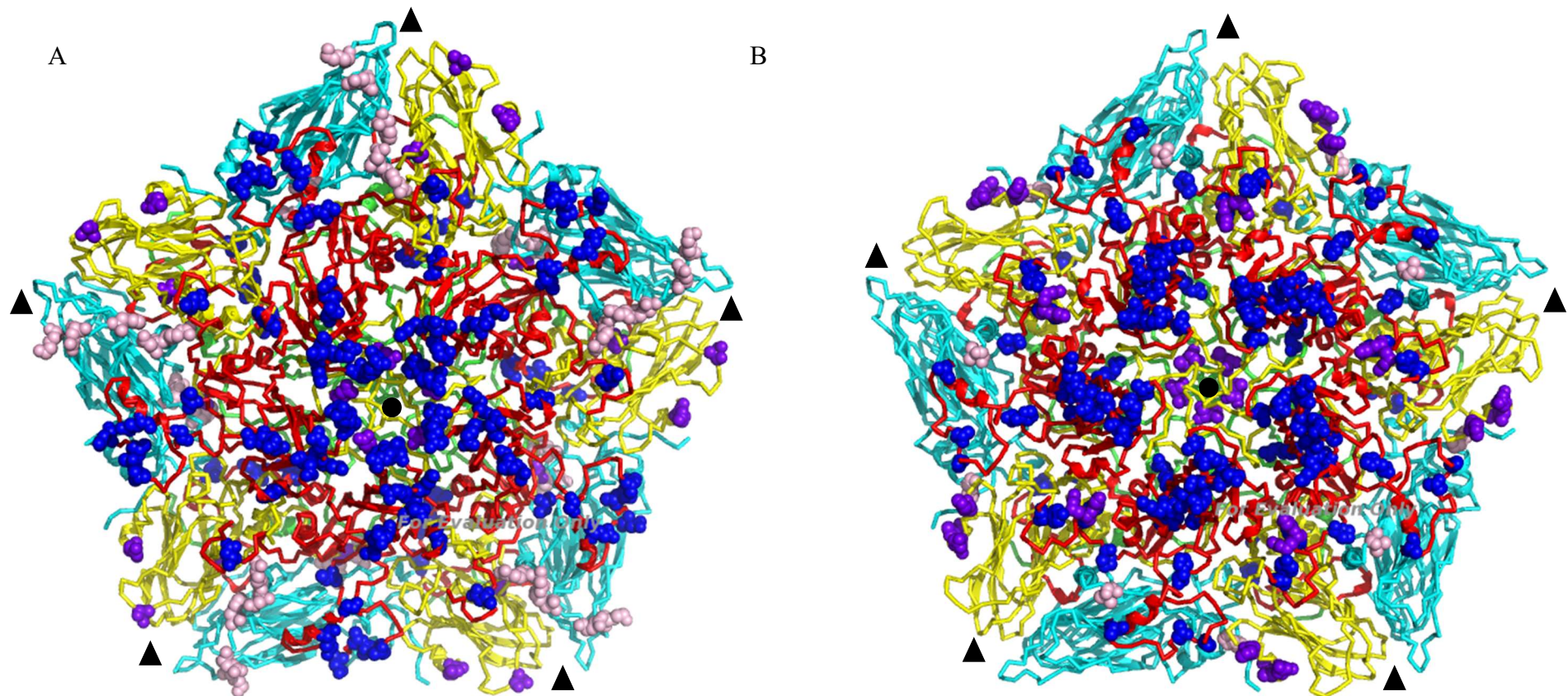


Figure 4.10: The aa variation (entropy >1) occurring during sequence alignments was plotted on a ribbon protein diagram of a crystallographic pentamer of SAT1 (protein data bank ID: 2wzr, r2wrsf; Reeve *et al.*, 2010) (A) and a modelled pentamer for SAT3 viruses (B). The protein subunits and structural features are colour coded for VP1 (red), VP2 (light blue), VP3 (yellow) and VP4 (green). The pore, located at the 5-fold axis of the capsid (black circle), is shown in the middle of the structure. The 3-fold axis is depicted by the black triangles. The spheres indicate the aa variation (entropy >1) in VP1 (blue), VP2 (pink) and VP3 (purple).

Table 4.7: Collation of regions of entropy >1 for the SAT1 and SAT3 FMDV aa alignments for the outer capsid proteins correlating with previously identified hypervariable regions or antigenic sites

	Amino Acid hypervariable region														
Capsid	1B	1B	1B	1B	1C	1C	1C	1C	1D	1D	1D	1D	1D	1D	1D
B-Sheets	A-B	B-C	D-D	E-F; H-I	A-B	B-C	E-F	G-H; H-I	N _T	B-C	E-F	F-G	G-H	H-I	C _T
Axis		3x		2x		3x	2x			5x			2x	5x	3x
SAT1 ¥	39, 41	71, 74			9	67	135		21, 24, 25, 28, 46, 47		84, 99	110, 112	130, 146, 157		204
SAT3 ¥				131, 214			131, 135, 139		21	44, 47	83, 84		143, 164	177, 179, 185	200
SAT1 \#	31-44	62-82*	97-101	130-134*	30-45	59-78*	124-141*	165-183	9-35	43-57*	93-102	113-123	135-151; 156-169	176-187	201-222
	FMDV antigenic sites														
Type O \square		Site 2: 70-77/78		Site 2: 131-134; T188I		Site 4: 56-58			T-cell	Site 3: 43-48			Site 1a, 5: 144-149, 154		Site 1b: 206-208
Type A \square		Site 3: 82-88; 196				Site 3: 58-61; Site 5: 69-70	Site 3: 136-139; 195	Site 3: 195					Site 1: 142-157	Site 4: 169, 175-179	Site 2: 200-212

¥ The hypervariable regions have been derived from the SAT1 and SAT3 virus alignments from this study (Appendix A3, A4).

\# Previously identified hypervariable regions for SAT1 from Maree *et al.*, 2011.

\square The antigenic sites are a summary of that described in Thomas *et al.*, (1988); Bolwell *et al.*, (1989); Saiz *et al.*, (1991); Kitson *et al.*, (1990); Crowther *et al.*, (1993a); Guzman *et al.*, (2010), Mahapatra *et al.*, 2012, Grazioli *et al.*, 2013.

*These regions have significant surface exposure (Maree *et al.*, 2011) and entropy.

4.4 Discussion

The LPBE for SAT1, SAT2 and SAT3 are well established assays, considering the high genetic diversity of the SAT-type viruses (Van Rensburg and Nel, 1999; Knowles and Samuel, 2003; Maree *et al.*, 2011; 2014), however there is still a need for improvement of these assays. Additionally, for FMD vaccine matching where the antigenic variability of field virus strains is measured against current vaccine strains, the virus neutralization assay is utilized. This assay, however, is laborious and can cause a delay in decision making regarding FMD control measures. To counter this strategy, the consideration into utilizing MAbs that recognize virus exposed antigenic epitopes in an ELISA format where results can be obtained timeously, was explored further in this study. These MAbs can also be beneficial in predicting epitopes, which can in turn be used in the design of improved FMD chimeric vaccines containing various antigenic sites that can elicit a wide immunological response or protection in vaccinated animals. To this end, phage display technology was explored.

The Nkuku® phage-display library has previously been used for FMDV to obtain novel scFv binders for serotype SAT2 (Opperman *et al.*, 2012). Opperman *et al.*, 2012 has shown that one SAT2-specific soluble scFv neutralized SAT2/ZIM/7/83 and this scFv was used to map a novel epitope at residue position 159 of VP1 and in a scFv-based ELISA assay. We broadened this study by focusing on FMDV serotype SAT1, SAT3 and A. Using naïve phage display libraries allows for the selection of recombinant antibodies when pre-existing paratopes bind to exposed and complementary parts of the immobilised antigen. Thus, the possibility of obtaining antigen-specific binders would depend on the presence and accessibility of suitable surface-exposed structures of the antigen, where in this case, it was the FMD virion. Another factor to consider using phage display technology, is that the quality and the size of the naïve library plays an important role in the success of phage display (Carmen and Jermutus, 2002), as paratopes that are not present within the library cannot be isolated.

In this study, the biopanning process against SAT1/KNP/196/91, SAT3/KNP/10/90 and A22 viruses resulted in unique, novel FMDV scFv binders *i.e.* one for SAT1, two for SAT3 and nine for serotype A. The low number of unique binders panned from the Nkuku® phage-display library for serotype SAT1 and SAT3 is not uncommon as two unique Bluetongue virus (BTV)-specific scFvs was obtained as well as three binders against the 16-kDa antigen of *M. tuberculosis* (Fehrsen *et al.*, 2005; Sixholo *et al.*, 2011) using the Nkuku® phage-display

library. However, the nine A22 binders attained in this study is novel. Although none of the SAT scFv binders showed neutralization capability, three of the nine A22 binders exhibited neutralization. Of the three A22 neutralizing binders, two binders *i.e.* A22scFv1 and A22scFv8 had the same heavy chain sequences and only differed in the light chain region sequences. This characteristic is of interest as Hamers-Casterman *et al.*, 1993 showed that the V_H are believed to play a more important role in the binding of antibody fragments to antigens than V_L . In addition, investigations by Williamson and Matthews (1999) showed that three neutralizing scFvs against pertussis toxin all had the same heavy chain sequences and were related. Thus, to obtain more unique neutralizing scFvs, one could modify only the heavy chain of non-neutralizing epitopes to be the same as their neutralizing counterparts.

For the generation of escape mutants for FMDV serotype A using the neutralizing scFvs, the aa substitutions for SRV1 and SRV3 occurred in the surface exposed and structurally flexible VP1 β G- β H loop, downstream of the RGD sequence, which is the identified FMDV serotype A antigenic site *i.e.* site I and the β G- β H loop residues 140-160 have been shown to play an important role in antigenicity in most FMDV serotypes (Pfaff *et al.*, 1988; Thomas *et al.*, 1988b; Barnett *et al.*, 1989; Baxt *et al.*, 1989; Bolwell *et al.*, 1989; Parry *et al.*, 1989; Crowther *et al.*, 1993a; Mahapatra *et al.*, 2011). For SRV1, there was a Pro to Ser aa change at VP1 position 149 (RGD +3 position) and for SRV3 the aa change occurred at VP1 position 150, RGD+4 *i.e.* from a Leu to a Phe. The residues succeeding the RGD motif are important for receptor recognition (Jackson *et al.* 2000a) and the RGD is flanked on both sides by hypervariable sequences, which delivers a domain that is capable of adopting different conformations. Opperman *et al.*, 2012 showed with scFv neutralization investigations of FMDV SAT2/ZIM/7/83, an aa change at the base of the GH loop *i.e.* VP1 position 159 where there was an Arg to His change. Furthermore, a synthetic peptide ELISA confirmed VP1 aa 159 as the epitope to which the SAT2 scFv binds (Opperman *et al.*, 2012). These investigations lead us to postulate that the epitope site for the A22scFv1 and A22scFv8 binding is the VP1 aa position 149 and 150 respectively. However, future investigations with SRV1 and SRV3, which was not the aim of this study, will be to derive a synthetic peptide from the predicted epitopic site and to confirm results with a synthetic peptide blocking ELISA.

A novel finding from this study is the result of two soluble, non-neutralizing scFvs, each from different FMDV serotypes but having the same heavy and light chain sequences *i.e.* SAT3scFv2 and A22scFv6. It is postulated that a common epitope between SAT3/KNP/10/90

and A22 resulted in the same soluble scFv from the antibody repertoire of the Nkuku library. However, complete sequence alignment investigations of A22, SAT1 and SAT3 viruses did not reveal probable epitope binding regions for SAT3scFv2 and A22scFv6. Monoclonal antibody studies are suggested to confirm the common epitope between A22 and SAT3.

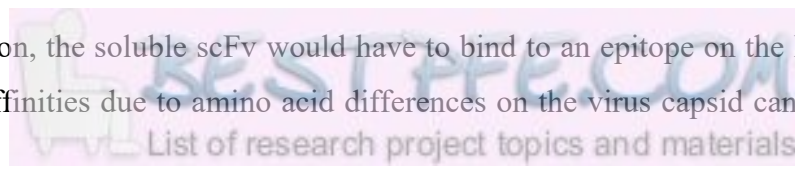
From the specificity analysis, the SAT1 and SAT3 soluble scFvs from this study bound to complete 146S virions of the virus used for biopanning *i.e.* SAT1/KNP/196/91 and SAT3/KNP/10/90 respectively. However, the phage displayed scFv formats did show cross-reactivity across the FMD serotype viruses tested, even though the binding profiles did vary. The SAT1 phage displayed scFv was found to bind to complete 146S virions of SAT2/ZIM/7/83 and SAT3/KNP/10/90 and similarly, the SAT3 phage-displayed scFvs were found to bind SAT1/KNP/196/91 and SAT2/ZIM/7/83 146S virions. Cross-reactivity of scFvs is not uncommon as in a study by Toth *et al.* (1999), which obtained scFv clones against the potato leafroll virus where 7 clones did not cross-react with other luteoviruses whilst 4 clones did. Additionally, Toth *et al.* (1999) proved that the cross-reacting scFvs are directed against continuous epitopes that are present on the coat proteins of certain related luteoviruses whereas the scFvs that did not show cross-reactivity, bound to discontinuous or conformation-dependant epitopes that are specific to potato leafroll virus. Thus, the cross-reacting phage-displayed SAT1 and SAT3 scFvs from this study may possibly be recognizing continuous epitopes of the SAT serotype viruses and should be investigated further in this regard.

The SAT soluble scFvs, which had reduced cross-reactivity compared to the phage displayed scFvs, were further investigated for their possible use as diagnostic reagents in an ELISA format as a FMDV capturing and a detecting reagent. For both ELISA formats, the one SAT1 soluble scFv was able to produce high positive ELISA reactivity to the various SAT1 viruses tested implying that it retained its native conformation following adsorption to polystyrene plates. However, the two SAT3 scFvs produced A_{450nm} signals just above the positive cut-off absorbance as a FMDV capturing reagent and a detecting reagent, which is not suitable as a positive result for a diagnostic ELISA. It is vital for a capturing antibody in an ELISA assay to be efficiently immobilised onto the ELISA plate such that it is able to retain both the antibody conformation and the antigen-binding activity (Jung *et al.*, 2008). Furthermore, important factors such as surface charge, hydrophobicity, co-adsorption of or exchange with surfactants and other proteins play a role in determining stability and specificity of absorbed antibodies in ELISA assays (Qian *et al.*, 2000). These factors may have played a role to reduce the

performance of the scFv ELISAs in this study. For conventional ELISAs where complete monoclonal or polyclonal antibodies are used, immobilisation onto the ELISA plates occur via physical adsorption (Kumada *et al.*, 2009a;b). Contrastingly, immobilisation of small antibody fragments such as scFvs onto plastic surfaces causes unfavorable conformational changes to occur (Kumada *et al.*, 2014). Essentially, a hydrophobic interaction occurs in the linked V_H and V_L regions forming a paratope and resulting in a conformational change of the antigen-binding domain, which in turn results in decreased antigen-binding activity (Torrance *et al.*, 2006; Wemmer *et al.*, 2010; Kumada *et al.*, 2014).

The analytical specificity of the SAT scFvs for the capturing and detecting SAT1 and SAT3 ELISAs showed that the soluble scFvs were specific for the respective serotype viruses tested and no cross-reactivity was observed. Additionally, the analytical sensitivity of both the capturing and detecting ELISAs for SAT1 and SAT3 scFvs against the SAT1 and SAT3 viruses respectively was found to detect all viruses at a 1:8 dilution tested albeit the low A_{450nm} signals for the SAT3 scFv ELISAs. The SAT1scFv1 shows promise as a good detecting and immunocapture reagent due to the high ELISA reactivity for the SAT1 viruses tested. Studies have shown that when scFv fragments are utilized as a soluble protein and are not within the phage display system, low expression levels or a low inherent affinity can occur (Van Wyngaardt *et al.*, 2004). Also, the monomeric scFv fragments can have moderate binding affinities when binding to a large multivalent antigen like FMDV, which is in contrast to greater binding affinities that can be achieved by the multivalent display on the phage (Hoogenboom and Winter, 1992; Griffiths *et al.*, 1993; O'Connell *et al.*, 2002). To overcome the low SAT3 scFv ELISA signals, random mutations can be introduced in the gene coding for the scFv and the length of the linker within the scFv, increasing the bacterial expression of the scFvs and thus increasing the ELISA signal (Sixholo *et al.*, 2011). Another approach is to stabilize the scFv to other proteins whilst retaining functionality. For example, fusion to other proteins such as constant light chain domain (Mcgregor *et al.*, 1994), leucine zipper dimerisation domain (Griep *et al.*, 2000), Fc fragment (CH2 and CH3 domains) of mouse IgG1 (Liu *et al.*, 2003) and alkaline phosphatase (Kerschbaumer *et al.*, 1997). Adapting such approaches to the SAT1 and SAT3 scFvs from this study could enhance these recombinant antibodies as diagnostic reagents.

In the ELISA reaction, the soluble scFv would have to bind to an epitope on the FMD virus, however, varying affinities due to amino acid differences on the virus capsid can lead to the



varying ELISA reactivities observed. For FMDV, there are various structural and functional similarities among the antigenic sites for the various serotypes even though their locations and epitopic residues differ (Usherwood and Nash, 1995; Maree *et al.*, 2011; Grazioli *et al.*, 2013). Antigenic sites of FMDV that are located close to the two-, three- and five-fold axes of symmetry are structurally related as they lie in close proximity to each other in the pentamer subunit of the viral capsid (Grazioli *et al.*, 2013). Thus, any changes in the amino acid sequences in the capsid protein can affect the antibody-antigen binding footprints. Mutations within antigenic sites have been shown in studies for FMDV (Dunn *et al.*, 1998) and in poliovirus (Rezapkin *et al.*, 2010) to completely abrogate binding with relevant virus-specific antibodies. Consequently, antibodies against a particular epitope will not be able to recognize it if a mutation occurs. Meloen *et al.* (1987) showed that a single amino acid change within a synthetic peptide sequence can alter the binding of the peptide to the MAb. Similarly, the investigations of the variation observed within the capsid-coding regions of the SAT1 and SAT3 viruses in this study could account for the differences in the ELISA affinity between the SAT1 and SAT3 scFvs and the antigen tested.

The highly disordered, flexible nature of the FMDV VP1 β G- β H loop plays a role in its antigenic diversity (Acharya *et al.*, 1989) where the flexible loop allows for greater sequence diversity without compromising the integrity of the capsid structure (Grazioli *et al.*, 2013). Additionally, the GH loop adopts conformations that can be distinguished among different FMDV serotypes (Curry *et al.*, 1995; Lea *et al.*, 1995). For example, studies have shown that serotype O viruses possess a disulphide bond at the base of the β G- β H loop and the presence of this bond is believed to account for MAbs against this serotype to recognize discontinuous epitopes, however, MAbs against serotype A strains not having this disulphide bond, recognize linear epitopes (Bolwell *et al.*, 1989; Parry *et al.*, 1989; Acharya *et al.*, 1990). This may be the case for the SAT serotypes as well. Mukonyora (2015) reported SAT1 viruses may potentially have a disulphide bond at the base of the VP1 GH loop between residues 135 of VP1 and 130 of VP2, however the SAT3 strains there was a Cys \rightarrow His substitution at residue 130 of VP2 preventing the formation of a disulphide bond. In this study, similar results were observed. It was found that the SAT1 viruses all had the Cys residue at VP1 135 and VP2 at 130 and for the SAT3 viruses there was a Cys residue at VP1 134 and but a His residue at VP2 130 (results not shown). If the SAT1 and SAT3 scFvs from this study had its binding footprint to FMDV in the β G- β H loop region, then the presence or lack of this disulphide bond may affect the affinity of the scFv-virus binding. This would explain the higher ELISA absorbance signals for

the SAT1scFv1 to SAT1 viruses (having the disulphide bond) and the lower signals of the SAT3scFvs to the SAT3 viruses (lacking the disulphide bond). The disulphide bond anchors the GH loop and is the main determinant of the conformation adopted by the loop as well as aiding in its flexibility (Lea *et al.*, 1994).

Comparison of the FMDV outer capsid aa sequences for SAT1 and SAT3 revealed that majority of the variation observed was not random but confined to hypervariable regions. These regions correlated to surface exposed loops on the virion and to previously identified neutralization sites for serotype A, O and SAT1 (Thomas *et al.*, 1988; Baxt *et al.*, 1989; Barnett *et al.*, 1989; Parry *et al.*, 1989; Kitson *et al.*, 1990; Crowther *et al.*, 1993; Maree *et al.*, 2011; Grazioli *et al.*, 2013). Additionally, the hypervariable regions may be regions of binding sites for the scFvs and the variation observed in ELISA reactivity of these soluble scFvs to the panel of SAT1 and SAT3 viruses might be a reflection of the amino acid variation in these regions. Studies with the SAT2 scFvs showed that ELISA reactivity was a consistently low binding profile for SAT2/ZIM/5/83 compared to the high binding profile for SAT2/ZIM/7/83 even though the P1 regions of these two SAT2 viruses vary by less than 1% at an aa level. This observation implied that the binding region for the SAT2 scFvs may be over the region of aa variability, thus resulting in the varying binding profiles (Opperman *et al.*, 2012). ELISA and sequence data alone is not sufficient to verify the binding region of the soluble SAT1 and SAT3 scFvs, but competition assays with overlapping synthetic peptides will provide tangible evidence.

Vaccines resulting in broadly neutralizing antibody responses is highly desirable to address the vast genetic and antigenic diversity seen in certain pathogens such as HIV and Influenza viruses (Corti *et al.*, 2017; Burton and Hangartner, 2016). One way to fulfil this task is the use of infectious cDNA technology in the development of chimeric vaccines where chimeric viruses containing the fine epitopic structure of interest are attained (Rieder *et al.*, 1993; Fowler *et al.*, 2008; Blignaut *et al.*, 2011; Opperman *et al.*, 2014). The approach followed in this study was combining ELISA reactivity data, r_1 -values, and aa sequence and structural data to determine regions that are antigenically relevant for the SAT1 and SAT3 viruses. Various regions of SAT1 and SAT3 hypervariability and entropy were identified that corresponded to previously identified antigenic sites for FMDV SAT1, A and O serotypes, however further studies are required to confirm antigenic and epitope sites. This study contributes to the future

identification of SAT1 and SAT3 epitopes, which is appealing for FMDV SAT serotype specific epitope vaccine development.

Furthermore, this study has been beneficial to gain novel recombinant antibodies against FMDV SAT1 and SAT3 serotype viruses. These scFvs, although not able to neutralize FMDV, have shown potential to be used as ELISA reagents, especially SAT1scFv1. Further investigation and validations of SAT1scFv is recommended to improve the ELISA absorbance signal. The ability of the phage displayed SAT1scFv to recognize SAT1, SAT2 and SAT3 viruses makes it a good candidate for consideration in pen-side tests, which will provide quick FMDV diagnostic results in a field situation. Furthermore, this repertoire of scFvs for the SAT serotypes can be expanded by constructing and panning from FMDV immune libraries.

CHAPTER 5

CONCLUDING REMARKS

Foot-and-mouth disease (FMD) was initially described in the 16th century, however, it still exists as one of the foremost economically important diseases of livestock (Grubman and Baxt, 2004). Although many countries have eradicated the disease, the risk of re-emergence exists due to the threat from neighbouring countries and trade of animals and animal products. Several parts of Asia, most of Africa and the Middle East remain endemic, thus emphasis on improved FMD vaccines, diagnostic assays and control measures are key research focus areas. The aims of this study included (i) investigating the effect of symmetrically arranged, positively charged residues on the foot-and-mouth disease virus (FMDV) capsid in cell entry; (ii) development and validation of a FMDV SAT serotype-specific 3ABC assay to differentiate infected from vaccinated animals and (iii) isolation and characterization of single-chain antibody fragments against FMD serotype A, SAT1 and SAT3 viruses using a Nkuku® phage display library. This conclusion will focus on how this study has achieved these aims and contributed to the advancement of such FMD research.

FMDV continue to evolve to produce novel strains, which sometimes break through vaccine-induced immunity and can result in major epidemics (Jamal and Belsham, 2013). Current commercial FMD vaccines consist of inactivated purified antigen, however, because there are seven immunologically distinct serotypes and a spectrum of antigenically distinct subtypes due to a high mutation rate, vaccination against one serotype, may not confer protection against another (Domingo *et al.*, 2005). Successful vaccine preparation depends on cell culture adaptation of FMDV field isolates, typically to BHK-21 cells (Doel 2003). This process tends to be laborious as some field FMDV strains can prove problematic to adapt to cell culture. Field isolates of FMDVs enter cells via the VP1 RGD-mediated attachment to integrin cell surface receptors. However, importantly for vaccine production, progeny viruses acquires the ability to bind to cell surface heparan sulphate proteoglycans (HSPGs), following serial cytolitic passages in cell culture, likely by the selection of rapidly replicating FMDV variants from the

quasi-species. This study has shown that fourteen FMDV Southern African Territories (SAT)1 and SAT2 serotype viruses, serially passaged in BHK-21 cells, were virulent in CHO-K1 cells and displayed an enhanced affinity for HSPGs, as opposed to their low-passage counterparts. Comparative sequence analysis of several cell-culture adapted SAT virus isolates revealed the accumulation of positively charged residues at deduced amino acid positions 83-85 in the β D- β E loop and 110-112 in the β F- β G loop of VP1 upon adaptation to cultured cells. The use of GRID indicated putative enhanced binding of heparan sulphate to the region around VP1 arginine 112 contributing the most energetically favorable binding site. This data was utilized to construct two inter-serotype and six intra-serotype chimeric, mutant viruses with a net gain of positive charges in repeated clusters on the virion surface. Five of the eight chimeric viruses attained the ability to utilize heparan sulphate as an alternate receptor and the positively charged amino acid substitutions expanded the cell tropism of the chimera FMD viruses. However, only positively charged amino acid residues at position 110-112 of VP1 significantly enhanced infectivity of BHK-21 cells. This study has proven that the symmetrical arrangement of even a single amino acid residue change in the FMD virion, is a powerful strategy deployed by the virus to generate novel receptor binding and alternative host-cell interactions. Understanding which amino acid substitutions in the FMDV capsid region contribute favorably to rapid virus adaptation to cell culture will improve vaccine production using reverse genetics.

FMD is controlled in southern Africa essentially through vaccination, restriction of animal movement and frequent animal inspections in the controlled areas. However, the effective control of FMD requires not only effective vaccines but also sensitive, specific and rapid diagnostic tools (reviewed in Longjam *et al.*, 2011). In addition, the control and eradication of FMD in Africa is complicated by, among other factors, the existence of five of the seven FMDV serotypes, including the SAT-serotypes 1, 2 and 3 that are genetically and antigenically the most variable FMDV serotypes (Maree *et al.*, 2013; 2014). The genetic heterogeneity of the FMDV 3ABC-coding region of the SAT type viruses indicates that the current commercial tests may not be sensitive in the southern African sub-region. Additionally, a key diagnostic assay to enable a country to re-gain its FMD-free status and for FMD surveillance, is the 3ABC or the non-structural protein (NSP) enzyme-linked immunosorbent assay (ELISA). Although many kits are available to detect 3ABC antibodies, none has been developed specifically for the variable SAT serotypes. This study compared the performance of a SAT-specific NSP ELISA with two validated NSP assays (PrioCheck®-NSP and IZSLER-NSP), using panels of

field and experimental sera, vaccinated and/or infected with FMDV SAT1, SAT2 or SAT3. The sensitivity and specificity (95% confidence interval) of the SAT-NSP was estimated as 76% (70%, 81%) and 96% (95%, 98%), respectively. In addition, high sensitivities and specificities were observed for the PrioCheck®-NSP (82% and 99% respectively) and IZSLER-NSP (78% and 98% respectively) and good correlations were observed for all three assays. The high sensitivity and specificity of the SAT-NSP makes this test an ideal tool for FMD eradication, surveillance and control programs.

FMDV populations are quasispecies, which is due to the lack of the proofreading mechanism of the RNA-dependent RNA polymerase during FMDV replication resulting in genomes that are related but non-identical (Domingo *et al.*, 2002; 2004). Thus, the impediment that arises is a broad spectrum of antigenic and genetic FMDV variants within each serotype. The location of identified epitopic residues of the antigenic sites tend to differ even though there are several structural and functional similarities within the structural proteins across serotypes. This poses serious implications in vaccine design and efficacy where an effective vaccine should include multiple independent neutralizing epitopes to elicit an immune response (Longjam and Tayo, 2011). The hypervariable regions on surface-exposed loops of the FMDV that link β -sheets in the capsid proteins (VP1-3) have been shown to contribute to immunogenic variation (Acharya *et al.*, 1989; 1990; Aktas and Samuel, 2000; Hogle *et al.*, 1985). Further investigation of the residues that comprise the antigenic determinants of the virus will allow the identification of mutations in outbreak strains that potentially lessen the efficacy of a vaccine. Thus, if sufficient epitopes are identified, it may be possible to predict the protection afforded by a vaccine against a specific outbreak strain. Neutralizing antigenic sites have been identified through several studies for serotype A (Thomas *et al.*, 1988a; Baxt *et al.*, 1989; Bolwell *et al.*, 1989; Mahapatra *et al.*, 2011), O (Kitson, *et al.*, 1990; Crowther *et al.*, 1993), C (Mateu *et al.*, 1990) and Asia-1 (Grazioli *et al.*, 2003). However, information regarding the epitopes of the SAT serotypes, which are confined geographically to occur in Africa, is scarce.

A naïve semi-synthetic chicken IgY phage display library, known as the Nkuku® library (Van Wyngaardt *et al.*, 2004) was used for bio-panning against FMD SAT1/KNP/196/91, SAT3/KNP/10/90 and A22 viruses. Unique, novel single chain variable fragments (scFvs) were obtained *i.e.* one, two and nine soluble scFv binders for each of the SAT1, SAT3 and A22 viruses, respectively. These binders were used in virus neutralization assays where it was

observed that the SAT1 and SAT3 soluble scFvs did not neutralize the SAT1 and SAT3 viruses; however, three of the nine A22 binders *i.e.* A22scFv1, A22scFv2 and A22scFv8 were able to neutralize A22. Successive virus passage under scFv pressure, revealed three scFv resistant viruses (SRV), one of which had no amino acid variation occurring when sequences before and after passage was determined, whilst the remaining two SRVs had amino acid mutations occurring in the RGD+3 and +4 positions respectively. Further characterization of these escape mutants was performed at Plum Island Animal Disease Centre (PIADC), USA, due to the restrictions of working with A22 virus at the ARC-OVR.

Phage libraries have additionally proven useful for the generation of diagnostic reagents for the detection of a wide variety of viruses such as influenza virus (Rajput *et al.*, 2015), noroviruses (Hurwitz *et al.*, 2017) and human immunodeficiency virus (Haard *et al.*, 2000). The SAT1 and SAT3 soluble scFvs resulting from the biopanning process was also exploited as immunoreagents for the design of improved diagnostic tests. Soluble scFvs were tested in an ELISA as detecting or capturing reagents and although the SAT1svFv1 retained its native conformation, following adsorption to polystyrene plates, the SAT3scFv's did not. As a detecting reagent in the LPBE, the SAT1 soluble scFv reacted specifically with a panel of SAT1 viruses, albeit with different binding affinities, and did not cross-react with SAT2, SAT3, A or O and showed potential to be used as a detecting reagent, in an ELISA. Unfavourable ELISA signals for the two SAT3 scFvs were shown to be possibly attributed to the sequence variability occurring in the viral capsid proteins of the SAT3 viruses tested which could play a role in altering the epitope to which the scFv favourably binds to the virus.

In conclusion, the symmetrical arrangement of surface exposed clusters of positively charged amino acid residues around the 5-fold axis of the virus has confirmed alternative host-cell interactions and enhanced adaptation of FMD viruses to cultured BHK-21 cells necessary for downstream vaccine production. Utilizing and introducing these amino acid substitutions especially the VP1 110-112 mutation, can result in viruses being easily grown on a large scale in cell culture to produce increased 146S antigen yield. Thus, vaccines can easily be produced for virus strains that are currently circulating and causing a threat, evading the need to isolate on primary cell lines. The development and validation of a SAT-specific 3ABC ELISA is the first study that investigated a truncated SAT 3ABC polyprotein for the use in differentiating vaccinated from infected animals (DIVA) ELISA. The validation study that resulted from this work included a vast number of sera from FMDV vaccinated populations as well as

experimentally infected animals, thus providing a significant performance of the NSP assays investigated in this study. Conclusions could be inferred that the PrioCheck®-NSP, IZSLER-NSP and SAT-NSP ELISA performed similarly and the commercially available PrioCheck®-NSP kit is a dependable kit to use for FMDV NSP testing. This study has successfully obtained three soluble SAT single-chain variable antibody fragments where the analytical sensitivity and specificity of the SAT1 scFv showed potential as a diagnostic reagent. The two SAT3 scFvs can be altered to enhance its performance as a diagnostic reagent by stabilizing the soluble scFv to other proteins whilst retaining functionality. Additionally, the potential use of the SAT scFvs in point of care tests must not be ruled out and should also be investigated in future work. The use of the SAT1 and SAT3 soluble scFvs in this study, resulted in the use of ELISA and structural data to predict potential SAT1 and SAT3 epitopes. The results obtained from this study has contributed to the increase of knowledge on the FMDV SAT serotypes and will be of benefit to the SADC region as well as the FMD global research community when considering future FMDV investigations such as improved diagnostic assays and vaccine development.

REFERENCES

- Abu Samra, N., Jori, F., Xiao, L., Rikhotso, O. and Thompson, P. N. (2013). Molecular characterization of *Cryptosporidium* species at the wildlife/livestock interface of the Kruger National Park, South Africa. *Comparative immunology, microbiology and infectious diseases*, **36**: 295–302. doi: 10.1016/j.cimid.2012.07.004.
- Acharya, R., Fry, E., Stuart, D., Fox, G., Rowlands, D. and Brown, F. (1989). The three-dimensional structure of foot-and-mouth disease virus at 2.9 Å resolution. *Nature*, **337**: 709–716. doi: 10.1038/337709a0.
- Acharya, R., Fry, E., Stuart, D., Fox, G., Rowlands, D. and Brown, F. (1990). The structure of foot-and-mouth disease virus: implications for its physical and biological properties. *Veterinary Microbiology*, **23**: 21–34. doi: 10.1016/0378-1135(90)90134-H.
- Ahmed, H. A., Salem, S. A. H., Habashi, A. R., Arafa, A. A., Aggour, M. G. A., Salem, G. H., Gaber, A. S., Selem, O., Abdelkader, S. H., Knowles, N. J., Madi, M., Valdazo-González, B., Wadsworth, J., Hutchings, G. H., Mioulet, V., Hammond, J. M. and King, D. P. (2012). Emergence of foot-and-mouth disease virus SAT 2 in Egypt during 2012. *Transboundary and emerging diseases*, **59**: 476–481. doi: 10.1111/tbed.12015.
- Airaksinen, A., Roivainen, M. and Hovi, T. (2001). Coxsackievirus A9 VP1 Mutants with Enhanced or Hindered A Particle Formation and Decreased Infectivity. *Journal of Virology*, **75**: 952–960. doi: 10.1128/JVI.75.2.952-960.2001.
- Aktas, S. and Samuel, A. R. (2000). Identification of antigenic epitopes on the foot and mouth disease virus isolate O1/Manisa/Turkey/69 using monoclonal antibodies. *Revue scientifique et technique (International Office of Epizootics)*, **19**: 744–753.
- Aldabe, R., Irurzun, A. and Carrasco, L. (1997). Poliovirus protein 2BC increases cytosolic free calcium concentrations. *Journal of Virology*, **71**: 6214–6217.
- Alexandersen, S., Zhang, Z. and Donaldson, A. I. (2002). Aspects of the persistence of foot-and-mouth disease virus in animals—the carrier problem. *Microbes and Infection*, **4**: 1099–1110. doi: 10.1016/S1286-4579(02)01634-9.
- Alexandersen, S., Zhang, Z., Donaldson, A. I. and Garland, A. J. M. (2003). The pathogenesis and diagnosis of foot-and-mouth disease. *Journal of Comparative Pathology*, **129**: 1–36. doi: 10.1016/S0021-9975(03)00041-0.
- Alexandersen, S. and Mowat, N. (2005). Foot-and-mouth disease: host range and pathogenesis. *Current topics in microbiology and immunology*, **288**: 9–42. doi: 10.1007/b138628.
- Almeida, M. R., Rieder, E., Chinsangaram, J., Ward, G., Beard, C., Grubman, M. J. and Mason, P. W. (1998). Construction and evaluation of an attenuated vaccine for foot-and-mouth disease: Difficulty adapting the leader proteinase-deleted strategy to the serotype O1 virus. *Virus Research*, **55**: 49–60. doi: 10.1016/S0168-1702(98)00031-8.
- Amadori, M., Archetti, I. L., Verardi, R. and Berneri, C. (1992). Isolation of mononuclear cytotoxic cells from cattle vaccinated against foot-and-mouth disease. *Archives of Virology*, **122**: 293–306. doi: 10.1007/BF01317191.

Amaral-Doel, C. M., Owen, N. E., Ferris, N. P., Kitching, R. P. and Doel, T. R. (1993). Detection of foot-and-mouth disease viral sequences in clinical specimens and ethyleneimine-inactivated preparations by the polymerase chain reaction, *Vaccine*, **11**: 415–421.

Arzt, J., Juleff, N., Zhang, Z., Rodriguez, L. (2011). The Pathogenesis of Foot-and-Mouth Disease I: Viral Pathways in Cattle. *Transboundary and emerging diseases*, **58**: 291-304.

Arzt, J., Pacheco, J., Stenfeldt, C., Rodriguez, L. (2017). Pathogenesis of virulent and attenuated foot-and-mouth disease virus in cattle. *Virology Journal*, **14**: 89 doi: 10.1186/s12985-017-0758-9

Asagoe, T., Inaba, Y., Jusa, E. R., Kouno, M., Uwatoko, K. and Fukunaga, Y. (1997). Effect of heparin on infection of cells by equine arteritis virus. *The Journal of veterinary medical science*, **59**: 727–728.

Ayebazibwe, C., Mwiine, F. N., Balinda, S. N., Tjørnehøj, K., Masembe, C., Muwanika, V. B., Okurut, A. R. A., Siegismund, H. R. and Alexandersen, S. (2010a). Antibodies against foot-and-mouth disease (FMD) virus in African buffalos (*Syncerus caffer*) in selected National Parks in Uganda (2001-2003). *Transboundary and emerging diseases*, **57**: 286–292. doi: 10.1111/j.1865-1682.2010.01147.x.

Ayebazibwe, C., Mwiine, F. N., Tjørnehøj, K., Balinda, S. N., Muwanika, V. B., Ademun Okurut, A. R., Belsham, G. J., Normann, P., Siegismund, H. R. and Alexandersen, S. (2010b). The role of African buffalos (*Syncerus caffer*) in the maintenance of foot-and-mouth disease in Uganda. *BMC veterinary research*, **6**: 54. doi: 10.1186/1746-6148-6-54.

Bablanian, G. M. and Grubman, M. J. (1993). Characterization of the foot-and-mouth disease virus 3C protease expressed in *Escherichia coli*. *Virology*, **197**: 320–327. doi: 10.1006/viro.1993.1593.

Bachrach, H. L., Trautman, R. and Breese, S. S. (1964). Chemical and physical properties of virtually pure foot-and-mouth disease virus. *American Journal of Veterinary Research*, **25**: 333–342.

Balinda, S. N., Belsham, G. J., Masembe, C., Sangula, A. K., Siegismund, H. R. and Muwanika, V. B. (2010a). Molecular characterization of SAT 2 foot-and-mouth disease virus from post-outbreak slaughtered animals: implications for disease control in Uganda. *Epidemiology and infection*, **138**: 1204–1210. doi: 10.1017/S0950268809991427.

Balinda, S. N., Sangula, A. K., Heller, R., Muwanika, V. B., Belsham, G. J., Masembe, C. and Siegismund, H. R. (2010b). Diversity and transboundary mobility of serotype O foot-and-mouth disease virus in East Africa: implications for vaccination policies. *Infection, genetics and evolution: Journal of molecular epidemiology and evolutionary genetics in infectious diseases*, **10**: 1058–1065. doi: 10.1016/j.meegid.2010.06.017.

Baranowski, E., Sevilla, N., Verdaguer, N., Ruiz-Jarabo, C. M., Beck, E. and Domingo, E. (1998). Multiple virulence determinants of foot-and-mouth disease virus in cell culture. *Journal of Virology*, **72**: 6362–6372.

Baranowski, E., Ruiz-Jarabo, C. M., Sevilla, N., Andreu, D., Beck, E. and Domingo, E. (2000). Cell recognition by foot-and-mouth disease virus that lacks the RGD integrin-binding motif: flexibility in aphthovirus receptor usage. *Journal of Virology*, **74**: 1641–7.

- Barnett, P. V., Ouldrige, E. J., Rowlands, D. J., Brown, F., Parry, N. R. (1989). Neutralizing epitopes of type O foot-and-mouth disease virus. I. Identification and characterization of three functionally independent, conformational sites. *Journal of General Virology*, **70**:1483-91.
- Barnett, P. V., Cox, S. J., Aggarwal, N., Gerber, H. and McCullough, K. C. (2002). Further studies on the early protective responses of pigs following immunisation with high potency foot and mouth disease vaccine. *Vaccine*, **20**: 3197–208.
- Barteling, S. J. (2002). Development and performance of inactivated vaccines against foot and mouth disease. *Revue scientifique et technique* (International Office of Epizootics), **21**: 577–588.
- Bartley, L. M., Donnelly, C. A. and Anderson, R. M. (2002). Review of foot-and-mouth disease virus survival in animal excretions and on fomites. *The Veterinary Record*, **151**: 667–669.
- Bastos, A. D. S. (1998). Detection and characterisation of foot-and-mouth disease virus in sub-Saharan Africa. *Onderstepoort Journal of Veterinary Research*, **65**: 37–47.
- Bastos, A. D. S., Anderson, E. C., Bengis, R. G., Keet, D. F., Winterbach, H. K. and Thomson, G. R. (2003a). Molecular Epidemiology of SAT3-Type Foot-and-Mouth Disease. *Virus Genes*. **27**: 283–290, doi: 10.1023/A:1026352000959.
- Bastos, A. D. S., Haydon, D. T., Sangaré, O., Boshoff, C. I., Edrich, J. L. and Thomson, G. R. (2003b). The implications of virus diversity within the SAT 2 serotype for control of foot-and-mouth disease in sub-Saharan Africa. *Journal of General Virology*, **84**: 1595–1606. doi: 10.1099/vir.0.18859-0.
- Bautista, E. M., Ferman, G. S. and Golde, W. T. (2003). Induction of lymphopenia and inhibition of T cell function during acute infection of swine with foot and mouth disease virus (FMDV). *Veterinary Immunology and Immunopathology*, **92**: 61–73.
- Bautista, E. M., Ferman, G. S., Gregg, D., Brum, M. C. S., Grubman, M. J. and Golde, W. T. (2005). Constitutive Expression of Alpha Interferon by Skin Dendritic Cells Confers Resistance to Infection by Foot-and-Mouth Disease Virus Constitutive Expression of Alpha Interferon by Skin Dendritic Cells Confers Resistance to Infection by Foot-and-Mouth Disease. *Journal of Virology*. **79**: 4838–4847, doi: 10.1128/JVI.79.8.4838.
- Baxi, M. K., Baxi, S., Clavijo, A., Burton, K. M. and Deregt, D. (2006). Microarray-based detection and typing of foot-and-mouth disease virus. *Veterinary Journal* (London, England : 1997). **172**: 473–481, doi: 10.1016/j.tvjl.2005.07.007.
- Baxt, B., Morgan, D. O., Robertson, B. H. and Timpone, C. (1984). Epitopes on foot-and-mouth disease virus outer capsid protein VP1 involved in neutralization and cell attachment. *Journal of Virology*, **51**: 298–305.
- Baxt, B. and Morgan, D. (1985). Nature of the interaction between foot-and-mouth disease virus and cultured cells, in Richard L. Crowell, Karl Lonberg-Holm, A. S. for M. (ed.) Virus Attachment and Entry into Cells, *Proceedings of an ASM Conference*. American Society for Microbiology.
- Baxt, B., Vakharia, V., Moore, D. M., Franke, A. J. and Morgan, D. O. (1989). Analysis of neutralizing antigenic sites on the surface of type A12 foot-and-mouth disease virus. *Journal of Virology*, **63**: 2143–51.

- Baxt, B. and Becker, Y. (1990). The effect of peptides containing the arginine-glycine-aspartic acid sequence on the adsorption of foot-and-mouth disease virus to tissue culture cells. *Virus Genes*, **4**: 73–83. doi: 10.1007/BF00308567.
- Baxt, B. and Mason, P. W. (1995). Foot-and-mouth disease virus undergoes restricted replication in macrophage cell cultures following Fc receptor-mediated adsorption. *Virology*, **10**: 503–509. doi: S0042-6822(85)71110-5 [pii]r10.1006/viro.1995.1110.
- Beck, E. and Strohmaier, K. (1987). Subtyping of European foot-and-mouth disease virus strains by nucleotide sequence determination. *Journal of Virology*, **61**: 1621–1629.
- Belsham, G. J. and Bostock, C. J. (1988). Studies on the infectivity of foot-and-mouth disease virus RNA using microinjection. *The Journal of General Virology*, **69**: 265–74. doi: 10.1099/0022-1317-69-2-265.
- Belsham, G. J. (1993). Distinctive features of foot-and-mouth disease virus, a member of the picornavirus family; aspects of virus protein synthesis, protein processing and structure. *Progress in biophysics and molecular biology*, **60**: 241–60.
- Belsham, G. J. and Martínez-Salas, E. (2004). Genome organisation, translation and replication of foot-and-mouth disease virus RNA, in Domingo, E., Sobrino, F. N. (ed.) *Foot and Mouth Disease: Current Perspectives*. United Kingdom: Horizon Bioscience, pp. 19–52.
- Belsham, G. (2005). Translation and replication of FMDV RNA. *Current topics in microbiology and immunology*, **288**: 43–70.
- Bengis, R. G., Thomson, G. R., Hedger, R. S., De Vos, V. and Pini, A. (1986). Foot-and-mouth disease and the African buffalo (*Syncerus caffer*). 1. Carriers as a source of infection for cattle. *The Onderstepoort Journal of Veterinary Research*, **53**: 69–73.
- Bergmann, I. E., de Mello, P. A., Neitzert, E., Beck, E. and Gomes, I. (1993). Diagnosis of persistent aphthovirus infection and its differentiation from vaccination response in cattle by use of enzyme-linked immunoelectrotransfer blot analysis with bioengineered nonstructural viral antigens. *American Journal of Veterinary Research*, **54**: 825–831.
- Bergmann, I.E., Malirat, V. and Neitzert, E. (2005). Non-capsid proteins to identify foot-and-mouth disease viral circulation in cattle irrespective of vaccination. *Biologicals*, **33**: 235–239.
- Berinstein, A., Roivainen, M., Hovi, T., Mason, P. W. and Baxt, B. (1995). Antibodies to the vitronectin receptor (integrin $\alpha\beta 3$) inhibit binding and infection of foot-and-mouth disease virus to cultured cells. *Journal of Virology*, **69**: 2664–2666.
- Berryman, S., Clark, S., Kakker, N. K., Silk, R., Seago, J., Wadsworth, J., Chamberlain, K., Knowles, N. J. and Jackson, T. (2013). Positively charged residues at the 5-fold symmetry axis of cell-culture adapted foot-and-mouth disease virus permit novel receptor interactions. *Journal of Virology*, **87**: 8735–8744. doi: 10.1128/jvi.01138-13.
- Blanco, E., Blanco, E., Garcia-briones, M., Garcia-briones, M., Sanz-parra, A., Sanz-parra, A., Gomes, P., Gomes, P., Oliveira, E. D. E., Oliveira, E. D. E., Valero, M. L. U. Z., Valero, M. L. U. Z., Andreu, D., Andreu, D., Ley, V., Ley, V., Sobrino, F. and Sobrino, F. (2001). Identification of T-Cell Epitopes in Nonstructural Proteins of Foot-and-Mouth Disease Virus. *Journal of Virology*, **75**: 3164–3174. doi: 10.1128/JVI.75.7.3164.
- Blignaut, B., Visser, N., Theron, J., Rieder, E. and Maree, F. F. (2011). Custom-engineered

chimeric foot-and-mouth disease vaccine elicits protective immune responses in pigs. *The Journal of General Virology*, **92**: 849–59. doi: 10.1099/vir.0.027151-0.

Bolwell, C., Clarke, B. E., Parry, N. R., Ouldrige, E. J., Brown, F. and Rowlands, D. J. (1989). Epitope mapping of foot-and-mouth disease virus with neutralizing monoclonal antibodies. *The Journal of General Virology*, **70**: 59–68. doi: 10.1099/0022-1317-70-1-59.

Breuss, J. M., Gallo, J., DeLisser, H. M., Klimanskaya, I. V, Folkesson, H. G., Pittet, J. F., Nishimura, S. L., Aldape, K., Landers, D. V and Carpenter, W. (1995). Expression of the beta 6 integrin subunit in development, neoplasia and tissue repair suggests a role in epithelial remodeling. *Journal of Cell Science*, **108**: 2241–51.

Brito, B. P., Jori, F., Dwarka, R., Maree, F. F., Heath, L. and Perez, A. M. (2016). Transmission of Foot-and-Mouth Disease SAT2 Viruses at the Wildlife–Livestock Interface of Two Major Transfrontier Conservation Areas in Southern Africa. *Frontiers in Microbiology*, **7**: Article 528- doi: 10.3389/fmicb.2016.00528.

Brocchi, E., De Diego, M. I., Berlinzani, A, Gamba, D. and De Simone, F. (1998). Diagnostic potential of Mab-based ELISAs for antibodies to non-structural proteins of foot-and-mouth disease virus to differentiate infection from vaccination. *The Veterinary Quarterly*, **20**: S20–S24. doi: 10.1080/01652176.1998.9694957.

Brocchi, E., Bergmann, I. E., Dekker, A., Paton, D. J., Sammin, D. J., Greiner, M., Grazioli, S., De Simone, F., Yadin, H., Haas, B., Bulut, N., Malirat, V., Neitzert, E., Goris, N., Parida, S., Sørensen, K. and De Clercq, K. (2006). Comparative evaluation of six ELISAs for the detection of antibodies to the non-structural proteins of foot-and-mouth disease virus. *Vaccine*, **24**: 6966–6979. doi: 10.1016/j.vaccine.2006.04.050.

Bronsvort, B. M. D. C., Radford, A. D., Tanya, V. N., Nfon, C., Kitching, R. P. and Morgan, K. L. (2004a). Molecular Epidemiology of Foot-and-Mouth Disease Viruses in the Adamawa Province of Cameroon Molecular Epidemiology of Foot-and-Mouth Disease Viruses in the Adamawa Province of Cameroon. *Journal of Clinical microbiology*, **42**: 2186–2196. doi: 10.1128/JCM.42.5.2186.

Bronsvort, B. M. D. C., Sørensen, K. J., Anderson, J., Corteyn, A., Tanya, V. N., Kitching, R. P. and Morgan, K. L. (2004b). Comparison of Two 3ABC Enzyme-Linked Immunosorbent Assays for Diagnosis of Multiple-Serotype Foot-and-Mouth Disease in a Cattle Population in an Area of Endemicity Comparison of Two 3ABC Enzyme-Linked Immunosorbent Assays for Diagnosis of Multiple-Serotyp. *Journal of Clinical Microbiology*, **42**: 2108–2114. doi: 10.1128/JCM.42.5.2108.

Brooksby, J. B. (1967). Foot-and-mouth disease--a world problem. *Nature*, **213**: 120–2.

Brown, F. (1999). Foot-and-mouth disease and beyond: vaccine design, past, present and future. *Archives of virology*, Supplementum, **15**: 179–88.

Bruderer, U., Swam, H., Haas, B., Visser, N., Brocchi, E., Grazioli, S., Esterhuysen, J.J., Vosloo, W., Forsyth, M., Aggarwal, N., Cox, S., Armstrong, R. and Anderson, J. (2004). Differentiating infection from vaccination in foot-and-mouth disease: evaluation of an ELISA based on recombinant 3ABC. *Veterinary Microbiology*, **101**: 187–197.

Burman, A., Clark, S., Abrescia, N. G. A., Fry, E. E., Stuart, D. I. and Jackson, T. (2006). Specificity of the VP1 GH Loop of Foot-and-Mouth Disease Virus for v Integrins. *Journal of*

Virology, **80**: 9798–9810. doi: 10.1128/JVI.00577-06.

Burton, D. R., Hangartner, L. (2016). Broadly Neutralizing Antibodies to HIV and Their Role in Vaccine Design. *Annual Reviews in Immunology*, **20**: 635-59.

Byrnes, A. P. and Griffin, D. E. (1998). Binding of Sindbis virus to cell surface heparan sulfate. *Journal of Virology*, **72**: 7349–7356.

Calvete, J. J., Henschen, A. and González-Rodríguez, J. (1991). Assignment of disulphide bonds in human platelet GPIIIa. A disulphide pattern for the beta-subunits of the integrin family. *The Biochemical Journal*, **274**: 63–71.

Capozzo, A. V. E., Burke, D. J., Fox, J. W., Bergmann, I. E., La Torre, J. L. and Grigera, P. R. (2002). Expression of foot and mouth disease virus non-structural polypeptide 3ABC induces histone H3 cleavage in BHK21 cells. *Virus Research*, **90**: 91–99.

Capozzo, A. V., Wilda, M., Bucafusco, D., de los Ángeles Lavoria, M., Franco-Mahecha, O. L., Mansilla, F. C., Pérez-Filgueira, D. M. and Grigera, P. R. (2011). Vesicular Stomatitis Virus glycoprotein G carrying a tandem dimer of Foot and Mouth Disease Virus antigenic site A can be used as DNA and peptide vaccine for cattle. *Antiviral Research*, **92**: 219–227. doi: 10.1016/j.antiviral.2011.08.006.

Carmen, S. and Jermutus, L. (2002). Concepts in antibody phage display. *Briefings in Functional Genomics and Proteomics*, **1**: 189–203. doi: 10.1093/bfgp/1.2.189.

Caron, A., Miguel, E., Gomo, C., Makaya, P., Pfukenyi, D. M., Foggin, C., Hove, T. and de Garine-Wichatitsky, M. (2013). Relationship between burden of infection in ungulate populations and wildlife/livestock interfaces. *Epidemiology and Infection*, **141**: 1522–1535. doi: 10.1017/S0950268813000204.

Carrillo, C., Tulman, E. R., Delhon, G., Lu, Z., Carreno, A., Vagnozzi, A., Kutish, G. F. and Rock, D. L. (2005). Comparative genomics of Foot-and-Mouth Disease Virus. *The Journal of Virology*, **79**: 6487–6504. doi: 10.1128/JVI.79.10.6487.

Carrillo, C., Lu, Z., Borca, M. V, Vagnozzi, A., Kutish, G. F. and Rock, D. L. (2007). Genetic and Phenotypic Variation of FMDV During Serial Passages in a Natural Host. *Journal of Virology*, **81**: 11341-11351. doi: 10.1128/JVI.00930-07.

Carroll, M. C. (2004). The complement system in regulation of adaptive immunity. *Nature Immunology*, **5**: 981–986. doi: 10.1038/ni1113.

Caspersen, K., Park, J.-H., Patil, S. and Dumler, J. S. (2002). Genetic variability and stability of *Anaplasma phagocytophila* msp2 (p44). *Infection and Immunity*, **70**: 1230–4.

Chamberlain, K., Fowler, V. L., Barnett, P. V., Gold, S., Wadsworth, J., Knowles, N. J. and Jackson, T. (2015). Identification of a novel cell culture adaptation site on the capsid of foot-and-mouth disease virus. *The Journal of General Virology*, **96**: 2684–2692. doi: 10.1099/jgv.0.000222.

Chang, K. H., Auvinen, P., Hyypia, T. and Stanway, G. (1989). The nucleotide sequence of Coxsackievirus A9; Implications for receptor binding and enterovirus classification. *Journal of General Virology*, **70**: 3269–3280. doi: 10.1099/0022-1317-70-12-3269.

Charleston, B., Bankowski, B. M., Gubbins, S., Chase-Topping, M. E., Schley, D., Howey, R.,

Barnett, P. V, Gibson, D., Juleff, N. D. and Woolhouse, M. E. J. (2011). Relationship between clinical signs and transmission of an infectious disease and the implications for control. *Science* (New York, N.Y.), **332**: 726–9. doi: 10.1126/science.1199884.

Charpentier, N., Davila, M., Domingo, E. and Escarmis, C. (1996). Long-term, large-population passage of aphthovirus can generate and amplify defective noninterfering particles deleted in the leader protease gene. *Virology*, **223**: 10–18. doi: S004268229690450X [pii].

Chase-Topping, M. E., Handel, I., Bankowski, B. M., Juleff, N. D., Gibson, D., Cox, S. J., Windsor, M. A., Reid, E., Doel, C., Howey, R., Barnett, P. V., Woolhouse, M. E. J. and Charleston, B. (2013). Understanding foot-and-mouth disease virus transmission biology: Identification of the indicators of infectiousness. *Veterinary Research*, **44** :46. doi: 10.1186/1297-9716-44-46.

Cavanagh, D., Rowlands, D. J. and Brown, F. (1978). Early events in the interaction between foot-and-mouth disease virus and primary pig kidney cells. *Journal of General Virology*, **41**: 255-64.

Chen, Y., Maguire, T., Hileman, R. E., Fromm, J. R., Esko, J. D., Linhardt, R. J. and Marks, R. M. (1997). Dengue virus infectivity depends on envelope protein binding to target cell heparan sulfate. *Nature Medicine*, **3**: 866–871. doi: 10.1038/nm0897-866.

Chung, C. S., Hsiao, J. C., Chang, Y. S. and Chang, W. (1998). A27L protein mediates vaccinia virus interaction with cell surface heparan sulfate. *Journal of Virology*, **72**: 1577–1585. doi: 10.1128/JVI.75.16.7517-7527.2001.

Clackson, T., Hoogenboom, H. R., Griffiths, A. D. and Winter, G. (1991). Making antibody fragments using phage display libraries. *Nature*, **352**: 624–628. doi: 10.1038/352624a0.

Clarke, B. E., Sangar, D. V., Burroughs, J. N., Newton, S. E., Carroll, A. R. and Rowlands, D. J. (1985). Two initiation sites for foot-and-mouth disease virus polyprotein in vivo. *Journal of General Virology*, **66**: 2615–2626. doi: 10.1099/0022-1317-66-12-2615.

Clavijo, A., Wright, P. and Kitching, P. (2004). Developments in diagnostic techniques for differentiating infection from vaccination in foot-and-mouth disease. *The Veterinary Journal*, **167**: 9–22. doi: 10.1016/S1090-0233(03)00087-X.

Cloete, M., Dungu, B., Van Staden, L. I., Ismail-Cassim, N. and Vosloo, W. (2008). Evaluation of different adjuvants for foot-and-mouth disease vaccine containing all the SAT serotypes. *The Onderstepoort journal of veterinary research*, **75**: 17–31.

Clopper, C.J. and Pearson, E.S. (1934). The use of confidence or fiducial limits illustrated in the case of the binomial. *Biometrika*, **26**: 404–413.

Collen, T. (1994). Cell-mediated immunity. In Ruminants, (Goddeeris, B. M. L. and Morrison, W. I., eds.). pp. 173-198, CRC Press, London.

Collins, R. A., Ko, L.-S., Fung, K. Y., Lau, L.-T., Xing, J. and Yu, A. C. H. (2002). A method to detect major serotypes of foot-and-mouth disease virus. *Biochemical and biophysical research communications*, **297**: 267–74.

Compton T., Nowlin D.M. and Cooper, N.R. (1993). Initiation of human cytomegalovirus infection requires initial interaction with cell surface heparan sulfate. *Virology*, **193**: 834–841.

Condy, J. B. and Hedger, R. S. (1974). The survival of foot and mouth disease virus in African buffalo with non transference of infection to domestic cattle. *Research in Veterinary Science*, **16**: 182–185.

Condy, J. B., Hedger, R. S., Hamblin, C. and Barnett, I. T. (1985). The duration of the foot-and-mouth disease virus carrier state in African buffalo (i) in the individual animal and (ii) in a free-living herd. *Comparative immunology, microbiology and infectious diseases*, **8**: 259–65.

Corti, D., Cameroni, E., Guarino, B., Kallewaard, N. L., Zhu, Q. and Lanzavecchia, A. (2017). Tackling influenza with broadly neutralizing antibodies. *Current Opinion in Virology*, **24**: 60–69.

Crowther, J. R., Rowe, C. A. and Butcher, R. (1993). Characterization of monoclonal antibodies against a type SAT 2 foot-and-mouth disease virus. *Epidemiology and Infection*, **111**: 391–406.

Curry, S., Abrams, C. C., Fry, E., Crowther, J. C., Belsham, G. J., Stuart, D. I. and King, A. M. Q. (1995). Viral-RNA Modulates the Acid Sensitivity of Foot-and-Mouth-Disease Virus Capsids. *Journal of Virology*, **69**: 430–438.

Curry, S., Fry, E., Blakemore, W., Abu-Ghazaleh, R., Jackson, T., King, A., Lea, S., Newman, J., Rowlands, D. and Stuart, D. (1996). Perturbations in the surface structure of A22 Iraq foot-and-mouth disease virus accompanying coupled changes in host cell specificity and antigenicity. *Structure (London, England : 1993)*, **4**: 135–45.

Danner, S. and Belasco, J. G. (2001). T7 phage display: a novel genetic selection system for cloning RNA-binding proteins from cDNA libraries. *Proceedings of the National Academy of Sciences of the United States of America*, **98**: 12954–9. doi: 10.1073/pnas.211439598.

Davidson, F. L., Crowther, J. R., Nqindi, J., Knowles, N. J., Thevasagayam, S. J. and Van Vuuren, C. J. (1995). Antigenic analysis of SAT 2 serotype foot-and-mouth disease virus isolates from Zimbabwe using monoclonal antibodies. *Epidemiology and Infection*, **115**: 193–205.

Dawe, P.S., Flanagan, F.O., Madekurozwa, R.L., Sorensen, K.J., Anderson, E.C., Foggin, C.M., Ferris, N.P., Knowles, N.J. (1994). Natural transmission of foot-and-mouth disease virus from African buffalo (*Syncerus caffer*) to cattle in a wildlife area of Zimbabwe. *Veterinary Record*, **134**: 230–232.

Dedhar, S. and Hannigan, G. E. (1996). Integrin cytoplasmic interactions and bidirectional transmembrane signalling. *Current opinion in cell biology*, **8**: 657–69.

Devaney, M. A., Vakharia, V. N., Lloyd, R. E., Ehrenfeld, E. and Grubman, M. J. (1988). Leader protein of foot-and-mouth disease virus is required for cleavage of the p220 component of the cap-binding protein complex. *Journal of Virology*, **62**: 4407–9.

De Diego, M., Brocchi, E., Mackay, D. and De Simone, F. (1997). The non-structural polyprotein 3ABC of foot-and-mouth disease virus as a diagnostic antigen in ELISA to differentiate infected from vaccinated cattle. *Archives of Virology*, **142**: 2021–2033. doi: 10.1007/s007050050219.

De Los Santos, T., Diaz-San Segundo, F. and Grubman, M. J. (2007). Degradation of nuclear factor kappa B during foot-and-mouth disease virus infection. *Journal of Virology*, **81**: 12803–

12815. doi: 10.1128/JVI.01467-07.

Di Nardo, A., Knowles, N. and Paton, D. (2011). Combining livestock trade patterns with phylogenetics to help understand the spread of foot and mouth disease in sub-Saharan Africa, the Middle East and Southeast Asia. *Revue scientifique et technique de l'Office international des épizooties*, **30**: 63–85.

Ding, Y., Liu, Y., Zhou, J., Chen, H., Zhang, J., Ma, L. and Wei, G. (2011). A highly sensitive detection for foot-and-mouth disease virus by gold nanoparticle improved immuno-PCR. *Virology Journal*, **8**: 148. doi: 10.1186/1743-422X-8-148.

Dintzis, H. M., Dintzis, R. Z. and Vogelstein, B. (1976). Molecular determinants of immunogenicity: the immunon model of immune response. *Proceedings of the National Academy of Sciences of the United States of America*, **73**: 3671–5. doi: 10.1073/pnas.73.10.3671.

Doel, T. R. and Baccharini, P. J. (1981). Thermal stability of foot-and-mouth disease virus. *Archives of Virology*, **70**: 21–32.

Doel, T. R. and Mowat, G. N. (1985). An international collaborative study on foot-and-mouth disease virus assay methods. 2. Quantification of 146S particles. *Journal of Biological Standards*, **13**: 335-44.

Doel, T. R. (1996). Natural and vaccine-induced immunity to foot and mouth disease: the prospects for improved vaccines. *Revue scientifique et technique (International Office of Epizootics)*, **15**: 883–911.

Doel, T. R. (2003). FMD vaccines. *Virus Research*, **91**: 81–99. doi: 10.1016/S0168-1702(02)00261-7.

Doel, T. R. (2005). Natural and vaccine induced immunity to FMD, in *Foot-and-Mouth Disease Virus*, pp. 103–131. doi: 10.1007/3-540-27109-0_5.

Domingo, E., Martínez-Salas, E., Sobrino, F., de la Torre, J. C., Portela, A., Ortín, J., López-Galindez, C., Pérez-Breña, P., Villanueva, N. and Nájera, R. (1985). The quasispecies (extremely heterogeneous) nature of viral RNA genome populations: biological relevance--a review. *Gene*, **40**: 1–8.

Domingo, E., Diez, J., Martinez, M. A., Hernandez, J., Holguin, A., Borrego, B. and Mateu, M. G. (1993). New observations on antigenic diversification of RNA viruses. Antigenic variation is not dependent on immune selection. *Journal of General Virology*, **74**: 2039–45

Domingo, E., Baranowski, E., Escarmís, C. and Sobrino, F. (2002). Foot-and-mouth disease virus. *Comparative Immunology, Microbiology and Infectious Diseases*, **25**: 297–308. doi: 10.1016/S0147-9571(02)00027-9.

Domingo, E., Escarmís, C., Baranowski, E., Ruiz-Jarabo, C. M., Carrillo, E., Núñez, J. I. and Sobrino, F. (2003). Evolution of foot-and-mouth disease virus. *Virus Research*, **91**: 47–63. doi: 10.1016/S0168-1702(02)00259-9.

Domingo, E., Ruiz-Jarabo, C. M., Arias, A., Garcia-Arriaza, J. and Escarmis, C. (2004) Quasispecies dynamics and evolution of foot-and-mouth disease virus, in *Foot and mouth disease: Current Perspectives*, ed. Esteban Domingo and Francisco Sobrino, pp. 262–304. doi.org/10.1201/9781420037968.ch10

Domingo, E., Gonzalez-Lopez, C., Pariente, N., Airaksinen, A., Escarmís, C. (2005). Population dynamics of RNA viruses: the essential contribution of mutant spectra. *Archives of Virology Suppl.* **19**: 59-71.

Donaldson, A. I. (1972). The influence of relative humidity on the aerosol stability of different strains of foot-and-mouth disease virus suspended in saliva. *The Journal of General Virology*, **15**: 25–33. doi: 10.1099/0022-1317-15-1-25.

Donaldson, A. I. and Kitching, R. P. (1989). Transmission of foot-and-mouth disease by vaccinated cattle following natural challenge. *Research in Veterinary Science*, **46**: 9–14.

Donaldson A. I. and Kitching R. P. (2000). Manual of Standards for Diagnostic Tests and Vaccines, in *OIE Standards Commission*. 4th edn. Paris, pp. 77–92.

Dreyfuss, J. L., Regatieri, C. V., Jarrouge, T. R., Cavalheiro, R. P., Sampaio, L. O. and Nader, H. B. (2009). Heparan sulfate proteoglycans: structure, protein interactions and cell signaling. *Anais da Academia Brasileira de Ciências*, **81**: 409–429. doi: 10.1590/S0001-37652009000300007.

Dukes, J. P., King, D. P. and Alexandersen, S. (2006). Novel reverse transcription loop-mediated isothermal amplification for rapid detection of foot-and-mouth disease virus. *Archives of Virology*, **151**: 1093–106. doi: 10.1007/s00705-005-0708-5.

Dunn, C. S., Samuel, A. R., Pullen, L. A. and Anderson, J. (1998). The Biological Relevance of Virus Neutralisation Sites for Virulence and Vaccine Protection in the Guinea Pig Model of Foot-and-Mouth Disease. *Virology*, **247**: 51–61. doi: 10.1006/viro.1998.9175.

Duque, H. and Baxt, B. (2003). Foot-and-Mouth Disease Virus Receptors : Comparison of Bovine α V Integrin Utilization by Type A and O Viruses. *Journal of Virology*, **77**: 2500–2511. doi: 10.1128/JVI.77.4.2500.

Duque, H., LaRocco, M., Golde, W. T. and Baxt, B. (2004). Interactions of Foot-and-Mouth Disease Virus with Soluble Bovine V 3 and V 6 Integrins. *Journal of Virology*, **78**: 9773–9781. doi: 10.1128/JVI.78.18.9773-9781.2004.

Dyason, E. (2010). Summary of foot-and-mouth disease outbreaks reported in and around the Kruger National Park, South Africa, between 1970 and 2009. *Journal of South African Veterinary Association*, **81**: 201–206.

Edelman, G. M., Cunningham, B. A., Gall, W. E., Gottlieb, P. D., Rutishauser, U. and Waxdal, M. J. (1969). The covalent structure of an entire gammaG immunoglobulin molecule. *Proceedings of the National Academy of Sciences of the United States of America*, **63**: 78–85. doi: 10.1073/pnas.63.1.78.

Elnekave, E., Shilo, H., Gelman, B. and Klement, E. (2015). The longevity of anti NSP antibodies and the sensitivity of a 3ABC ELISA – A 3 years follow up of repeatedly vaccinated dairy cattle infected by foot and mouth disease virus. *Veterinary Microbiology* **178**: 14–18.

Emsley P and Cowtan, K. (2004). Coot: model-building tools for molecular graphics. *Acta Crystallogr D Biol Crystallogr*, **60**: 2126–2132.

Etchison, D., Milburn, S. C., Edery, I., Sonenberg, N. and Hershey, J. W. (1982). Inhibition of HeLa cell protein synthesis following poliovirus infection correlates with the proteolysis of a 220,000-dalton polypeptide associated with eucaryotic initiation factor 3 and a cap binding

protein complex. *The Journal of Biological Chemistry*, **257**: 14806–10.

Eygelaar, D., Jori, F., Mokopasetso, M., Sibeko, K. P., Collins, N. E., Vorster, I., Troskie, M. and Oosthuizen, M. C. (2015). Tick-borne haemoparasites in African buffalo (*Syncerus caffer*) from two wildlife areas in Northern Botswana. *Parasites & Vectors*, **8**: 26. doi: 10.1186/s13071-014-0627-y.

Falk, M. M., Grigera, P. R., Bergmann, I. E., Zibert, A., Multhaup, G. and Beck, E. (1990). Foot-and-mouth disease virus protease 3C induces specific proteolytic cleavage of host cell histone H3. *Journal of Virology*, **64**: 748–756.

Fehrsen, J., Van Wyngaardt, W., Mashau, C., Potgieter, A. C., Chaudhary, V. K., Gupta, A., Jordaan, F. A. and du Plessis, D. H. (2005). Serogroup-reactive and type-specific detection of bluetongue virus antibodies using chicken scFvs in inhibition ELISAs. *Journal of Virological Methods*, **129**: 31–9. doi: 10.1016/j.jviromet.2005.04.015.

Ferrer-Orta, C. and Fita, I. (2004). Structure of foot-and-mouth disease virus particles, in Sobrino, F., Domingo, E. (ed.) *Foot-and-mouth disease: Current perspectives*. Horizon Biosciences, pp. 77–92.

Filman, D. J., Syed, R., Chow, M., Macadam, A. J., Minor, P. D. and Hogle, J. M. (1989). Structural factors that control conformational transitions and serotype specificity in type 3 poliovirus. *The EMBO journal*, **8**: 1567–79.

Fors, S., Strebel, K., Beck, E. and Schaller, H. (1984). Nucleotide sequence and genome organization of foot-and-mouth disease virus. *Nucleic acids research*, **12**: 6587–601.

Fowler, V. L., Paton, D. J., Rieder, E. and Barnett, P. V. (2008). Chimeric foot-and-mouth disease viruses: evaluation of their efficacy as potential marker vaccines in cattle. *Vaccine*, **26**: 1982–9. doi: 10.1016/j.vaccine.2008.02.012.

Fowler, V. L., Knowles, N. J., Paton, D. J. and Barnett, P. V. (2010). Marker vaccine potential of a foot-and-mouth disease virus with a partial VP1 G-H loop deletion. *Vaccine*, **28**: 3428–3434. doi: 10.1016/j.vaccine.2010.02.074.

Fowler, V. L., Bankowski, B. M., Armson, B., Di Nardo, A., Valdazo-Gonzalez, B., Reid, S. M., Barnett, P. V., Wadsworth, J., Ferris, N. P., Mioulet, V. and King, D. P. (2014). Recovery of Viral RNA and Infectious Foot-and-Mouth Disease Virus from Positive Lateral-Flow Devices. *PLoS ONE*. (ed.) Y. E. Khudyakov, 9(10), p. e109322. doi: 10.1371/journal.pone.0109322.

Fox, G., Parry, N. R., Barnett, P. V., McGinn, B., Rowlands, D. J. and Brown, F. (1989). The cell attachment site on foot-and-mouth disease virus includes the amino acid sequence RGD (arginine-glycine-aspartic acid). *Journal of General Virology*, **70**: 625–37. doi: 10.1099/0022-1317-70-3-625.

Fromm, J. R., Hileman, R. E., Caldwell, E. E. O., Weiler, J. M. and Linhardt, R. J. (1995). Differences in the Interaction of Heparin with Arginine and Lysine and the Importance of these Basic Amino Acids in the Binding of Heparin to Acidic Fibroblast Growth Factor. *Archives of Biochemistry and Biophysics*, **323**: 279–287. doi: 10.1006/abbi.1995.9963.

Fry, E. E., Lea, S. M., Jackson, T., Newman, J. W. I., Ellard, F. M., Blakemore, W. E., Abu-Ghazaleh, R., Samuel, A., King, A. M. Q. and Stuart, D. I. (1999). The structure and function

of a foot-and-mouth disease virus-oligosaccharide receptor complex. *EMBO Journal*, **18**: 543–554. doi: 10.1093/emboj/18.3.543.

Fry, E. E., Newman, J. W. I., Curry, S., Najjam, S., Jackson, T., Blakemore, W., Lea, S. M., Miller, L., Burman, A., King, A. M. Q. and Stuart, D. I. (2005). Structure of Foot-and-mouth disease virus serotype A10 61 alone and complexed with oligosaccharide receptor: receptor conservation in the face of antigenic variation. *The Journal of General Virology*, **86**: 1909–20. doi: 10.1099/vir.0.80730-0.

Fukunaga, K. and Taki, M. (2012). Practical tips for construction of custom Peptide libraries and affinity selection by using commercially available phage display cloning systems. *Journal of Nucleic Acids*, Article ID 295719. doi: 10.1155/2012/295719.

Galloway, I. A., Henderson, W. M. and Brooksby, J. B. (1948). Strains of the virus of foot-and-mouth disease recovered from outbreaks in Mexico. *Proceedings of the Society for Experimental Biology and Medicine. Society for Experimental Biology and Medicine (New York, N.Y.)*, **69**: 57–63.

Gao, Y., Sun, S.-Q. and Guo, H.-C. (2016). Biological function of Foot-and-mouth disease virus non-structural proteins and non-coding elements. *Virology Journal*. **13**: 107. doi: 10.1186/s12985-016-0561-z.

Germain, R. N. (1994). MHC-dependent antigen processing and peptide presentation: Providing ligands for T lymphocyte activation. *Cell*, pp. 287–299. doi: 10.1016/0092-8674(94)90336-0.

Gerner, W., Hammer, S. E., Wiesmüller, K.-H. and Saalmüller, A. (2009). Identification of major histocompatibility complex restriction and anchor residues of foot-and-mouth disease virus-derived bovine T-cell epitopes. *Journal of virology*, **83**: 4039–50. doi: 10.1128/JVI.01534-08.

Giraud, A. T., Beck, E., Strelbel, K., de Mello, P. A., La Torre, J., Scodeller, E. A. and Bergmann, I. E. (1990). Identification of a nucleotide deletion in parts of polypeptide 3A in two independent attenuated aphthovirus strains. *Virology*, **177**: 780–783. doi: 10.1016/0042-6822(90)90549-7.

Glass, E. J., Oliver, R. A., Collen, T., Doel, T. R., Dimarchi, R. and Spooner, R. L. (1991). MHC class II restricted recognition of FMDV peptides by bovine T cells. *Immunology*, **74**: 594–9.

Golde, W. T., Nfon, C. K. and Toka, F. N. (2008). Immune evasion during foot-and-mouth disease virus infection of swine. *Immunological Reviews*, pp. 85–95. doi: 10.1111/j.1600-065X.2008.00672.x.

Golde, W. T., de los Santos, T., Robinson, L., Grubman, M. J., Sevilla, N., Summerfield, A. and Charleston, B. (2011). Evidence of Activation and Suppression during the Early Immune Response to Foot-and-Mouth Disease Virus. *Transboundary and Emerging Diseases*, **58**: 283–290. doi: 10.1111/j.1865-1682.2011.01223.x.

Goldman, A. S. and Prabhakar, B. S. (1996). Immunology Overview, In: *Baron SI*, (ed.) *Medical Microbiology. 4th edition. Galveston (TX): University of Texas Medical Branch at Galveston; 1996. Chapter 1.*



Grazioli, S., Fallacara, F. and Brocchi, E. (2003). Mapping of neutralising sites on FMD virus type Asia 1 and relationships with sites described in other serotypes. *In* Report of the Session of the Research Foot and Mouth Disease Group of the Standing Committee of the European Commission of Foot and Mouth Disease, pp. 277–287. Greece: Food and Agriculture Organization.

Grazioli, S., Moretti, M., Barbieri, I., Crosatti, M., and Brocchi, E. (2006). Use of monoclonal antibodies to identify and map new antigenic determinants involved in neutralization of FMD viruses type SAT 1 and SAT 2, *In: European Commission for the control of Foot-and-Mouth Disease: International control of Foot-and-Mouth disease: Tools, Trends and perspectives*. Paphos, Cyprus.

Grazioli, S., Fallacara, F. and Brocchi, E. (2013). Mapping of antigenic sites of foot-and-mouth disease virus serotype Asia 1 and relationships with sites described in other serotypes. *Journal of General Virology*, **94**: 559–569. doi: 10.1099/vir.0.048249-0.

Gregg, D. A., Schlafer, D. H. and Mebus, C. A. (1995). African swine fever virus infection of skin-derived dendritic cells in vitro causes interference with subsequent foot-and-mouth disease virus infection. *Journal of Veterinary Diagnostic Investigation*, **7**: 44–51.

Griep, R. A., Prins, M., Van Twisk, C., Keller, H. J., Kerschbaumer, R. J., Kormelink, R., Goldbach, R. W. and Schots, A. (2000). Application of Phage Display in Selecting Tomato spotted wilt virus-Specific Single-Chain Antibodies (scFvs) for Sensitive Diagnosis in ELISA. *Phytopathology*, **90**: 183–90. doi: 10.1094/PHYTO.2000.90.2.183.

Griffiths, A. D., Malmqvist, M., Marks, J. D., Bye, J. M., Embleton, M. J., McCafferty, J., Baier, M., Holliger, K. P., Gorick, B. D. and Hughes-Jones, N. C. (1993). Human anti-self antibodies with high specificity from phage display libraries. *The EMBO Journal*, **12**: 725–34.

Griffiths, A. D. and Duncan, A. R. (1998). Strategies for selection of antibodies by phage display. *Current Opinion in Biotechnology*, pp. 102–108. doi: 10.1016/S0958-1669(98)80092-X.

Grubman M. J., Baxt B. and Barach. H. L. (1979). Foot-and-mouth disease virion RNA: studies on the relation between the length of its 3'-poly(A) segment and infectivity. *Virology*, **97**: 22–31.

Grubman, M. and Baxt, B. (2004). Foot-and-mouth disease. *Clinical Microbiology Reviews*, **17**: 465–493. doi: 10.1128/CMR.17.2.465.

Grubman, M. J., Moraes, M. P., Diaz-San Segundo, F., Pena, L. and De Los Santos, T. (2008). Evading the host immune response: How foot-and-mouth disease virus has become an effective pathogen. *FEMS Immunology and Medical Microbiology*, **53**: 8–17. doi: 10.1111/j.1574-695X.2008.00409.x.

Guzman, E., Taylor, G., Charleston, B., Skinner, M. A. and Ellis, S. A. (2008). An MHC-restricted CD8⁺ T-cell response is induced in cattle by foot-and-mouth disease virus (FMDV) infection and also following vaccination with inactivated FMDV. *Journal of General Virology*, **89**: 667–675. doi: 10.1099/vir.0.83417-0.

Guzylack-Piriou, L., Piersma, S., McCullough, K. and Summerfield, A. (2006). Role of natural interferon-producing cells and T lymphocytes in porcine monocyte-derived dendritic cell maturation. *Immunology*, **118**: 78–87. doi: 10.1111/j.1365-2567.2006.02343.x.

- Haard, J. J. W. De, Kazemier, B., Oudshoorn, P., Boender, P., Gemen, B. Van, Koolen, M. J. M., Groen, G. Van Der, Hoogenboom, H. R. and Arends, J. W. (2000). Selection of human anti-human immunodeficiency virus type 1 envelope single-chain antibodies from a peripheral blood cell- based phage repertoire. *Culture*, pp. 2883–2894.
- Hall, T. (1999). BioEdit Sequence Alignment Editor for Windows 95/98/NT/XP/Vista/7. *Nucleic Acids Symposium Series*, **41**: 95–98.
- Hall, M. D., Knowles, N. J., Wadsworth, J., Rambaut, A. and Woolhouse, M. E. J. (2013). Reconstructing geographical movements and host species transitions of foot-and-mouth disease virus serotype SAT 2. *mBio*, **4** (5) e00591-13. doi: 10.1128/mBio.00591-13.
- Hamers-Casterman, C., Atarhouch, T., Muyldermans, S., Robinson, G., Hamers, C., Songa, E. B., Bendahman, N. and Hamers, R. (1993). Naturally occurring antibodies devoid of light chains. *Nature*, **363**: 446–8. doi: 10.1038/363446a0.
- Han, S.-C., Guo, H.-C., Sun, S.-Q., Jin, Y., Wei, Y.-Q., Feng, X., Yao, X.-P., Cao, S.-Z., Xiang Liu, D. and Liu, X.-T. (2016). Productive Entry of Foot-and-Mouth Disease Virus via Macropinocytosis Independent of Phosphatidylinositol 3-Kinase. *Scientific reports, Nature Publishing Group*, **6**: 19294. doi: 10.1038/srep19294.
- Hanley, J.A. and McNeil, B.J. (1982). The meaning and use of the area under the Receiver Operating Characteristic (ROC) curve. *Radiology*, **143**: 29–36.
- Harber, J. J., Bradley, J., Anderson, C. W. and Wimmer, E. (1991). Catalysis of poliovirus VP0 maturation cleavage is not mediated by serine 10 of VP2. *Journal of Virology*, **65**: 326–34.
- Hargreaves, S. K., Foggin, C. M., Anderson, E. C., Bastos, A. D. S., Thomson, G. R., Ferris, N. P. and Knowles, N. J. (2004). An investigation into the source and spread of foot and mouth disease virus from a wildlife conservancy in Zimbabwe. *Revue scientifique et technique (International Office of Epizootics)*, **23**: 783–90.
- Harlow, E. and Lane, D. (1988). *Antibodies: A Laboratory Manual*, p. 726. doi: 10.1016/0968-0004(89)90307-1.
- Harmsen, M. M., van Solt, C. B., Fijten, H. P. D., Van Keulen, L., Rosalia, R. A., Weerdmeester, K., Cornelissen, A. H. M., De Bruin, M. G. M., Eblé, P. L. and Dekker, A. (2007). Passive immunization of guinea pigs with llama single-domain antibody fragments against foot-and-mouth disease. *Veterinary Microbiology*, **120**: 193–206. doi: 10.1016/j.vetmic.2006.10.029.
- Harwood, L. J., Gerber, H., Sobrino, F., Summerfield, A. and McCullough, K. C. (2008). Dendritic cell internalization of foot-and-mouth disease virus: influence of heparan sulfate binding on virus uptake and induction of the immune response. *Journal of Virology*, **82**: 6379–6394. doi: 10.1128/JVI.00021-08.
- Hedger, R. S. (1972). Foot-and-mouth disease and the African buffalo (*Syncerus caffer*). *Journal of comparative pathology*, **82**: 19–28.
- Hogle, J. M., Chow, M. and Filman, D. J. (1985). Three-dimensional structure of poliovirus at 2.9 Å resolution. *Science (New York, N.Y.)*, **229**: 1358–65.
- Hoogenboom, H. R. and Winter, G. (1992). By-passing immunisation. Human antibodies from synthetic repertoires of germline VH gene segments rearranged in vitro. *Journal of Molecular*

Biology, **227**: 381–8.

Hoogenboom, H. R. (1997). Designing and optimizing library selection strategies for generating high-affinity antibodies. *Trends in Biotechnology*, **15**: 62–70. doi: 10.1016/S0167-7799(97)84205-9.

Hoogenboom, H. R., de Bruïne, A. P., Hufton, S. E., Hoet, R. M., Arends, J.-W. W., Roovers, R. C., de Bruïne, A. P., Hufton, S. E., Hoet, R. M., Arends, J.-W. W. and Roovers, R. C. (1998). Antibody phage display technology and its applications. *Immunotechnology: an international journal of immunological engineering*, **4**: 1–20. doi: 10.1016/S1380-2933(98)00007-4.

Hulst, M. M., Van Gennip, H. G. P. and Moormann, R. J. M. (2000). Passage of Classical Swine Fever Virus in Cultured Swine Kidney Cells Selects Virus Variants That Bind to Heparan Sulfate due to a Single Amino Acid Change in Envelope Protein Erns. *Journal of Virology*, **74**: 9553–9561. doi: 10.1128/JVI.74.20.9553-9561.2000.

Hunter, P. (1998). Vaccination as a means of control of foot-and-mouth disease in sub-saharan Africa. *Vaccine*, **16**: 261–4.

Hurwitz, A. M., Huang, W., Kou, B., Estes, M. K., Atmar, R. L. and Palzkill, T. (2017). Identification and Characterization of Single-Chain Antibodies that Specifically Bind GI Noroviruses. *Plos One*, 12(1), p. e0170162. doi: 10.1371/journal.pone.0170162.

Huston, J. S., Levinson, D., Mudgett-Hunter, M., Tai, M. S., Novotny, J., Margolies, M. N., Ridge, R. J., Bruccoleri, R. E., Haber, E. and Crea, R. (1988). Protein engineering of antibody binding sites: recovery of specific activity in an anti-digoxin single-chain Fv analogue produced in *Escherichia coli*. *Proceedings of the National Academy of Sciences*, **85**: 5879–5883. doi: 10.1073/pnas.85.16.5879.

Hynes, R. O. (1992). Integrins: Versatility, modulation, and signaling in cell adhesion. *Cell*, **69**:11-25. doi: 10.1016/0092-8674(92)90115-S.

Jackson, T., Ellard, F. M., Ghazaleh, R. A., Brookes, S. M., Blakemore, W. E., Corteyn, H., Stuart, D. I., Newman, J. W. and King, A. M. (1996). Efficient infection of cells in culture by type O foot-and-mouth disease virus requires binding to cell surface heparan sulfate. *Journal of Virology*, **70**: 5282–7.

Jackson, T., Sharma, A., Ghazaleh, R. A., Blakemore, W. E., Ellard, F. M., Simmons, D. L., Newman, J. W., Stuart, D. I. and King, A. M. (1997). Arginine-glycine-aspartic acid-specific binding by foot-and-mouth disease viruses to the purified integrin $\alpha(v)\beta_3$ in vitro. *Journal of Virology*, **71**: 8357–8361.

Jackson, T., Sheppard, D., Denyer, M., Blakemore, W. and King, A. M. Q. (2000a). The epithelial integrin $\alpha v \beta 6$ is a receptor for Foot-and-mouth disease virus. *Journal of Virology*, **74**: 4949–4956. doi: 10.1128/JVI.74.11.4949-4956.2000.

Jackson, T., Blakemore, W., Newman, J. W. I., Knowles, N. J., Mould, A. P., Humphries, M. J. and King, A. M. Q. (2000b). Foot-and-mouth disease virus is a ligand for the high-affinity binding conformation of integrin $\alpha 5 \beta 1$: Influence of the leucine residue within the RGD motif on selectivity of integrin binding. *Journal of General Virology*, **81**: 1383–1391. doi: 10.1099/0022-1317-81-5-1383.

Jackson, T., Mould, A. P., Sheppard, D. and King, A. M. Q. (2002). Integrin $\alpha v \beta 1$ is a

receptor for foot-and-mouth disease virus. *Journal of Virology*, **76**: 935–41. doi: 10.1128/JVI.76.3.935.

Jackson, T., King, A. M. Q., Stuart, D. I. and Fry, E. (2003). Structure and receptor binding. *Virus Research*, **91**: 33–46. doi: 10.1016/S0168-1702(02)00258-7.

Jackson, T., Clark, S., Berryman, S., Burman, A., Cambier, S., Mu, D., Nishimura, S. and King, A. M. Q. (2004). Integrin alphavbeta8 functions as a receptor for foot-and-mouth disease virus: role of the beta-chain cytodomain in integrin-mediated infection. *Journal of Virology*, **78**: 4533–4540. doi: 10.1128/JVI.78.9.4533.

Jae, K. O., Ferris, N. P., Lee, K.-N., Joo, Y.-S., Hyun, B.-H. and Park, J.-H. (2009). Simple and rapid lateral-flow assay for the detection of foot-and-mouth disease virus. *Clinical and Vaccine Immunology*, **16**: 1660–1664.

Jamal, S. M., Ferrari, G., Ahmed, S., Normann, P., Curry, S. and Belsham, G. J. (2011). Evolutionary analysis of serotype A foot-and-mouth disease viruses circulating in Pakistan and Afghanistan during 2002-2009. *The Journal of General Virology*, **92**: 2849–64. doi: 10.1099/vir.0.035626-0.

Jamal, S. M. and Belsham, G. J. (2013). Foot-and-mouth disease: Past, present and future. *Veterinary Research*, **44**: 1–14. doi: 10.1186/1297-9716-44-116.

James, H. E., Ebert, K., McGonigle, R., Reid, S. M., Boonham, N., Tomlinson, J. A., Hutchings, G. H., Denyer, M., Oura, C. A. L., Dukes, J. P. and King, D. P. (2010). Detection of African swine fever virus by loop-mediated isothermal amplification. *Journal of Virological Methods*, **164**: 68–74. doi: 10.1016/j.jviromet.2009.11.034.

Janeway, C. A. J., Travers, P. and Walport, M. (2001). Antigen recognition by B-cell and Tcell receptors. in *Immunobiology: The immune system in health and diseases*. 5th edn. New York: Garland Publishing.

Johnson, M. (2013). Antibody Structure and Fragments, *Materials and Methods*, doi: 10.13070/mm.en.3.160.

Jori, F., Vosloo, W., Du Plessis, B., Bengis, R., Brahmhatt, D., Gummow, B. and Thomson, G. R. (2009). A qualitative risk assessment of factors contributing to foot and mouth disease outbreaks in cattle along the western boundary of the Kruger National Park. *Revue scientifique et technique (International Office of Epizootics)*, **28**: 917–31.

Jori, F., Brahmhatt, D., Fosgate, G. T., Thompson, P. N., Budke, C., Ward, M. P., Ferguson, K. and Gummow, B. (2011). A questionnaire-based evaluation of the veterinary cordon fence separating wildlife and livestock along the boundary of the Kruger National Park, South Africa. *Preventive Veterinary Medicine*, **100**: 210–220. doi: 10.1016/j.prevetmed.2011.03.015.

Jori, F., Caron, A., Thompson, P.N., Dwarka, R., Foggin, C., de Garine-Wichatitsky, M., Hofmeyr, M., Van Heerden, J. and Heath, L. (2014). Characteristics of foot-and-mouth disease viral strains circulating at the wildlife/livestock interface of the great Limpopo transfrontier conservation area. *Transboundary Emerging Diseases*, **63**: e58–70.

Jori, F., Alexander, K. A., Mokopasetso, M., Munstermann, S., Moagabo, K. and Paweska, J. T. (2015). Serological Evidence of Rift Valley Fever Virus Circulation in Domestic Cattle and African Buffalo in Northern Botswana (2010-2011). *Frontiers in Veterinary Science*, **2**: 63.

doi: 10.3389/fvets.2015.00063.

Jori, F., Caron, A., Thompson, P. N., Dwarka, R., Foggin, C., de Garine-Wichatitsky, M., Hofmeyr, M., Van Heerden, J. and Heath, L. (2016). Characteristics of Foot-and-Mouth Disease Viral Strains Circulating at the Wildlife/livestock Interface of the Great Limpopo Transfrontier Conservation Area. *Transboundary and emerging diseases*, **63**: e58-70. doi: 10.1111/tbed.12231.

Juleff, N., Windsor, M., Reid, E., Seago, J., Zhang, Z., Monaghan, P., Morrison, I. W. and Charleston, B. (2008). Foot-and-mouth disease virus persists in the light zone of germinal centres. *PLoS ONE*, **3**: 10. doi: 10.1371/journal.pone.0003434.

Juleff, N. D. (2009). *Interactions of foot-and-mouth disease virus with cells in organised lymphoid tissue influence innate and adaptive immune responses*. Doctor of philosophy Dissertation, University of Edinburgh.

Jung, Y., Jeong, J. Y. and Chung, B. H. (2008). Recent advances in immobilization methods of antibodies on solid supports. *The Analyst*, **133**: 697–701. doi: 10.1039/b800014j.

Jusa, E. R., Inaba, Y., Kouno, M. and Hirose, O. (1997). Effect of heparin on infection of cells by porcine reproductive and respiratory syndrome virus. *American Journal of Veterinary Research*, **58**: 488–91.

Karber, G. (1931). 50% end-point calculation. *Arch. Exp. Pathol. Pharmacol*, **162**: 480-484.

Kasanga, C. J., Sallu, R., Kivaria, F., Mkama, M., Masambu, J., Yongolo, M., Das, S., Mpelumbe-Ngeleja, C., Wambura, P. N., King, D. P. and Rweyemamu, M. M. (2012). Foot-and-mouth disease virus serotypes detected in Tanzania from 2003 to 2010: conjectured status and future prospects. *The Onderstepoort journal of veterinary research*, **79**: 462.

Kasanga, C. J., Wadsworth, J., Mpelumbe-Ngeleja, C. A. R., Sallu, R., Kivaria, F., Wambura, P. N., Yongolo, M. G. S., Rweyemamu, M. M., Knowles, N. J. and King, D. P. (2015). Molecular Characterization of Foot-and-Mouth Disease Viruses Collected in Tanzania Between 1967 and 2009. *Transboundary and Emerging Diseases*, **62**: 5. doi: 10.1111/tbed.12200.

Katsunori O., Tomozumi M., Yasuhiro S., Junko O., Miki H., Yasuhiro I., Miya O., Tohru K., Michiyo S., Eiichi H. (1991). BHV-1 Adsorption is mediated by the interaction of glycoprotein gIII with heparinlike moiety on the cell surface. *Virology*, **181**: 666–670.

Kay, B.K. and Hoess, R. (1996). Principles and applications of phage display. In: Kay, B. K., Winter, J. and McCafferty, J. (eds.) *Phage display of peptides and proteins, a laboratory manual*. California: Academic Press. pp. 21–34. doi: 10.1016/B978-012402380-2/50004-6.

Keller, T., Kalt, R., Raab, I., Schachner, H., Mayrhofer, C., Kerjaschki, D. and Hantusch, B. (2015). Selection of scFv antibody fragments binding to human blood versus lymphatic endothelial surface antigens by direct cell phage display. *PLoS ONE*, **10**: 1–29. doi: 10.1371/journal.pone.0127169.

Kerschbaumer, R. J., Hirschl, S., Kaufmann, A., Ibl, M., Koenig, R. and Himmler, G. (1997). Single-chain Fv fusion proteins suitable as coating and detecting reagents in a double antibody sandwich enzyme-linked immunosorbent assay. *Analytical biochemistry*, **249**: 219–27. doi: 10.1006/abio.1997.2171.

- King, D. P., Dukes, J. P., Reid, S. M., Ebert, K., Shaw, A. E., Mills, C. E., Boswell, L. and Ferris, N. P. (2008). Prospects for rapid diagnosis of foot-and-mouth disease in the field using reverse transcriptase-PCR. *The Veterinary record*, **162**: 315–316. doi: 10.1136/vr.162.10.315.
- King, D. P., Madi, M., Mioulet, V., Wadsworth, J., Wright, C. F., Valdazo-González, B., Ferris, N. P., Knowles, N. J. and Hammond, J. (2012). New technologies to diagnose and monitor infectious diseases of livestock: Challenges for sub-Saharan Africa. *Onderstepoort Journal of Veterinary Research*, **79**: 1–6. doi: 10.4102/ojvr.v79i2.456.
- Kitching, R. P. (1998). A recent history of foot-and-mouth disease. *Journal of Comparative Pathology*, **118**: 89–108. doi: 10.1016/S0021-9975(98)80002-9.
- Kitching, R.P. and Hughes, G.J. (2002). Clinical variation in foot and mouth disease: sheep and goats. *Revue Scientifique et Technique*, Office International des Epizooties **21**, 505–512.
- Kitching, R.P., Hutber, A.M. and Thrusfield, M.V. (2005). A review of foot-and-mouth disease with special consideration for the clinical and epidemiological factors relevant to predictive modelling of the disease. *The Veterinary Journal*, **169**: 197-209.
- Kitson, J. D. A., McCahon, D. and Belsham, G. J. (1990). Sequence analysis of monoclonal antibody resistant mutants of type O foot and mouth disease virus: Evidence for the involvement of the three surface exposed capsid proteins in four antigenic sites. *Virology*, **179**: 26–34. doi: 10.1016/0042-6822(90)90269-W.
- Klimstra, W. B., Ryman, K. D. and Johnston, R. E. (1998). Adaptation of Sindbis virus to BHK cells selects for use of heparan sulfate as an attachment receptor. *Journal of Virology*, **72**: 7357–7366.
- Knipe, T., Rieder, E., Baxt, B., Ward, G. and Mason, P.W. (1997). Characterization of synthetic foot-and-mouth disease virus provirions separates acid-mediated disassembly from infectivity. *Journal of Virology* **71**: 2851-2856.
- Knowles, N. J., Davies, P. R., Henry, T., O'Donnell, V., Pacheco, J. M. and Mason, P. W. (2001). Emergence in Asia of Foot-and-Mouth Disease Viruses with Altered Host Range: Characterization of Alterations in the 3A Protein. *Journal of Virology*, **75**: 1551–1556. doi: 10.1128/JVI.75.3.1551-1556.2001.
- Knowles, N. and Samuel, A. (2003). Molecular epidemiology of foot-and-mouth disease virus. *Virus Research*, **91**: 65–80. doi: 10.1016/S0168-1702(02)00260-5.
- Köhler, G. and Milstein, C. (1975). Continuous cultures of fused cells secreting antibody of predefined specificity. *Nature*, **256**: 495–497. doi: 10.1038/256495a0.
- Kotecha, A., Seago, J., Scott, K., Burman, A., Loureiro, S., Ren, J., Porta, C., Ginn, H. M., Jackson, T., Perez-martin, E., Siebert, C. A., Paul, G., Huiskonen, J. T., Jones, I. M., Esnouf, R. M., Fry, E. E., Maree, F. F., Charleston, B. and Stuart, D. I. (2015). Structure-based energetics of protein interfaces guides foot-and-mouth disease virus vaccine design. *Nature Structural Molecular Biology*, **22**: 788-794 doi: 10.1038/nsmb.3096.
- Krusat, T. and Streckert, H. J. (1997). Heparin-dependent attachment of respiratory syncytial virus (RSV) to host cells. *Archives of Virology*, **142**: 1247–1254. doi: 10.1007/s007050050156.
- Ku, B.-K., Kim, S.-B., Moon, O.-K., Lee, S.-J., Lee, J.-H., Lyoo, Y.-S., Kim, H.-J. and Sur, J.-H. (2005). Role of apoptosis in the pathogenesis of Asian and South American foot-and-mouth

disease viruses in swine. *The Journal of veterinary medical science / the Japanese Society of Veterinary Science*, **67**: 1081–8. doi: 10.1292/jvms.67.1081.

Kumada, Y., Hamasaki, K., Shiritani, Y., Nakagawa, A., Kuroki, D., Ohse, T., Choi, D. H., Katakura, Y. and Kishimoto, M. (2009a). Direct immobilization of functional single-chain variable fragment antibodies (scFvs) onto a polystyrene plate by genetic fusion of a polystyrene-binding peptide (PS-tag). *Analytical and Bioanalytical Chemistry*, **395**: 759–65. doi: 10.1007/s00216-009-2999-y.

Kumada, Y., Hamasaki, K., Shiritani, Y., Ohse, T. and Kishimoto, M. (2009b). Efficient immobilization of a ligand antibody with high antigen-binding activity by use of a polystyrene-binding peptide and an intelligent microtiter plate. *Journal of Biotechnology*, **142**: 135–141. doi: 10.1016/j.jbiotec.2009.03.011.

Kumada, Y., Ishikawa, Y., Fujiwara, Y., Takeda, R., Miyamoto, R., Niwa, D., Momose, S., Kang, B. and Kishimoto, M. (2014). Efficient refolding and immobilization of PMMA-tag-fused single-chain Fv antibodies for sensitive immunological detection on a PMMA plate. *Journal of Immunological Methods*, **411**: 1–10. doi: 10.1016/j.jim.2014.05.015.

Kumar, S., Stecher, G. and Tamura, K. (2016). MEGA7: Molecular Evolutionary Genetics Analysis Version 7.0 for Bigger Datasets. *Molecular Biology and Evolution*, **33**: 1870–1874.

Kunicki, T. J., Kritzik, M., Annis, D. S. and Nugent, D. J. (1997). Hereditary variation in platelet integrin alpha 2 beta 1 density is associated with two silent polymorphisms in the alpha 2 gene coding sequence. *Blood*, **89**: 1939–43.

Lama, J., Paul, A. V, Harris, K. S. and Wimmer, E. (1994). Properties of purified recombinant poliovirus protein 3aB as substrate for viral proteinases and as co-factor for RNA polymerase 3Dpol. *The Journal of Biological Chemistry*, **269**: 66–70.

Lanier, L. L. (2005). NK cell recognition. *Annual Review of Immunology*, **23**: 225–74. doi: 10.1146/annurev.immunol.23.021704.115526.

Lau, L.-T., Reid, S. M., King, D. P., Lau, A. M.-F., Shaw, A. E., Ferris, N. P. and Yu, A. C.-H. (2008). Detection of foot-and-mouth disease virus by nucleic acid sequence-based amplification (NASBA). *Veterinary Microbiology*, **126**: 101–110. doi: 10.1016/j.vetmic.2007.07.008.

Lawrence, P., Rai, D., Conderino, J. S., Uddowla, S. and Rieder, E. (2016a). Role of Jumonji C-domain containing protein 6 (JMJD6) in infectivity of foot-and-mouth disease virus. *Virology*. Elsevier, **492**: 38–52. doi: 10.1016/j.virol.2016.02.005.

Lawrence, P., Pacheco, J., Stenfeldt, C., Arzt, J., Rai, D. K. and Rieder, E. (2016b). Pathogenesis and micro-anatomic characterization of a cell-adapted mutant foot-and-mouth disease virus in cattle: Impact of the Jumonji C-domain containing protein 6 (JMJD6) and route of inoculation. *Virology*. Elsevier, **492**: 108–117. doi: 10.1016/j.virol.2016.02.004.

Lazarus, D.D., Fosgate, G.T., van Schalkwyk, O.L., Burroughs, R.E.J., Heath, L., Maree, F.F., Blignaut, B., Reininghaus, B., Mpehle, A., Rikhotso, O., Thomson, G.R. (2017). Serological evidence of vaccination and perceptions concerning foot-and-mouth disease control in cattle at the wildlife-livestock interface of the Kruger National Park, South Africa. *Preventive Veterinary Medicine*, **147** 17–25.

Lea, S., Hernández, J., Blakemore, W., Brocchi, E., Curry, S., Domingo, E., Fry, E., Abu-Ghazaleh, R., King, A. and Newman, J. (1994). The structure and antigenicity of a type C foot-and-mouth disease virus. *Structure (London, England : 1993)*, **2**: 123–39.

Lea, S., Abu-Ghazaleh, R., Blakemore, W., Curry, S., Fry, E., Jackson, T., King, A., Logan, D., Newman, J. and Stuart, D. (1995). Structural comparison of two strains of foot-and-mouth disease virus subtype O1 and a laboratory antigenic variant, G67. *Structure*, **3**: 571–580. doi: 10.1016/S0969-2126(01)00191-5.

Lee, F., Jong, M.-H., Yang, D.W. (2006). Presence of antibodies to non-structural proteins of foot-and-mouth disease virus in repeatedly vaccinated cattle. *Veterinary Microbiology*, **115**: 14–20.

Leippert, M., Beck, E., Weiland, F. and Pfaff, E. (1997). Point mutations within the β G- β H loop of foot-and-mouth disease virus O1K affect virus attachment to target cells. *Journal of Virology*, **71**: 104–1051.

Leow, C. H., Jones, M., Cheng, Q., Mahler, S. and McCarthy, J. (2014). Production and characterization of specific monoclonal antibodies binding the Plasmodium falciparum diagnostic biomarker, histidine-rich protein 2. *Malaria journal*, **13**: 277. doi: 10.1186/1475-2875-13-277.

Levenhagen, M. A., de Almeida Araújo Santos, F., Fujimura, P. T., Caneiro, A. P., Costa-Cruz, J. M. and Goulart, L. R. (2015). Structural and functional characterization of a novel scFv anti-HSP60 of Strongyloides sp. *Scientific reports*, **5**: 10447. doi: 10.1038/srep10447.

Li, X., Liu, R., Tang, H., Jin, M., Chen, H. and Qian, P. (2008). Induction of protective immunity in swine by immunization with live attenuated recombinant pseudorabies virus expressing the capsid precursor encoding regions of foot-and-mouth disease virus. *Vaccine*, **26**: 2714–22. doi: 10.1016/j.vaccine.2008.03.020.

Litman, G. W., Rast, J. P., Shablott, M. J., Haire, R. N., Hulst, M., Roess, W., Litman, R. T., Hinds-Frey, K. R., Zilch, A. and Amemiya, C. T. (1993). Phylogenetic diversification of immunoglobulin genes and the antibody repertoire. *Molecular Biology and Evolution*, **10**: 60–72.

Liu, J., Wei, D., Qian, F., Zhou, Y., Wang, J., Ma, Y. and Han, Z. (2003). pPIC9-Fc: a vector system for the production of single-chain Fv-Fc fusions in Pichia pastoris as detection reagents in vitro. *Journal of Biochemistry*, **134**: 911–7.

Longjam, N. and Tayo, T. (2011). Antigenic variation of Foot and Mouth Disease Virus - An Overview. *Veterinary World*, **4**: 475-479. doi: 10.5455/vetworld.2011.475-479.

Luka, J., Arlen, P. M., and Bristol, A. (2011). Development of a serum biomarker assay that differentiates tumor-associated MUC5AC (NPC-1C ANTIGEN) from normal MUC5AC. *Journal of Biomedicine and Biotechnology*, Article ID 934757.

Mackay, D. K. J., Forsyth, M. A., Davies, P. R. and Salt, J. S. (1998). Antibody to the nonstructural proteins of foot-and-mouth disease virus in vaccinated animals exposed to infection. *Veterinary Quarterly*, **20** (November), pp. S9–S11. doi: 10.1080/01652176.1998.9694953.

Mackay, D. K. J., Bulut, A. N., Rendle, T., Davidson, F. and Ferris, N. P. (2001). A solid-phase

competition ELISA for measuring antibody to foot-and-mouth disease virus. *Journal of Virological Methods*, **97**: 33–48. doi: 10.1016/S0166-0934(01)00333-0.

Madshus, I. H., Olsnes, S. and Sandvig, K. (1984a). Different pH requirements for entry of the two picornaviruses, human rhinovirus 2 and murine encephalomyocarditis virus. *Virology*, **139**: 346–357. doi: 10.1016/0042-6822(84)90380-5.

Madshus, I. H., Olsnes, S. and Sandvig, K. (1984b). Mechanism of entry into the cytosol of poliovirus type 1: Requirement for low pH. *Journal of Cell Biology*, **98**: 1194–1200.

Mahapatra, M., Seki, C., Upadhyaya, S., Barnett, P. V., La Torre, J., and Paton, D. (2011). Characterisation and epitope mapping of neutralising monoclonal antibodies to A24 Cruzeiro strain of FMDV. *Veterinary Microbiology*, **149**: 242-247.

Makowski, L. and Russel, M. (1997). Structure and assembly of filamentous bacteriophages. In Kay, B., Winter, G. and McCafferty, J. (eds) *Structural Biology of Viruses*. New York: Oxford University Press, pp. 352–380.

Mandl, C. W., Kroschewski, H., Allison, S. L., Kofler, R., Holzmann, H., Meixner, T. and Heinz, F. X. (2001). Adaptation of Tick-Borne Encephalitis Virus to BHK-21 Cells Results in the Formation of Multiple Heparan Sulfate Binding Sites in the Envelope Protein and Attenuation In Vivo Adaptation of Tick-Borne Encephalitis Virus to BHK-21 Cells Results in the Forma. *Journal of Virology*, **75**: 5627–5637. doi: 10.1128/JVI.75.12.5627.

Maree, F. F., Blignaut, B., de Beer, T. A. P., Visser, N. and Rieder, E. A. (2010). Mapping of amino acid residues responsible for adhesion of cell culture-adapted foot-and-mouth disease SAT type viruses. *Virus Research*, **153**: 82–91. doi: 10.1016/j.virusres.2010.07.010.

Maree, F. F., Blignaut, B., Aschenbrenner, L., Burrage, T. and Rieder, E. (2011). Analysis of SAT1 type foot-and-mouth disease virus capsid proteins: Influence of receptor usage on the properties of virus particles. *Virus Research*. Elsevier B.V., **155**: 462–472. doi: 10.1016/j.virusres.2010.12.002.

Maree, F. F., Blignaut, B., de Beer, T. A. P. and Rieder, E. (2013). Analysis of SAT Type Foot-And-Mouth Disease Virus Capsid Proteins and the Identification of Putative Amino Acid Residues Affecting Virus Stability. *PLoS ONE*, **8** (5). doi: 10.1371/journal.pone.0061612.

Maree, F. F., Kasanga, C. J., Scott, K. A., Opperman, P. A., Chitray, M., Sangula, A. K., Sallu, R., Sinkala, Y., Wambura, P. N., King, D. P., Paton, D. J. and Rweyemamu, M. M. (2014). Challenges and prospects for the control of foot-and-mouth disease: an African perspective. *Veterinary Medicine: Research and Reports*, **5**: 119–138. doi: 10.2147/VMRR.S62607.

Maree, F. F., Nsamba, P., Mutowembwa, P., Rotherham, L. S., Esterhuysen, J. and Scott, K. (2015). Intra-serotype SAT2 chimeric foot-and-mouth disease vaccine protects cattle against FMDV challenge. *Vaccine*, **33**: 2909–2916. doi: 10.1016/j.vaccine.2015.04.058.

Market, E. and Papavasiliou, F. N. (2003). V(D)J Recombination and the Evolution of the Adaptive Immune System. *PLoS Biology*, **1**: e16.

Maroudam, V., Nagendrakumar, S. B., Rangarajan, P. N., Thiagarajan, D. and Srinivasan, V. A. (2010). Genetic characterization of Indian type O FMD virus 3A region in context with host cell preference. Infection, genetics and evolution: *Journal of molecular epidemiology and evolutionary genetics in infectious diseases*, **10**: 703–709. doi: 10.1016/j.meegid.2010.03.004.

Marquardt, O., Straub, O. C., Ahl, R. and Haas, B. (1995). Detection of foot-and-mouth disease virus in nasal swabs of asymptomatic cattle by RT-PCR within 24 hours. *Journal of Virological Methods*, **53**: 255–61.

Martínez, M.A., Dopazo, J., Hernández, J., Mateu, M.G., Sobrino, F., Domingo, E. and Knowles, N.J. (1992). Evolution of the capsid protein genes of foot-and-mouth disease virus. Antigenic variation without accumulation of amino acid substitutions over six decades. *Journal of Virology*, **66**: 3557-3565.

Martínez, M. A., Verdaguer, N., Mateu, M. G. and Domingo, E. (1997). Evolution subverting essentiality: dispensability of the cell attachment Arg-Gly-Asp motif in multiply passaged foot-and-mouth disease virus. *Proceedings of the National Academy of Sciences of the United States of America*, **94**: 6798–802. doi: 10.1073/pnas.94.13.6798.

Mason, P. W., Rieder, E. and Baxt, B. (1994). RGD sequence of foot-and-mouth disease virus is essential for infecting cells via the natural receptor but can be bypassed by an antibody-dependent enhancement pathway. *Proceedings of the National Academy of Sciences of the United States of America*, **91**: 1932–1936. doi: 10.1073/pnas.91.5.1932.

Mason, P. W., Grubman, M. J. and Baxt, B. (2003). Molecular basis of pathogenesis of FMDV. *Virus Research*, **91**: 9–32. doi: 10.1016/S0168-1702(02)00257-5.

Massicame, Z.E., 2012. *Serological Response of Cattle Vaccinated With a Bivalent (SAT1 and SAT 2) Foot-and-Mouth Disease Vaccine in Gaza Province, Mozambique*. MSc dissertation. University of Pretoria, South Africa, pp. 1–79.

Mateo, R., Diaz, A., Baranowski, E. and Mateu, M. G. (2003). Complete Alanine Scanning of Intersubunit Interfaces in a Foot-and-Mouth Disease Virus Capsid Reveals Critical Contributions of Many Side Chains to Particle Stability and Viral Function. *Journal of Biological Chemistry*, **278**: 41019–41027. doi: 10.1074/jbc.M304990200.

Mateo, R., Luna, E. and Mateu, M. G. (2007). Thermostable variants are not generally represented in foot-and-mouth disease virus quasispecies. *Journal of General Virology*, **88**: 859–864. doi: 10.1099/vir.0.82521-0.

Mateo, R., Luna, E., Rincón, V. and Mateu, M. G. (2008). Engineering viable foot-and-mouth disease viruses with increased thermostability as a step in the development of improved vaccines. *Journal of Virology*, **82**: 12232–12240. doi: 10.1128/JVI.01553-08.

Mateu, M.G., Da Silva, J.L., Rocha, E., De Brum, D.L., Alonso, A., Enjuanes, L., Domingo, E., Barahona, H.(1988). Extensive antigenic heterogeneity of foot-and-mouth disease virus of serotype C. *Virology*, **167**: 113-24.

Mateu, M. G., Martínez, M. A., Capucci, L., Andreu, D., Giralt, E., Sobrino, F., Brocchi, E. and Domingo, E. (1990). A single amino acid substitution affects multiple overlapping epitopes in the major antigenic site of foot-and-mouth disease virus of serotype C. *The Journal of general virology*, **71**: 629–37. doi: 10.1099/0022-1317-71-3-629.

Mateu, M. G., Camarero, J. A., Giralt, E., Andreu, D. and Domingo, E. (1995). Direct evaluation of the immunodominance of a major antigenic site of foot-and-mouth disease virus in a natural host. *Virology*, **206**: 298–306. doi: 10.1016/S0042-6822(95)80045-X.

Mateu, M. G., Valero, M. L., Andreu, D. and Domingo, E. (1996). Systematic replacement of

amino acid residues within an Arg-Gly-Asp-containing loop of foot-and-mouth disease virus and effect on cell recognition. *The Journal of Biological Chemistry*, **271**: 12814–9.

Maverakis, E., Kim, K., Shimoda, M., Gershwin, M. E., Patel, F., Wilken, R., Raychaudhuri, S., Ruhaak, L. R. and Lebrilla, C. B. (2015). Glycans in the immune system and The Altered Glycan Theory of Autoimmunity: A critical review. *Journal of Autoimmunity*, **57**: 1–13. doi: 10.1016/j.jaut.2014.12.002.

McCullough, K. C., Crowther, J. R., Butcher, R. N., Carpenter, W. C., Brocchi, E., Capucci, L. and De Simone, F. (1986). Immune protection against foot-and-mouth disease virus studied using virus-neutralizing and non-neutralizing concentrations of monoclonal antibodies. *Immunology*, **58**: 421–428.

McCullough, K. C., Crowther, J. R., Carpenter, W. C., Brocchi, E., Capucci, L., De Simone, F., Xie, Q. and McCahon, D. (1987). Epitopes on foot-and-mouth disease virus particles. I. Topology. *Virology*, **157**: 516–25.

McCullough, K. C., Parkinson, D. and Crowther, J. R. (1988). Opsonization-enhanced phagocytosis of foot-and-mouth disease virus. *Immunology*, **65**: 187–191.

McCullough, K. C., De Simone, F., Brocchi, E., Capucci, L., Crowther, J. R. and Kihm, U. (1992). Protective immune response against foot-and-mouth disease. *Journal of Virology*, **66**: 1835–40.

McCullough, K. C. (2004). Immunology of foot-and-mouth disease, *In Sobrino, F. and Domingo, E. (eds) Foot and Mouth disease: current perspectives*. United Kingdom: Horizon Bioscience.

Mcgregor, D. P., Molloy, P. E., Cunningham, C. and Harris, W. J. (1994). Spontaneous assembly of bivalent single chain antibody fragments in *Escherichia coli*. *Molecular Immunology*, **31**: 219–226. doi: 10.1016/0161-5890(94)90002-7.

McLeish, N. J., Williams, C. H., Kaloudas, D., Roivainen, M. M. and Stanway, G. (2012). Symmetry-Related Clustering of Positive Charges Is a Common Mechanism for Heparan Sulfate Binding in Enteroviruses. *Journal of Virology*, **86**: 11163–11170. doi: 10.1128/JVI.00640-12.

Mechaly, A., Zahavy, E. and Fisher, M. (2008). Development and implementation of a single-chain Fv antibody for specific detection of *Bacillus anthracis* spores. *Applied and Environmental Microbiology*, **74**: 818–822. doi: 10.1128/AEM.01244-07.

Meloan, R. H., Puyk, W. C., Meijer, D. J. A., Lankhof, H., Posthumus, W. P. A. and Schaaper, W. M. M. (1987). Antigenicity and Immunogenicity of Synthetic Peptides of Foot-and-Mouth Disease Virus. *Journal of General Virology*, **68**: 305–314. doi: 10.1099/0022-1317-68-2-305.

Mettenleiter, T. C., Zsak, L., Zuckermann, F., Sugg, N., Kern, H. and Ben-Porat, T. (1990). Interaction of glycoprotein gIII with a cellular heparinlike substance mediates adsorption of pseudorabies virus. *Journal of Virology*, **64**: 278–86.

Meyer, K., Petersen, A., Niepmann, M. and Beck, E. (1995). Interaction of eukaryotic initiation factor eIF-4B with a picornavirus internal translation initiation site. *Journal of Virology*, **69**: 2819–24.

Michel, A. L. and Bengis, R. G. (2012). The African buffalo: a villain for inter-species spread

of infectious diseases in southern Africa. *The Onderstepoort journal of veterinary research*, **79**: 453.

Miguel, E., Grosbois, V., Caron, a, Boulinier, T., Fritz, H., Cornelis, D., Foggin, C., Makaya, P. V, Tshabalala, P. T. and de Garine-Wichatitsky, M. (2013). Contacts and foot and mouth disease transmission from wild to domestic bovines in Africa. *Ecosphere*, **4**. doi: 10.1890/es12-00239.1.

Miller, L. C., Blakemore, W., Sheppard, D., Atakilit, A., King, A. M. Q. and Jackson, T. (2001). Role of the Cytoplasmic Domain of the α -Subunit of Integrin $\alpha 6$ in Infection by Foot-and-Mouth Disease Virus. *Journal of Virology*, **75**: 4158–4164. doi: 10.1128/JVI.75.9.4158-4164.2001.

Moffat, K., Howell, G., Knox, C., Graham, J., Monaghan, P., Ryan, M. D., Belsham, G. J., Wileman, T., Monaghan, P., Ryan, M. D. and Wileman, T. (2005). Effects of Foot-and-Mouth Disease Virus Nonstructural Proteins on the Structure and Function of the Early Secretory Pathway : 2BC but Not 3A Blocks Endoplasmic Reticulum-to-Golgi Transport Effects of Foot-and-Mouth Disease Virus Nonstructural Proteins. *Society*, **79**: 4382–4395. doi: 10.1128/JVI.79.7.4382.

Moffat, K., Knox, C., Howell, G., Clark, S. J., Yang, H., Belsham, G. J., Ryan, M. and Wileman, T. (2007). Inhibition of the Secretory Pathway by Foot-and-Mouth Disease Virus 2BC Protein Is Reproduced by Coexpression of 2B with 2C, and the Site of Inhibition Is Determined by the Subcellular Location of 2C. *Journal of Virology*, **81**: 1129–1139. doi: 10.1128/JVI.00393-06.

Monaghan, P., Gold, S., Simpson, J., Zhang, Z. D., Weinreb, P. H., Violette, S. M., Alexandersen, S. and Jackson, T. (2005). The $\alpha 6 \beta 1$ integrin receptor for Foot-and-mouth disease virus is expressed constitutively on the epithelial cells targeted in cattle. *Journal of General Virology*, **86**: 2769–2780. doi: 10.1099/vir.0.81172-0.

Moraes, M. P., De Los Santos, T., Koster, M., Turecek, T., Wang, H., Andreyev, V. G. and Grubman, M. J. (2007). Enhanced antiviral activity against foot-and-mouth disease virus by a combination of type I and II porcine interferons. *Journal of Virology*, **81**: 7124–7135. doi: 10.1128/JVI.02775-06.

Moulard, M., Lortat-Jacob, H., Mondor, I., Roca, G., Wyatt, R., Sodroski, J., Zhao, L., Olson, W., Kwong, P. D. and Sattentau, Q. J. (2000). Selective Interactions of Polyanions with Basic Surfaces on Human Immunodeficiency Virus Type 1 gp120. *Journal of Virology*, **74**: 1948–1960. doi: 10.1128/JVI.74.4.1948-1960.2000.

Mukonyora, M. (2015). *The in silico prediction of foot-and-mouth disease virus (FMDV) epitopes on the South African territories*. Master of Science Dissertation, University of South Africa.

Nayak, A., Goodfellow, I. G. and Belsham, G. J. (2005). Factors Required for the Uridylylation of the Foot-and-Mouth Disease Virus 3B1, 3B2, and 3B3 Peptides by the RNA-Dependent RNA Polymerase (3Dpol) *In Vitro*. *Journal of Virology*, **79**: 7698–7706. doi: 10.1128/JVI.79.12.7698-7706.2005.

Nayak, A., Goodfellow, I. G., Woolaway, K. E., Birtley, J., Curry, S. and Belsham, G. J. (2006). Role of RNA Structure and RNA Binding Activity of Foot-and-Mouth Disease Virus 3C Protein in VPg Uridylylation and Virus Replication. *Journal of Virology*, **80**: 9865–9875. doi: 10.1128/JVI.00561-06.

- Neff, S., Sá-Carvalho, D., Rieder, E., Mason, P. W., Blystone, S. D., Brown, E. J. and Baxt, B. (1998). Foot-and-mouth disease virus virulent for cattle utilizes the integrin alpha(v)beta3 as its receptor. *Journal of Virology*, **72**: 3587–94.
- Neff, S., Mason, P. W. and Baxt, B. (2000). High-efficiency utilization of the bovine integrin alpha(v)beta(3) as a receptor for foot-and-mouth disease virus is dependent on the bovine beta(3) subunit. *Journal of Virology*, **74**: 7298–7306. doi: 10.1128/JVI.74.16.7298-7306.2000.
- Newman, J. F. E., Cartwright, B., Doel, T. R. and Brown, F. (1979). Purification and Identification of the RNA-dependent RNA Polymerase of Foot-and-Mouth Disease Virus. *Journal of General Virology*, **45**: 497–507. doi: 10.1099/0022-1317-45-2-497.
- Nsamba, P. (2015a). *Genetic and phenotypic characterisation of selected African foot-and-mouth disease virus isolates*. Doctor of Philosophy Dissertation, University of Pretoria.
- Nsamba, P., de Beer, T. A. P., Chitray, M., Scott, K., Vosloo, W. and Maree, F. F. (2015b). Determination of common genetic variants within the non-structural proteins of foot-and-mouth disease viruses isolated in sub-Saharan Africa', *Veterinary Microbiology*. Elsevier B.V., **177**: 106–122. doi: 10.1016/j.vetmic.2015.03.007.
- Nukarinen, T. (2016). *Production and characterisation of scFv binders against selected enteroviruses*. Master of Science Dissertation, University of Eastern Finland.
- Nunez, J. I., Baranowski, E., Molina, N., Ruiz-Jarabo, C. M., Sanchez, C., Domingo, E. and Sobrino, F. (2001). A Single Amino Acid Substitution in Nonstructural Protein 3A Can Mediate Adaptation of Foot-and-Mouth Disease Virus to the Guinea Pig. *Journal of Virology*, **75**: 3977–3983. doi: 10.1128/JVI.75.8.3977-3983.2001.
- O'Connell, D., Becerril, B., Roy-Burman, A., Daws, M. and Marks, J. D. (2002). Phage versus phagemid libraries for generation of human monoclonal antibodies. *Journal of Molecular Biology*, **321**: 49–56.
- O'Donnell, V., Larocco, M., Duque, H. and Baxt, B. (2005). Analysis of Foot-and-Mouth Disease Virus Internalization Events in Cultured Cells. *Journal of Virology*, **79**: 8506–8518. doi: 10.1128/JVI.79.13.8506–8518.2005.
- O'Donnell, V., Larocco, M. and Baxt, B. (2008). Heparan Sulfate-Binding Foot-and-Mouth Disease Virus Enters Cells via Heparan Sulfate-Binding Foot-and-Mouth Disease Virus Enters Cells. **82**: 9075–9085. doi: 10.1128/JVI.00732-08.
- OIE 2017. *Manual of Diagnostic Tests and Vaccines for Terrestrial Animals*, Paris, Office International des Epizooties.
- O'Toole, T. E., Katagiri, Y., Faull, R. J., Peter, K., Tamura, R., Quaranta, V., Loftus, J. C., Shattil, S. J. and Ginsberg, M. H. (1994). Integrin cytoplasmic domains mediate inside-out signal transduction. *Journal of Cell Biology*, **124**: 1047–1059. doi: 10.1083/jcb.124.6.1047.
- Opperman, P. A., Maree, F. F., Van Wyngaardt, W., Vosloo, W. and Theron, J. (2012). Mapping of antigenic determinants on a SAT2 foot-and-mouth disease virus using chicken single-chain antibody fragments. *Virus Research*. Elsevier B.V., **167**: 370–379. doi: 10.1016/j.virusres.2012.05.026.
- Opperman, P. A. (2013). *Antigenic site determination on a SAT2 foot-and-mouth disease virus using a chicken antibody phage display library*. Doctor of philosophy Dissertation, University

of Pretoria.

Opperman, P.A., Rotherham, L.S., Esterhuysen, J., Charleston, B., Juleff, N., Capozzo, A.V, Theron, J. and Maree, F.F. (2014). Determining the epitope dominance on the capsid of a serotype SAT2 foot-and-mouth disease virus by mutational analyses. *Journal of Virology*, **88**: 8307-18.

Ostrowski, M., Vermeulen, M., Zabal, O., Zamorano, P. I., Sadir, A. M., Geffner, J. R. and Lopez, O. J. (2007). The Early Protective Thymus-Independent Antibody Response to Foot-and-Mouth Disease Virus Is Mediated by Splenic CD9+ B Lymphocytes. *Journal of Virology*, **81**: 9357–9367. doi: 10.1128/JVI.00677-07.

Pacheco, J. M., Gladue, D. P., Holinka, L. G., Arzt, J., Bishop, E., Smoliga, G., Pauszek, S. J., Bracht, A. J. and O'Donnell, V., Fernandez-Sainz, I., Fletcher, P., Piccone, M. E., Rodriguez, L. L. and Borca, M. V. (2013). A partial deletion in non-structural protein 3A can attenuate foot-and-mouth disease virus in cattle. *Virology*, **446**: 260–267. doi: 10.1016/j.virol.2013.08.003.

Paiba, G. A., Anderson, J., Paton, D. J., Soldan, A. W., Alexandersen, S., Corteyn, M., Wilsden, G., Hamblin, P., MacKay, D. K. J. and Donaldson, A. I. (2004). Validation of a foot-and-mouth disease antibody screening solid-phase competition ELISA (SPCE). *Journal of Virological Methods*, **115**: 145–58.

Pallansch, M. A., Kew, O. M., Semler, B. L., Omilianowski, D. R., Anderson, C. W., Wimmer, E. and Rueckert, R. R. (1984). Protein processing map of poliovirus. *Journal of Virology*, **49**: 873–80.

Palm, N. W. and Medzhitov, R. (2009). Pattern recognition receptors and control of adaptive immunity. *Immunological Reviews*, **227**: 221–33. doi: 10.1111/j.1600-065X.2008.00731.x.

Pandey, S. (2010). Hybridoma technology for the production of monoclonal antibodies. *International Journal of Pharmaceutical Sciences Review and Research*, **1**: 88–94.

Panina, G. F., Civardi, A., Massirio, I., Scatozza, F., Baldini, P. and Palmia, F. (1989). Survival of foot-and-mouth disease virus in sausage meat products (Italian salami). *International Journal of Food Microbiology*, **8**: 141–148. doi: 10.1016/0168-1605(89)90068-8.

Parida, S., Cox, S.J., Reid, S.M., Hamblin, P., Barnett, P.V., Inoue, T., Anderson, J. and Paton, D.J. (2005). The application of new techniques to the improved detection of persistently infected cattle after vaccination and contact exposure to foot-and-mouth disease. *Vaccine*, **23**: 5186–5195.

Parmley, S. F. and Smith, G. P. (1988). Antibody-selectable filamentous fd phage vectors: affinity purification of target genes. *Gene*, **73**: 305–318. doi: 10.1016/0378-1119(88)90495-7.

Parry, N. R., Barnett, P. V., Ouldrige, E. J., Rowlands, D. J. and Brown, F. (1989). Neutralizing epitopes of type O foot-and-mouth disease virus. II. Mapping three conformational sites with synthetic peptide reagents. *Journal of General Virology*, **70**: 1493–1503. doi: 10.1099/0022-1317-70-6-1493.

Paton, D. J., Valarcher, J. F., Bergmann, I., Matlho, O. G., Zakharov, V. M., Palma, E. L. and Thomson, G. R. (2005). Selection of foot and mouth disease vaccine strains--a review. *Revue scientifique et technique (International Office of Epizootics)*, **24**: 981–993.

- Paton, D. J., Sumption, K. J. and Charleston, B. (2009). Options for control of foot-and-mouth disease: knowledge, capability and policy. *Philosophical transactions of the Royal Society of London. Series B, Biological sciences*, **364**: 2657–67. doi: 10.1098/rstb.2009.0100.
- Pay, T. W. F. and Rweyemamu, M. M. (1978). Experiences with Type SAT 2 foot-and-mouth disease vaccines in Southern Africa., in *XVth Conference of the Office International Des Epizooties Permanent Commission on foot-and-mouth disease*, pp. 1–25.
- Pay, T. W. and Hingley, P. J. (1987). Correlation of 140S antigen dose with the serum neutralizing antibody response and the level of protection induced in cattle by foot-and-mouth disease vaccines. *Vaccine*, **5**: 60–64.
- Peiris, J. S. M., Gordon, S., Unkeless, J. C. and Porterfield, J. S. (1981). Monoclonal anti-Fc receptor IgG blocks antibody enhancement of viral replication in macrophages. *Nature*, **289**: 189–191. doi: 10.1038/289189a0.
- Perelson, A. S. and Oster, G. F. (1979). Theoretical studies of clonal selection: Minimal antibody repertoire size and reliability of self-non-self discrimination. *Journal of Theoretical Biology*, **81**: 645–670. doi: 10.1016/0022-5193(79)90275-3.
- Pfaff, M., Tangemann, K., Müller, B., Gurrath, M., Müller, G., Kessler, H., Timpl, R. and Engel, J. (1994). Selective recognition of cyclic RGD peptides of NMR defined conformation by alpha IIb beta 3, alpha V beta 3, and alpha 5 beta 1 integrins. *The Journal of Biological Chemistry*, **269**: 20233–8.
- Preston, K. J., Owens, H. and Mowat, G. N. (1982). Sources of variations encountered during the selection and production of three strains of FMD virus for the development of vaccine for use in Nigeria. *Journal of Biological Standardization*, **10**: 35–45. doi: 10.1016/S0092-1157(82)80046-2.
- Pringle, C. R. (1999). Virus taxonomy. *Archives of Virology*, **144**: 2060–2070. doi: 10.1007/s007050050515.
- Putnam, F., Sheng, Y., Liu, V. and Low, T. (1979). Primary structure of a human IgA1 the alpha 1 heavy chain . Primary Structure of a Human IgA1 Immunoglobulin. *Journal Biology Chemicals*, **254**: 2865–2874.
- Qian, W., Yao, D., Yu, F., Xu, B., Zhou, R., Bao, X. and Lu, Z. (2000). Immobilization of antibodies on ultraflat polystyrene surfaces. *Clinical chemistry*, **46**: 1456–1463.
- Quan, M., Murphy, C. M., Zhang, Z. and Alexandersen, S. (2004). Determinants of early foot-and-mouth disease virus dynamics in pigs. *Journal of Comparative Pathology*, **131**: 294–307. doi: 10.1016/j.jcpa.2004.05.002.
- Rajan, S. R. K. (2001). Chemistry of the blood, in Ltd, O. L. P. (ed.) *Textbook of medical biochemistry*. 3rd edn. Hyderabad, pp. 154–171.
- Rajput, R., Sharma, G., Rawat, V., Gautam, A., Kumar, B., Pattnaik, B., Pradhan, H. K. and Khanna, M. (2015). Diagnostic potential of recombinant scFv antibodies generated against hemagglutinin protein of influenza A virus. *Frontiers in Immunology*, **6**: 1–9. doi: 10.3389/fimmu.2015.00440.
- Rakabe, M. (2008). *Selection of chicken single-chain antibody fragments directed against recombinant VP7 of bluetongue virus*. Master of Science Dissertation, University of Pretoria.

doi: 10.1080/09540105.2011.575122.

Reading, S. A. and Dimmock, N. J. (2007). Neutralization of animal virus infectivity by antibody. *Archives of Virology*, **152**: 1047–1059. doi: 10.1007/s00705-006-0923-8.

Reeve, R., Blignaut, B., Esterhuysen, J. J., Opperman, P., Matthews, L., Fry, E. E., Beer, T. A. P. De, Theron, J., Rieder, E., Vosloo, W., Hester, G., Neill, O., Haydon, D. T. and Maree, F. F. (2010). Sequence-Based Prediction for Vaccine Strain Selection and Identification of Antigenic Variability in Foot-and- Mouth Disease Virus. *PLOS Computational Biology*, **6** (12): e1001027 doi: 10.1371/journal.pcbi.1001027.

Reid, S. M., Ferris, N. P., Brüning, A., Hutchings, G. H., Kowalska, Z. and Åkerblom, L. (2001). Development of a rapid chromatographic strip test for the pen-side detection of foot-and-mouth disease virus antigen. *Journal of Virological Methods*, **96**: 189–202. doi: 10.1016/S0166-0934(01)00334-2.

Reid, S.M., Grierson, S.S., Ferris, N.P., Hutchings, G.H. and Alexandersen, S. (2003). Evaluation of automated RT-PCR to accelerate the laboratory diagnosis of foot-and mouth disease virus. *Journal of Virological Methods*, **107**: 129–139.

Reid, S. M., Ebert, K., Bachanek-Bankowska, K., Batten, C., Sanders, A., Wright, C., Shaw, A. E., Ryan, E. D., Hutchings, G. H., Ferris, N. P., Paton, D. J. and King, D. P. (2009). Performance of real-time reverse transcription polymerase chain reaction for the detection of foot-and-mouth disease virus during field outbreaks in the United Kingdom in 2007. *Journal of veterinary diagnostic investigation : official publication of the American Association of Veterinary Laboratory Diagnosticians, Inc*, **21**: 321–30. doi: 10.1177/104063870902100303.

Rémond, M., Kaiser, C. and Lebreton, F. (2002). Diagnosis and screening of foot-and-mouth disease. *Comparative Immunology, Microbiology and Infectious Diseases*, **25**: 309–320. doi: 10.1016/S0147-9571(02)00028-0.

Rezapkin, G., Neverov, A., Cherkasova, E., Vidor, E., Sarafanov, A., Kouivskaia, D., Dragunsky, E. and Chumakov, K. (2010). Repertoire of antibodies against type 1 poliovirus in human sera. *Journal of Virological Methods*, **169**: 322–331. doi: 10.1016/j.jviromet.2010.07.037.

Ribeiro, V. da S., Araújo, T. G., Gonzaga, H. T., Nascimento, R., Goulart, L. R. and Costa-Cruz, J. M. (2013). Development of specific scFv antibodies to detect neurocysticercosis antigens and potential applications in immunodiagnosis. *Immunology Letters*, **156**: 59–67. doi: 10.1016/j.imlet.2013.09.005.

Rieder, E., Bunch, T., Brown, F. and Mason, A. P. W. (1993). Genetically Engineered Foot-and-Mouth Disease Viruses with Poly (C) Tracts of Two Nucleotides Are Virulent in Mice. **67**: 5139–5145.

Rieder, E., Baxt, B. and Mason, P. W. (1994). Animal-derived antigenic variants of foot-and-mouth disease virus type A12 have low affinity for cells in culture. *Journal of Virology*, **68**: 5296–5299.

Rieder, E., Berinstein, A., Baxt, B., Kangt, A. and Mason, P. W. (1996). Propagation of an attenuated virus by design: Engineering a novel receptor for a noninfectious foot-and-mouth disease virus. *Microbiology*, **93**: 10428–10433. doi: 10.1073/pnas.93.19.10428.

- Rieder, E., Henry, T., Duque, H. and Baxt, B. (2005). Analysis of a Foot-and-Mouth Disease Virus Type A24 Isolate Containing an SGD Receptor Recognition Site In Vitro and Its Pathogenesis in Cattle. *Journal of Virology*, **79**: 12989–12998. doi: 10.1128/JVI.79.20.12989-12998.2005.
- Rigden, R. C., Carrasco, C. P., Summerfield, A. and McCullough, K. C. (2002). Macrophage phagocytosis of foot-and-mouth disease virus may create infectious carriers. *Immunology*, **106**: 537–548. doi: 10.1046/j.1365-2567.2002.01460.x.
- Ritter, M. A. (2000). *Diagnostic and therapeutic antibodies*. XIV. Edited by Geroge, A.J.T; Urch. Humana press.
- Roderiquez, G., Oravec, T., Yanagishita, M., Bou-Habib, D. C., Mostowski, H. and Norcross, M. A. (1995). Mediation of human immunodeficiency virus type 1 binding by interaction of cell surface heparan sulfate proteoglycans with the V3 region of envelope gp120-gp41. *Journal of Virology*, **69**: 2233–2239.
- Rodi, D. J. and Makowski, L. (1999). Phage-display technology - Finding a needle in a vast molecular haystack. *Current Opinion in Biotechnology*, **10**: 87–93. doi: 10.1016/S0958-1669(99)80016-0.
- Roitt, I., Brostoff, J. and Male, D. (1998). Antibodies and their receptors', in Mosby International Ltd (ed.) *Immunology*. 8th edn. London.
- Roivainen, M., Piirainen, L., Hovi, T., Virtanen, I., Riikonen, T., Heino, J. and Hyypiä, T. (1994). Entry of coxsackievirus A9 into host cells: specific interactions with alpha v beta 3 integrin, the vitronectin receptor. *Virology*, **203**: 357–65. doi: 10.1006/viro.1994.1494.
- Rowlands, D. J., Harris, T. J. and Brown, F. (1978). More precise location of the polycytidylic acid tract in foot and mouth disease virus RNA. *Journal of Virology*, **26**: 335–43.
- Ruiz-Sáenz, J., Goez, Y., Tabares, W. and López-Herrera, A. (2009). Cellular receptors for foot and mouth disease virus. *Intervirology*, **52**: 201–212. doi: 10.1159/000226121.
- Ruoslahti, E. (1996). RGD and Other Recognition Sequences for Integrins. *Annual Review of Cell and Developmental Biology*, **12**: 697–715. doi: 10.1146/annurev.cellbio.12.1.697.
- Rweyemamu, M.M and Garland, A.J.M. (2006). The design of vaccines and diagnostics for use in endemic FMD settings, in *Global Endemic FMD roadmap workshop*. Agra.
- Rweyemamu, M.M, Roeder, P., Mackay, D., Sumption, K., Brownlie, J., Leforban, Y., Valarcher, J.-F., Knowles, N. J. and Saraiva, V. (2008a). Epidemiological patterns of foot-and-mouth disease worldwide. *Transboundary and emerging diseases*, **55**: 57–72. doi: 10.1111/j.1865-1682.2007.01013.x.
- Rweyemamu, M., Roeder, P., MacKay, D., Sumption, K., Brownlie, J. and Leforban, Y. (2008b). Planning for the progressive control of foot-and-mouth disease worldwide. *Transboundary and emerging diseases*, **55**: 73–87. doi: 10.1111/j.1865-1682.2007.01016.x.
- Sa-Carvalho, D., Rieder, E., Baxt, B., Rodarte, R., Tanuri, A. and Mason, P. W. (1997). Tissue culture adaptation of foot-and-mouth disease virus selects viruses that bind to heparin and are attenuated in cattle. *Journal of Virology*, **71**: 5115–23.
- Saitou, N., Nei, M. (1987). The neighbor-joining method: a new method for reconstructing

phylogenetic trees. *Molecular Biological Evolution*, **4**: 406-425.

Sáiz, M., Núñez, J. I., Jimenez-Clavero, M. A., Baranowski, E. and Sobrino, F. (2002). Foot-and-mouth disease virus: Biology and prospects for disease control. *Microbes and Infection*, **4**: 1183–1192. doi: 10.1016/S1286-4579(02)01644-1.

Salt, J. S. (1993). The carrier state in foot and mouth disease-an immunological review. *British Veterinary Journal*, **149**: 207–223. doi: 10.1016/S0007-1935(05)80168-X.

Salt, J. S., Mulcahy, G. and Kitching, R. P. (1996). Isotype-specific antibody responses to foot-and-mouth disease virus in sera and secretions of "carrier" and "non-carrier" cattle', *Epidemiology and infection*, **117**: 349–360. doi: 10.1017/S0950268800001539.

Sambrook, J. and Russell, D. (2001). *Molecular Cloning: A Laboratory Manual*, Cold Spring Harbor Laboratory Press, Cold Spring Harbor, NY, p. 999.

Sammin, D.J., Paton, D.J., Parida, S., Ferris, N.P., Hutchings, G.H., Reid, S.M., Shaw, A.E., Holmes, C., Gibson, D., Corteyn, M., Knowles, N.J., Valarcher, J.-F., Hamblin, P.A., Fleming, L., Gwaze, G. and Sumption, K.J., 2007. Evaluation of laboratory tests for SAT serotypes of foot-and-mouth disease virus with specimens collected from convalescent cattle in Zimbabwe. *Veterinary Record*, **160**: 647–654.

Sammin, D., Ryan, E., Ferris, N. P., King, D. P., Zientara, S., Haas, B., Yadin, H., Alexandersen, S., Sumption, K. and Paton, D. J. (2010). Options for decentralized testing of suspected secondary outbreaks of foot-and-mouth disease. *Transboundary and emerging diseases*, **57**: 237–43. doi: 10.1111/j.1865-1682.2010.01141.x.

Samuel, A. R., Knowles, N. J. and Kitching, R. P. (1988). Serological and biochemical analysis of some recent type A foot-and-mouth disease virus isolates from the Middle East. *Epidemiology and infection*, **101**: 577–90. doi: 10.1017/S0950268800029447.

Samuel, A.R. and Knowles, N.J. (2001). Foot-and-mouth disease type O viruses exhibit genetically and geographically distinct evolutionary lineages (topotypes). *Journal of General Virology*, **82**: 609–621.

Sánchez-Aparicio, M. T., Rosas, M. F., Ferraz, R. M., Delgui, L., Veloso, J. J., Blanco, E., Villaverde, A. and Sobrino, F. (2009). Discriminating foot-and-mouth disease virus-infected and vaccinated animals by use of β -galactosidase allosteric biosensors. *Clinical and Vaccine Immunology*, **16**: 1228–1235. doi: 10.1128/CVI.00139-09.

Sangula, A. K., Belsham, G. J., Muwanika, V. B., Heller, R., Balinda, S. N., Masembe, C. and Siegismund, H. R. (2010a). Evolutionary analysis of foot-and-mouth disease virus serotype SAT 1 isolates from east Africa suggests two independent introductions from southern Africa. *BMC Evolutionary Biology*, **10**: 371. doi: 10.1186/1471-2148-10-371.

Sangula, A. K., Belsham, G. J., Muwanika, V. B., Heller, R., Balinda, S. N. and Siegismund, H. R. (2010b). Co-circulation of two extremely divergent serotype SAT 2 lineages in Kenya highlights challenges to foot-and-mouth disease control. *Archives of Virology*, **155**: 1625–1630. doi: 10.1007/s00705-010-0742-9.

Sangula, A. K., Siegismund, H. R., Belsham, G. J., Balinda, S. N., Masembe, C. and Muwanika, V. B. (2011). Low diversity of foot-and-mouth disease serotype C virus in Kenya:

evidence for probable vaccine strain re-introductions in the field. *Epidemiology and Infection*, **139**: 189–96. doi: 10.1017/S0950268810000580.

Sanyal, A., Venkataramanan, R. and Pattnaik, B. (1997). Antigenic features of foot-and-mouth disease virus serotype Asia1 as revealed by monoclonal antibodies and neutralization-escape mutants. *Virus Research*, **50**: 107–17.

Sanyal, A., Subramaniam, S., Mohapatra, J. K., Tamilselvan, R. P., Singh, N. K., Hemadri, D. and Pattnaik, B. (2010). Phylogenetic analysis of Indian serotype Asia1 foot-and-mouth-disease virus isolates revealed emergence and reemergence of different genetic lineages. *Veterinary Microbiology*, **144**: 198–202. doi: 10.1016/j.vetmic.2009.12.034.

Sanz-Parra, A., Sobrino, F. and Ley, V. (1998). Infection with foot-and-mouth disease virus results in a rapid reduction of MHC class I surface expression. *Journal of General Virology*, **79**: 433–436. doi: 10.1099/0022-1317-79-3-433.

Sarangi, L. N., Mohapatra, J. K., Subramaniam, S., Pandey, L. K., Das, B., Sanyal, A., Misri, J. and Pattnaik, B. (2015). Spectrum of VP1 region genetic variants in the foot-and-mouth disease virus serotype O populations derived from infected cattle tongue epithelium. *Acta Virologica*, **59**: 305–10.

Schlesinger, J. J. and Brandriss, M. W. (1981). Growth of 17D yellow fever virus in a macrophage-like cell line, U937: role of Fc and viral receptors in antibody-mediated infection. *Journal of Immunology*, **127**: 659–665.

Schneider, T.D. and Stephens, R.M. (1990). Sequence logos: a new way to display consensus sequences. *Nucleic Acids Res.* **18**: 6097-6100.

Schroeder, H. W. J. and Cavacini, L. (2010). Structure and Function of Immunoglobulins. *Journal of Allergy and Clinical Immunology*, **125**: S41–S52. doi: 10.1016/j.jaci.2009.09.046.Structure.

Sellers, R. F., Herniman, K. A. and Donaldson, A. I. (1971). The effects of killing or removal of animals affected with foot-and-mouth disease on the amounts of airborne virus present in looseboxes. *The British Veterinary Journal*, **127**: 358–65.

Sevilla, N. and Domingo, E. (1996). Evolution of a persistent aphthovirus in cytolytic infections: partial reversion of phenotypic traits accompanied by genetic diversification. *Journal of Virology*, **70**: 6617–24.

Sharma, G.K., Mohapatra, J.K., Mahajan, S., Matura, R., Subramaniam, S., Pattnaik, B. (2014). Comparative evaluation of non-structural protein-antibody detecting ELISAs for foot-and-mouth disease sero-surveillance under intensive vaccination. *Journal of Virological Methods*, **207**: 22–28.

Shirley, M. W., Charleston, B. and King, D. P. (2010). New opportunities to control livestock diseases in the post-genomics era. *The Journal of Agricultural Science*, **149**: 115–121. doi: 10.1017/S0021859610001103.

Simel, D., Samsa, G., Matchar, D. (1991). Likelihood ratios with confidence: sample size estimation for diagnostic test studies. *Journal of Clinical Epidemiology*, **44**: 763–770.

Sinkala, Y., Pfeiffer, D., Kasanga, C., Muma, J. B., Simuunza, M. and Mweene, A. (2012).

Foot-and-mouth disease control in Zambia: A review of the current situation. *Onderstepoort Journal of Veterinary Research*, **79** (2). doi: 10.4102/ojvr.v79i2.472.

Sinkala, Y., Simuunza, M., Muma, J. B., Pfeiffer, D. U., Kasanga, C. J. and Mweene, A. (2014). Foot and mouth disease in Zambia: Spatial and temporal distributions of outbreaks, assessment of clusters and implications for control. *Onderstepoort Journal of Veterinary Research*, **81** (2). doi: 10.4102/ojvr.v81i2.741.

Sixholo, J., Van Wyngaardt, W., Mashau, C., Frischmuth, J., Du Plessis, D. H. and Fehrsen, J. (2011). Improving the characteristics of a mycobacterial 16 kDa-specific chicken scFv. *Biologicals : Journal of the International Association of Biological Standardization*, **39**: 110–6. doi: 10.1016/j.biologicals.2011.01.007.

Smith, G. P. (1985). Filamentous fusion phage: novel expression vectors that display cloned antigens on the virion surface. *Science (New York, N.Y.)*, **228**: 1315–7.

Smith, G. P. and Petrenko, V. a (1997). Phage Display. *Chemical Reviews*, **97**: 391–410. doi: 10.1016/1380-2933(95)00013-5.

Sobrino, F., Sáiz, M., Jiménez-Clavero, M. A., Núñez, J. I., Rosas, M. F., Baranowski, E. and Ley, V. (2001). Foot-and-mouth disease virus: a long known virus, but a current threat. *Veterinary Research*, **32**: 1–30. doi: 10.1051/vetres:2001106.

Sørensen, K. J., Madsen, K. G., Madsen, E. S., Salt, J. S., Nqindi, J. and Mackay, D. K. (1998). Differentiation of infection from vaccination in foot-and-mouth disease by the detection of antibodies to the non-structural proteins 3D, 3AB and 3ABC in ELISA using antigens expressed in baculovirus. *Archives of Virology*, **143**: 1461–76.

Sørensen, K. J., De Stricker, K., Dyrting, K. C., Grazioli, S. and Haas, B. (2005). Differentiation of foot-and-mouth disease virus infected animals from vaccinated animals using a blocking ELISA based on baculovirus expressed FMDV 3ABC antigen and a 3ABC monoclonal antibody. *Archives of Virology*, **150**: 805–814. doi: 10.1007/s00705-004-0455-z.

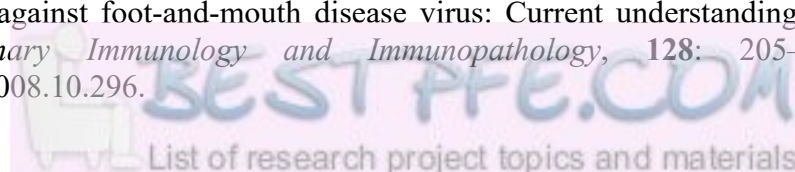
Sparks, A.B., Adey, N.B., Cwirla, S. and Kay, B. (1996). Screening phage-displayed random peptide libraries, In: B.K. Kay, J. and McCafferty, W. and J. (eds) *Phage display of peptides and proteins*. Academic Press, pp. 227–253.

Stanway, G. (1990). Structure, function and evolution of picornaviruses. *Journal of General Virology*, **71**: 2483–2501.

Storey, P., Theron, J., Maree, F. F. and O'Neill, H. G. (2007). A second RGD motif in the 1D capsid protein of a SAT1 type foot-and-mouth disease virus field isolate is not essential for attachment to target cells. *Virus Research*, **124**: 184–192. doi: 10.1016/j.virusres.2006.11.003.

Subramaniam, S., Mohapatra, J. K., Sharma, G. K., Das, B., Dash, B. B., Sanyal, A. and Pattnaik, B. (2013). Phylogeny and genetic diversity of foot and mouth disease virus serotype Asia1 in India during 1964-2012. *Veterinary Microbiology*, **167**: 280–288. doi: 10.1016/j.vetmic.2013.08.023.

Summerfield, A., Guzylack-Piriou, L., Harwood, L. and McCullough, K. C. (2009). Innate immune responses against foot-and-mouth disease virus: Current understanding and future directions. *Veterinary Immunology and Immunopathology*, **128**: 205–210. doi: 10.1016/j.vetimm.2008.10.296.



- Summerford, C. and Samulski, R. J. (1998). Membrane-Associated Heparan Sulfate Proteoglycan Is a Receptor for Adeno-Associated Virus Type 2 Virions. *Journal of Virology*, **72**: 1438–1445.
- Sumption, K., Rweyemamu, M. and Wint, W. (2008). Incidence and distribution of foot-and-mouth disease in Asia, Africa and South America; Combining expert opinion, official disease information and livestock populations to assist risk assessment. *Transboundary and Emerging Diseases*, **55**: 5–13. doi: 10.1111/j.1865-1682.2007.01017.x.
- Sutmoller, P. and Gaggero, A. (1965). Foot-and mouth diseases carriers. *The Veterinary Record*, **77**: 968–9.
- Sutmoller, P., Cottral, G. E. and McVicar, J. W. (1967). A review of the carrier state in foot-and-mouth disease. *Proceedings, annual meeting of the United States Animal Health Association*, **71**: 386–95.
- Sutmoller, P., Thomson, G. R., Hargreaves, S. K., Foggin, C. M. and Anderson, E. C. (2000). The foot-and-mouth disease risk posed by African buffalo within wildlife conservancies to the cattle industry of Zimbabwe. *Preventive Veterinary Medicine*, **44**: 43–60.
- Sutmoller, P., Barteling, S. S., Olascoaga, R. C. and Sumption, K. J. (2003). Control and eradication of foot-and-mouth disease. *Virus Research*, **91**: 101–44.
- Sweeney, T. R., Cisnetto, V., Bose, D., Bailey, M., Wilson, J. R., Zhang, X., Belsham, G. J. and Curry, S. (2010). Foot-and-Mouth Disease Virus 2C Is a Hexameric AAA+ Protein with a Coordinated ATP Hydrolysis Mechanism. *Journal of Biological Chemistry*, **285**: 24347–24359. doi: 10.1074/jbc.M110.129940.
- Takamatsu, H.-H., Denyer, M. S., Stirling, C., Cox, S., Aggarwal, N., Dash, P., Wileman, T. E. and Barnett, P. V (2006). Porcine gammadelta T cells: possible roles on the innate and adaptive immune responses following virus infection. *Veterinary Immunology and Immunopathology*, **112**: 49–61. doi: 10.1016/j.vetimm.2006.03.011.
- Takeda, A., Tuazon, C. and Ennis, F. (1988). Antibody-enhanced infection by HIV-1 via Fc receptor-mediated entry. *Science*, **242**: 580–583. doi: 10.1126/science.2972065.
- Takemoto, K. K. and Liebhaver, H. (1961). Virus-polysaccharide interactions. *Virology*, **14**: 456–462. doi: 10.1016/0042-6822(61)90338-5.
- Thomas, A. A. M., Woortmeijer, R. J., Puijk, W. and Barteling, S. J. (1988). Foot-and-mouth disease virus type A10. *Journal of Virology*, **62**: 2782–2789.
- Thompson, J. D., Gibson, T. J., Plewniak, F., Jeanmougin, F. and Higgins, D. G. (1997). The CLUSTAL _ X windows interface : flexible strategies for multiple sequence alignment aided by quality analysis tools. *Nucleic Acids Research*, **25**: 4876–4882.
- Thomson, G. R., Vosloo, W., Esterhuysen, J. J. and Schuldt, T, J. (1992). Maintenance of foot and mouth disease viruses in buffalo (*syncerus caffer* Sparrman, 1779) in southern Africa. *Revue Scientifique et Technique de l'OIE*, **11**(4), pp. 1097–1107. doi: 10.20506/rst.11.4.646.
- Thomson, G. R. (1994). Foot-and-mouth disease, *In*: Coetzer, J.A.W., Thomson G.R., Tustin, R.C., Kriek, N. P. J. (ed.) *Infectious diseases of livestock with special reference to Southern Africa*. Cape Town: Oxford University Press, pp. 825–852.

- Thomson, G. R., Vosloo, W. and Bastos, A. D. S. (2003). Foot and mouth disease in wildlife. *Virus Research*, **91**: 145–61.
- Thomson, G.R. and Bastos, A. D. (2004). Foot-and-mouth disease, *In*: Coetzer, J.A.W., Tustin, R. . (ed.) *Infectious Diseases of Livestock*. 2nd edn. Oxford University Press, pp. 1324–1365.
- Thomson, G. and Vosloo, W. (2004). Natural Habitats in Which Foot-and-Mouth Disease Virus is Maintained, *In: Foot and Mouth Disease*. CRC Press, pp. 384–410. doi: 10.1201/9781420037968.ch14.
- Tizard, I. R. (2000). Dendritic cells and antigen processing, *In*: W.B. Saunders Company (ed.) *Veterinary Immunology: An Introduction*. Pennsylvania.
- Torrance, L., Ziegler, A., Pittman, H., Paterson, M., Toth, R. and Eggleston, I. (2006). Oriented immobilisation of engineered single-chain antibodies to develop biosensors for virus detection. *Journal of Virological Methods*, **134**: 164–70. doi: 10.1016/j.jviromet.2005.12.012.
- Toth, R. L., Harper, K., Mayo, M. A. and Torrance, L. (1999). Fusion proteins of single-chain variable fragments derived from phage display libraries are effective reagents for routine diagnosis of potato leafroll virus infection in potato. *Phytopathology*, **89**: 1015–21. doi: 10.1094/PHYTO.1999.89.11.1015.
- Towner, J. S., Ho, T. V and Semler, B. L. (1996). Determinants of membrane association for poliovirus protein 3AB. *The Journal of Biological Chemistry*, **271**: 26810–8.
- Twomey, T., Newman, J., Burrage, T., Piatti, P., Lubroth, J. and Brown, F. (1995). Structure and immunogenicity of experimental foot-and-mouth disease and poliomyelitis vaccines. *Vaccine*, **13**: 1603–10.
- Usherwood, E. J. and Nash, A. A. (1995). Lymphocyte recognition of picornaviruses. *Journal of General Virology*, **76**: 499–508. doi: 10.1099/0022-1317-76-3-499.
- Vakharia, V. N., Devaney, M. A., Moore, D. M., Dunn, J. J. and Grubman, M. J. (1987). Proteolytic processing of foot-and-mouth disease virus polyproteins expressed in a cell-free system from clone-derived transcripts. *Journal of Virology*, **61**: 3199–207.
- Valarcher, J., Knowles, N.J., Fernandez, R., Davies, P.R., Midgley, R.J., Statham, B., Hutchings, G., Newman, B.J., Ferris, N.P., Paton, D. (2004). Global Foot-and-mouth Disease situation 2003-2004, *In: Report of the session of the research group of the standing technical committee of the European Commission for the control of foot-and-mouth disease (EuFMD)*, pp. 137–148.
- Vance, L. M., Moscufo, N., Chow, M. and Heinz, B. A. (1997). Poliovirus 2C region functions during encapsidation of viral RNA. *Journal of Virology*, **71**: 8759–8765.
- Vasquez, C., Denoya, C. D., La Torre, J. and Palma, E. L. (1979). Structure of foot-and-mouth disease virus capsid. *Virology*, **97**: 195–200. doi: 10.1016/0042-6822(79)90387-8.
- Van Kuppeveld, F. J. M., Van Den Hurk, P. J. J. C., Van Der Vliet, W., Galama, J. M. D. and Melchers, W. J. G. (1997). Chimeric coxsackie B3 virus genomes that express hybrid coxsackievirus-poliovirus 2B proteins: Functional dissection of structural domains involved in RNA replication. *Journal of General Virology*, **78**: 1833–1840. doi: 10.1099/0022-1317-78-8-1833.

- Van Rensburg, H. G. and Nel, L. H. (1999). Characterization of the structural-protein-coding region of SAT 2 type foot-and-mouth disease virus. *Virus Genes*, **19**: 229–233. doi: 10.1023/A:1008140815045.
- Van Rensburg, H., Haydon, D., Joubert, F., Bastos, A., Heath, L. and Nel, L. (2002). Genetic heterogeneity in the foot-and-mouth disease virus Leader and 3C proteinases. *Gene*, **289**: 19–29. doi: 10.1016/S0378-1119(02)00471-7.
- Van Rensburg, H. G., Henry, T. M. and Mason, P. W. (2004). Studies of genetically defined chimeras of a European type A virus and a South African Territories type 2 virus reveal growth determinants for foot-and-mouth disease virus. *Journal of General Virology*, **85**: 61–68. doi: 10.1099/vir.0.19509-0.
- Van Vlijmen, H. W., Curry, S., Schaefer, M. and Karplus, M. (1998). Titration calculations of foot-and-mouth disease virus capsids and their stabilities as a function of pH. *Journal of Molecular Biology*, **275**: 295–308. doi: 10.1006/jmbi.1997.1418.
- Van Wyngaardt, W., Malatji, T., Mashau, C., Fehrsen, J., Jordaan, F., Miltiadou, D. and Du Plessis, D. H. (2004). A large semi-synthetic single-chain Fv phage display library based on chicken immunoglobulin genes. *BMC Biotechnology*, **4**: 6. doi: 10.1186/1472-6750-4-6.
- Vosloo, W., Bastos, A.D., Kirkbride, E., Esterhuysen, J.J., Van Rensburg, J., Bengis, R.G., Keet, D.F. and Thomson, G.R. (1996). Persistent infection of African buffalo (*Syncerus caffer*) with SAT-type foot-and-mouth disease viruses: rate of fixation of mutations, antigenic change and interspecies transmission. *Journal of General Virology*, **77**:1457–1467.
- Vosloo, W., Bastos, A. D. S., Sangare, O., Hargreaves, S. K. and Thomson, G. R. (2002). Review of the status and control of foot and mouth disease in sub-Saharan Africa. *Revue scientifique et technique (International Office of Epizootics)*, **21**: 437–449. doi: <http://web.oie.int/boutique/extrait/11vosloo.pdf>.
- Vosloo, W., Bastos, A.D.S., Sahle, M., Sangare, O. and Dwarka, R. M. (2005). Virus topotypes and the role of wildlife in foot and mouth disease in Africa', *In: Osofsky, S. A. (ed.) Conservation and development interventions at the wildlife/livestock interface: Implications for wildlife, livestock and human health*. United Kingdom: IUCN Publications Services Unit.
- Webster, R. E. (1996). Biology of the filamentous bacteriophage, *In: Phage Display of Peptides and Proteins*. California: Academic Press Inc, pp. 1–20.
- Wemmer, S., Mashau, C., Fehrsen, J., van Wyngaardt, W. and du Plessis, D. H. (2010). Chicken scFvs and bivalent scFv-C(H) fusions directed against HSP65 of Mycobacterium bovis. *Biologicals : Journal of the International Association of Biological Standardization*, **38**: 407–14. doi: 10.1016/j.biologicals.2010.02.002.
- Willats, W. G. T. (2002). Phage display: Practicalities and prospects. *Plant Molecular Biology*, **50**: 837–854. doi: 10.1023/A:1021215516430.
- Williams, F., A. and Barclay, A. N. (1988). The immunoglobulin superfamily--domains for cell surface recognition. *Annual Review of Immunology*, **6**: 381–405. doi: 10.1146/annurev.iy.06.040188.002121.
- Williamson, P. and Matthews, R. (1999). Development of neutralising human recombinant antibodies to pertussis toxin. *FEMS Immunology and Medical Microbiology*, **23**: 313–9.

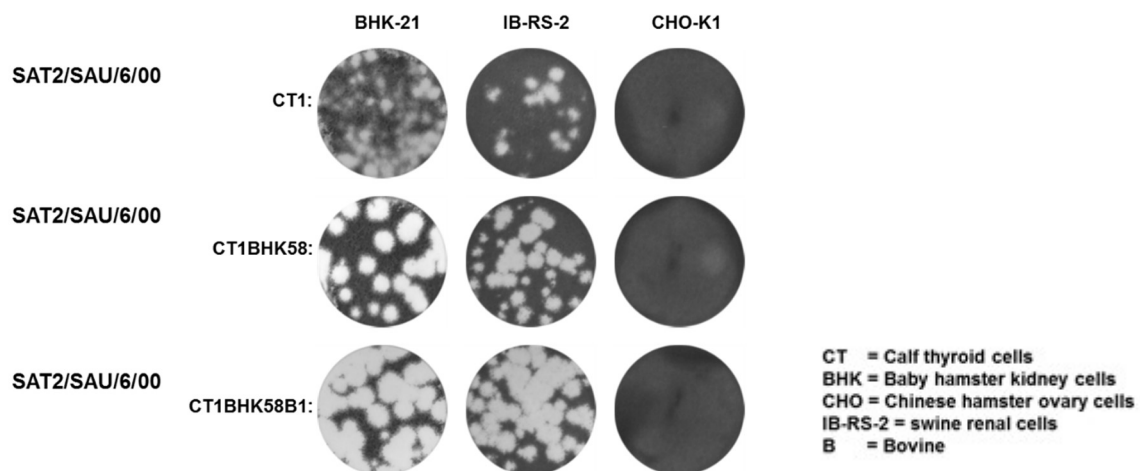
- Winter, G., Griffiths, A. D., Hawkins, R. E. and Hoogenboom, H. R. (1994). Making antibodies by phage display technology. *Annual Review of Immunology*, **12**: 433–55. doi: 10.1146/annurev.iy.12.040194.002245.
- WuDunn, D. and Spear, P. G. (1989). Initial interaction of herpes simplex virus with cells is binding to heparan sulfate. *Journal of Virology*, **63**: 52–58.
- Xie, Q-C, McCahon, D., Crowther, J.R., Belsham, G.R. and McCullough, K.C. (1987). Neutralization of Foot-and-Mouth Disease virus can be mediated through any of at least three separate antigenic sites. *Journal of general Virology*, **68**: 1637-1647
- Yamaguchi, Y., Inatani, M., Matsumoto, Y., Ogawa, J. and Irie, F. (2010). Roles of heparan sulphate in mammalian brain development: current views based on the findings from Ext1 conditional knockout studies, *In: Progress in molecular biology and translational science*. Vol. **93**. Elsevier Inc, p. 377.
- Yang, M., Goolia, M., Xu, W., Bittner, H. and Clavijo, A. (2013). Development of a quick and simple detection methodology for foot-and-mouth disease virus serotypes O, A and Asia 1 using a generic RapidAssay Device. *Virology Journal*, **10**, p. 125. doi: 10.1186/1743-422X-10-125.
- Yu, Y., Wang, H., Zhao, L., Zhang, C., Jiang, Z. and Yu, L. (2011). Fine mapping of a foot-and-mouth disease virus epitope recognized by serotype-independent monoclonal antibody 4B2. *The Journal of Microbiology*, **49**: 94–101. doi: 10.1007/s12275-011-0134-1.
- Yuan, Q., Clarke, J. R., Zhou, H. R., Linz, J. E., Pestka, J. J. and Hart, L. P. (1997). Molecular cloning, expression, and characterization of a functional single-chain Fv antibody to the mycotoxin zearalenone. *Applied and environmental microbiology*, **63**: 263–9. Available at: <http://www.ncbi.nlm.nih.gov/pubmed/8979354>.
- Yun, Y. H., Eteshola, E., Bhattacharya, A., Dong, Z., Shim, J. S., Conforti, L., Kim, D., Schulz, M. J., Ahn, C. H. and Watts, N. (2009). Tiny medicine: Nanomaterial-based biosensors. *Sensors*, **9**: 9275–9299. doi: 10.3390/s91109275.
- Zadoks, R. N. and Schukken, Y. H. (2006). Use of molecular epidemiology in veterinary practice. *The Veterinary clinics of North America. Food animal practice*, **22**: 229–61. doi: 10.1016/j.cvfa.2005.11.005.
- Zhang, Z. D., Hutching, G., Kitching, P. and Alexandersen, S. (2002). The effects of gamma interferon on replication of foot-and-mouth disease virus in persistently infected bovine cells, *Arch Virol*, **147**: 2157–2167. doi: 10.1007/s00705-002-0867-6.
- Zhang, Z., Ahmed, R., Paton, D. and Bashiruddin, J. B. (2009). Cytokine mRNA responses in bovine epithelia during foot-and-mouth disease virus infection. *Veterinary Journal*, **179**: 85–91. doi: 10.1016/j.tvjl.2007.08.012.
- Zhou, X.-H., Obuchowsky, N.A., McClish, D.K. (2002). *Statistical Methods in Diagnostic Medicine*. John Wiley and Sons, New York.
- Zhao, Q. Z., Pacheco, J. M. and Mason, P. W. (2003). Evaluation of genetically engineered derivatives of a Chinese strain of foot-and-mouth disease virus reveals a novel cell-binding site which functions in cell culture and in animals. *Journal of Virology*, **77**: 3269–3280. doi: 10.1128/jvi.77.3269-3280.2003.

Zibert, A., Maass, G., Strebel, K., Falk, M. M. and Beck, E. (1990). Infectious foot-and-mouth disease virus derived from a cloned full-length cDNA. *Journal of Virology*, **64**: 2467–73. doi: 10.1360/03wc0567.

APPENDICES

Appendix A1:

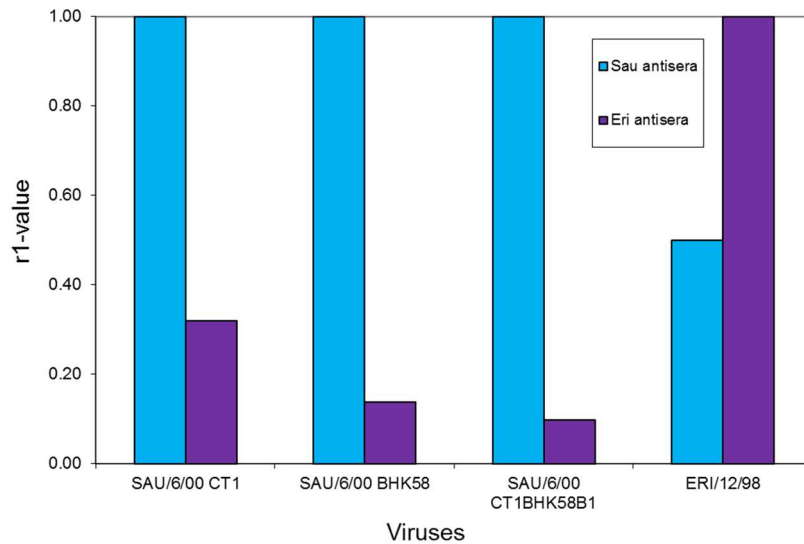
A SAT2 isolate causing a severe outbreak in dairy herds in Saudi Arabia in 2000, *i.e.* SAT2/SAU/6/00, have been passaged 58 times in BHK-21 suspension cells (designated SAU^{BHK58}). The plaque morphology on BHK-21 cells of the SAT2/SAU/6/00 calf thyroid (CT₁) isolate was medium sized opaque plaques as reported by Maree *et al.* (1), whereas SAU^{BHK58} produced large, clear plaques (Figure A1.1). On a porcine kidney cell line (IB-RS-2 cells), known to express mainly the integrin, $\alpha V\beta 8$ (2) the plaques were not as distinctly different, with clear medium sized plaques. None of the SAT2/SAU/6/00 viruses produced plaques on CHO-K1 cell monolayers (Figure A1.1) and infectivity is therefore independent of cell surface glycosaminoglycans (GAG) for cell entry.



Appendix Figure A1.1: Plaque morphologies of SAT2/SAU/6/00 field isolate (CT₁), cell culture derived virus (CT₁BHK₅₈) and bovine passaged virus (CT₁BHK₅₈B₁), obtained using monolayers of BHK-21, swine renal (IB-RS-2) and CHO-K1 cells. Cells infected with the indicated viral strains were incubated with tragacanth overlay for 42 h prior to staining with 1% methylene blue. Plaques for SAT2/SAU/6/00 wild-type virus (CT₁) are medium size (3-5 mm) with opaque edges whilst the CT₁BHK₅₈ displayed medium and large (6-8 mm) plaques with clear edges. None of the viruses replicated in CHO-K1 cells.

One-way antigenic relationships (r_1 -values) were used to compare the antigenic cross-reactivity of the SAT2/SAU/6/00 isolates with each other. Bovine sera raised against the CT₁BHK₅₈

reacted similarly against CT₁, CT₁BHK₅₈ and CT₁BHK₅₈B₁ isolates (Figure A1.2). Correspondingly, sera raised against a related SAT2 virus, *i.e.* SAT2/ERI/12/98, reacted similarly to SAT2/SAU/6/00 CT₁, CT₁BHK₅₈ and CT₁BHK₅₈B₁ isolates (Figure A1.2). However, based on the cross neutralization data, the antigenic features of SAU/6/00 seem to be unchanged following 58 passages on BHK-21 cells.

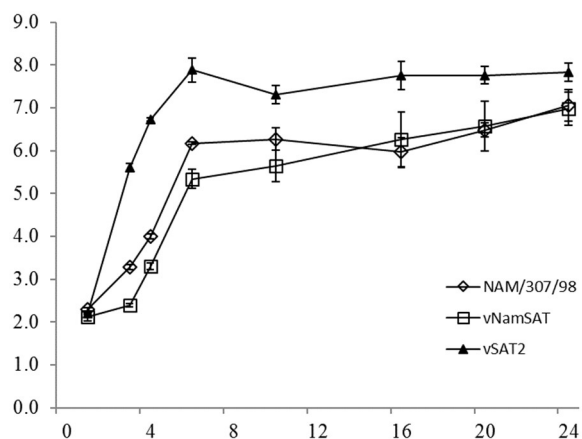


Appendix Figure A1.2: Cross reactivity of the SAT2/SAU/6/00 CT₁, CT₁BHK₅₈ and CT₁BHK₅₈B₁ isolates measured against cattle sera raised to CT₁BHK₅₈. VNTs were done in duplicate. r1-values are expressed as the ratio between the heterologous/homologous end point serum titres of the largest dilution of serum to neutralize 100 TCID₅₀ in 50% of the wells in VN tests.

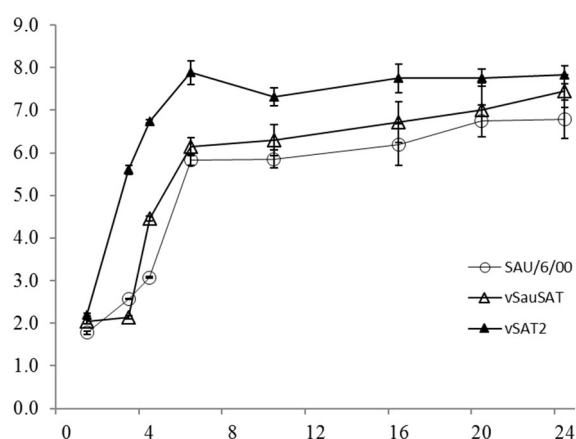
Appendix A2:

Relative infectivity titres of chimeric v^{SAU}SAT and v^{NAM}SAT viruses after recovery of five passages in BHK-21 cells was 1.6 x 10⁶ pfu/ml and 6.2 x 10⁶ pfu/ml, respectively. Neither were able to replicate in CHO-K1 cells. One-step growth studies were performed for the vSAT2, v^{NAM}SAT2 and v^{SAU}SAT2 and the parental viruses SAT1/NAM/307/98 and SAT2/SAU/6/00 in BHK-21 cells. The one-step growth kinetics illustrated that the growth of the chimeric viruses were similar to that of the parental viruses at MOI of two (Figure A2.1). A substantial increase in virus titre were observed during 4-10 hpi, but slower than that of vSAT2. A growth plateau was reached between 12 h and 24hpi with titres of the chimeric and parental viruses 10 to 30-fold lower than vSAT2 (Figure A2.1).

A)



B)



Appendix Figure A2.1. One-step growth kinetic studies were performed in BHK-21 cells. For comparison of the relative release of virus particles from cells infected with A) vSAT2, v^{NAM}SAT and SAT1/NAM/307/98 and B) vSAT2, v^{SAU}SAT2 and SAT2/SAU/6/00 viruses are shown as the average log virus titres at different times p.i. (1, 3, 4, 6, 10, 16, 20 and 24 hpi). The standard deviations of the titres determined from quadruple wells are indicated on the graph.

References

1. Maree FF, Blignaut B, de Beer TAP, Visser N, Rieder EA. 2010. Mapping of amino acid residues responsible for adhesion of cell culture-adapted foot-and-mouth disease SAT type viruses. *Virus Res* 153:82–91.
2. Burman A, Clark S, Abrescia NGA, Fry EE, Stuart DI, Jackson T. 2006. Specificity of the VP1 GH Loop of Foot-and-Mouth Disease Virus for v Integrins. *J Virol* 80:9798–9810.

Appendix A3: Table showing the amino acid sequence variation (entropy >1) that was observed for the SAT1 panel of viruses for this study for the outer capsid coding regions, when aligned to the panned SAT1/KNP/196/91 virus. The characteristic type of amino acid variation that was observed was evaluated and is indicated by the key.

Virus capsid protein	Amino acid position	SAT1/ZAM/2/93 Amino acid change	SAT1/SAR/9/81 Amino acid change	SAT1/KNP/10/03 Amino acid change	SAT1/NAM/272/98 Amino acid change	SAT1/SAR/2/10 Amino acid change	SAT1/KNP3/03 Amino acid change	SAT1/ZIM/14/98 Amino acid change	SAT1/BOT/1/06 Amino acid change	SAT1/SAR/9/03 Amino acid change	SAT1/SAR/33/00 Amino acid change
VP1	21	D-N	D-N	-	D-A	-	-	-	D-V	-	-
VP1	24	T-A	T-G	T-V	-	-	T-V	-	-	T-A	T-A
VP1	25	-	T-V	T-A	T-A	T-V	T-A	T-A	T-A	T-A	-
VP1	28	H-Q	H-Q	-	H-V	-	H-Q	-	H-P	-	-
VP1	46	Q-V	-	Q-E	Q-V	Q-R	-	-	Q-K	-	-
VP1	47	D-E	D-N	-	D-N	D-N	D-K	-	D-N	-	D-N
VP1	84	D-T	D-E	D-K	D-V	D-V	D-K	D-A	D-A	D-T	-
VP1	99	A-S	A-E	A-S	A-S	A-N	A-S	A-S	A-T	A-T	A-E
VP1	110	K-H	K-N	K-A	K-H	-	K-A	K-H	K-H	K-R	-
VP1	112	R-G	R-G	-	R-N	R-N	R-G	R-N	-	R-N	-
VP1	130	A-T	A-T	A-S	A-V	A-T	A-S	A-T	A-V	-	A-L
VP1	146	E-T	E-D	E-D	E-T	-	-	E-T	-	-	E-T
VP1	157	-	A-Q	A-D	A-E	A-E	A-G	A-E	-	-	A-E
VP1	204	G-Q	G-N	G-K	-	-	G-S	-	G-A	-	G-A
VP2	39	S-T	-	-	S-A	-	-	-	S-T	-	S-L
VP2	41	-	R-H	R-H	R-T	-	R-H	R-L	R-K	R-L	R-Q
VP2	71	L-S	-	L-P	L-T	-	-	L-T	-	-	L-T
VP2	74	R-K	R-Q	R-Q	R-E	R-K	R-Q	R-K	R-Q	R-K	R-S
VP3	09	V-D	V-D	V-H	V-D	V-D	V-H	V-D	V-D	V-A	V-A
VP3	67	A-N	A-S	-	A-N	-	A-S	A-N	A-N	-	-
VP3	135	E-T	-	E-D	-	E-D	E-A	E-N	E-K	E-D	E-A

KEY

	Change to Polar
	Change to Non-polar/hydrophobic
	Change to basic side chains
	Change to acidic side chains (polar)
	Amino acid variation results in same characteristic
Bold	Loss of +ve charge
<i>Bold italics</i>	<i>Gain of +ve charge</i>
-	Amino acid same as reference sequence

Appendix A4: **Table showing the amino acid sequence variation (entropy >1) that was observed for the outer capsid coding regions for the SAT3 panel of viruses for this study, when aligned to SAT3/KNP/10/90 virus (panned virus). The characteristic type of amino acid variation that was observed was evaluated and is indicated by the key in Appendix A4.

Virus protein	Position	SAT3/KN P/14/96 Aacid change	SAT3/BO T/6/98 Aacid change	SAT3/SA R/14/01 Aacid change	SAT3/SA R/1/06 Aacid change	SAT3/KN P/2/03 Aacid change	SAT3/ZA M/5/93 Aacid change	SAT3/KN P/8/02 Aacid change	SAT3/KN P/1/03 Aacid change	SAT3/ZI M/5/91 Aacid change	SAT3/ZI M/11/94 Aacid change	SAT3/KN P/6/08 Aacid change
VP1	21	A-T	A-V	-	A-T	A-T	A-E	A-T	A-V	A-T	A-E	-
	44	T-E	T-S	-	T-Q	-	-	T-P	T-S	T-S	T-A	T-E
	47	G-A	-	-	G-N	G-A	G-S	G-A	-	G-A	-	G-A
	83	T-E	T-D	-	-	T-N	T-D	-	-	T-E	T-D	T-E
	84	G-A	G-A	-	-	G-A	G-A	G-D	G-S	G-A	G-A	G-A
	143	V-T	-	-	V-T	V-Q	V-S	-	V-A	V-K	V-T	V-T
	164	R-I	R-I	-	-	R-I	R-L	-	R-I	R-K	R-I	R-M
	177	T-S	T-S	-	-	-	T-S	-	T-A	T-S	T-G	T-S
	179	D-N	-	-	D-E	D-E	-	D-E	D-E	-	D-E	D-N
	185	E-N	E-Q	-	E-K	-	-	-	E-K	-	-	E-K
	200	A-V	A-T	-	A-T	A-T	A-T	A-T	A-R	A-T	A-T	A-V
VP2	131	T-S	T-S	-	T-K	T-A	-	T-S	T-S	T-A	T-K	T-S
	214	K-M	K-R	-	K-R	K-R	K-M	K-R	K-R	-	K-R	K-M
VP3	131	D-E	D-S	-	D-E	D-E	D-N	D-E	D-E	D-E	D-S	D-E
	135	D-K	D-N	-	D-K	D-K	D-N	-	-	D-S	-	D-N
	139	A-E	A-K	-	A-E	A-E	-	A-K	A-E	A-E	A-Q	A-S

** Key as per Appendix A3



Development and validation of a foot-and-mouth disease virus SAT serotype-specific 3ABC assay to differentiate infected from vaccinated animals



M. Chitray^{a,b}, S. Grazioli^c, T. Willems^d, T. Tshabalala^a, A. De Vleeschouwer^d, J.J. Esterhuysen^a, E. Brocchi^c, K. De Clercq^d, F.F. Maree^{a,b,*}

^a Transboundary Animal Diseases, Onderstepoort Veterinary Institute, Agricultural Research Council, Private Bag X05, Onderstepoort, 0110, South Africa

^b Department of Microbiology and Plant Pathology, Faculty of Agricultural and Natural Sciences, University of Pretoria, Pretoria 0002, South Africa

^c Istituto Zooprofilattico Sperimentale della Lombardia e dell'Emilia Romagna (IZSLER), Via Bianchi 7/9, 25124 Brescia, Italy

^d Unit Vascular and Exotic Diseases, Department of Virology, CODA-CERVA-VAR, Gosselberg 99, B-1180 Ukkel, Belgium

ARTICLE INFO

Keywords:
FMD
ELISA
NSP
SAT
SABC

ABSTRACT

The effective control of foot-and-mouth disease (FMD) requires sensitive, specific and rapid diagnostic tools. However, the control and eradication of FMD in Africa is complicated by, among other factors, the existence of five of the seven FMD virus (FMDV) serotypes, including the SAT-serotypes 1, 2 and 3 that are genetically and antigenically the most variable FMDV serotypes. A key diagnostic assay to enable a country to re-gain its FMD-free status and for FMD surveillance, is the 3ABC or the non-structural protein (NSP) enzyme-linked immunosorbent assay (ELISA). Although many kits are available to detect 3ABC antibodies, none has been developed specifically for the variable SAT serotypes. This study designed a SAT-specific NSP ELISA and determined whether this assay could better detect NSP-specific antibodies from FMDV SAT-infected livestock. The assay's performance was compared to validated NSP assays (PrioCheck[®]-NSP and IZSLER-NSP), using panels of field and experimental sera, vaccinated and/or infected with FMDV SAT1, SAT2 or SAT3. The sensitivity () of the SAT-NSP was estimated as 76% (70%, 81%) whereas the specificity was 96% (95%, 98%) at a 95% confidence interval. The sensitivity and specificity were comparable to the commercial NSP assays, PrioCheck[®]-NSP (92% and 99%, respectively) and IZSLER-NSP (78% and 98%, respectively). Good correlations were observed for all three assays.

1. Introduction

Foot-and-mouth disease (FMD) is one of several contagious transboundary diseases that can spread rapidly within livestock populations with a devastating effect on the economy of a country or region. The causative agent, FMD virus (FMDV), an *Aphthovirus* in the family *Picornaviridae*, though clinically indistinguishable, exist as seven distinct serotypes (Knowles and Samuel, 2003). The epidemiology of FMD in Africa is unique in the sense that five of the seven serotypes of FMDV [South African Territories [(SAT) 1, 2, 3, A and O]], with the exception of types C and Asia-1, occur. Another unique feature is the two different epidemiological patterns in Africa i.e. a cycle involving wildlife, in particular the African buffalo (*Syncerus caffer*), and an independent cycle maintained within domestic animals (Vosloo et al., 1996). The presence of large numbers of African buffalo provides a potential source of sporadic spill-over to domestic livestock (Hedger, 1972; Vosloo et al., 1996). Although the precise mechanism of transmission of FMDV from buffalo to cattle is not well understood, it is facilitated by direct contact

between these two species. Once cattle are infected they may maintain FMDV infections without the further involvement of buffalo (Dawe et al., 1994). Outbreaks of the disease can cause high mortality of young animals due to myocarditis, as well as decreased production of milk and meat in older animals (Grubman and Baxi, 2004).

Considering the complex epidemiology of FMDV in Africa, in the Southern African Development Community (SADC) emphasis is placed on control rather than eradication of the disease. Countries implement control strategies to separate wildlife and livestock creating areas free of FMD, either through physical separation and movement restrictions or by creating an immunological 'barrier' via repeated vaccination of cattle herds potentially exposed to wildlife. The costs of control are substantial and trade restrictions severely affect economies that are reliant on agricultural production (reviewed in Maree et al., 2014).

In southern Africa, where an increase in the incidence of outbreaks in livestock has been experienced over the last 10 years, a fast and reliable assay to distinguish between infected and vaccinated animals is essential in the decision making for the implementation of control

* Corresponding author at: Transboundary Animal Diseases, Onderstepoort Veterinary Institute, Private Bag X05, Onderstepoort 0110, South Africa.
E-mail address: mareef@arc.agric.za (F.F. Maree).

<https://doi.org/10.1016/j.jviromet.2018.02.006>

Received 6 September 2017; Received in revised form 31 January 2018; Accepted 6 February 2018

Available online 08 February 2018

0166-0934/ © 2018 Elsevier B.V. All rights reserved.

PUBLICATIONS AND CONFERENCE CONTRIBUTIONS

PUBLISHED MANUSCRIPTS

Nsamba P, de Beer TA, **Chitray M**, Scott K, Vosloo W, Maree FF. (2015). Determination of common genetic variants within the non-structural proteins of foot-and-mouth disease viruses isolated in sub-Saharan Africa. *Vet Microbiol.* 177(1-2):106-22

Maree FF, Kasanga CJ, Scott KA, Opperman PA, **Chitray M**, Sangula AK, Sallu R, Sinkala Y, Wambura PN, King DP, Paton DJ, Rweyemamu MM. (2014). Review: Challenges and prospects for the control of foot-and-mouth disease: an African perspective. *DovePress Journal: Veterinary Medicine: Research and Reports* (5) 119–138.

Chitray M, Grazioli S, Willems T, Tshabalala T, De Vleeschauwerd A, Esterhuysen JJ, Brocchi E, De Clercq K and Maree FF. (2018). The development and evaluation of a SAT-specific 3ABC DIVA test for Foot-and-mouth disease virus in the Southern Africa context. *J. Virol Methods* (255) 44-51.

MANUSCRIPTS IN PREPARATION

Chitray M*, Kotecha A*, Nsamba P, Ren J, Maree S, Paul G, Theron J, Fry EE, Stuart DI and Maree FF. Symmetrical arrangement of positively charged residues around the five-fold pore of Foot-and-mouth disease SAT type virus capsids results in the enhanced binding to heparan sulphate. *Submitted to the Journal of Virology.*

Chitray M, Rotherham LS, Frischmuth J, Rieder E, Maree FF and Opperman PA. Vaccine strain selection: Determining the antigenic composition of a Type A and SAT serotype foot-and-mouth viruses using chicken single-chain antibody fragments. *In preparation*

NATIONAL CONFERENCE CONTRIBUTIONS

Chitray M, Maree S, Theron J and Maree FF. (Poster presentation). The introduction of positively charged residues at the five-fold axis of the foot- and-mouth virus capsid enhances infection of cultured cells. SASM 2013, 24-27 November, 2013, Bela Bela, South Africa.

Chitray M, Kotecha A, Turkki P, Maree S, Nsamba P, Fry EE, Theron J and Maree FF (Poster Presentation). The introduction of positively charged residues at the five-fold axis of the foot-and-mouth virus capsid enhances infection of cultured cells. Virology Africa 2015, 30 November - 03 December 2015, Cape Town, South Africa.

Chitray M, Fershen J, Frischmuth J, Maree F, Opperman P (Oral presentation). FMDV-specific scFvs as diagnostic reagents and tools to map epitopes. SASM 2018, 4-7 April, 2018, Muldersdrift, South Africa

INTERNATIONAL CONFERENCE CONTRIBUTIONS

Chitray M, Esterhuysen JJ, Blignaut B, Tshabalala T and Maree FF. (Poster presentation). The development and evaluation of a SAT-specific 3ABC DIVA test for Foot-and-mouth disease virus in the Southern Africa context. EuFMD 2010, 28 September to 1 October, Vienna, Austria.

Chitray M, Esterhuysen JJ, Tshabalala T and Maree FF. (Oral presentation). The development and evaluation of a FMDV SAT-specific 3ABC DIVA assay for SADC. FAO PCP workshop, 16-18 March 2011, Gaborone, Botswana.

Chitray M, Tshabalala T, Fosgate GT, Brocchi E, Grazioli S, De Clercq K, Willems T, Esterhuysen JJ and Maree FF. (Oral presentation). The development and evaluation of a SAT-specific 3ABC DIVA test for Foot-and-mouth disease virus in the Southern Africa context. EuFMD 2012, 28-31 October 2012, Jerez de la Frontera, Spain

Chitray M, Maree S, Theron J and Maree FF. (Poster presentation). The introduction of positively charged residues at the five-fold axis of the foot-and-mouth virus capsid enhances infection of cultured cells. Europic XVII 2014, 9-14 March, 2014, Blankenberge, Belgium.

***Chitray M**, Maree S, Theron J and Maree F. (Oral presentation). The introduction of positively charged residues at the five-fold axis of the foot-and-mouth virus capsid enhances infection of cultured cells. EuFMD 2014, 28 to 31 October 2014, Cavtat, Croatia.

* Won an award for best presentation for the session

Chitray M, Kotecha A, Turkki P, Maree S, Nsamba P, Fry EE, Theron J and Maree FF (Oral Presentation). The introduction of positively charged residues at the five-fold axis of the foot-and-mouth virus capsid enhances infection of cultured cells. GFRA 2015, 20-22 October 2015, Hanoi, Vietnam